STRUCTURAL RELIABILITY ANALYSIS OF FPSOs TOWARDS A RATIONAL DESIGN PROCEDURE

by

André Maerli, BEng

Thesis Submitted for the Degree of Master of Science

UNIVERSITY
of
GLASGOW

Department of Naval Architecture and Ocean Engineering
University of Glasgow

December 1998

To my father Kai on his 50th birthday.

Declaration

Except where reference is made to the work of others,
this thesis is believed to be original.

Acknowledgements

I would like to thank Dr. P.K. Das for his valuable guidance, assistance and encouragement during this project. Thanks are also due to Professor Nigel Barltrop for insightful comments and recommendations.

Special thanks to Stuart N. Smith and Amerada Hess Ltd., for financial support and for making this project possible by providing necessary data.

Warm and heartfelt thanks to Angelo Palos Teixeira and Iason Papageorgiou Lambos for invaluable help and support.

Abstract

This report presents the structural reliability analysis of the hull girder ultimate strength for the ship shaped FPSO Triton. The ultimate strength of the hull girder was calculated using a component approach, where the behaviour of the hull is evaluated based on the behaviour of the single structural components. Three collapse conditions were investigated; failure initiated by plate compression, failure initiated by stiffener tension and failure initiated by stiffener compression.

Only vertical bending moment has been considered and the hull girder loads are divided into stillwater and wave induced components. The two loading components have been considered independent and Ferry Borges – Castenheta load combination method has been applied to obtain load combination factors for the Full Load, Partial Load (50 % loaded) and Ballast condition.

The distributions of the extreme values of the vertical wave bending moments (VWBM) were calculated, based on linear strip theory and a long-term formulation. The vertical mooring forces are small and they were considered to have an insignificant influence on the bending moment response.

The reliability analysis was carried out using a SORM analysis. Annual reliability indices (β) and probabilities of failures were calculated for hogging and sagging conditions. The calculated β values were higher than the annual reliability indices proposed in DNV Classification Notes 30.6 for serious failures in redundant structures. This indicates that the design is safe and reliable for operation in this particular location.

Table of Contents

List of Figures

List of Tables

Nomenclature

b - Breadth of plate (Chapter 2)

b -Weibull shape parameter (Chapter 3)

b_f - Breadth of flange

d_w - Depth of web

f_l - Material factor

f_{sl} - Slam related extreme stresses

f_w - Wave related extreme stresses

k - Weibull scale parameter

k_i - Main curvature of failure surface equation

m_0 - Variance of response

$m_{0_{rm}}$ - Variance of relative motion

$m_{0_{rv}}$ - Variance of relative velocity

m_n - Moments of Response Spectra

n_{sw} - Number of occurrences of load condition per year

n_w - Number of wave peaks in reference period

p_i - Cargo pressure

r - Radius of curvature

t_f - Thickness of flange

t_w - Thickness of web

u_{sw} - Gumbel parameter

u_w - Gumbel parameter

v - Ship speed

v_{cr} - Critical velocity

x - Basic variable

$\bar{x}^*$ - Design point

$\bar{x}_d$ - Design values

x_{sp_i} - Nominal value of resistance

x_{sp_l} - Nominal value of loading

y - Vertical distance from neutral axis

y_e - Vertical position of element

y_n - Vertical position of instantaneous neutral axis

z - Limit state function

A - Area

A_e - Element Area

B - Greatest moulded breadth in metres

C - Curvature

C_b - Block coefficient

COV – Coefficient of variation

C_w - Wave load coefficient

E - Young's Modulus

E_e - Young's Modulus for an element

G - Spreading function

H_{max}- Maximum wave height

H_s - Significant wave height

I - Rule requirement moment of inertia

I_{tr} - Inertia of transformed section

K - Optimisation parameter

L - Length of ship (Chapters 2 and 3)

L - Load (Chapter 4)

L_e - Panel length

M - Bending moment

M_c - Combined bending moment

M_e - Elastic bending moment

M_p - Plastic bending moment

M_{se}- Extreme stillwater induced bending moments

M_{sl}- Slam induced bending moment

M_{sw}- Stillwater induced bending moments

M_{te}- Total bending moment

M_{te}- Total extreme bending moment

M_u - Ultimate longitudinal bending moment

M_{ut}- Target ultimate longitudinal bending moment

M_w- Wave induced bending moment

M_{we}- Extreme wave induced bending moment

M_x - Bending moment related to a specific curvature

P_f - Probability of failure

Q - Probability of exceedance

R - Resistance

$\mathcal{R}$ - Probability of survival

S - Shape factor

S_B - Directional response spectrum

S_i - Transformation factor

S_ζ - Wave spectrum

T - Draught

T_m - Average wave period

T_{sw} - Total time per year in load condition

T_z - Wave period

Z - Rule requirement section modulus

Z_e - Elastic section modulus

Z_p - Plastic section modulus

α - Angle between neutral axis and x-axis

α_i - Sensitivity factor

α_{sw} - Gumbel parameter

α_w - Gumbel parameter

β - Reliability index

β - Annual reliability index

β_g - Generalised reliability index

β_{HL} - Hasofer-Lind reliability index

β_t - Target reliability Index

γ - Euler's constant

γ_i - Partial safety factors

γ_s - Partial safety factor on stillwater loading

γ_s^* - Redefined partial safety factor on stillwater loading

γ_u - Partial safety factor on ultimate bending moment

γ_w - Partial safety factor on wave loading

γ_w^* - Redefined partial safety factor on wave loading

δ_0 - Initial deformation

ε - Bending strain

ε_e - Longitudinal strain in element

θ - Ship heading

χ_m - Modelling uncertainty

χ_{nl} - Non-linear effects

χ_u - Uncertainty on ultimate capacity

χ_w - Uncertainty on wave Load

μ - Wave direction

μ_g - Mean of limit state function

μ_L - Mean of load

μ_R - Mean of resistance

μ_{sw}- Mean of stillwater normal distribution

μ_{se} - Mean of stillwater Gumbel distribution

ρ - Density of sea-water

σ - Stress

σ_0 - Nominal yield stress

σ_g - Standard deviation of limit state function

σ_e - Element stress

σ_r - Residual stress

σ_{sw}- Standard deviation of stillwater normal distribution

σ_{se} - Standard deviation of stillwater Gumbel distribution

σ_y - Yield stress

σ_{yp} - Yield stress of plating

τ_{sw} - Duration of load condition

ω - Wave frequency

$\Delta_{0,p}$- Overall deformation, towards plating

$\Delta_{0,s}$ - Overall deformation, towards stiffener

Φ - Transfer function (Chapter 3)

Φ - Normal distribution (Chapter 4)

Ψ_{sw}- Stillwater load combination factor

Ψ_w - Wave load combination factor

1 Introduction

The Floating Production Storage and Off-loading Vessel (FPSO) has become a well-established development concept in offshore oil and gas production. FPSOs have been chosen for an increasing number of field developments in recent years. High payload capacity, short development schedule and in-built cargo storage capacity are some important advantages that make 'Ship Shaped' FPSOs very attractive for field developers. The operation and maintenance profiles of a FPSO differ from those of a traditional merchant ship, and these differences will significantly influence the structural reliability of the vessel. This report presents the structural reliability analysis of the hull girder ultimate strength for the ship shaped FPSO Triton.

Both new-build FPSOs and tanker conversions have a role to play, with selection being based on the particular field requirements. A site-specific assessment of the global structural response must be carried out. FPSOs are designed to endure long-term deployment, often in very harsh environment, minimum production downtime may dictate that the vessels operate without dry-docking and survey on station. The vertical bending moment and shear forces for a production vessel have been estimated to be approximately 30% higher than for a tanker with the same main particulars (Sogstad (1995)).

The Triton FPSO is a double-skin tanker conversion fitted with a passive turret mooring system. It will be moored close to the Gannet field, producing from the Bittern and Guillemot west fields. The vessel's Oil-storage capacity is 630,000 BBLS, which equals 6 days of production. The main Particulars of the FPSO are:

Length Between Perpendiculars	233.0 m
Breadth Moulded	42.0 m
Depth Moulded	21.3 m
Design Draught	13.6 m
Scantling Draught	14.7 m
Tonnage	105,000 DWT

Table 1.1 Main Particulars of Triton

The overall aims of the project are to establish a realistic structural response of FPSOs with a probabilistic environmental loading and to carry out a structural reliability analysis of Triton considering the ultimate limit-state. The methodology will ensure a procedure to design a structure with consistent levels of safety, ensuring that the structure is safe throughout its lifetime. The report compares the as-built FPSO design with the initial tanker design and comments on the reliability levels.

1.1 Ultimate Longitudinal Strength of Ships

It is difficult to define theoretically the ultimate limit state of a complex structure like a ship. The hull girder is a three-dimensional structure containing many members, and its collapse involves various combinations of plastic deformation and inelastic bifurcation buckling of members. For the purpose of ultimate limit state analysis, it is necessary to move from classic linear elastic approaches to more effective theories, able to take into account the influence of non-linear behaviour of structural components on the ultimate strength evaluation.

This report only addresses the case of ultimate longitudinal bending moment (UBM); that is the moment causing the global collapse of the ship. Simplified methods for determining the ultimate limit state of the hull girder have been developed throughout the last 30 years. Smith (1977) developed an iterative approach, where a sequence of increasing curvatures is imposed on the hull girder, and a complete moment curvature relationship for the ship's hull is obtained. Other methods based on the same general approach were later developed, including the simplified approaches by Billingsley (1980), Adamchak (1984) and Dow et al (1981).

The Lloyds Register's LRPASS Program 20203 uses this type of simplified component approach, where the behaviour of the hull is evaluated based on the behaviour of the single structural components. The cross section of the hull is subdivided into beam column elements, which are assumed to act independently. Each element is composed of longitudinal stiffeners and an effective breadth of plate. Three collapse conditions are investigated; failure initiated by plate compression, failure initiated by stiffener tension and failure initiated by stiffener compression.

1.2 Loads and Load Combination

For adequate and safe ship design, appropriate values of design loads have to be established. The hull girder loads may be divided into stillwater loads and wave loads. The two types of loading are of a very different nature. The stillwater loads relate to cargo loading and other controllable factors, it is therefore relatively easy to predict their characteristic values and their distribution parameters. The procedure of evaluating the wave loads is far more complex. Wave loads are probabilistic and it is a complicated task to calculate the wave bending moments on a ship structure in a sea state.

In addition to the hull girder loads, local loads may be important in the design of local structures. However, only vertical bending moment will be considered in this project and the loads due to external and internal hydrostatic pressure will be accounted for during calculation of the Ultimate Bending Moment of the hull girder. The other extreme local loads have not been included in the analysis.

The hull girder loads are divided into still water induced (SWBM) and wave induced components (VWBM). Autohydro 4.0 will be used to calculate stillwater vertical bending moments for each loading condition. A procedure for calculating the long-term distribution of the wave induced bending moments, based on short-term response, is presented. As a final step of the load analysis, the loads are combined using Ferry Borges – Castenheta load combination model to obtain load combination. The results from load calculations will together with the ultimate strength calculations make up the basis of the structural reliability analysis.

1.3 Structural Reliability Analysis

Traditionally structural engineering as been dominated by deterministic methods, where all factors affecting the strength of the structure and applied loads are assumed known. In reality, there will be a high degree of uncertainty associated with all these factors. To handle the design in a realistic way, the probabilistic approach considers each parameter as a statistical variable characterised by the probability density function.

The probability of all values of all variables are then considered and combined, to give an estimate of the safety or reliability of the structure. Lewis (1994) defined reliability as "the probability that a system will perform its intended function for a specified period of time

under a given set of conditions". Structural reliability is concerned with the calculation and estimation of the probability of limit state violation, violation of both serviceability criteria and the ultimate limit state. The failure surface for the longitudinal strength of the hull girder may be defined by;

$$g(X) = \chi_u M_u - M_{sw} - \psi_w \chi_{nl} \chi_w M_w = 0 \qquad \text{Eq. 1.1}$$

The goal for the structural design is to achieve some target reliability for the total structure, and the objective of the structural reliability analysis is then to achieve this target reliability. A reliability analysis is carried out for Triton and safety indices obtained for various limit states. The safety indices are compared with target reliabilities, depending on consequence of failure and type of failure, proposed by the classification societies. A partial safety factor optimisation is carried out for Triton to establish a code format.

The structural reliability program *CALREL* is used to calculate the generalised reliability index β_g and P_f. *CALREL* incorporates four techniques for computing these quantities; FORM, SORM, Directional simulation and Monte Carlo simulation. FORM and SORM are applicable to component reliability analysis, FORM is applicable to series system reliability. Directional simulation in conjunction with FORM or SORM is applicable to component or system reliability analysis, and Monte Carlo simulation is applicable to all classes of problems.

2 Ultimate Longitudinal Strength of Ships

2.1 Ultimate Limit State

This report only addresses the case of ultimate longitudinal bending moment (UBM); that is the moment causing the global collapse of the ship. Research have shown that for a production ship always heading onto waves in operation, although the waves are not collinear, the horizontal bending and shear are negligible. Other combinations of sectional forces could be critical, in particular for non-conventional vessels. It may be useful for these vessels to extend the calculation of the limit state of the hull to include; the effects of shear, torque and transverse bending moment.

It is difficult to define theoretically the ultimate limit state of a complex structure like a ship. The hull girder is a three-dimensional structure containing many members, and its collapse involves various combinations of plastic deformation and inelastic bifurcation buckling of members. For the purpose of ultimate limit state analysis, it is necessary to move from classic linear elastic approaches to more effective theories, able to take into account the influence of non-linear behaviour of structural components on the ultimate strength evaluation. The elasto-plastic methods almost invariably over-predict the ultimate bending moment. These elastic and plastic bending moments capacities have been evaluated using conventional elastic and plastic theories.

The interaction of the individual components that contribute to the collapse may be evaluated using a finite element method, which would consider the material and geometrical non-linearity. These analyses require vast computational effort and are at the time being too uneconomical for design purposes. A much simpler methodology for determining the ultimate limit state of the hull girder has been developed throughout the last 30 years.

Caldwell (1965) proposed a simplified procedure where the ultimate moment of the mid-ship section was calculated introducing a "knockdown" factor for the compressed panels. This factor would account for the reduced strength of the cross-section due to early failure and unloading of some elements. Considerable effort was spent on improving the formulation of the compressive behaviour of stiffened plate panels; Faulkner (1975) and Dow et al (1981) amongst others made valuable contributions. Smith (1977) developed a method to incorporate the load shortening curves of the plate elements in the calculation of the hull girder collapse. By an iterative approach, where a sequence of increasing curvatures is

imposed on the hull girder, a complete moment curvature relationship for the ship's hull can be obtained.

Other methods based on the same general approach were later developed, including the simplified approaches by Billingsley (1980), Adamchak (1984) and Dow et al (1981). The Lloyds Register's LRPASS Program 20203 uses this type of simplified component approach, where the behaviour of the hull is evaluated based on the behaviour of the single structural components. The most important hypothesis of these "component" approaches is that the global collapse of the hull is a sequence of localised collapses of individual components rather than a global collapse of the whole section. It is assumed that the collapse values of the individual elements are very different from each other, and therefore interaction of the different collapse modes is neglected.

2.2 Ultimate Bending Moment

2.2.1 Stiffened panel analysis

As a first step in the analysis, the selected cross-section of the hull is subdivided into beam column elements, which are assumed to act independently. Each element is composed of longitudinal stiffeners and an effective breadth of plate as shown in figure 2.1. The hull girder subdivision of Triton into discrete elements is presented Figure 2.7. Some further assumptions are made in the theory:

- The overall collapse of the hull may be subdivided into two distinct and independent modes of collapse, the longitudinal and the transverse one.
- Any stresses acting in the transverse direction have a negligible effect on the elements' behaviour under longitudinal stress. This can be justified on the basis that the panels between transverse frames are longitudinally stiffened only, thus generating a predominantly longitudinal stress field.
- Any incompatibility of out-of-plane displacements between adjacent elements is negligible. Again, the typical design of stiffened plates between transverse frames and deep girders in the main strength zones of the deck and bottom involves panels whose element sections and properties are uniform across the plate width. Relative displacements between adjacent elements will consequently be small or zero.
- The overall grillage collapse of the deck and bottom structure is avoided by using sufficiently strong transverse frames.

- Longitudinal Collapse occurs only between two adjacent frames.
- The longitudinal girders are strong enough to support the panels adequately, the longitudinal girder failure is due to yielding only.

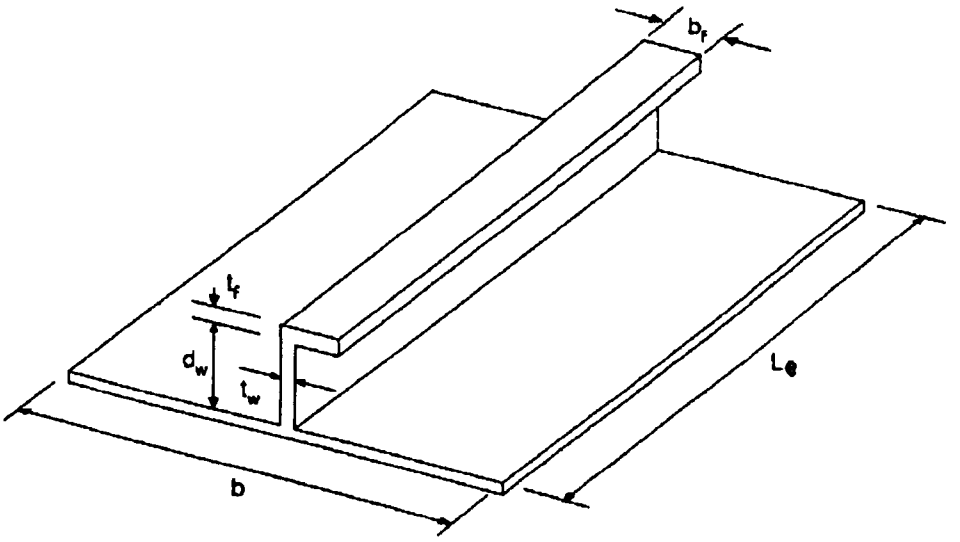

Figure 2.1 Beam Column Element

The LRPASS Program 20202 was used for obtaining load-shortening curves for the stiffened plate elements. The program is based on a formulation of the ultimate strength of stiffened panels outlined by Rutherford (1982). The ultimate strength of stiffened panels is assessed using a beam-column approach. The panel behaviour is typified by that of a single stiffener, together with an effective width of plating. The overall axial strength is obtained from a strut formulation in which the individual plate and stiffener strengths provide the limiting extreme fibre stresses.

Two predictions of ultimate strength of stiffened plate elements are given by the program, one relating to plate-induced failure and the other to stiffener-induced failure. The lowest of these defines the ultimate condition and identifies the mode to be used in selecting a load-shedding response beyond the ultimate stress. In this respect, four separate theories are included in the program, two for plate failure and two for stiffener failure; in both cases, one theory allows for buckling while the other assumes pure plastic action. Panels in tension behave without unloading after yield, while panels in compression behave with an unloading pattern after collapse.

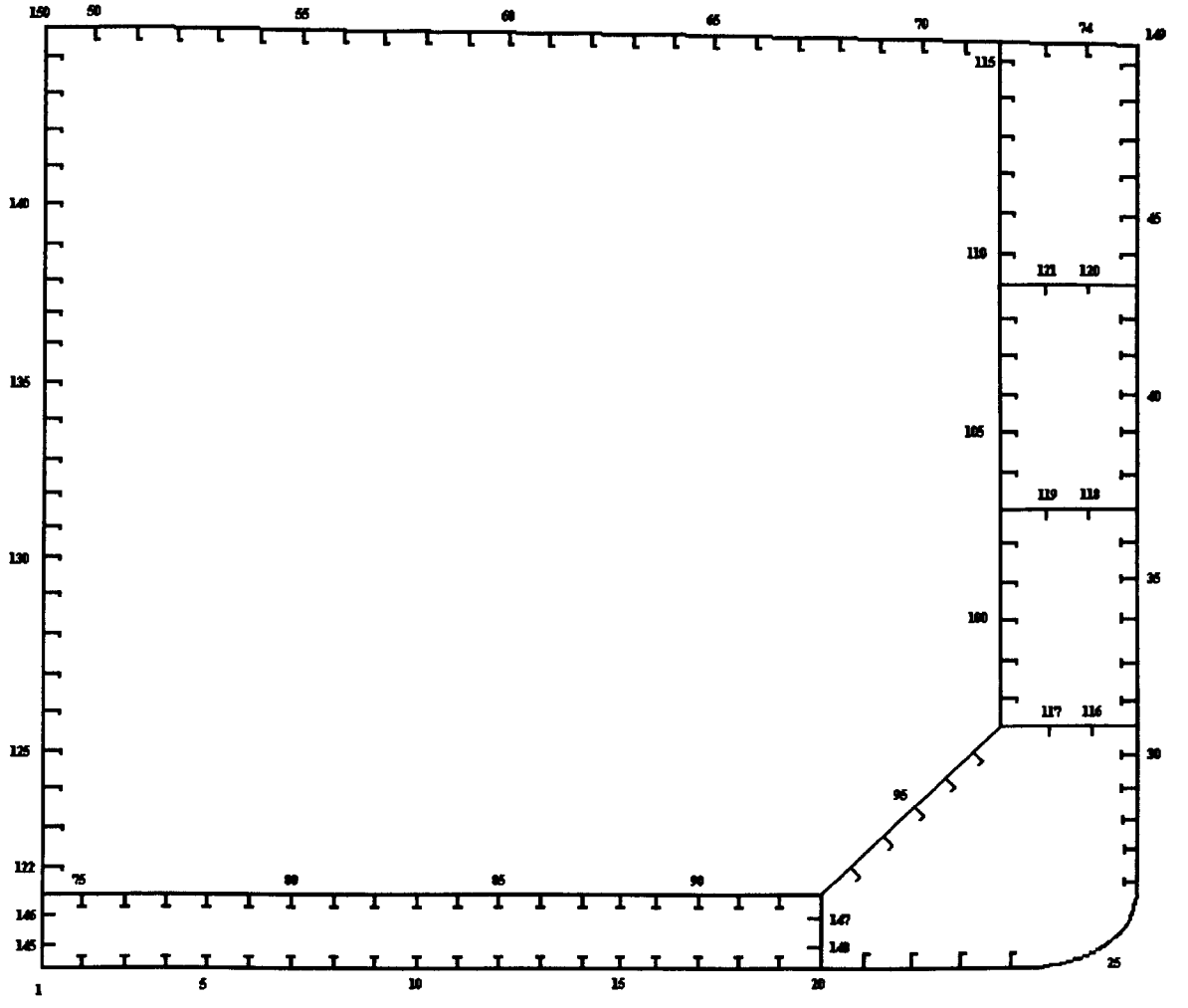

Figure 2.2 Hull Girder Subdivision

All the elements have been assumed to have residual stresses and initial deformations. The default values given in LRPASS 20202 have been used. These values are given by:

Residual stress, σ_r $= 0.1 \times \sigma_{yp}$ Eq. 2.1

Local deformation, δ_0 $= \frac{b}{200} \times \left[\frac{\sigma_{yp}}{\sigma_0} \right]^{1/2}$ Eq. 2.2

Overall deformation, $\Delta_{0,s}$ $= \frac{L_e}{900}$ (towards the stiffener) Eq. 2.3

Overall deformation, $\Delta_{0,p}$ $= \frac{L_e}{1200}$ (towards the plating) Eq. 2.4

In addition to these initial imperfections, lateral sea- and cargo-pressures on the plate panels are included in the analysis. These pressures give rise to both local and overall bending effects. The *DNV Rules pt. 3 Ch.1 Sec. 4C 200* gives the cargo pressure as;

$$p_i = \rho g h_s + 25 \text{ kN/m}^2 \qquad \text{Eq. 2.5}$$

If the tank is assumed full, a pressure of 0.19 N/mm^2 will act on the top of the double bottom. In a half-full tank the cargo pressure will be 0.11 N/mm^2. The cargo pressure on the inner side shell is assumed to decrease linearly from the tank bottom to the tank top. A situation where the tank on one side of the longitudinal bulkhead is full, and the other is empty has not been analysed, although it would be necessary to do so in the local strength assessment.

The same section in the DNV rules states that the design sea pressures are to be taken as corresponding to full draught including dynamic sea pressures. Dynamic sea pressures have been neglected at this stage of the analysis. The scantling draught of 14.7 m gives a pressure on the bottom of approximately 0.15 N/mm^2. The water pressure on the side shell decreases linearly from approximately 0.15 N/mm^2 at the bilge keel, to zero at the water line. Figure 2.3 shows the effect of lateral pressure on a typical bottom plate panel from Triton.

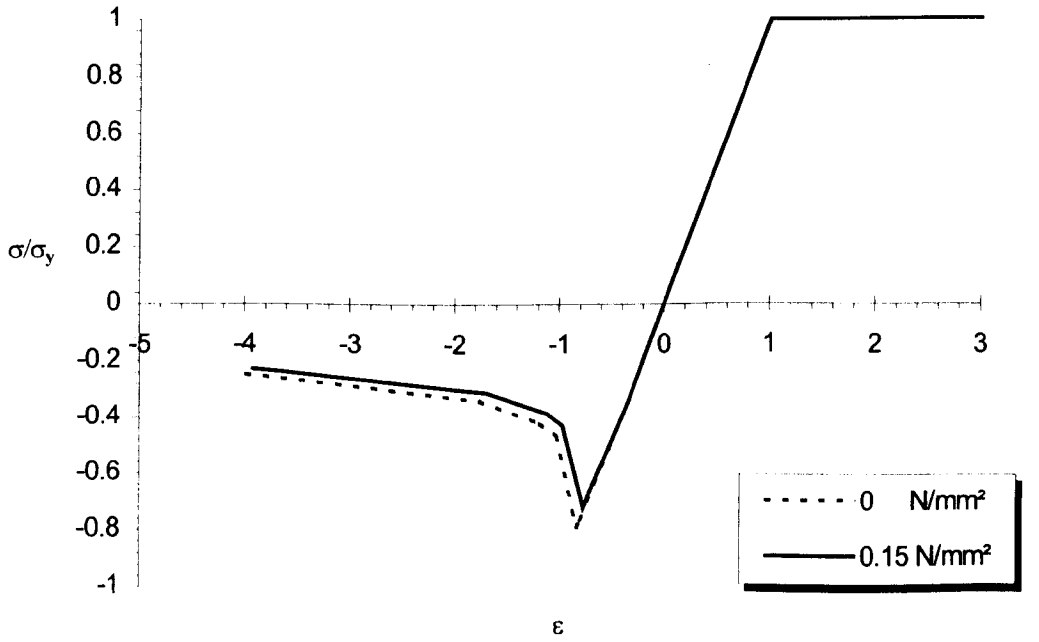

Figure 2. 3 Lateral Pressure on Bottom Panel

The hydrostatic pressure acting on the side shell will also induce transverse stresses in the bottom plating. If a plate is subjected to two orthogonal compressive stresses, elastic and inelastic buckling and ultimate strength all involves a strong interaction between these two stresses. The nature of the interaction depends mainly on the aspect ratio and plate slenderness. The problem is very complex and an exact solution requires a rigorous numerical analysis. However, the stress in the bottom structure resulting from pressure on the side shell has been estimated to be close to 20 N/mm^2 as a worst case scenario, that is approximately 6 % of the yield stress. This level of stress will have a negligible influence on the axial load carrying capacity of the structure, and it has therefore been ignored. Lateral pressure effects considered in the analysis are therefore restricted to local bending of the plate panels between stiffeners and overall bending of the stiffened panels between frames. Both of these are accounted for automatically in the theory used to generate element stress-strain data.

Elements close to deck corners and longitudinal bulkheads will sometimes have adequate stiffness to avoid premature collapse. These hard corners may be modelled by elements where no unloading takes place after the stiffened panel has reached yield collapse, as shown in Figure 2.4. The LRPASS Program 20202 does not have a built-in feature to treat this phenomenon, so the stress-strain curves have to be modified or created manually. The inclusion of hard corners increases the ultimate hull bending moment, and gives a better representation of the actual behaviour of the hull girder.

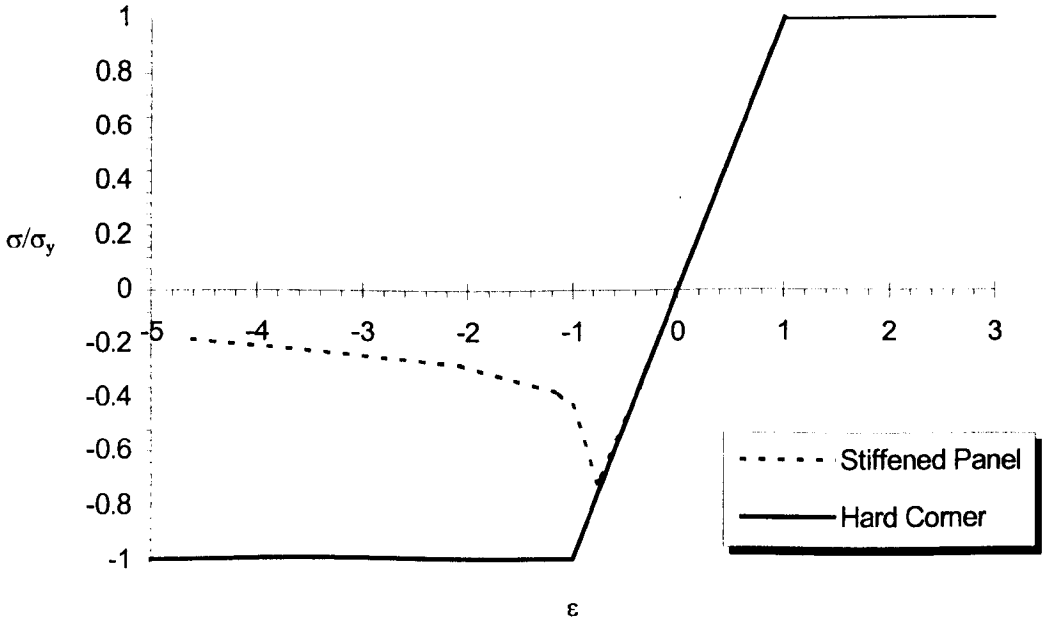

Figure 2.4 The Effect of Hard Corners

2.2.2 Ultimate Bending Moment Analysis

The phenomenon of longitudinal collapse is shown in Figure 2.4 where the curvature $C = 1/r$, is progressively increased due to an externally applied hogging or sagging bending moment. The internal moment of resistance M of the hull cross-section increases, up to a point at which dM/dC becomes zero, or changes sign. This point defines the ultimate longitudinal bending strength M_u of the hull. In general, M_u will be different for hogging and sagging conditions.

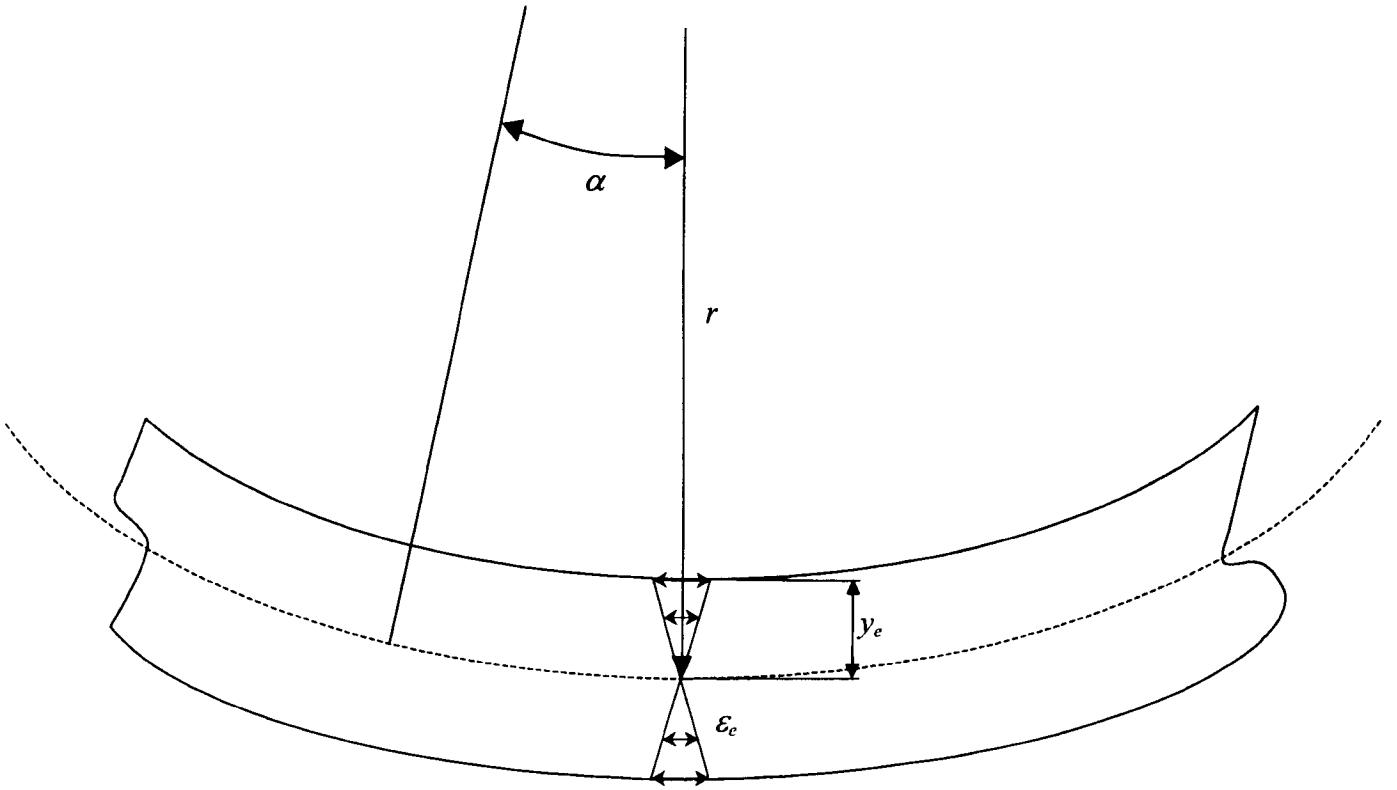

Figure 2.5 Hull Girder Bending Concept

On the assumption that plane sections remain plane in bending, the strain corresponding to an applied curvature, C, can be calculated for each element of the cross-section using a simple beam bending theory. Combined vertical and horizontal bending can be accommodated if their relative magnitude and phasing are known and can be represented by incrementing horizontal and vertical curvature. For an element e the following relationship applies, when curvature C is imposed in the horizontal plane only:

$$\varepsilon_e = C \cdot y_e \qquad \text{Eq. 2.6}$$

where ε is the longitudinal strain in the element. Using this information in conjunction with input element stress-strain curves, the stress state around the hull is established and a simple summation process follows to determine the bending moment resulting from the applied curvature. For a curvature C the moment is;

$$M_x = \sum \sigma_e \cdot A_e \cdot y_e \qquad \text{Eq. 2.7}$$

where σ_e is the element stress related to the strain ε_e via the stress-strain curve for the element, y_e is the vertical position of the element and A_e is the effective sectional area of the element. By performing this process in predefined steps, a trace of the moment curvature response of the hull incorporating the non-linear response of individual elements is achieved. A typical moment-curvature relationship is shown in Figure 2.6.

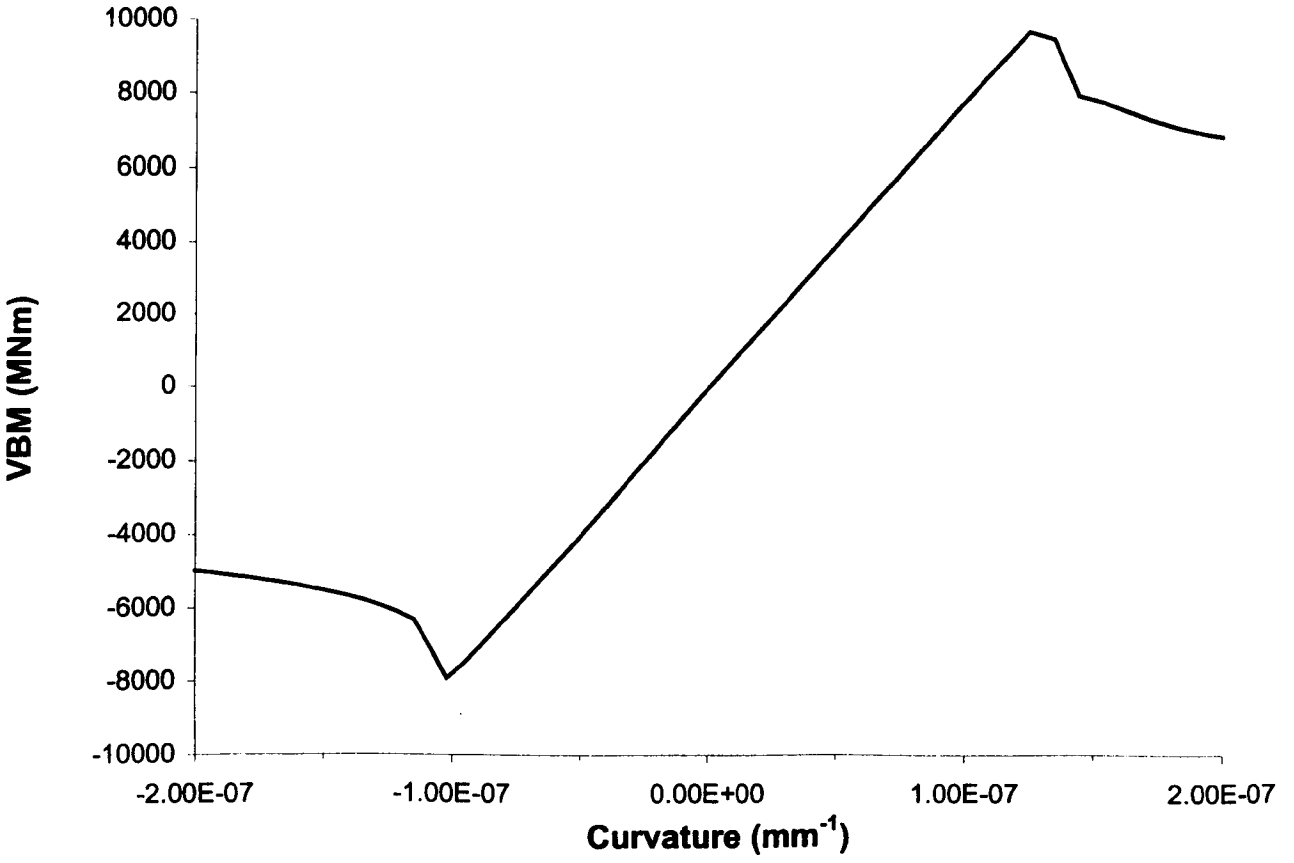

Figure 2.6 Bending Moment-Curvature Relationship for Triton 2

Initially it is necessary to estimate the position of the neutral (or zero strain) axis through elastic analysis, because when the curvature is small the section behaves in the elastic

domain. If the section is symmetric and the origin of the reference system is located at the underside of the bottom plating, the elastic neutral axis passes through a point with co-ordinates:

$$y_n = \frac{\sum y_e \cdot A_e}{\sum A_e} \qquad \text{Eq. 2.8}$$

Since the stress distribution may not be linear, the neutral axis position is adjusted using Eq. 2.8 to maintain equilibrium of the system, during the incremental procedure.

$$\text{SHIFT} = \frac{\sum (A_e \cdot \sigma_e)}{C \cdot \sum E_e \cdot A_e} \qquad \text{Eq. 2.9}$$

where E_e is the value of Young's modulus for the element.

At high curvatures, several of the initial assumptions made on page 6 could be violated. Thus, the estimation of the capacity beyond the ultimate bending moment is approximate. Other methods of analysis, such as FEA, should be used to investigate the post-UBM behaviour. However, the procedure utilised in LRPASS 20203 gives a satisfactory estimation of the UBM, which is of great importance in the assessment of ship safety.

2.3 Elastic and Plastic Theory

It is of interest to compare the ultimate bending moment of a cross section to the elastic and plastic bending moments. The comparison will give an indication on how well the midship section is designed. One would generally try to achieve values of UBM as close to the elastic bending moment as possible. A Fortran code was developed to determine the elastic and plastic properties of the midship section. The theory behind this code is described on the following pages.

2.3.1 Elastic Theory

Triton has high tensile steel in the upper deck, inner and outer bottom, and to some extent in the side shells. The assessment of the elastic bending moment of a cross section fabricated of two (or more) materials requires more effort than the straightforward case of a single material-hull. Hughes (1983) outlines a composite beam theory that is intended for beams of

solid cross section, with dissimilar materials. The technique has direct application to a hull girder if the dissimilar portion is part of the cross section of the main hull; for example, a deck constructed of titanium or high tensile steel.

The fundamental assumption of beam bending theory is that plane sections remain plane. It is now assumed that the dissimilar portion is an integral part of the hull girder, such that the bending strain ε is still linearly proportional to the distance y from the neutral axis; that is

$$\varepsilon = \frac{y}{r} \qquad \text{Eq. 2.10}$$

The corresponding value of the bending stress at any point is $\sigma = E\varepsilon$, and the following relationship can be derived;

$$\sigma = \frac{Ey}{r} \qquad \text{Eq. 2.11}$$

The next step in the derivation of elementary beam theory is the requirement that there is no net axial force in the beam:

$$\int \sigma \, dA = \int E \frac{y}{r} dA = \frac{1}{r} \int Ey \, dA = 0 \qquad \text{Eq. 2.12}$$

If there are two or more portions of the beam which have different values of s then the integral must be evaluated separately for each portion. An alternative approach is to chose one of the values of σ_i (say σ_1) as a reference value and relate the other values to it by means of a transformation factor S_i which is defined as.

$$S_i = \frac{\sigma_i}{\sigma_1} \qquad \text{Eq. 2.13}$$

S_i is a variable, which is a function of position within the beam cross section. Within any one material its value is constant, but the value changes abruptly when passing from one material to another. We can now write Eq. 2.12 as:

$$\int \sigma_1 \, dA + \int \sigma_2 \, dA + \ldots + \int \sigma_n \, dA = \frac{E}{R} \int S_i y \, dA = 0 \qquad \text{Eq. 2.14}$$

The next step in elementary beam theory is the requirement of equilibrium between the external bending moment acting on the section and the moment of internal stress forces.

$$M_e = \sigma_1 \int S_i y \, dA = \frac{E}{r} \int S_i y^2 \, dA \qquad \text{Eq. 2.15}$$

The transformation factor S_i can be regarded as multiplying dA and giving either a reduced or an enlarged area for each non-standard portion of the cross section. Therefore, the integral in (Eq. 2.14) is simply the moment of inertia of the transformed section, which can be denoted as I_{tr}:

$$I_{tr} = \int S_i y^2 \, dA \qquad \text{Eq. 2.16}$$

This definition holds, as if the beam were a homogenous beam of σ_1, with I_{tr} in place of I:

$$\frac{1}{R} = \frac{M}{EI_{tr}} \qquad \text{Eq. 2.17}$$

Combining Eq. 2.11 and Eq. 2.17 gives us an expression for the elastic bending moment:

$$M_e = \frac{I_{tr}\sigma_1}{y} \qquad \text{Eq. 2.18}$$

2.3.2 Plastic Theory

Plastic theory is based on an idealised "elastic-perfectly plastic" stress-strain curve. As shown in Figure 2.7, this idealisation is quite suitable for mild steel, with its definite yield point, and it is conservative since it ignores the subsequent strain hardening of the material.

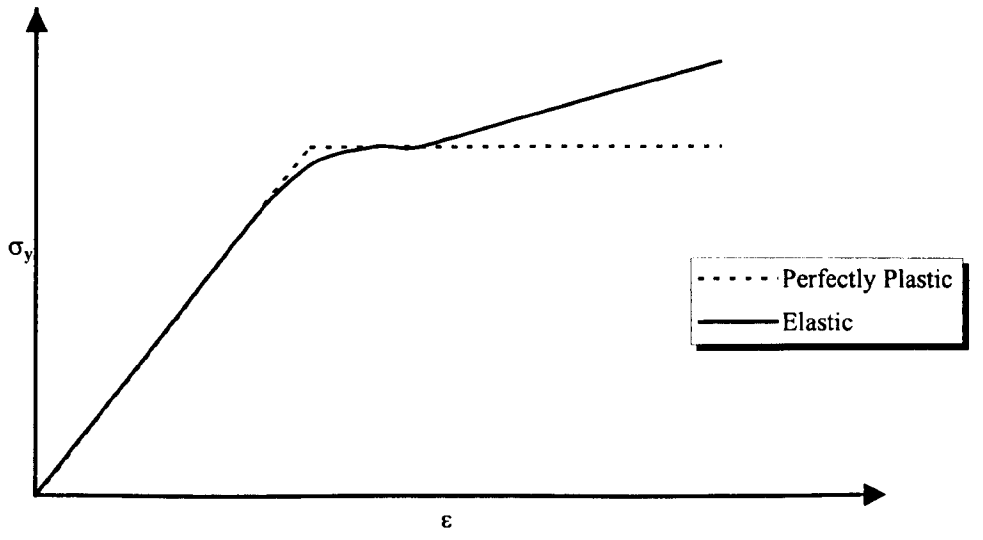

Figure 2.7 Idealised Elastic-Plastic Stress-Strain Curve.

Within the elastic range, the local curvature of the beam (hull girder) is linearly proportional to M, and the load-deflection curve is also linear. At some value of M, say M_y, the maximum bending stress will reach the yield stress of the material. If the curvature of the beam, and therefore the bending moment, is further increased plasticity will spread through the depth of the cross-section until the section is fully plastic. The local bending moment corresponding to this condition is known as the plastic moment of the section M_p. Because all of the fibres have now reached their load-carrying capacity, the beam can absorb no further bending moment at this section. In practice the strain hardening of the material would delay the collapse slightly, to some value of M marginally greater than M_p, but nevertheless at $M = M_p$ the deflection would already be so large as to constitute effective collapse.

Equilibrium in the longitudinal direction requires that the net axial force is zero. If there is no axial force, the force taken by the upper and lower portions of the cross section must be equal and opposite. When dealing with bending about an axis which is not an axis of symmetry, it is important to notice that the *plastic neutral axis,* where the stress reverses sign, does not coincide with the usual neutral axis for elastic bending. The equilibrium of forces can be given as:

$$F_{upper} = F_{lower} \qquad \text{Eq. 2.19}$$

This can be expressed in terms of stresses and areas as:

$$A_{upper} \cdot \sigma_y = A_{lower} \cdot \sigma_y \qquad \text{Eq. 2.20}$$

If the section is made up of different steel qualities, with different σ_y, then equivalent areas have to be used in the calculations. This is done by choosing one of the σ_y's as a reference yield stress and dividing on both sides of Eq. 2.20 by this σ_y. This generalisation of Eq. 2.20 may be written as:

$$\sum A_{1,u} + A_{2,u} \cdot \frac{\sigma_2}{\sigma_1} + \ldots + A_{n,u} \cdot \frac{\sigma_n}{\sigma_1} = \sum A_{1,l} + A_{2,l} \cdot \frac{\sigma_2}{\sigma_1} + \ldots + A_{n,l} \cdot \frac{\sigma_n}{\sigma_1} \qquad \text{Eq. 2.21}$$

Finding the *plastic neutral axis* is then an iterative process solving equation Eq. 2.21. Having fixed the *plastic neutral axis* in this way, it is a simple matter to calculate the first moment of area about that axis in order to determine the section modulus.

$$Z_p = \sum A_{1,u} \cdot \bar{y} + A_{1,l} \cdot \bar{y} + A_{2,u} \cdot \frac{\sigma_2}{\sigma_1} \cdot \bar{y} + A_{2,l} \cdot \frac{\sigma_2}{\sigma_1} \cdot \bar{y} + \ldots + A_{n,u} \cdot \frac{\sigma_n}{\sigma_1} \cdot \bar{y} + A_{n,l} \cdot \frac{\sigma_n}{\sigma_1} \cdot \bar{y} \qquad \text{Eq. 2.22}$$

The full plastic moment is given by:

$$M_p = Z_p \cdot \sigma_1 \qquad \text{Eq. 2.23}$$

Both Z_p and the elastic section modulus, Z, are geometric quantities which depend on the shape of the section, and it may be shown that Z_p is always larger than Z. A shape factor, S, can be calculated:

$$S = \frac{Z_p}{Z} = \frac{M_p}{M_e} \qquad \text{Eq. 2.24}$$

Thus, the shape factor has physical significance; it is the ratio by which the plastic hinge moment exceeds the initial yield moment, at any given section of the beam. If the beam is statically determinate, so that only one hinge is required for collapse, then S also indicates the margin between yielding and collapse. However, beams in structures generally have

more than this minimum degree of fixity and consequently their reserve of strength is somewhat larger than *S*.

2.4 Hull Strength Results and Discussion

Three different mid-ship sections have been analysed and compared. Triton 1 is the initial tanker design, Triton 2 is the improved, as built, FPSO design and Triton 3 is an intermediate design, where only the bottom panels have been strengthened. Although all three designs have been analysed, the focus of the analysis has been on Triton 2, as this is the as-built design.

It can be seen from Table 2.1 that the main modifications from Triton 1 to Triton 2 are; the bottom plating has been increased by 3 mm, the deck plating has been increased by 2-3 mm and the steel has been upgraded to Grade D steel. The increase in plate thickness will affect the ultimate bending moment capacity, whereas the change of steel grade will improve fatigue characteristics. A drawing of the midship section is shown in Appendix A.

Ship	Bottom Plating	Deck Plating	Material
Triton 1	16.5 – 18 mm	16.5-17.5 mm	High Tensile, Grade A
Triton 2	19.5 – 21 mm	19.5 mm	High Tensile, Grade D
Triton 3	19.5 – 21 mm	16.5-17.5 mm	High Tensile, Grade D

Table 2.1 Plate Thickness and Material Properties for Different Designs

2.4.1 Elasto-Plastic Analysis

The area of the midship section has been increased by approximately 5% from Triton 1 to Triton 2. The weight of the added material is estimated to 4% of the hull weight, equalling 800 tonnes. In the Triton 3 design, the cross section area was increased by 2.5% from Triton 1, and the weight increase estimated to 400 tonnes. A summary of the results of the elasto-plastic analysis is shown in Table 2.1.

	Triton 1	Triton 2	Triton 3	Rule Req.	Units
Area of Cross Section	$5.35 \cdot 10^{6}$	$5.61 \cdot 10^{6}$	$5.48 \cdot 10^{6}$		mm^2
Vertical N.A.	9384	9455	9164		mm
2nd Moment of Area	$3.65 \cdot 10^{14}$	$3.96 \cdot 10^{14}$	$3.76 \cdot 10^{14}$	$2.40 \cdot 10^{14}$	mm^4
Elastic Section Modulus Bottom	$5.17 \cdot 10^{10}$	$5.57 \cdot 10^{10}$	$5.46 \cdot 10^{10}$	$3.43 \cdot 10^{10}$	mm^3
Elastic Section Modulus Deck	$3.93 \cdot 10^{10}$	$4.25 \cdot 10^{10}$	$3.93 \cdot 10^{10}$	$3.43 \cdot 10^{10}$	mm^3
Plastic Section Modulus	$4.98 \cdot 10^{10}$	$5.32 \cdot 10^{10}$	$5.04 \cdot 10^{10}$		mm^3
Elastic Bending Moment	9626	10421	9604		MNm
Plastic Bending Moment	12211	13036	12359		MNm
Shape Factor	1.27	1.25	1.29		

Table 2.2 Elastic/Plastic results

2.4.2 Ultimate Bending Moment

The sagging moment-curvature relationship for Triton 2 is plotted in Figure 2.8, and the state of the cross section at significant curvatures is shown in sequential drawings in appendix C. The moment-curvature (M-C) graph follows a linear relationship up to a curvature of $-60 \cdot 10^{-9}$ mm^{-1}, where the slope decreases slightly. The first failure occurs in the stringer stiffeners at a curvature of $-90 \cdot 10^{-9}$ mm^{-1}, as the curvature increases to $-100 \cdot 10^{-9}$ mm^{-1} the deck plates near the centre line collapses. Element 112 in the longitudinal bulkhead and element 144 in the centre longitudinal bulkhead also fails at this stage. These, somewhat premature plate failures could be avoided by using thicker plating in the longitudinal bulkheads.

The ultimate bending moment of 7887 MNm is reached at a curvature of $-102 \cdot 10^{-9}$ mm^{-1}, a further increase in curvature dramatically reduces the stiffness of the cross section. The plate failure in the deck propagates outwards from the centre line towards the deck edge, at the same time as members of the side shell and longitudinal bulkhead fails. When a curvature of $-108 \cdot 10^{-9}$ mm^{-1} is reached all the deck elements have failed, and the moment decreases slowly with increasing curvature.

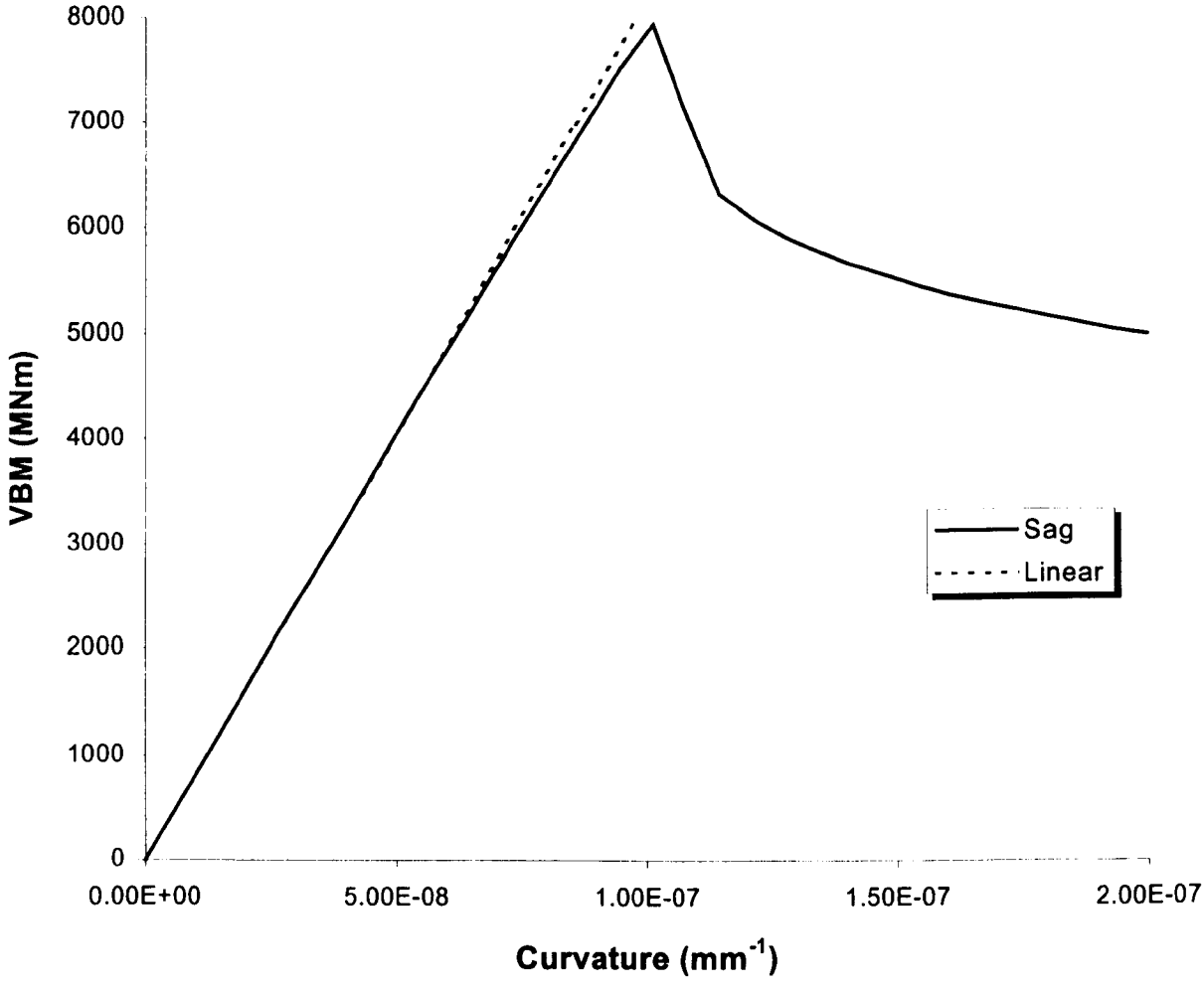

Figure 2.8 Sagging Moment-Curvature Relationship for Triton 2

A plot of the hogging moment-curvature relationship for Triton 2 indicates an onset of first buckling at a curvature of around $60 \cdot 10^{-9}$ mm^{-1}. At this point the moment-curvature relationship becomes non-linear and falls below the linear values. It is the elements in the longitudinal girders that fail due to stiffener failure. When the curvature is increased up to $120 \cdot 10^{-9}$ mm^{-1}, the first element in the centre longitudinal bulkhead fails and the slope of the M-C decreases even more.

At a curvature of $125 \cdot 10^{-9}$ mm^{-1} the ultimate bending moment is reached, and the dM/dC becomes zero. This is the curvature where the first elements in the bottom experience plate failure. The plate buckling starts at element 19, close to the longitudinal wing girder, and propagates all the way to element 6 where the plate thickness changes from 19.5 to 21 mm. From this point, the stiffness of the cross-section decreases rapidly with an increase in curvature. The rest of the stiffened plate elements in the bottom fail when the curvature reaches $127.5 \cdot 10^{-9}$ mm^{-1}. The members in the inner bottom fail at a curvature of

approximately $135 \cdot 10^{-9}$ mm^{-1}, this is represented by a dramatic drop in the M-C. From this point onwards the moment decreases slowly, at a steady rate, as the plate failure propagates up trough the side shells, the inner side shells and the longitudinal centre bulkhead.

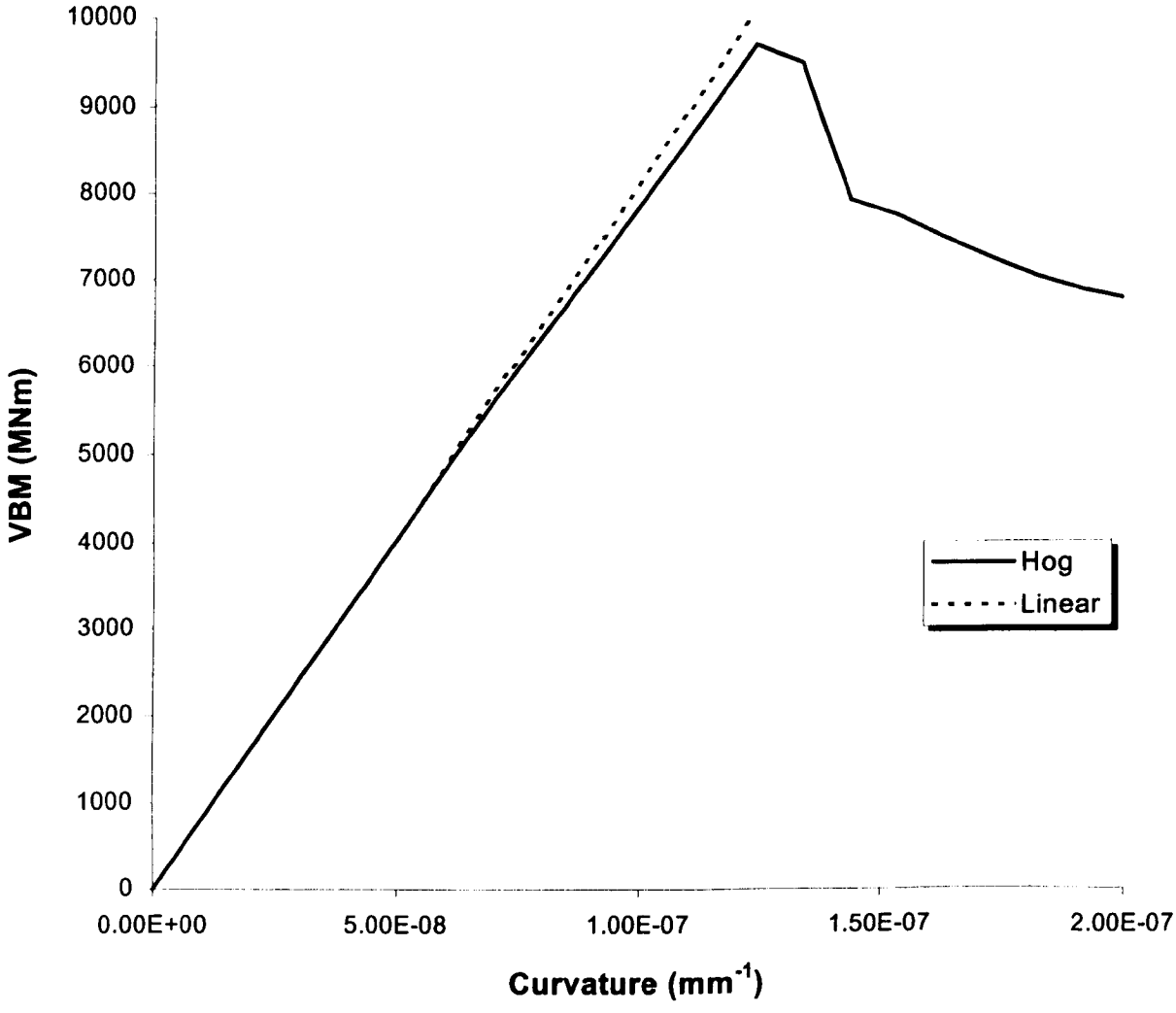

Figure 2.9 Hogging Moment-Curvature Relationship for Triton 2

The moment-curvature relationships in sagging and hogging were obtained for each of the three different midship sections. A summary of the results is shown in Table 2.3. The full output from LRPASS is shown in appendix B.

	Triton 1	Triton 2	Triton 3	Units
UBM_{Sag}	6693	7887	6885	MNm
UBM_{Hog}	8329	9701	9603	MNm
UBM_{Sag}/ UBM_{Hog}	0.80	0.81	0.72	

Table 2.3 Ultimate Bending Moments

A well-designed cross-section has an Ultimate Bending Moment close its elastic (M_e) and plastic (M_p) bending moment capacities. If the UBM is considerably lower than these values, the design does not take full advantage of the material in the cross section. As a part of the design-process, the scantlings should be optimised so that the final UBM is close to the elastic bending capacity of that cross-section. The comparison in Table 2.4 shows that the values for the UBM in hogging condition are reasonably close to M_e and M_p, especially for Triton 2 and 3. However, the UBM values for the sagging condition fall well below the elastic bending moment capacities.

	Triton 1	Triton 2	Triton 3
UBM_{Sag} / M_e	0.695	0.757	0.717
UBM_{Hog} / M_e	0.865	0.931	0.9998
UBM_{Sag} / M_p	0.548	0.605	0.557
UBM_{Hog} / M_p	0.682	0.744	0.777

Table 2.4 UBM Compared with Elastic and Plastic Bending Moment Capacities

2.4.3 Effect of Lateral Pressure on UBM

The effect of lateral sea and cargo pressures on the buckling strength of stiffened plate panels was discussed in section 2.2.1. It was shown that the collapse strength of the beam column element was reduced when a lateral pressure was applied. These pressures act predominantly on members below the neutral axis, thus the strength of the members in the double bottom and lower parts of the side shell are reduced. As the buckling strength of these elements significantly influences the ultimate strength in hogging, the hogging UBM will be reduced when lateral pressures are included in the model.

In sagging, the buckling characteristics of the deck elements will be the governing factor influencing the UBM. No lateral pressures are applied to the deck plating, so the buckling strength of the deck structure will remain unchanged. Figure 2.10 shows how the lateral pressures affect the ultimate bending moment of the whole cross section. The ultimate hogging bending moment was reduced from 9920 to 9150, approximately 8%, whereas the sagging UBM was virtually unchanged.

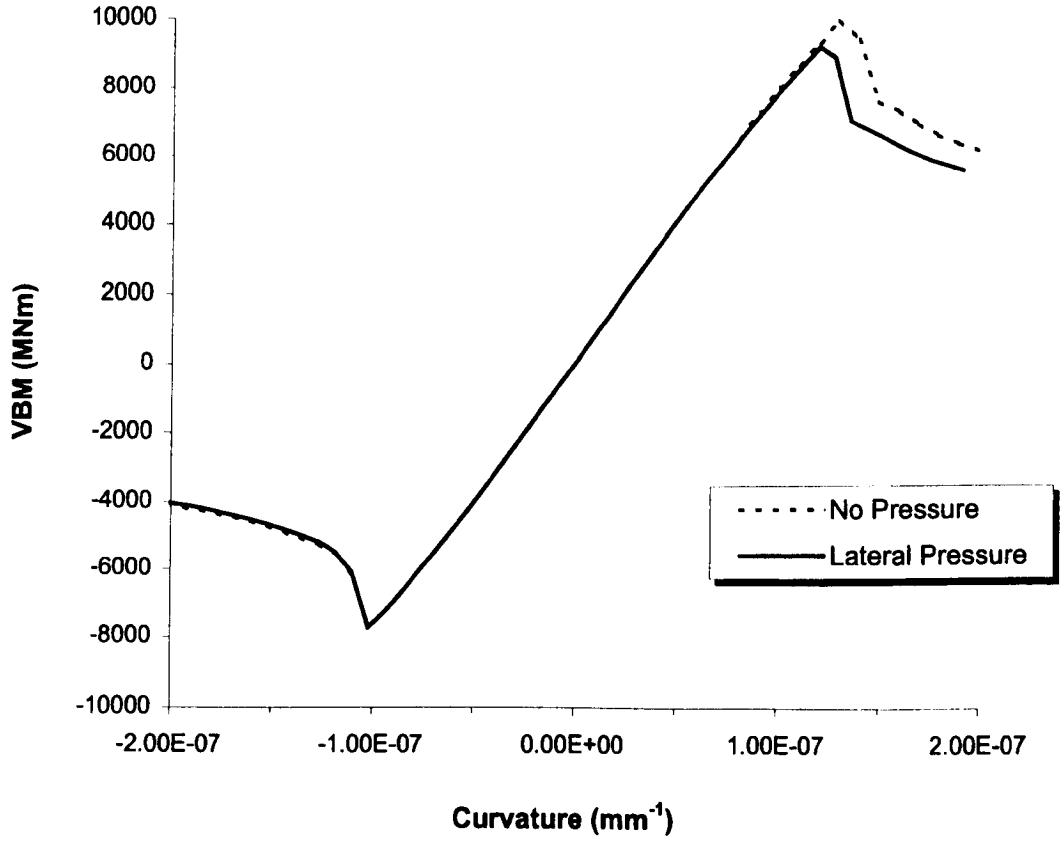

Figure 2.10 Effect of Lateral Pressure in Strength Model

2.4.4 Effect of Hard Corners on UBM

The effect of hard corners on the ultimate bending moment could be explained using the same reasoning as for the effect of lateral pressure. The deck and bottom elements buckling capacities are dominating the sagging and hogging UBMs respectively. The bottom structure contains four elements (1, 20, 25 and 31) that are treated as hard corners, thus the inclusion of these in the model will increase the calculated hogging UBM. The calculated increase in ultimate bending moment for Triton 2 was from 9150 to 9700, or approximately 6%.

As for the deck structure, it only contains three rather small elements (72, 149 and 150) that may be taken as hard corners. From Figure 2.11 it can be seen that the UBM in sagging is not significantly increased. However, the behaviour beyond the UBM is somewhat different as no load shedding takes place in the hard corner elements.

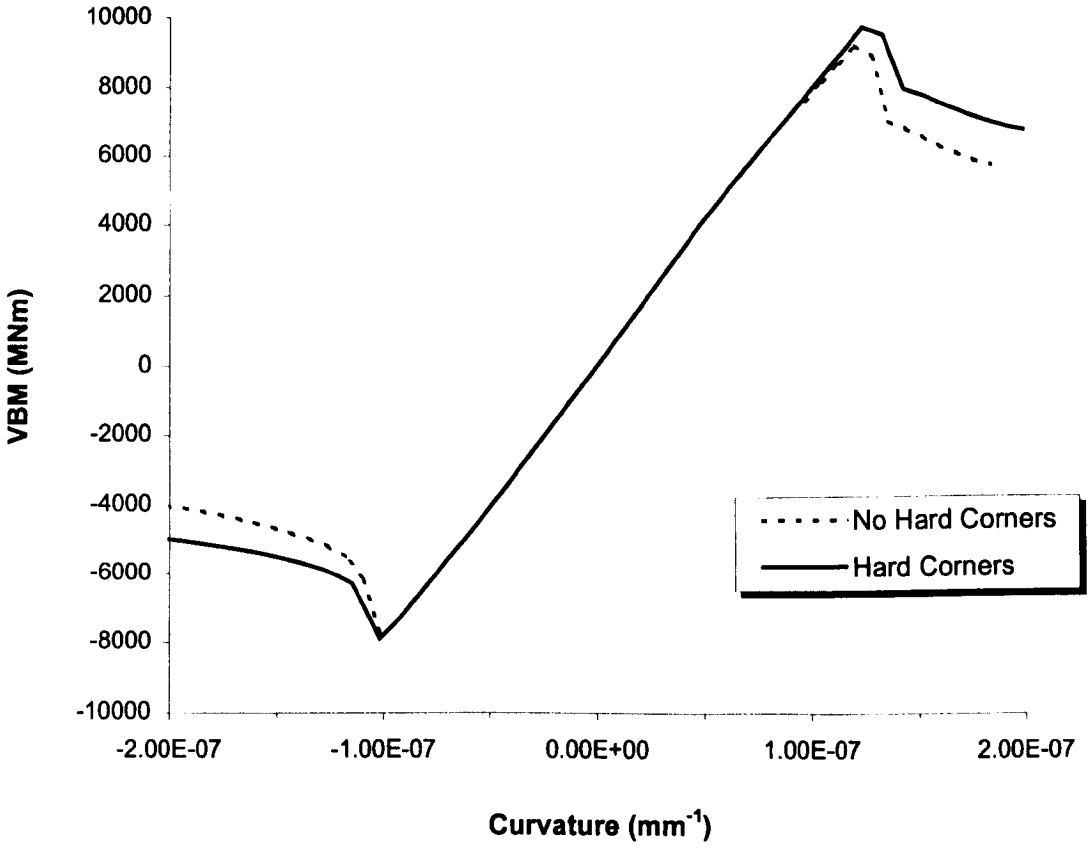

Figure 2.11 Effect of Hard Corners in Strength Model

2.5 Conclusions

Three different mid-ship sections for Triton were analysed. A traditional elastic analysis showed that all three designs satisfied the IACS rule requirements for section modulus and 2nd moment of area. The next step was to perform a ultimate bending moment analysis, which showed that the ultimate bending moment capacity was increased by 18% and 16 % in sagging and hogging respectively from Triton 1 to Triton 2. This increase in ultimate bending moment was achieved by strengthening the bottom and deck structure of the vessel.

A calculation based on changes in cross-sectional areas estimated the weight of the added material to be roughly 4% of the hull weight, equalling 800 tonnes. For Triton 3 an increase of 15% in the hogging UBM is achieved by increasing the plate thickness in the bottom plates by 3 mm. The sagging capacity was just marginally increased (3%). The weight of the added material from Triton 1 to Triton 3 is around 2% of the hull weight, or approximately 400 tonnes.

The ultimate bending moment in sagging (UBM_{Sag}) for Triton 2 is 7887 MNm, which is just 76% of the elastic bending moment and 61% of the plastic bending moment. These rather

low ratios suggest that element failure occurs prematurely and that a more effective design would take advantage of more of the material in the cross-section. An improved design could be achieved by optimising the stiffener spacing and properties as well as plate thickness. For Triton1 and Triton 3 the ratios between UBM_{Sag} and elastic and plastic bending moments are even lower.

The ultimate bending moment in hogging (UBM_{Hog}) for Triton 2 is 9701 MNm, or 93% of the elastic bending moment capacity, which is better than the ratio of 87% found for Triton 1. For Triton 3 a value of almost 100% was achieved, implying a very effective design of the cross-section.

The analysis showed that plate induced failure was the dominating failure mode in all designs and conditions. This, combined with the results from the elastic analysis, indicate that the stiffener spacing in the deck is too large to give an effective design from a structural point of view. The stiffeners have adequate strength, the plates are sufficiently thick, but the elements are too wide, resulting in plate failure. Optimising the cross-section to have acceptable properties in both sagging and hogging is a time consuming iterative process. The goal of the structural optimisation will be to fulfil predefined requirements based on some knowledge of the loads to which the hull girder will be exposed. In addition to the structural strength, there will be other parameters influencing the choice of cross-sectional properties in practise. These factors could typically be material cost, total labour content and construction methods, and it may be considered to increase the steelweight of the ship to minimise production cost.

The inclusion of lateral sea and cargo pressures in the buckling strength model was shown to reduce the hogging UBM by approximately 8%, no reduction was found on UBM_{Sag}. The use of hard corners to represent longitudinal girders and corners increased UBM_{Hog} by approximately 6%. It is worth noting that the effects of lateral pressures and hard corners almost cancels each other out, so that a simplified model, neglecting both effects, would give a UBM_{Hog} only 2.35% higher than the more accurate model.

3 Loads and Load Combination

3.1 Introduction

For adequate and safe ship design, appropriate values of design loads have to be established. The hull girder loads may be divided into stillwater loads and wave loads. The two types of loading are of a very different nature. The stillwater loads relate to cargo loading and other controllable factors, it is therefore relatively easy to predict their characteristic values and their distribution parameters. The major uncertainty in the prediction of stillwater loads is associated with deviations from the loading manual. These deviations are difficult to estimate, as they are dependent on factors as; the type of vessel, the quality of the crew and whether the vessel has a loading instrument or not.

The procedure of evaluating the wave loads is far more complex than calculation of stillwater loads. Wave loads are probabilistic and it is a complicated task to calculate the wave bending moments on a ship structure in a sea state. The wave loads are usually divided into low and high frequency wave loads. The low frequency wave loads consists of vertical, horizontal and torsional loads, while the high frequency loads are due to slamming and springing. Procedures of extrapolation of these loads to their extreme lifetime values are reviewed and models for their combinations discussed in this report.

In addition to the hull girder loads, local loads may be important in the design of local structures. These local loads consist of external and internal loads. The external loads are due to stillwater loads (static head), low-frequency wave loads (dynamic pressure due to waves) and high frequency local slamming loads. The internal loads can result from weight of cargo, inertia forces of cargo associated with ship motions and accelerations, and from sloshing of liquid cargo. The loads due to external and internal hydrostatic pressure are accounted for during calculation of the Ultimate Bending Moment of the hull girder. The other extreme local loads have not been included in the analysis.

3.2 Rule Requirements

Ship structural safety is normally taken into account by the Rules of Classification Societies, and IACS (International Association of Classification Societies) plays an important role in achieving common standards. The rules determine the extreme wave loads (global and local) which are to be considered as minimum requirements (safety standards). These requirements

are generally based on extensive calculations and tests and are verified by means of the statistics of damages gathered during the years of supervision. They therefore represent the outcome of an experience derived from more than a century of classification activity.
The rule requirements for the midship section modulus and midship section moment of inertia about the transverse axis are;

$$Z_0 = \frac{C_w}{f_1} L^2 B(C_B + 0.7) \text{ cm}^3 \quad \text{and} \quad I = 3C_w L^3 B(C_b + 0.7) \text{ cm}^4 \quad \text{Eq. 3.1-2}$$

where Z_0 and I are the section modulus and section moment of inertia receptively, f_1 material factor depending on material strength group and C_W is the wave load coefficient given by;

$$C_w = 10.75\text{-}((300\text{-}L)/100)^{1.5} \qquad for\ 90 \le L \le 300 \qquad \text{Eq. 3. 3}$$

$$C_w = 10.75 \qquad for\ 300 < L < 350$$

$$C_w = 10.75\text{-}((L\text{-}350)/150)^{1.5} \qquad for\ 350 \le L \le 500$$

IACS gives the following recommendations for the minimum design midship still-water bending moments, Msw:

In hog: $M_{sw} = C_w L^2 B(122.5\text{-}15C_b)$ Eq. 3.4

In sag: $M_{sw} = 65C_w L^2 B(C_b + 0.7)$ Eq. 3.5

For the Triton FPSO, these values would be approximately 2577 MNm and 2238 MNm for hogging and sagging respectively. The rules also state that larger values based on load conditions are to be applied when relevant. The minimum design midship wave-induced bending moments are as follows:

In hog: $M_w = 190\ C_w L^2 B C_b$ Nm Eq. 3.6

In sag: $M_w = 110\ C_w L^2 B(C_b + 0.7)$ Nm Eq. 3.7

The values obtained for Triton are approximately 3447 MNm in the hogging condition and 3787 MNm in sagging. The calculations of the rule values for minimum design loads and cross-sectional properties are shown in Appendix D.

3.3 Stillwater Bending Moment

A ship floating in still water is subjected to vertical forces of weight and buoyancy which, although equal as a whole, are distributed differently along the length. These vertical forces cause shearing forces and bending moments (SWBM) at each section and the ship behaves like a girder under continuos uneven loading. As can be seen from Figure 3.1, a diagram of weight will have a series of discontinuities caused by concentrated loads such as bulkheads, machinery, different densities of cargo in each hold, etc. The buoyancy, which is dependent upon the shape of each section (Figure 3.2), will give an upward force that at certain sections will be less than the weight while at others it will exceed the weight.

The variation of the still-water loads largely depends on the amount of cargo and its distribution along the ship. Traditionally, a load manual is used to ensure that the specified maximum value is not exceeded. The more frequent application of on-board computerised load distribution equipment gives masters as much freedom to load the ship as they want, as long as the maximum loads are within the limits specified by Classification Societies. The consequence is the loading manual is less likely to be strictly followed with a resulting larger variability of load conditions. This fact also produces a larger probability of exceeding the maximum operational load due to human decisions involved in the choice of load conditions. However, the reliability analysis only considers the small variations in loading conditions associated with the daily operation of the vessel, gross errors are not accounted for.

Mano et al (1977) showed that the still-water midship bending moment in container ships could be adequately modelled by a normal distribution. Several subsequent studies have shown that the normal distribution is a good description for other ocean going vessels as well. For offshore production ships however, due to completely different loading procedures, and in particular to the frequent changes in the load distribution on board, the statistical model for still-water load substantially differs from that of conventional ships. Wang *et al* (1996) reported the outcomes of 453 actual still-water load conditions, recorded during the first two operational years of an offshore production ship. It was found that the cumulative distribution function of the individual sagging Still-Water Bending Moment is well fitted by a Rayleigh distribution, while the hogging SWBM follows an exponential distribution.

Rayleigh and exponential distributions are more complicated in mathematical terms than normal distributions. Thus as a slightly conservative approximation in order to simplify the

extreme model, the SWBM was assumed to follow a normal distribution in both hog and sag. It is believed that the effect of this simplification will be insignificant.

3.3.1 Characteristic Values of Stillwater Loads

Prediction of the still-water load effects raises no difficulty once the loading procedures of the vessel are specified. The primary hull structure is modelled as a beam and the load effects are determined by integration over the length of the ship. This can readily be done in a number of computer packages. In determining the design value of the still-water load-effects, several representative load conditions must be considered. The reference value adopted for deterministic design is the maximum that occurs in these conditions or the minimum design requirement of classification societies' Rules, whichever is greater. In a reliability-based analysis, the SWBM for each condition is taken as the mean or characteristic value, and an uncertainty (e.g. σ or COV) is assigned.

The SWBM for each loading condition were calculated using *Autohydro 4.5.0*, which is a part of the *Autoship* package. SWBM calculation is just one of many modules in *Autohydro*, other features include calculation of hydrostatics, hull data, cross curves etc. The main input to the program, the weight distribution and the hull geometry, are shown in Appendix E. The hull geometry (Figure 3.2) was modelled in *Model Maker*, and then exported to *Autohydro* where weight distributions (Figure 3.1) were added to the model.

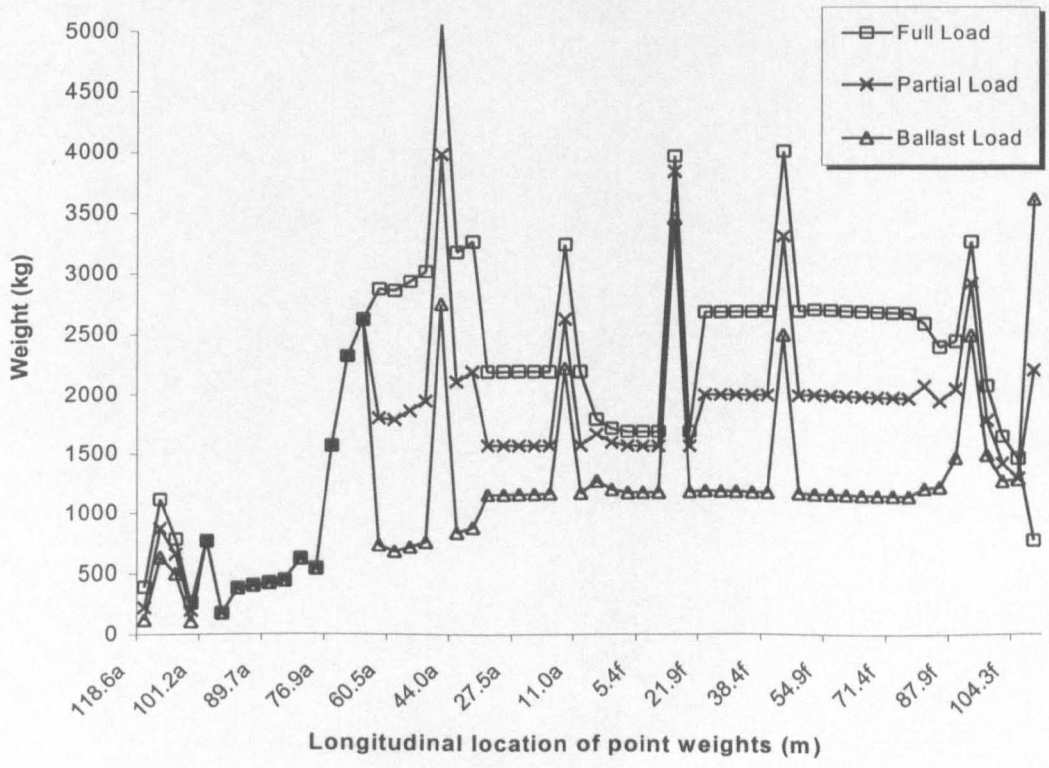

Figure 3.1 Weight Distributions, Triton

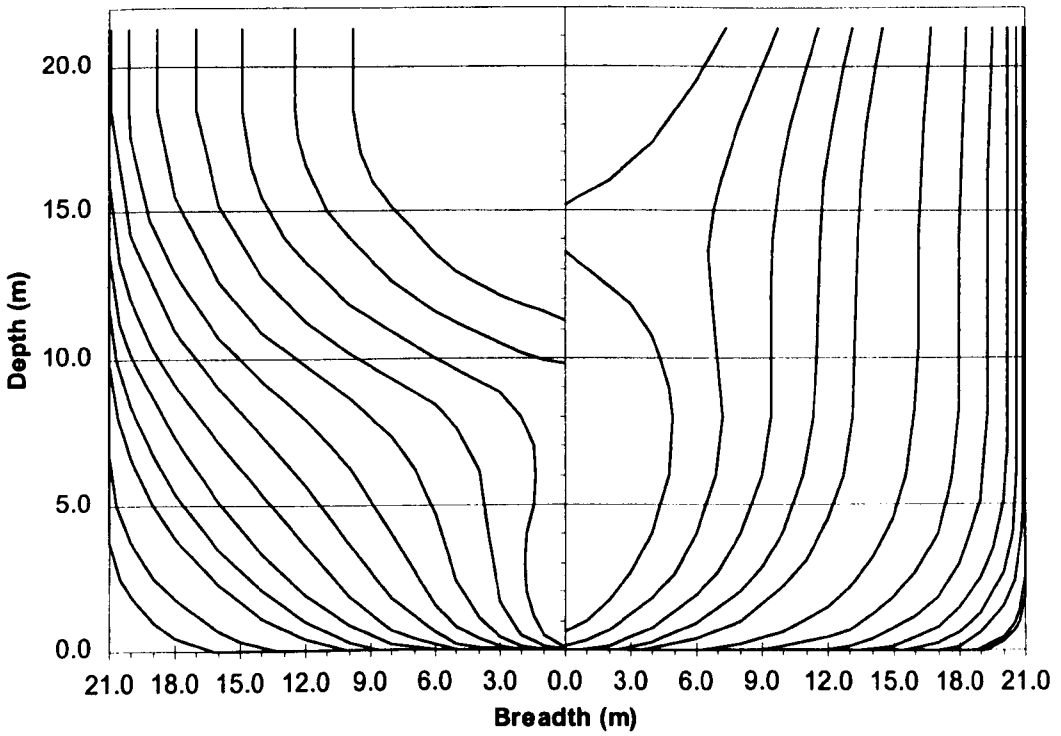

Figure 3.2 Cross Sectional Offsets

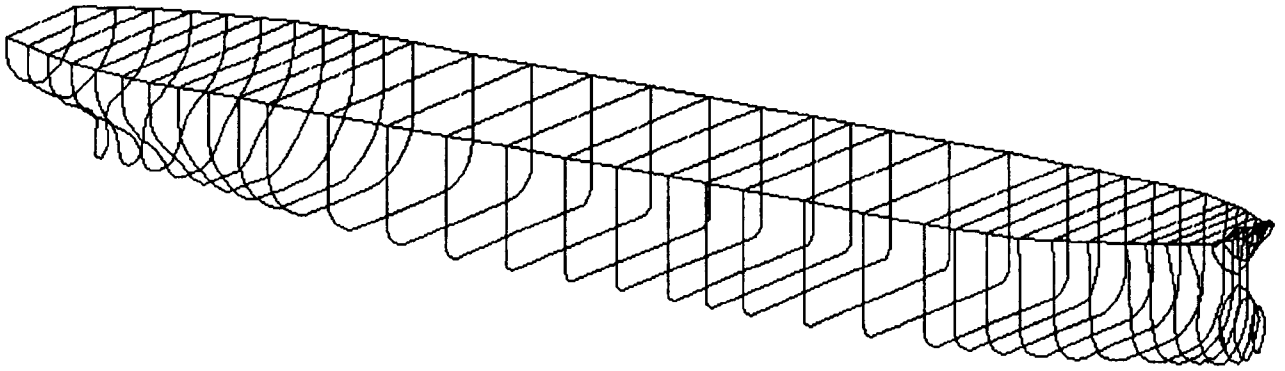

Figure 3.3 Hull Geometry Model of Triton

As soon as the vessel is properly modelled, it is straightforward to calculate the longitudinal loads on the hull girder. The characteristic values of the SWBM were taken as the highest value in each loading condition. The output from *Autohydro*, plots of the SWBM and shear force distributions, the section area curves and curves of form may be found in Appendix F.

SWBM	Full Load	Partial Load	Ballast Load
[Tonne-m]	57517	147971	234425
[MNm]	564	1452	2300

Table 3.1 Characteristic Values of SWBM

3.3.2 Uncertainties in Still Water Loading

It is reasonable to expect the uncertainty on the mean SWBM for a loading condition to be quite high. The variation of the extreme SWBM will be somewhat smaller. While not strictly a "modelling error", one aspect of variability related to still water loads is that they can, with a given probability distribution, exceed the design value. This probability distribution can be expected to depend on the type of vessel, the quality of the crew, constraints on vessel operation, and whether the vessel has a loading instrument or not.

Little data exists on this aspect of still water load variability, because of the admission of such occurrences is not often desirable, making the collection of such data difficult. Wang et al. (1996) indicate that the maximum allowed value might be exceeded by 5 % within the first two years of operation. Thus, a COV of 5% on the extreme SWBM, M_{se}, might be reasonable to apply in the reliability calculations. The relationship between mean and extreme values suggests that a COV of 15% could be used on the mean SWBM.

The mean SWBM in ballast condition for Triton condition is 2300 MNm and the extreme value is close to 3200 MNm, 23 % higher than the rule minimum value of 2600 MNm. As an extreme weather countermeasure, the ship's master will probably try to avoid being in ballast condition in heavy weather for several reasons. This will reduce the probability of the extreme VWBM and extreme SWBM occurring at the same time. A truncated normal density could be used to represent this effect, and to account for differing loading patterns during the long term. As the extents of these countermeasures are not known, the effect of these has not been included in the analysis. Consequently, the reliability results for the ballast load condition will tend to be somewhat conservative.

3.3.3 Operation Profile

No information on the loading procedures for the FPSO was available. Thus, a simplified operation profile based on the production and storage capacities was estimated, and a rectangular pulse process was fitted. The storage capacity of the vessel is 630,000 BBLS, which equals 6 days production. It is supposed that offloading will take place before the vessel is completely full, consequently load cycles of 5 days were assumed. The number of occurrences of each load condition per year is given by;

$$n_{sw} = \frac{T_{sw}}{\tau_{sw}} \qquad \text{Eq.3.8}$$

where τ_{sw} is the duration and T_{sw} is the total time per year spent in each load condition.

Loading Condition	T_{sw}	τ_{sw}	n_{sw}
Full Load	73 days	24 hours	73
Partial Load	219 days	72 hours	73
Ballast Load	73 days	24 hours	73

Table 3. 2 Operation Profile

The extreme model (ref. Chapter 3.3.4) is only dependent on the number of occurrences, not on the total time spent in that condition. One interpretation of this could be that the uncertainty is associated with changes in the loading, and not with the duration of the condition. This is a suitable assumption for merchant ships, where the same loading condition is maintained over the whole duration of the voyage. The assumption might not hold for a FPSO, which experience continually changing loading each day, where higher uncertainties would be expected. On the other hand, FPSOs are generally fitted with better loading monitoring instruments than traditional tankers, resulting in better load control, thus reducing the uncertainties on SWBM. These points were considered when assigning uncertainties to the SWBM in the extreme model. It should be noted that the number of occurrences of a particular load condition in a year, n_{sw} for Triton is the same for all three conditions. This might not be the case for other operation profiles, where some loading condition might occur more often than others.

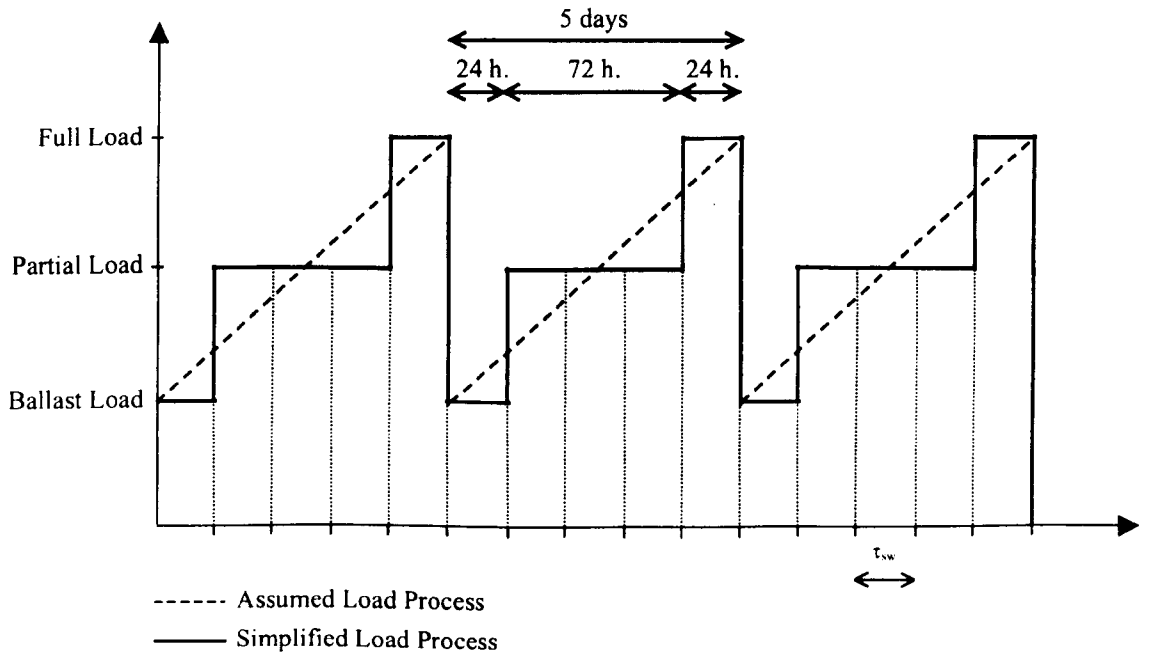

Figure 3.4 Assumed Operation Profile

3.3.4 Extreme Model

The SWBM was assumed to follow a normal distribution in both hog and sag. This slightly conservative approximation was applied in order to simplify the extreme model. When the values μ_{sw} and σ_{sw} of the normal distribution are known the extreme values may be approximated as a Gumbel law. The Gumbel parameters were estimated by:

$$u_{sw} = F_{sw}^{-1}(1 - \frac{1}{n_{sw}}) \quad \text{Eq. 3.9}$$

$$\alpha_{sw} = \left(\frac{1 - F_{sw}}{f_{sw}} \right) \quad \text{Eq. 3.10}$$

where n_{sw} is the number of occurrences of a particular load condition in the reference period, F_{sw}^{-1} is the inverse cumulative probability distribution, F_{sw} is the cumulative probability distribution and f_{sw} is the probability density function. The mean and standard deviation of the Gumbel distribution could then be calculated as;

$$\mu_{se} = u_{sw} + \frac{\gamma}{\alpha_{sw}} \quad \text{Eq. 3.11}$$

$$\sigma_{se} = \frac{\pi}{\alpha_{sw}\sqrt{6}} \quad \text{Eq. 3.12}$$

Figure 3.5 and Figure 3.6 show the Gumbel probability density function f_{se} and distribution functions F_{se} respectively for the SWBM of each of the three loading conditions. F_{se} and f_{se} are given by:

$$f_{se}(x) = \alpha_{sw} exp(-\alpha_{sw}(M_{se} - u_{sw}) - exp(-\alpha_{sw}(M_{se} - u_{sw}))) \quad \text{Eq. 3.13}$$

$$F_{se}(x) = exp(-exp(-\alpha_{sw}(M_{se} - u_{sw}))) \quad \text{Eq. 3.14}$$

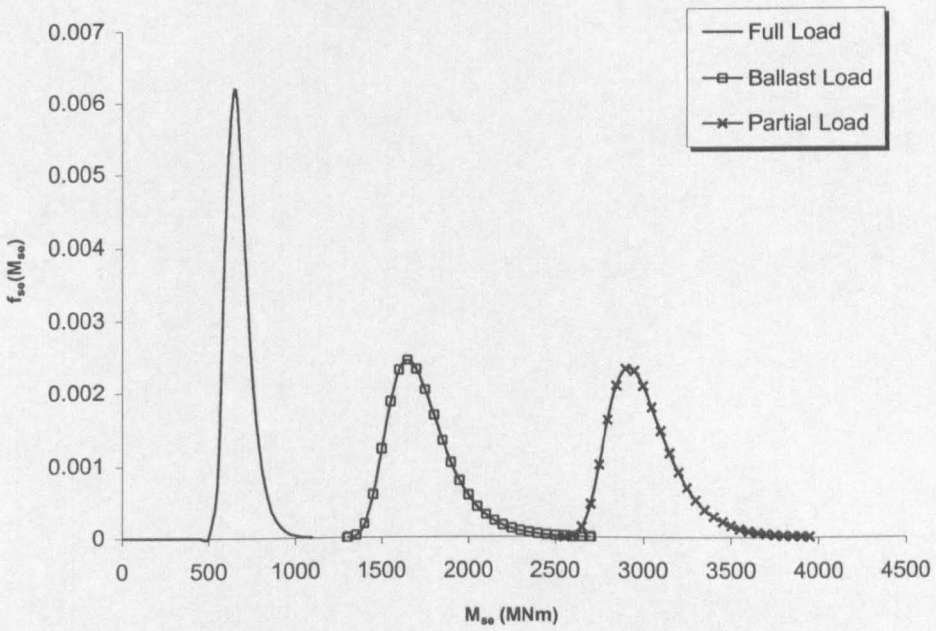

Figure 3.5 Extreme SWBM Probability Density Functions

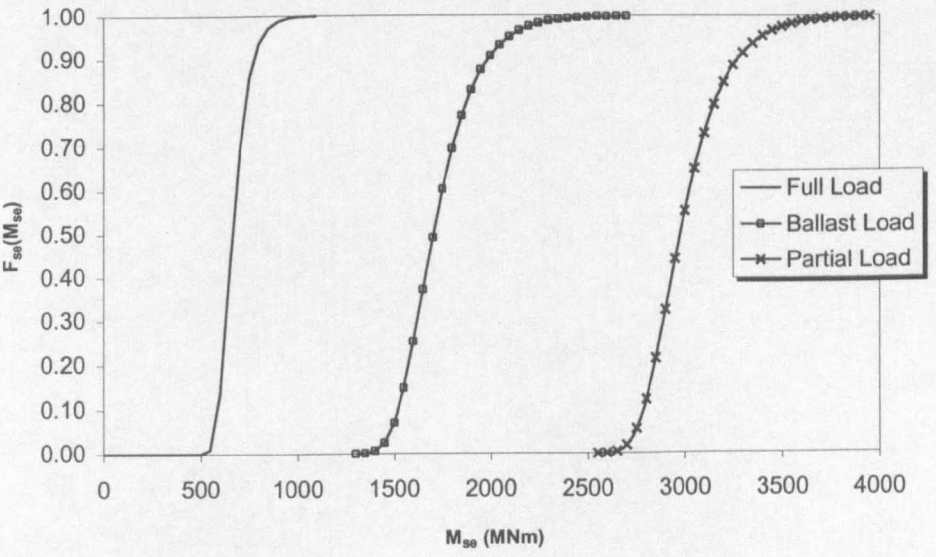

Figure 3.6 Extreme SWBM Probability Distribution Functions

The extreme SWBM calculations were carried out as a part of the load combination factor calculations shown in Appendix H. Table 3.3 gives a summary of the extreme values of SWBM obtained for Triton. The differences between sagging and hogging extreme values are quite significant, keeping in mind the sign convention, positive values for hogging and negative values for sagging. In hog the wave load and SWBM will have the same sign, both will give hogging moments, whereas in sag there will be a hogging SWBM and a sagging

VWBM. This is a very significant factor when considering the reliability of the vessel in hog and sag, as shown in the reliability analysis.

	Load Condition	μ_{sw} (MNm)	σ_{sw} (MNm)	μ_{se} (MNm)	σ_{se} (MNm)
Hog	Full Load	564	84.6	770	42.4
	Partial Load	1452	218	1982	109.3
	Ballast Load	2300	345	3139	173.1
Sag	Full Load	564	85	358	42.4
	Partial Load	1452	218	922	109.3
	Ballast Load	2300	345	1461	173.1

Table 3.3 Summary of Stillwater Results

3.4 Quasi Static Wave Bending

When a ship encounter irregular waves or swells with wave components in the range of 1/2 to 2 times the length of the ship (shorter at oblique angles), significant bending moments are developed. Estimating these wave-induced loads, particularly vertical bending moments (VWBM), is one of the most important and complex tasks in ship design. Four methods has been suggested by which wave-induced loads can be determined:

- approximate methods
- strain and/or pressure measurements for full scale ships
- laboratory measures of loads on models
- direct computation of wave induced fluid loads

Historically, approximate methods have been the most commonly used design tool for the prediction of a characteristic extreme load. One such method is the linear strip theory. Linear strip theory has shown good agreement with model and full-scale tests for small excitations and responses. For larger motions, however, both wave excitation and the ship responses are non-linear. These non-linearities have to be accounted for in the reliability analysis. The 2-D strip theory program *TRIBON Hydro* from Kockums Computer Systems was used to obtain transfer functions for the ship.

The wave load analysis was performed for three operating conditions; full load, partial load and ballast load. The ship was assumed moored and free to weathervane within ±30° from the predominant wave direction. The vertical mooring forces are small and have been considered to have an insignificant influence on the bending moment response.

The wave-induced response serves as input to a post-processing program, *LongTerm* that calculates the long-term distribution of the VWBM. Short-term responses in irregular waves are calculated using the principle of linear superposition and wave statistics. The short-term responses are combined with long-term wave statistics for a specific ocean area in order to determine the long-term distribution of VWBM. When the long-term distribution is known, the most probable extreme value in any reference period may be found. The reference period will typically be one year for the reliability analysis, where the target reliability is given as an annual reliability index.

3.4.1 Short Term

These wave-induced moments were first determined by model tests in waves (Lewis, 1957 and Vosser, Swaan and Rijken). Korvin-Kroukovsky developed the strip theory approach to the calculation of ship motions, which subsequently led to methods for calculating stress and bending moments in regular waves (Gerritsma and Beukelman (1967) and Salvesen, Tuck and Faltinsen (1970)).

St. Denis and Pierson (1953) accomplished the extension of regular wave results to predicting ship responses to short-crested irregular seas, on the assumption that both the irregular waves and the ship short-term responses are stationary stochastic processes. The response of a ship in irregular waves can be taken as the summation of the individual responses to the regular waves, which form the confused sea. By short-term is meant periods of typically a few hours during which sea conditions remain essentially constant. Hence under these assumptions, the bending moment response can be predicted for any ship for which transfer functions are available. The square of the transfer functions are called response amplitude operators (RAO), and they can be multiplied by the directional wave spectra to produce the directional response spectra,

Not a normal usage I think!

$$S_B(\omega,\mu) = S_\zeta(\omega,\mu)\cdot|\Phi(\omega,\mu)|^2 \qquad \text{Eq. 3.15}$$

where S_B is the bending moment spectrum given by the product of the non-linear transfer function Φ for a specified relative heading and significant wave height (RAO), and the

seaway spectrum S_ζ. When these components are integrated over wave direction a single response spectrum is obtained, whose area and shape define the bending moment response,

$$S_B(\omega) = \int S_B(\omega, \mu) d\mu \qquad \text{Eq. 3.16}$$

Short-term statistics can be derived from the response spectrum by taking the various moments of $S_B(\omega)$,

$$m_n = \int_0^\infty \omega^n \cdot S_B(\omega) d\omega \qquad \text{Eq. 3.17}$$

For the modelling of the response the variance given by;

$$m_0 = \int_0^\infty S_B(\omega) d\omega \qquad \text{Eq. 3.18}$$

has special interest.

The fundamental assumption in this approach is that the wave induced stresses are a linear function of suitably defined wave elevations and that the response spectrum may be estimated from computer packages or model test. A consequence of this assumption is that the wave-induced stresses must be a zero mean random Gaussian process. A further consequence is that the process must be statistically symmetrical. That is, the short-term statistics for the wave induced bending moment maxima in hogging are assumed the same as for sagging.

For a broad-banded response spectrum, the Rayleigh distribution is not immediately applicable, a more generalised distribution, involving the spectrum broadness parameter ε, is required. The statistics of a broad-banded response are different in many respects from those of a narrow banded spectrum having the same m_0 and m_2. However, Ochi (1973) showed that the most probable extreme value and the mean extreme value are still theoretically predicted by the narrow band formulae. Dalzell et al (1979) proved that for a slow, ocean going ship with high C_b (0.84), a Rayleigh distribution is an adequate statistical description of the short-term response amplitudes of bending moment.

3.4.2 Long-Term

The long-term cumulative approach was first developed by Bennet (1962), Band (1966), Lewis (1967) and Nordenstrøm (1971) as a means of analysing full-scale stress data obtained over periods of one to three years, and extrapolating to longer periods. The approach was then applied to calculating predicted long-term probabilities of exceedance for bending moment (or stress), for design use. It gave the designer an indication of the magnitude of the most probable wave bending moments in the ship's lifetime. Different writers have presented many variations of the basic long-term prediction procedure, including Compton (1968), Lewis et al. (1973), Nordenstrøm (1971), Söding (1974), Dalzell et al. (1979), Ochi (1981) and Guedes Soares (1993). They are all based on the idea of predicting short-term probabilities and then combining them based on assumed lifetime service profiles to obtain long-term probabilities. Some variations in the various methods:

- Choice of wave spectra.
- Sequence of dealing with various factors.
- Whether or not component and final distributions are fitted to specific mathematical formulations.

The first step in all methods is the selection of suitable sea spectra covering a wide range of both severity and spectral shape. It could be the ISSC version of the Pierson-Moskowitz spectrum given by Warnsick (1964):

$$S_\zeta = 0.11 H_s T_m \left(T_m \frac{\omega}{2\pi}\right)^{-5} exp\left(-0.44\left(T_m \frac{\omega}{2\pi}\right)^{-4}\right) \qquad \text{Eq. 3.19}$$

where T_m is the average period and H_s is the significant wave height.

The next step is to obtain RAOs for bending moment by either model test or calculation. A number of computer programs are available for calculating the RAOs at all headings, typically in increments of 10, 30 or 45°. Having the RAOs, the bending moment response spectra can be calculated by superposition for all of the selected wave spectra. The directional spectrum represents the distribution of wave energy both in frequency of the wave components and in direction θ. The analysis of directional buoy records has shown that

the spreading function is a function of both direction and frequency. If the one-dimensional or point spectrum is $S_\zeta(\omega)$, the directional spectrum is assumed to be,

$$S_\zeta(\omega,\mu) = S_\zeta(\omega)\cdot G(\omega,\mu) \qquad \text{Eq. 3.20}$$

The frequency spectrum gives the absolute value of wave energy while the directional spreading function, $G(\omega,\mu)$, represents the relative magnitude of the directional spreading of wave energy. The directional spreading function is a dimensionless quantity that is normalised as:

$$\int_{-\pi}^{\pi} G(\omega,\mu)d\mu = 1 \qquad \text{Eq. 3.21}$$

Pierson and St Denis used a directional spreading function that became somewhat generalised because of its simplicity. It is a frequency independent formulation given by:

$$G(\mu) = \frac{2}{\pi}\cos^2\mu \quad , \quad |\theta| \le \frac{\pi}{2} \qquad \text{Eq. 3.22}$$

$$G(\mu) = 0 \quad , \quad |\theta| \ge \frac{\pi}{2} \qquad \text{Eq. 3.23}$$

where μ is the angle between an angular wave component and the dominant wave direction. The long-term formulation may be expressed in many ways, but it is essentially a joint probability of x and m_0, expressed as:

$$q(x,m_0) = p(x|m_0)\cdot p(m_0) \qquad \text{Eq. 3.24}$$

where $p(x|m_0)$, the probability of x for a given m_0, is the conditional density function of x with respect to m_0, which is assumed to be Rayleigh distributed. Thus,

$$p(x|m_0) = (\frac{x}{m_0})e^{-\frac{x^2}{2m_0}} \quad \text{Eq. 3.25}$$

and $p(m_0)$ is the probability density of response variance in the considered sea states. It depends on several variables such as the wave climate represented by significant wave height (H_s) and wave period (T_z), the ship heading (θ), speed (v) and loading condition (c),

$$f_R(r)dr = f(h_s, t_z, \theta, v, c)dh_s dt_z \, d\theta \, dv \, dc \quad \text{Eq. 3.26}$$

The most important of these variables to consider is the ship heading relative to dominant wave direction. Ship speed, which has relatively small effect on wave bending moment, is not applicable for a FPSO. In a more general analysis, ship speed can be eliminated as a variable by assuming either the design speed or the highest practicable speed for the particular sea condition and the ship heading under consideration. The effect of amounts and distribution of cargo and weights, which in turn affect draft and trim, transverse stability, longitudinal radius of gyration, etc., can be a complicated problem. Usually, however, it can be simplified by assuming two or more representative conditions of loading, such as normal full load, partial load and ballast condition. Then completely independent short and long-term calculations can be carried out for all load conditions.

With the above simplifications, we are left with the following variables, to be considered in the probability calculation; H_s, T_z and θ. The variables are assumed mutually independent. The probabilities of different combinations of H_s and T_z are given in a wave scatter diagram. The probabilities of each ship heading θ have to be established for different cases, but in general, one can say that they are random.

The cumulative long-term distribution is defined by,

$$Q(x > x_i) = \int_{x_i}^{\infty}\int_{0}^{\infty} p(x|m_0) \cdot f_R(r)dr \quad \text{Eq. 3.27}$$

And since the cumulative Rayleigh distribution is,

$$\int_{x_i}^{\infty} p(x|m_0) = e^{-\frac{x^2}{2m_0}} \qquad \text{Eq. 3.28}$$

the probability of exceeding amplitude x for a given m_0 is given by:

$$Q(x > x_i) = \int_0^{\infty} e^{-\frac{x^2}{2m_0}} \cdot f_R(r)dr \qquad \text{Eq. 3.29}$$

Figure 3.7 shows a typical long-term distribution of Vertical Bending Moments. The Weibull parameters for scale (k) and shape (b), can then be estimated from this plot of VWBM against $Q(M_w>M_i)$ using the following expression:

$$Q(M_w > M_i) = exp\left(-\left(\frac{M_w}{k}\right)^b\right) \qquad \text{Eq. 3.30}$$

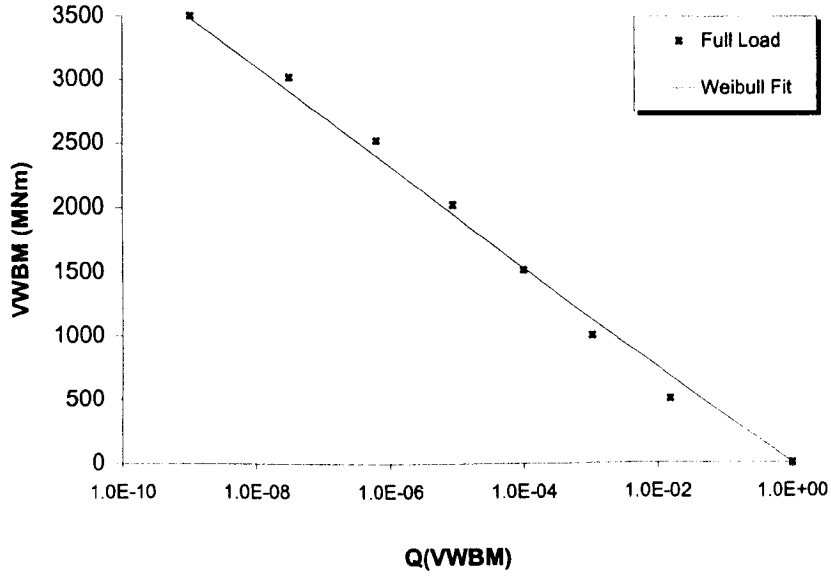

Figure 3.7 Long-term distribution of Vertical Bending Moments

3.4.3 Extreme Model

The rationally based design of ships requires the consideration of the largest value (extreme value) of the wave loading, especially the wave-induced bending moment, which is expected to occur within the ship's lifetime. The prediction of the *characteristic value,* which is associated with a certain probability of nonexceedance in that time, is of particular interest. The *characteristic value* is that magnitude of extreme value, which has an appropriate probability of exceedance.

For a very wide class of parent distributions, the distribution functions of the maximum (or minimum) values of large random samples taken from the parent distribution tend towards certain limiting distributions, as the sample becomes larger. These are called *asymptotic extreme-value distributions*. There are usually good theoretical grounds for expecting the variable to have a distribution function which is very close to one of the asymptotic extreme-value distributions. It has been shown that the extreme VWBM can be described by a Type I extreme-value distribution, generally called Gumbel distribution:

$$F_{Gumb}(M_{we}) = exp[-exp(-\alpha_w(M_{we} - u_w))] \qquad \text{Eq. 3.31}$$

Guedes Soares (1985) showed that the Gumbel parameters can be estimated from the initial Weibull fit using the following equations:

$$u_w = k \cdot [ln(n_w)]^{\frac{1}{b}} \qquad \text{Eq. 3.32}$$

$$\alpha_w = \frac{b}{k}[ln(n_w)]^{-\frac{1-b}{b}} \qquad \text{Eq. 3.33}$$

where n_w is the number of peaks counted in the period τ_{sw} given by:

$$n_w = \frac{\tau_{sw}}{\overline{T}_z} \qquad \text{Eq. 3.34}$$

$\overline{T}_z$ is the average mean zero crossing period of waves.

The parameters u_w and α_w are respectively measures of location and dispersion. u_w is the *mode* of the asymptotic extreme-value distribution. The mean and standard deviation of the Gumbel distribution are related to the u_w and α_w parameters as follows:

$$\mu_{we} = u_w + \frac{\gamma}{\alpha_w} \qquad \text{Eq. 3.35}$$

$$\sigma_{we} = \frac{\pi}{\alpha_w \sqrt{6}} \qquad \text{Eq. 3.36}$$

where γ is Euler's constant equal to 0.5772.

3.4.4 Results and Discussion

The transfer functions for the load conditions where calculated using *TRIBON Hydro*. The calculations are based on the hull geometry and the weight distributions shown in Appendix E. The response was calculated in increments of 10°, and the results served as input to the *LongTerm* program. The transfer functions for Triton in full load are shown in Figure 3.8, plots of transfer functions for all loading conditions are found in appendix G.

Due to the scantling variations, the three designs will have slightly different weight distributions. These differences have been deemed to have an insignificant effect on the wave bending response. Hence, the same transfer functions, and consequently the same wave loads, have been used for Triton 1, 2 and 3. ISSC '91 showed that the vertical mooring forces are small, and have insignificant influence on the bending moment response.

The largest amplitudes of response are found at 180° and 0°, which represent following seas and head seas respectively. The lowest response is found at 90°, when the vessel encounters the waves sideways. These results are both reasonable and in good agreement with other analyses. The magnitude of the maximum response is approximately 500 MNm.

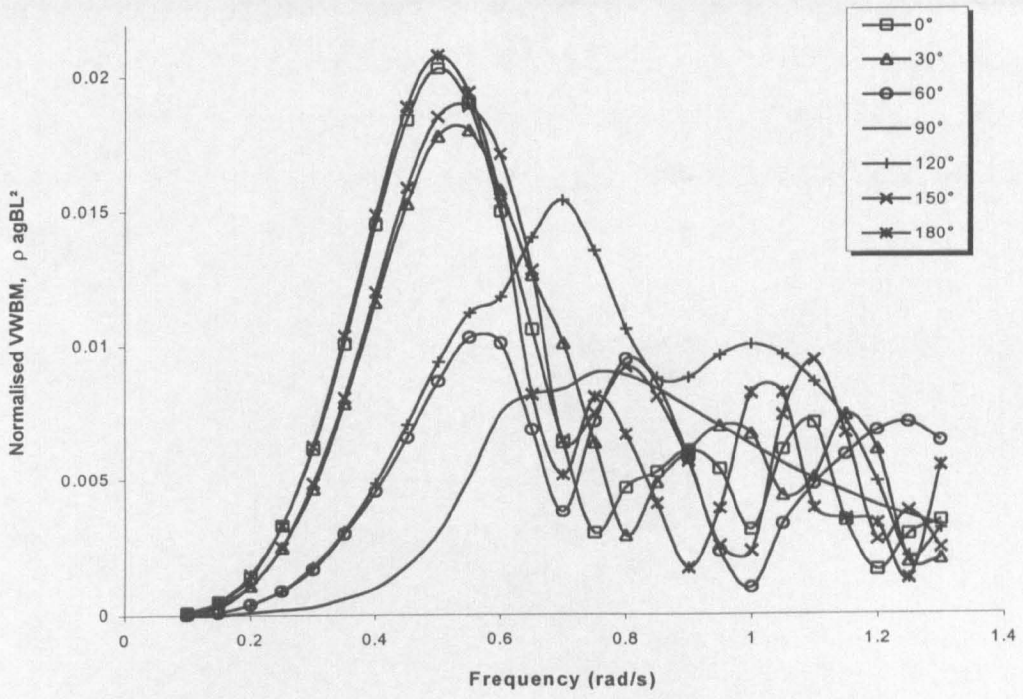

Figure 3.8 Transfer Functions for Triton in Full Load

The long-term prediction of wave induced bending moments takes into account the environment in which the vessel is operated. A FPSO is a stationary vessel, so a site-specific analysis has to be carried out. The Triton FPSO will be positioned close to the Gannet complex in the North Sea, hence Hogben's Global Wave Statistics Area 11 was assumed to represent the wave statistics for this location. Measurements of the directional spectrum at the site over many years (2-5 years) would have been the preferred basis for the wave statistical analysis. However, there are few sites where spectra are available for a five-year period, so the Global Wave Statistics are widely used for design purposes.

$H_s \backslash T_z$	1.75	3.5	6.5	8.5	10.5	12.5	14.5	16.5	18.5	20.5	21
0.25	6.33E-02	4.13E-02	2.35E-03	9.16E-04	5.23E-04	0.00E+00	0.00E+00	0.00E+00	0.00E+00	1.31E-04	6.54E-04
0.5	4.45E-03	1.13E-01	1.43E-02	3.40E-03	9.16E-04	1.31E-04	1.31E-04	1.31E-04	0.00E+00	0.00E+00	3.40E-03
1	4.97E-03	1.68E-01	6.17E-02	1.07E-02	2.62E-03	9.16E-04	3.92E-04	5.23E-04	3.92E-04	0.00E+00	1.57E-03
1.5	3.79E-03	7.42E-02	8.28E-02	2.14E-02	6.80E-03	1.57E-03	5.23E-04	5.23E-04	1.31E-04	1.31E-04	1.31E-04
2	2.88E-03	2.04E-02	5.18E-02	2.46E-02	6.41E-03	1.05E-03	3.92E-04	1.31E-04	0.00E+00	0.00E+00	3.92E-04
2.5	1.57E-03	9.68E-03	2.81E-02	2.18E-02	7.98E-03	1.83E-03	2.62E-04	0.00E+00	1.31E-04	0.00E+00	1.31E-04
3	5.23E-04	5.23E-03	1.74E-02	1.16E-02	7.45E-03	1.83E-03	2.62E-04	3.92E-04	1.31E-04	0.00E+00	0.00E+00
3.5	1.44E-03	1.70E-03	9.16E-03	1.36E-02	5.89E-03	2.62E-03	1.31E-04	1.31E-04	0.00E+00	0.00E+00	0.00E+00
4	5.23E-04	1.70E-03	4.71E-03	5.89E-03	3.92E-03	1.44E-03	3.92E-04	0.00E+00	1.31E-04	0.00E+00	0.00E+00
4.5	5.23E-04	7.85E-04	4.05E-03	4.71E-03	2.62E-03	1.57E-03	5.23E-04	3.92E-04	0.00E+00	1.31E-04	0.00E+00
5	1.31E-04	2.62E-04	3.92E-04	5.23E-04	7.85E-04	2.62E-04	0.00E+00	0.00E+00	0.00E+00	0.00E+00	0.00E+00
5.5	3.92E-04	1.31E-04	5.23E-04	1.05E-03	9.16E-04	0.00E+00	0.00E+00	0.00E+00	0.00E+00	0.00E+00	0.00E+00
6	2.62E-04	1.31E-04	5.23E-04	1.05E-03	5.23E-04	3.92E-04	1.31E-04	1.31E-04	0.00E+00	0.00E+00	0.00E+00
6.5	0.00E+00	0.00E+00	6.54E-04	6.54E-04	1.05E-03	3.92E-04	1.31E-04	0.00E+00	0.00E+00	0.00E+00	0.00E+00
7	1.31E-04	1.31E-04	0.00E+00	2.62E-04	1.31E-04	2.62E-04	0.00E+00	0.00E+00	0.00E+00	0.00E+00	0.00E+00
7.5	0.00E+00	0.00E+00	0.00E+00	2.62E-04	2.62E-04	1.31E-04	1.31E-04	0.00E+00	0.00E+00	0.00E+00	0.00E+00
8	1.31E-04	1.31E-04	2.62E-04	3.92E-04	0.00E+00	0.00E+00	0.00E+00	0.00E+00	0.00E+00	0.00E+00	0.00E+00
8.5	0.00E+00	0.00E+00	0.00E+00	0.00E+00	1.31E-04	0.00E+00	0.00E+00	1.31E-04	0.00E+00	0.00E+00	0.00E+00
9	0.00E+00	0.00E+00	0.00E+00	1.31E-04	1.31E-04	0.00E+00	0.00E+00	0.00E+00	0.00E+00	0.00E+00	0.00E+00
9.5	0.00E+00	0.00E+00	0.00E+00	2.62E-04	1.31E-04	0.00E+00	0.00E+00	0.00E+00	0.00E+00	0.00E+00	0.00E+00

Table 3.4 Scatter Diagram Area 11

Based on the theory outlined in chapters 3.4.1 and 3.4.2, the *LongTerm* program processes the transfer functions and scatter diagram to calculate the long-term distribution of the VWBM. Each load condition has to be considered separately, so three runs where required for Triton. The output from the program presents the probability of exceeding certain wave bending moments.

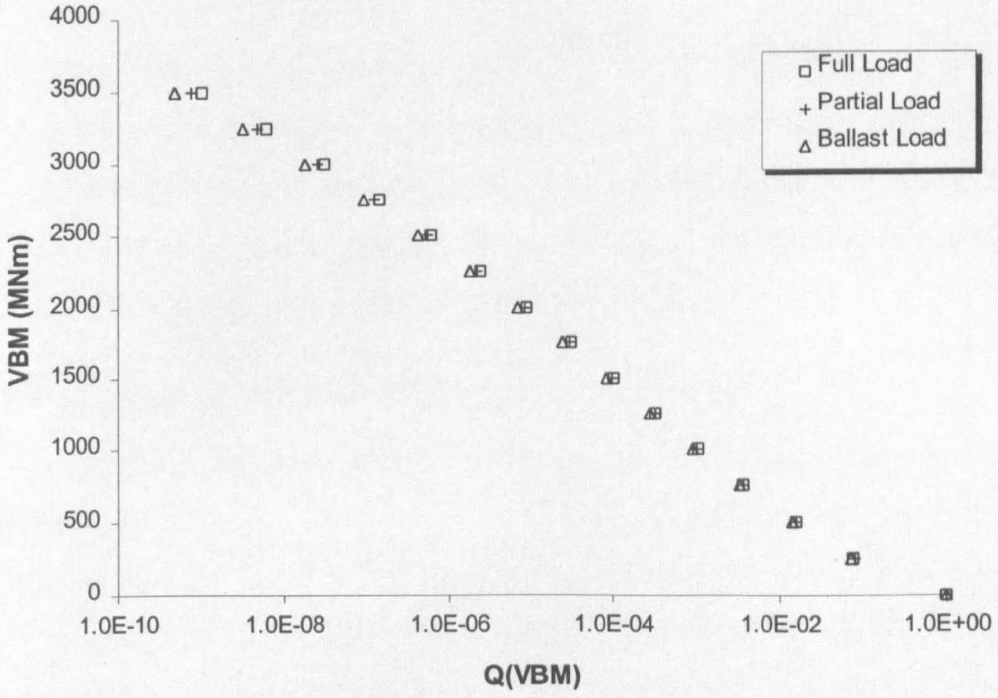

Figure 3.9 Long-Term Distribution of Vertical Wave Bending Moments

A Weibull distribution may be fitted to the long-term distribution, and by using the Weibull parameters k and b, the most probable extreme values for each load condition are found. The extreme value calculations and Weibull fits are performed as a part of the load combination procedure shown in Appendix H.

Load Condition	k (MNm)	b	μ_{we} (MNm)	σ_{we} (MNm)	10^{-8} (MNm) ~ 20 years	$10^{-8.7}$ (MNm) ~ 100 years
Full Load	124.9	0.898	2358	239.8	3211	3452
Partial Load	127.8	0.908	2538	236.8	3188	3421
Ballast Load	127.6	0.914	2289	228.9	3137	3360

Table 3.5 Summary of Wave Bending Moment Analysis

As this is a non-linear analysis, no distinction has been made between the hogging and sagging moments at this stage. The effect of non-linearity is incorporated by introducing a correction factor, χ_{nl}, in the reliability analysis (ref. Chapter *4.3.1 Modelling Uncertainties*).

The values obtained for each condition are very similar; the values extracted direct from the long-term distribution at 10^{-8} and $10^{-8.7}$ probability levels are virtually identical (1.5-2.5% difference). However, there is a 10% difference between the mean extreme values in partial load and ballast load, this difference advocate the use of three separate conditions in the analysis.

It is worth noting that the highest extremes value, μ_{we}, is found in the partial load condition, whereas the highest value at any probability level is found in full load. The explanation is that μ_{we} is the most probable extreme value in one year based on the operation profile. The FPSO spends more time in the partial load condition per year than in full load; thus, it encounters a higher number of waves per year in that condition.

3.4.4.1 The Influence of Predominant Wave Direction on VWBM results

It was shown on page 44 that the largest VWBM response is found when the wave direction is predominately head-on or from the stern. It is obvious that this difference in response to waves from different angles will affect the overall probabilities of exceedance, depending on the vessels heading. It is assumed that traditional tankers have equal probability of encountering waves at all headings during a voyage, as opposed to FPSOs, where the waves will have higher probabilities of approaching the vessel from certain angles. It is important to keep in mind that by wave direction we mean the predominant direction of the waves in the sea-state, relative to the ship heading. Although the wave direction is 0°, waves will approach from other directions at the same time. This short-crestedness is achieved by introducing the spreading function (Eq. 3.21).

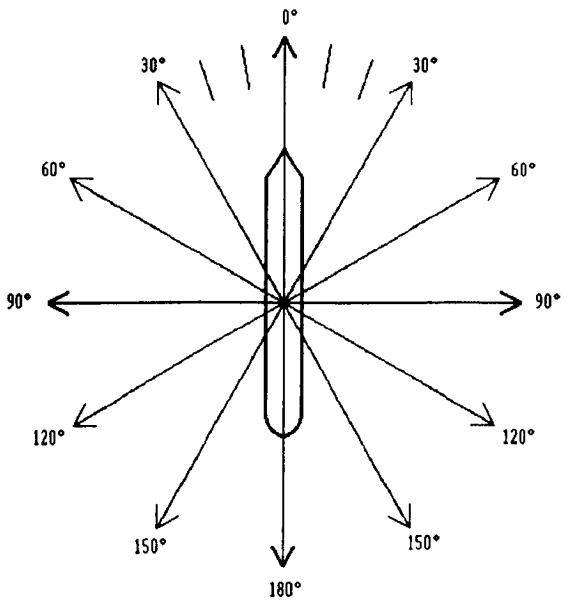

Figure 3. 10 Wave Directions

Using the *LongTerm* program, five different models were adopted to investigate the effect of ship heading on VWBM results. The first case considered was the "Tanker" situation where there is equal probability of each heading. This was modelled by calculating the probability of exceedance of VWBM for

seven headings from 0-180° with increments of 30°. The long-term distribution was taken as the average of all headings.

The heading of a FPSO with a passive mooring system is mainly dependent on the wave-direction, but wind and current will also influence the heading of the vessel. It was assumed that the vessel weathervanes between ±30 degrees from the head sea due to of wind and current. In order to model this (Case 2) equal weighting was applied to 0° and 30°, whereas the other directions where given zero weight.

In case 2, only two headings (0° and 30°) were used in the computations. It was believed that the precision could be improved by performing the calculations in the range from 0° to 30° with 10° increments, i.e. four steps instead of two. The *LongTerm* program was rewritten to accommodate four headings, and a situation with equal probability in the range 0°-30° was analysed as case 3. Case 4 was based on estimated probabilities for each of the four headings. The assumption was that it was most likely that most waves approached the vessel's bow, with decreasing probabilities for larger offsets. For reference, a last case where all waves encounter the vessel from 0° (head waves) was included. The main characteristics of each case are tabulated in Table 3.6, and plots of the results are shown in Figure 3.11.

Case	Weighting	Range	Increment	10^{-8} prob. [MNm]	$10^{-8.7}$ prob. [MNm]
1	1/7, 1/7, 1/7, 1/7, 1/7, 1/7, 1/7	0°-180°	30°	2633	2786
2	½, ½, 0, 0, 0, 0, 0	0°-180°	30°	3130	3268
3	¼, ¼, ¼, ¼	0°-30°	10°	3180	3281
4	0.55, 0.30, 0.10, 0.05	0°-30°	10°	3211	3452
5	1, 0, 0, 0	0°-30°	10°	3221	3464

Table 3.6 The Influence of Wave Direction on VWBM results

The VWBM value for 10^{-8} probability was increased by 18% from case 1, the traditional tanker approach, to the FPSO approach in case 4. This significant increase shows how importance of considering the wave direction when calculating the vertical wave bending moments or indeed any wave induced response. Another point of interest are the relatively small deviation in VWBM for the cases 2 trough to 5, where there is virtually no difference between the results obtained. This shows that as long the wave direction is limited to within 30° of the head seas, the methods give reasonable predictions of the long-term distribution of VWBM.

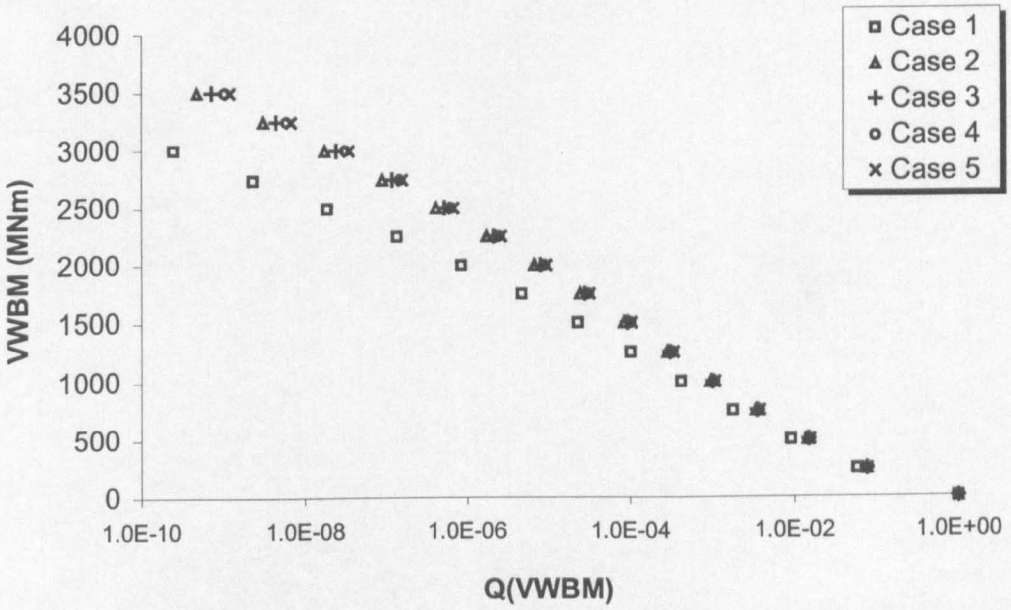

Figure 3.11 The Influence of Wave Direction on the Long-Term Distribution of VWBM

3.4.4.2 The Influence of Ocean Data on VWBM results

It was stated in chapter 3.4.4 that the Area 11 wave statistics was believed to give a good representation of the actual location of the Triton FPSO. Different fields may have different wave statistic, which may lead to variations in the wave induced loads acting on the vessel. The recent trend in offshore development is to develop marginal oil fields, with shorter field life and lower field value. Under these circumstances, it may be desirable to design the FPSO with a longer service life, and then operate the vessel at new locations after a field is depleted. If this is the case, thorough consideration during the design procedure should be given to where the vessel may be operated in its lifetime. Getting the design right in the first place may save costly improvements at a later stage.

A sensitivity study was carried to investigate the influence of the wave statistics (H_s and T_z) on the VWBM calculations. Table 3.7 shows the most probable values for the VWBM at probability levels corresponding to approximately 20 and 100 year return period at different locations.

The VWBM results for Area 11 are fairly close to the rule requirements, whereas the West of Shetlands wave statistics generates a VWBM almost 45% higher than the rule value. The results for different areas in the North Sea range from 2447 MNm to 4110 MNm with 20-year return period.

Area	10^{-8} prob. [MNm]	$10^{-8.7}$ prob. [MNm]
Area 11	3211	3452
Central North Sea	2447	2500
Northern North Sea	4110	4456
West of Shetlands	4983	5425
IACS Requirement	3447	3757[1]

Table 3.7 Most Probable Values at Different Locations (Full Load)

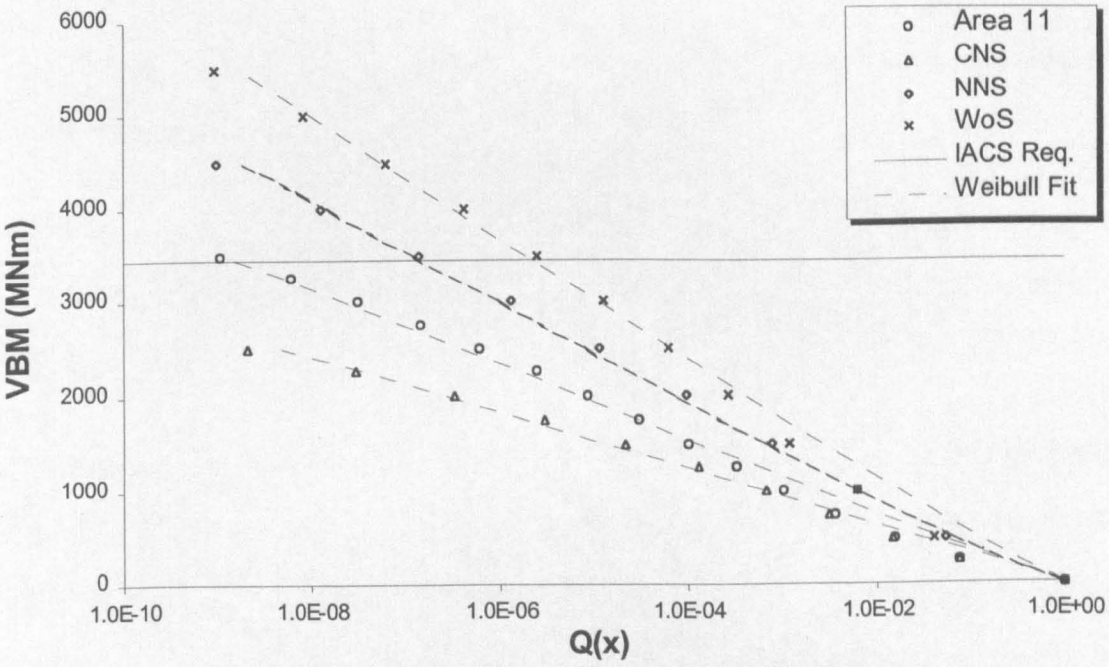

Figure 3.12 The Influence of Ocean Data on the Long-Term Distribution of VWBM

3.5 Slamming

Slamming related to local and hull girder loads arise from bottom impact or bow flare immersion. Rigorous calculation of the slam impact forces includes addressing changes in fluid momentum, buoyancy and impulsive pressure variations as a function of time. The dynamic slam transient load effects are superposed on the steady state wave induced load effect. There is also a slam-related deceleration, which is superposed on the wave acceleration. In obtaining combined wave bending and slam effects, the phasing between wave induced and slamming load effects is important.

[1] DNV Rules for Classification of Ships, Part 5, Chapter 9, 'Oil Production and Storage vessels': "The relation between probability level $10^{-8.7}$ (100 year return period) and 10^{-8} (20 year return period) may be taken as 1.09"

Slamming does not occur with every wave encounter, and it only affects the sagging response. The incidences of slamming are dependent on vessel speed, heading and heavy weather countermeasures. The master of the vessel will usually take measures to limit the incidences of slamming, however this might not be possible for a FPSO with a passive mooring system. Slamming is known to occur on FPSOs operated in harsh weather condition, with steep waves. The magnitude of the slamming loads may be as much as 50% of the extreme Vertical Wave Bending Moment (Chalmers (1993)).

Ochi and Motter (1973) proposed a probabilistic formulation for the prediction of slamming. The probability of slamming was estimated by:

$$P(slam) = exp\left[-\left(\frac{T^2}{2m_{0_m}} + \frac{v_{cr}^2}{2m_{0_v}}\right)\right] \qquad \text{Eq. 3. 37}$$

where T is the draught of the vessel, v_{cr} is the critical velocity which is related to the length of the vessel through an empirical formula. The two variances in the equation are associated with relative motion and velocity respectively. For Triton the probability of slamming was found to be ~ 0, when this formula was applied in a sea state with $H_{max} = 33$ m and $T_z = 8$ s. The draught in ballast load is 8.6 meters at the FP, whereas there appear to be a threshold draught of around 7 meters, below which the probability of slamming becomes significant, with one slam expected in 25 years.

If slamming occurs it could be taken into account by combining it with the wave induced bending moments. In this case, the combined extreme value M_c for a sea state, heading and speed is given on the basis of the Square Root of Sum of Squares (SRSS) rule, by

$$M_c = \sqrt{M_{we}^2 + M_{sl}^2} \qquad \text{Eq. 3. 38}$$

where M_{we} and M_{sl} are the individual (wave and slam related) extreme bending moments, with the two processes considered uncorrelated because of their typical frequency separation. These extreme values can then be combined with the stillwater loads as described in chapter 3.6. If a peak value of the slamming induced bending moment of 50% of the VWBM is used,

M_c will be only 12 % larger than M_{we}. Taking this M_c value into the load combination calculations will reduce the effect of slamming further, to less than 6 % of M_{we}.

Considering the low probability of slamming for Triton, and keeping in mind, that slamming is only associated with sagging, and that hogging is the dominating condition for Triton, it was decided to ignore slamming induced VBM in the load calculations. However, if effect of slamming is proven significant, it could easily be accounted for by modifications to the non-linear correction factor, χ_{nl}, in the reliability analysis.

3.6 Stochastic Combination of Hull Girder Bending Moments

Combining the vertical bending moments in an appropriate way is not a straightforward task, given the different random nature of the loads. Still water induced loads are very slow varying, wave induced loads have low frequency whereas slamming induces high frequency loads. Only the still water induced and wave induced components of the hull girder loads have been considered. These two loading components have been considered independent and Ferry Borges – Castenheta load combination method has been applied to obtain the load combination factor, Ψ_w, for the Full Load, Partial Load (50 % loaded) and Ballast condition. The effect of slamming was disregarded for reasons discussed in chapter 3.5.

Historically several deterministic methods have been applied to derive load combination factors for M_w and M_{sw} for both sagging and hogging condition. The correlation between these two loads is negligible for the estimation of the extreme combined bending moment. In the existing ship rules (e.g. IACS Requirements) SWBM and VWBM are simply added together, assuming that the maximum values of the two loads occur at the same instant during a ship's design life. IACS also specifies that the maximum SWBM and VWBM should not exceed their respective allowable values, even if one of the moments is negligible.

As the stillwater and wave bending moments are stochastic processes, the maximum SWBM and VWBM do not necessarily occur simultaneously in a ship's service lifetime. Söding combined the two loads by modelling them as random variables, although this was a step in the right direction, it was a simplistic model. Moan and Jiao (1988) considered both SWBM and VWBM as stochastic processes, and, based on a particular solution by Larrabee (1981),

they introduced a load combination factor, derived by the combination of two stochastic processes:

$$M_{te} = M_{we} + \Psi_{sw} M_{se} = \Psi_w M_{we} + M_{se} \qquad \text{Eq. 3.39}$$

where Ψ_s and Ψ_w are load combination factors, while M_{se} and M_{we} are the extremes of the still-water and wave induced bending moments.

Wang and Moan (1996) and Wang, Jiao and Moan (1996) presented a comparison of the five most used load combination methods; the Turkastra's rule, the square root sum of the squares (SRSS) rule, the Ferry-Borges Castenheta method, the point-crossing method and the load coincidence method. The peak coincidence method turned out to be very conservative with an over-prediction of the maximum total load of 24.1%. The other deterministic methods are all under-predictive: Turkastra's rule giving a deviation of 8.3% and SRSS gave a deviation of 9.4%. As a conclusion, it was found that, in the case of an offshore production tanker, considered the point-crossing method as a reference solution, the Ferry-Borges's method is the more reliable and its use was therefore recommended by the authors.

3.6.1 Ferry Borges - Castenheta Method

In the Ferry Borges-Castenheta Method the real loading processes are greatly simplified in such a way that the mathematical problems connected with estimating the distribution function of the maximum value of a sum of loading processes are avoided. The method assumes that the loads change intensity after prescribed deterministic, equal time interval, during which they remain constant. The intensity of the loads in the different elementary time intervals is an outcome of identically distributed and mutually independent variables. A time interval for still-water loads would typically be one voyage for a conventional ship. For a production ship, the period between different loading conditions must be defined from the operational profile.

In the method, the point-in-time distribution for load process $\{x\}$ is defined as f_{x_i} (density function) and the corresponding distribution function is F_{x_i}. The cumulative distribution function of the maximum value in the reference period T is then given by $(F_{x_i})^{n_i}$, i.e.:

$$F_{max,x_i}(x_i) = (F_{x_i}(x_i))^{n_i} \quad \text{Eq. 3.40}$$

From load combination theory, we have that the density functions $f_{x_i+x_j}$ are determined by the convolution integral:

$$f_{x_i+x_j}(x) = \int_{-\infty}^{\infty} f_{x_i}(z) \cdot f_{x_j}(x-z)dz \quad \text{Eq. 3.41}$$

and from basic statistics we have:

$$F_{x_i}(x) = \int_{-\infty}^{\infty} f_{x_i}(z)dz \quad \text{Eq. 3.42}$$

by combining these three formulas (3.37-39) we end up with the following expression:

$$F_{max,x_i+x_j}(x) = \left\{ \int_{-\infty}^{\infty} f_{x_i}(z) \cdot \left[F_{x_j}(x-z)\right]^{n_j} dz \right\}^{n_i} \quad \text{Eq. 3.43}$$

Taking x_i and x_j as M_{sw} and M_w respectively, Equation 3.40 may be applied directly to the combination of stillwater and wave induced bending moments. The total vertical bending moment, M_t, may then be estimated by:

$$F_t(M_t) = \left\{ \int_{-\infty}^{M_t} f_{sw}(z) \cdot \left[F_w(M_t - z)\right]^{n_w} dz \right\}^{n_{sw}} \quad \text{Eq. 3.44}$$

The density distribution function f_{sw} is the still-water bending moment in one year, which is a normal distribution. The number of occurrences of each load condition, n_{sw}, is defined by the operation profile in chapter 3.3.3. $[F_w]^{n_w}$ is the Gumbel distribution of the extreme wave induced bending moment in one load condition derived from the Weibull distribution assuming n_w wave loads in each load condition.

$$n_w = \frac{\tau_{sw}}{T_Z} \quad \text{Eq. 3.45}$$

Introducing a load combination factor, the total load might be defined as:

$$F_t = F_{sw}(x) + \Psi_w F_w(x) \qquad \text{Eq. 3.46}$$

where the extreme distributions are considered at 0.5 exceedance level. The load combination factor can then be determined by the following relationship:

$$\Psi_w = \frac{F_t^{-1}(0.5) - F_{sw}^{-1}(0.5)}{F_w^{-1}(0.5)} \qquad \text{Eq. 3.47}$$

3.6.2 Load Combination Results

The load combination factors were calculated for the three loading conditions, based on the operation profile and the extreme loads. The load combination factors were calculated for all load conditions in all events considered (i.e. different locations, different load models etc.). The calculations for the conditions that make up the basis of the reliability analysis may be found in Appendix H. The cumulative distribution functions for the individual loads and the combined effect are shown in figures 3.13-15.

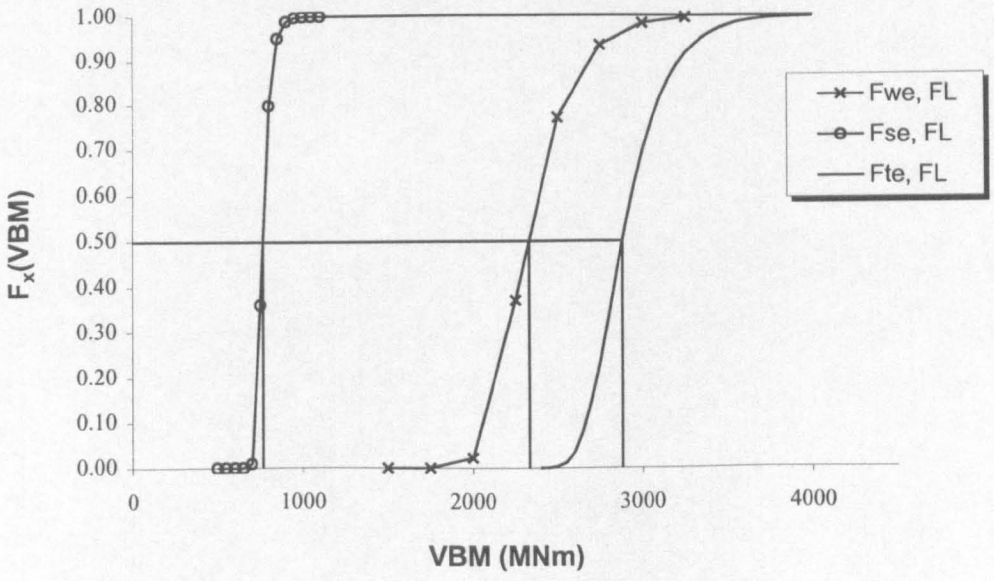

Figure 3.13 Load Distribution Functions in Full Load Condition

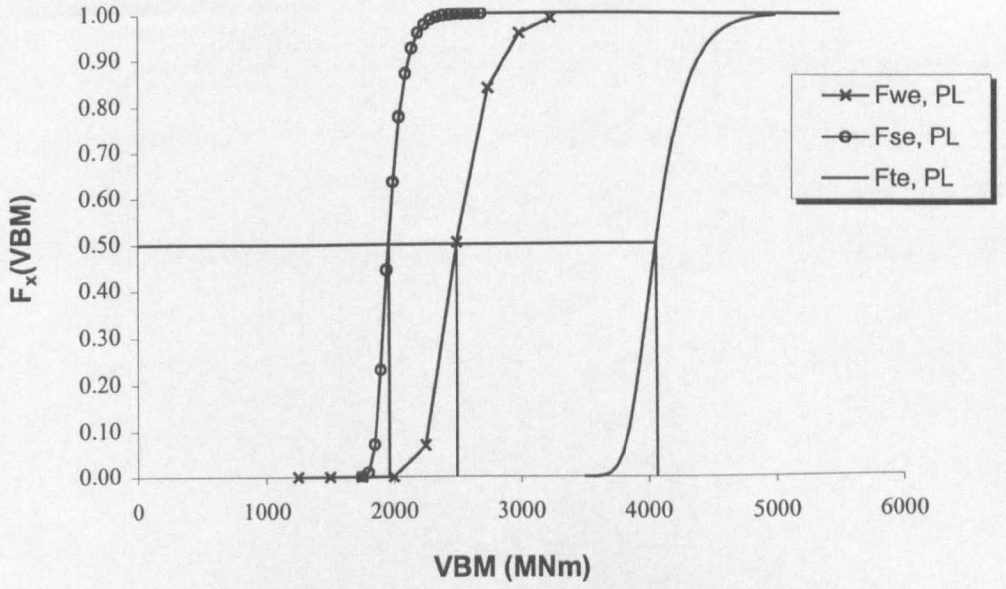

Figure 3.14 Load Distribution Functions in Partial Load Condition

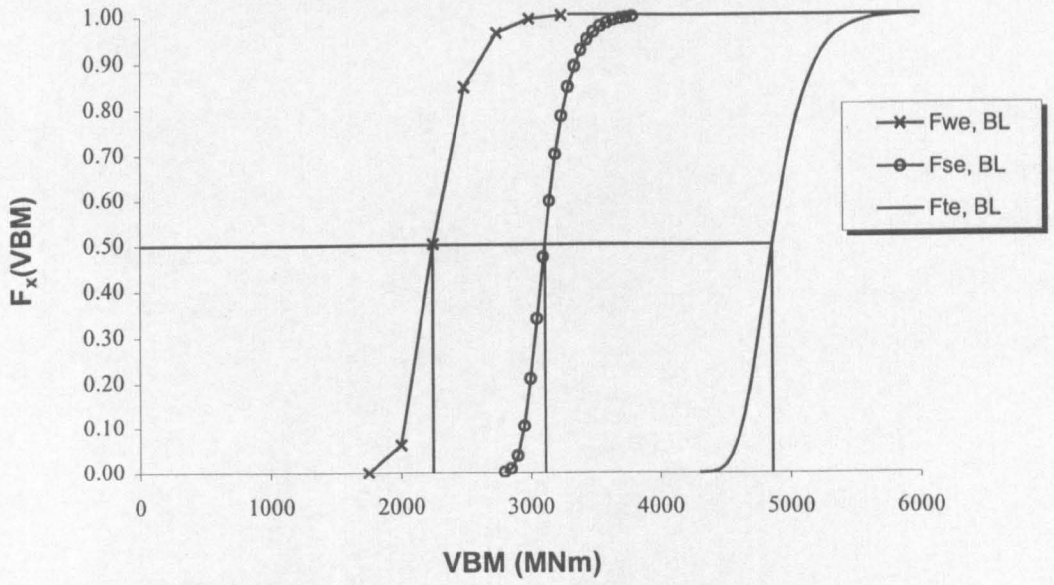

Figure 3.15 Load Distribution Functions in Ballast Load Condition

The only values of interest for the load combination, are the VBMs that have exactly 50% probability of being exceeded. These values, shown in Table 3.8, are used in Eq. 3.46 to calculate the load combination factor.

	Load Condition	$M_{sw}(0.5)$ [MNm]	$M_w(0.5)$ [MNm]	$M_t(0.5)$ [MNm]	Ψ_w
Hog	Full Load	763	2319	2882	0.91
	Partial Load	1964	2500	4065	0.84
	Ballast Load	3111	2251	4859	0.78
Sag	Full Load	-365	2319	1754	0.91
	Partial Load	-940	2500	1162	0.84
	Ballast Load	-1490	2251	259	0.78

Table 3.8 Load Combination Factors

3.7 Conclusions

IACS requirements give the minimum M_{sw} for Triton as 2577 MNm and 2238 MNm for hogging and sagging respectively. The values obtained for minimum M_w are 3447 MNm in the hogging condition and 3787 MNm in sagging. By combining M_{sw} and M_w the minimum total vertical bending moment is found to be 6025 MNm in both sagging and hogging.

The operational profile of the vessel is such that the ship will always have a hogging stillwater bending moment, ranging from 564 MNm in full load to 2300 MNm in the ballast condition. The extreme SWBM values for the ballast load condition will tend to be conservative due to two assumptions. Firstly, the SWBM was assumed to follow a normal distribution in both hog and sag, and secondly the effect of heavy weather countermeasures was not included in the analysis. Both these assumptions will give higher values for the extreme SWBM than what might be found in reality.

The Triton FPSO will be stationed in the North Sea, close to the Gannet complex and Hogben's Global Wave Statistics Area 11 was assumed to represent the wave statistics for this location. The vertical mooring forces on the FPSO are small, and have insignificant influence on the bending moment response. The same transfer functions, and consequently the same wave loads, was used for Triton 1, 2 and 3, neglecting the slightly different weight distributions caused by variations in the scantling.

Different wave statistic may lead to variations in the wave induced loads acting on the vessel, thus three other sites were investigated for reference. The VWBM results for Area 11 are fairly close to the rule requirement at the 10^{-8} probability level, whereas the wave bending moment response for West of Shetlands is almost 45% higher than the recommended rule value.

The two loads, stillwater and wave bending moments, were considered to be independent and Ferry Borges – Castenheta load combination model was applied to obtain load combination factors. As no information on the loading procedures for the FPSO was available, a simplified operation profile based on the production capacity was used, and a rectangular pulse process was fitted. The load combination factor was found to vary significantly with the ratio of stillwater load to the total load. It was also found that the load combination factors for hogging and sagging remain the same within each loading condition.

4 Structural Reliability Analysis

4.1 Introduction

Traditionally structural engineering has been dominated by deterministic design methods, where all factors affecting the strength of the structure and applied loads are assumed known. In reality, there will be a high degree of uncertainty associated with all these factors. In order to account for this, the methods of structural analysis give lower bound solutions to collapse loads, empirical design rules are formulated to give safe estimates of strength and high margins of safety are applied in the deterministic analysis to ensure some degree of safety. Because of this rather arbitrary way of treating the uncertainties, the reserve strength of the structure is rarely known, and it is in most cases far too high.

To handle the design in a more realistic way, the probabilistic approach considers each parameter as a statistical variable characterised by the probability density function. The probability of all values of all variables are then considered and combined, to give an estimate of the safety of the structure. Thus, structural reliability is concerned with the calculation and prediction of the probability of limit state violation. In particular, the violation of the ultimate limit state is evaluated as a governing criterion, which controls the major disposition of material and hence cost. Structures fail when they encounter some extreme load (or load combination), of sufficient magnitude that exceeds the strength capacity of the structure. The problem of estimating the ultimate limit state consists of combining the probabilistic models for these extreme loads with estimates for the structural strength.

Several methods have been developed to evaluate the safety of structures. These reliability methods are usually classified in three levels of generally increasing complexity:

Level 1: Code level methods in which reliability based partial safety factors (PSF) are applied to characteristic values of load components and resistance factors in the safety check equations used in design; this is a deterministic format most commonly advocated for limit state design codes at present.

Level 2: Second moment methods in which the random variables are defined in terms of means and variances with some distribution. The joint probabilistic behaviour is reflected in a covariance matrix. The measure of reliability is based on the reliability index β. In *Advanced* or *Extended* level 2 methods the design variables can have any type of probability distribution.

Level 3: Methods in which calculations are made to determine the "exact" probability of failure for a structure, making use of a full probabilistic description of the joint occurrence of the various design variables, taking into account the true nature of the failure domain. The measure of reliability is the calculated probability of failure P_f.

Structural systems are composed of individual structural components. Well-designed structures are often redundant, so failure of an individual component does not usually constitute collapse. The overall goal for the structural design is to achieve some target reliability for the total structure, and the aim for the structural reliability analysis is then to document that this target reliability is achieved. Target reliabilities, depending on consequence of failure and type of failure, are proposed by the classification societies.

The results from ultimate strength calculations and load calculations serve as input to the reliability analysis, where the first step is to define a limit state function. This function could typically be on the form;

$$g(X) = \chi_u M_u - M_{sw} - \psi_w \chi_{nl} \chi_w M_w \qquad \text{Eq. 4.1}$$

for the ultimate hull girder strength. Where χ_u , χ_{nl} and χ_w are the uncertainties associated with ultimate capacity, non-linear effects and uncertainty on wave load respectively.

4.2 Structural Reliability Theory

Level II analyses have shown to give acceptable results compared to the accurate Level III method. The philospohy behind the the level II methods is that each basic variable in the limit state function can be represented by their mean value and standard deviation. That is the first and second moments of their probability distributions. A level III analysis requires knowledge of the joint probability of the variables, such information is hardly ever avaliable for practical problems.

The most commonly used level II analyses are the *first-order reliability method* (FORM) and the *second-order reliability method* (SORM). The basic concepts of theses two methods are simple; transformation of arbitrary random uncertainty vectors into independent, standard normal vectors and approximation of the failure surface so that the probability of failure can simply be estimated from the probabilities of linear (FORM) or quadratic (SORM) forms in normal variables.

Freudenthal et al. (1966) proposed a formulation where the strength of the structure is made dependent on only one load (L) and one resistance (R) that are described by their probability density functions. The probability of failure is;

$$P_f = P(R - L) \le 0 = \int_{-\infty}^{\infty} F_R(x) f_l(x) dx \qquad \text{Eq. 4.2}$$

The geometrical relationship between the probability distribution functions for strength and load effect is shown in Figure 4.1. The probability of survival $\mathcal{R}$, or the probability that structure will satisfy a defined serviceability requirement, is given by;

$$\Re = 1 - P_f = 1 - \int_{-\infty}^{\infty} (1 - F_l(x)) f_r(x) dx \qquad \text{Eq. 4.3}$$

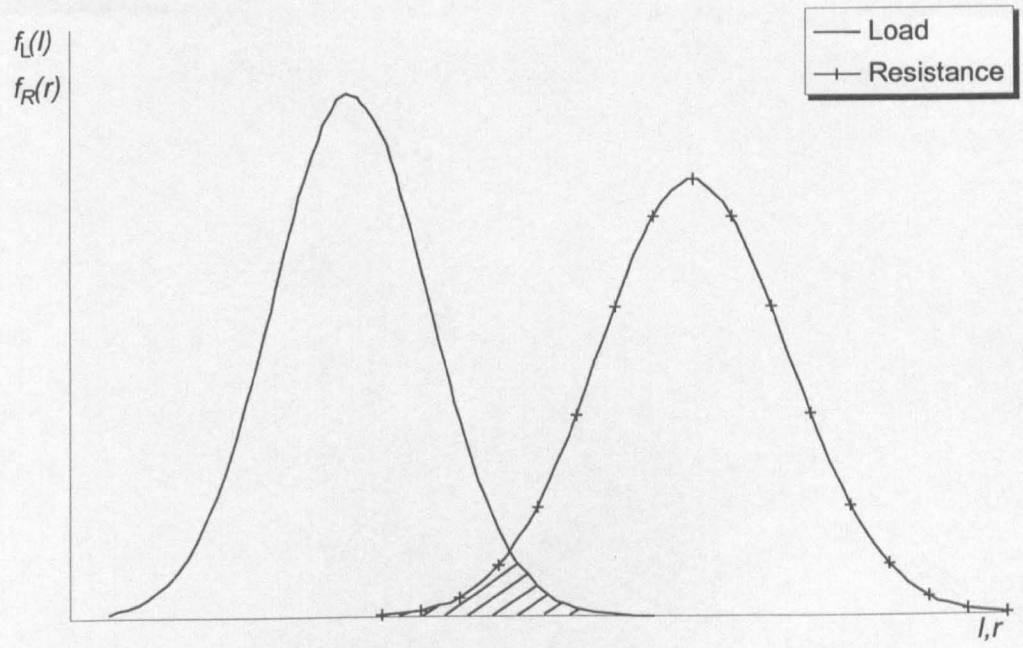

Figure 4.1 Probability distribution functions for strength and load effect

Although the overlapping area in Figure 4.1 gives an indication to the probaility of failure, it is not a direct measure. In general there do not exist close form solutions to the integrals in Eq. 4.2-3, except for some special cases. One such special case is the event involving two independent normally distributed variables. Assuming a limit state equation,

$$g(R,L) = R - L \qquad \text{Eq. 4.4}$$

the mean and the standard deviation of the limit state may be calculated as,

$$\mu_g = \mu_R - \mu_L \qquad \text{Eq. 4.5}$$

$$\sigma_g = \sqrt{\sigma_R^2 + \sigma_L^2} \qquad \text{Eq. 4.6}$$

The failure surface is a hyperplane defined by,

$$P_f = \Phi\left(-\frac{\mu_g}{\sigma_g}\right) = \Phi\left(\frac{\mu_L - \mu_R}{\sqrt{\sigma_R^2 + \sigma_L^2}}\right) \qquad \text{Eq. 4.7}$$

4.2.1 Cornell's Reliability Index

Cornell (1969) proposed a reliability measure for cases with linear safety margins *g(R,L)* as a ratio of the expected value to its standard deviation, or the number of standard deviations by which μ_g exceeds zero;

$$\beta = \frac{\mu_g}{\sigma_g} \qquad \text{Eq. 4.8}$$

The geometrical properties of β are shown in Figure 4.2.

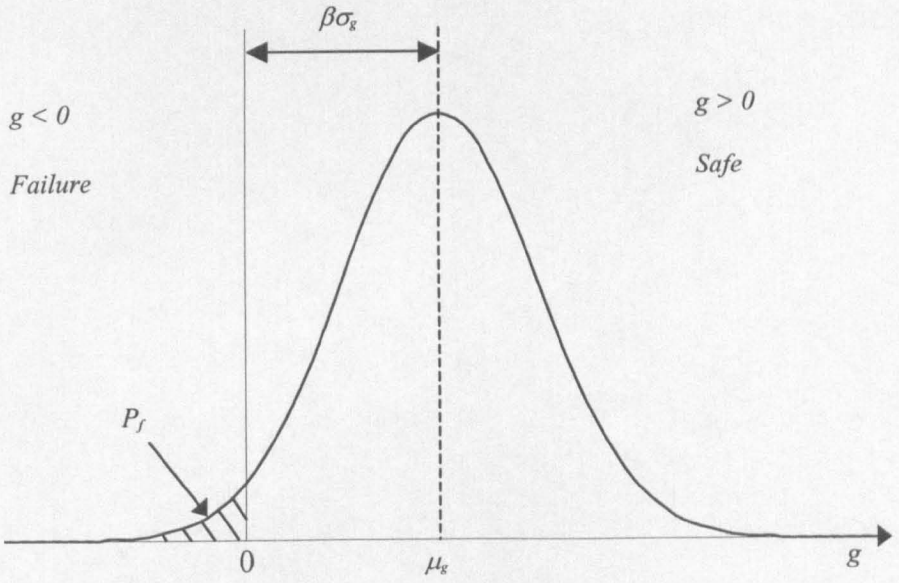

Figure 4.2 Reliability Index β

The probability of failure of a structure with independent normally distributed variables may then be expressed as;

$$P_f = \Phi(-\frac{\mu_g}{\sigma_g}) = \Phi(-\beta) \qquad \text{Eq. 4.9}$$

The main problem with the Cornell reliability index is that there is a 'lack of invariance' in the failure function. The reliability index as defined by Eq. 4.8 will change when the different, but equivalent non-linear failure functions are used. Cornell's estimate of the reliability index for non-linear functions will depend on the choice of linearisation point. The easiest method, and thus most used, is to linearise the failure function at the mean point.

Experience shows that that calculations based on the mean point should not be used, and that a linearisation about a point on the failure surface where $g(R,L)=0$ is more reasonable.

Structural systems often involve more than two variables, and if $x_1, x_2, \ldots, x_n$ are the n independent variables, a general expression for any limit state equation is

$$z = g(x_1, x_2, \ldots, x_n) > 0 \qquad \text{Eq. 4.10}$$

where z is the safety margin. The failure surface $z = 0$ divides the n-dimensional space into a safe ($z > 0$) and a failure region ($z < 0$). The failure probability is the probability content in the failure set;

$$P_f = \int_{g(x)\le 0} f_{x_1,\ldots,x_n}(x_1,x_2,\ldots,x_n)dx \qquad \text{Eq. 4.11}$$

$$\beta = -\Phi^{-1}(P_f) \qquad \text{Eq. 4.12}$$

Where $f_{x_1,\ldots,x_n}(x_1,x_2,\ldots,x_n)$ is the joint probability distribution density function for the n variables x_n. These joint probability distributions are almost impossible to define in practice. Even if they are known, the multi-dimensional integration of Eq. 4.11 is very complex and time-consuming, if at all solvable. To overcome these problems new level II methods, involving iterative procedures where developed.

4.2.2 Hasofer & Lind Reliability Index

The Hasofer & Lind (1974) transformation provided a major advance in second-moment methods, extending the concept of reliability index to include correlated basic variables and solving the invariance problem. The set of basic variables is normalised using the following transformation:

$$x_i' = \frac{x_i - \mu_{X_i}}{\sigma_{X_i}} \quad , \qquad i = 1, 2, \ldots, n \qquad \text{Eq. 4.13}$$

The Hasofer and Lind reliability index is defined as the shortest distance from the origin to the failure surface in normalised X'-space. This point $\bar{x}^*$ on the failure surface is called the design point. The formal definition of β_{HL} is:

$$\beta_{HL} = \frac{\mu_{g_{HL}}}{\sigma_{g_{HL}}} = \frac{-\sum_{i=1}^{n} (\bar{x}_i^*) \left(\frac{\partial g(x)}{\partial x'_i} \right)}{\sqrt{\sum_{k=1}^{n} \left(\frac{\partial g(x)}{\partial x'_k} \right)^2}} \qquad \text{Eq. 4.14}$$

β_{HL} may also be expressed in tems of the sensitivity factors α_i, which show the relative importance of each variable within a given limit state function.

$$\beta_{HL} = -\sum_{i=1}^{n} x_i^* \alpha_i \qquad \text{Eq. 4.15}$$

where,

$$\alpha_i = \frac{-\frac{\partial g(x)}{\partial x'_i}(\beta \bar{\alpha})}{\sqrt{\sum_{k=1}^{n} \left(\frac{\partial g(x)}{\partial x'_k}(\beta \bar{\alpha}) \right)^2}} \qquad \text{Eq. 4.16}$$

From this, the probability of failure can be approximated by:

$$P_f = \Phi\left(-\frac{\mu_{G_{HL}}}{\sigma_{G_{HL}}}\right) = \Phi(-\beta_{HL}) \qquad \text{Eq. 4. 17}$$

By using this definition of the reliability index, where β is related to the failure surface, not the mean point, an invariant safety measure is obtained (ref. page 61).

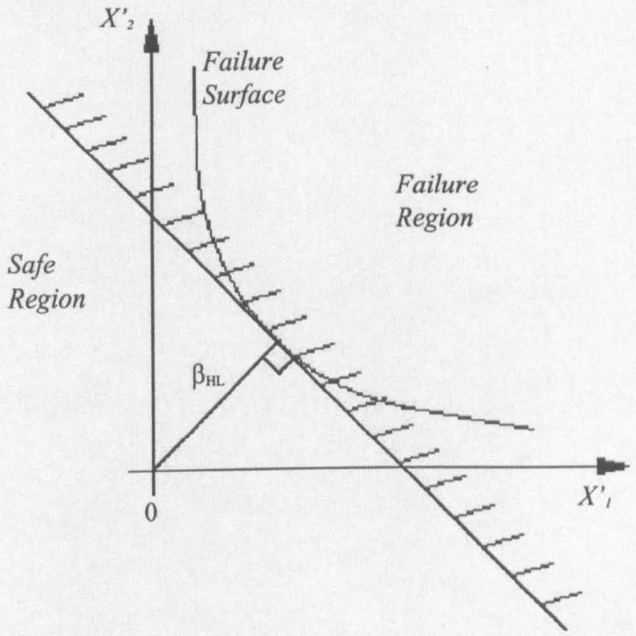

Figure 4.3 Hasofer-Lind Reliability Index in Standard Normal Space.

4.2.3 Non-Normal Basic Variables

When dealing with non-normal basic variables Rackwitz and Fiessler (1977) formulated a method for transforming the variables into standard normal space. This transformation is performed in such a way that the values of the original density functions f_{X_i} and the original distribution function F_{X_i} for the random variables are equal to the corresponding values of the density functions f_{X_i} and the distribution function for a normally distributed variable at the design point $\bar{x}^*$.

$$F_{X_i}(x_i^*) = \Phi\left(\frac{x_i^* - \mu'_{X_i}}{\sigma'_{X_i}}\right) \qquad \text{Eq. 4.18}$$

$$f_{X_i}(x_i^*) = \frac{1}{\sigma'_{X_i}}\varphi\left(\frac{x_i^* - \mu'_{X_i}}{\sigma'_{X_i}}\right) \qquad \text{Eq. 4.19}$$

Where the design point is defined by $(x_1^*, \ldots, x_i^*, \ldots, x_n^*)$, and where μ'_{X_i} and σ'_{X_i} are the (unknown) mean and standard deviation of the approximate normal distribution. Solving Eq. 4.18 and 4.19 with respect to μ'_{X_i} and σ'_{X_i} we get;

$$\sigma'_{X_i} = \frac{\varphi\left(\Phi^{-1}\left(F_{X_i}\left(x_i^*\right)\right)\right)}{f_{X_i}\left(x_i^*\right)} \qquad \text{Eq. 4.20}$$

$$\mu'_{X_i} = x_i^* - \Phi^{-1}\left(F_{X_i}(x_i^*)\right)\sigma'_{X_i} \qquad \text{Eq. 4.21}$$

The iterative procedure described in chapter 4.2.2 for calculating the reliability index must be modified when this transformation is used. On each step of the iteration new values for μ'_{X_i} and σ'_{X_i} must be calculated for those variables where such a transformation has been used.

4.2.4 Second-Order Reliability Method

In the foregoing FORM approach, the failure surface was linearised at the design point. It is obvious that this approximation will become more inaccurate for failure surfaces with higher curvatures. To correct for potential errors second-order methods, where the failure surface is replaced by a quadratic surface at the design point, were developed by Ditlevsen (1979), Breitung (1984), Tvedt (1988), Madsen (1986) and others.

The definitions of P_f and β in 4.2.2 were based on the assumption of a linear safety margin z. If z is non-linear, approximate values for μ_g and σ_g was obtained by using a linearised safety margin. z is obtained by expanding the safety margin in a Taylor series about the design point $\bar{x}^*$ and retaining only the linear terms;

$$z = g(x_1,x_2,\ldots,x_n) = g(x_1^*,\ldots,x_i^*,\ldots,x_n^*) + \sum_{i=1}^{n}\left(\frac{\partial g(x_i - x_i^*)}{\partial x'_i}\right) \qquad \text{Eq. 4.22}$$

To improve the accuracy achieved by FORM, the failure surface in SORM is expanded into Taylor series around the design point up to second order;

$$z = g(x_1,x_2,...,x_n) = g(x_1^*,...,x_i^*,...,x_n^*) + \sum_{i=1}^{n}\left(\frac{\partial g(x_i - x_i^*)}{\partial x'_i}\right) \qquad \text{Eq. 4.23}$$

$$+ \tfrac{1}{2}\sum_{i=1}^{n}(x_i - x_i^*)\sum_{j=1}^{n}\left(\frac{\partial^2 g(x_i - x_i^*)}{\partial x'_i \partial x'_j}\right)$$

Several formulations exist for evaluating the second-order approximation of the failure probability. Breitung proposed the following relationship;

$$P_f \approx \Phi(-\beta)\prod_{i=1}^{n-1}\frac{1}{\sqrt{1+\beta k_i}} \qquad \text{Eq. 4.24}$$

Where k_i are the main curvatures of the failure surface equation.

The second-order corrections become more significant with increasing dimension, but vanishes as the surfaces $(g_i = 0)$ approaches linearity, or if the failure surface is sufficiently far from the origin. The possible improvement of classical FORM results by second-order corrections must be judged in view of the large numerical effort involved and the magnitude of other non-computational uncertainties in the reliability problem.

4.2.5 CALREL

CALREL is a general-purpose structural reliability analysis program developed in *Department of Civil Engineering at University of California at Berkeley*. It is designed to compute probability integrals of the form,

$$P_f = \int_{g(x)\le 0} f_{x_1,...,x_n}(x_1,x_2,...,x_n)dx \qquad \text{ref. Eq. 4.11}$$

The program also calculates the generalised reliability index β_g, the sensitivities α of P_f and β_g with respect to deterministic parameters defining the probability distribution or the limit-state function. *CALREL* incorporates four techniques for computing these quantities; FORM, SORM, Directional simulation and Monte Carlo simulation.

CALREL uses Improved Breitiung and Tvedt's methods for the SORM analysis, these methods are based the Breitung formulation described above, but they are slightly more

complex. The pros and cons of SORM were discussed in chapter 4.2.4, where the main objection to the method was the large numerical effort involved. With programs like *CALREL*, however, there is virtually no extra computational time associated with the more accurate SORM analysis, so these results have been used in this report. A study of the sensitivity of β to the reliability method applied, showed good agreement between FORM and SORM for the ultimate hull girder reliability problem.

4.3 Uncertainty Modelling

The uncertainty sources that are relevant for the reliability evaluation may be classified according to their nature into physical, statistical, knowledge and model uncertainties. Physical uncertainty may be subdivided into the inherent uncertainty of the physical properties of the variable itself and the inherent uncertainty of the measuring device. Natural fluctuations of the strength parameters through a specimen of material or fluctuations in the wave loads on a vessel are examples of inherent uncertainty in variables.

Statistical uncertainty originates from lack of sufficiently large number of observations. Appropriate probability density functions for each basic variable must then be estimated through mean and higher moments derived from the available data. However, these observations of the variable do not perfectly represent it, so a statistical uncertainty is present. The numerical value of this uncertainty is seldom calculated by the engineer, but could be based on Bayesian analysis or expert opinion.

The knowledge about some unique variable may be more or less uncertain. Such uncertainty may conveniently be modelled in probabilistic terms. This type of model does not describe properties of the variable but properties of the knowledge about the variable. Model uncertainty is caused by the requirement of simplicity of the models so that they can be operational tools for the reliability evaluation. The errors in more elaborate models may be known, but at any level of detailed modelling there are errors relating to some unknown reality.

4.3.1 Modelling Uncertainties

Structural design and analysis use simplified, often deterministic, mathematical models to represent physical phenomena or behaviour. In the case of ultimate bending moment it is difficult to calculate the collapse load exactly, even if the actual value of all parameters are known. Thus, there is uncertainty associated with the mathematical model, in addition to the

uncertainty in the input parameters. This uncertainty, which is not just found in the strength model, is called model uncertainty and it reflects the confidence in the calculations. Model uncertainty is usually incorporated in the reliability analysis by a parameter, χ, which is defined as:

$$\chi_m = \frac{Actual\ response}{Predicted\ (modelled)\ response} \qquad \text{Eq. 4.25}$$

The model uncertainties are defined by a mean value and a standard deviation, and assumed normally distributed. In the analysis of the ultimate limit state of the hull girder, three model uncertainties have been used. These are; uncertainty on ultimate strength, non-linear effects and uncertainty in wave load prediction.

4.3.1.1 Uncertainty on ultimate strength

The parameter χ_u is introduced in the reliability analysis to account for the uncertainties in the ultimate strength model and in the material properties. The method for predicting the ultimate strength is continually being improved and verified by tests on statically determinate models or full-size elements, but some modelling uncertainty still exists. The modelling uncertainty have been estimated by different authors to lie in the range from 5 to 15%, depending on the strength model used and the material properties considered.

The main uncertainty in material properties stems from the variations in yield stress that may be found in steel from different steel mills, different batches or indeed within the same batch. CIRIA (1977) stated that there is very little practical evidence to suggest that the frequency of occurrence of low strengths (i.e. below the specified strength) becomes attenuated as a result of quality control procedures. This is because only a very small fraction of the total bulk of any material is actually tested, so that the chances of detecting occasional low strength material are very low. Common practice is to apply COV of 8%, if the steel is from the same batch.

Teixeira (1997) estimated a realistic COV for the total uncertainty on ultimate strength to be 15%, which is in good agreement with Faulkner (1992) who proposed a COV of 10-15% for the modelling uncertainty for flat panel collapse. As the ultimate bending moment calculations are directly dependent on for flat panel collapse, a COV value of 15% seems

reasonable to adopt for the reliability calculations. Thus, the basic variable χ_u is assumed normally distributed, with a mean value of 1.0 and a standard deviation of 0.15.

4.3.1.2 Non-linear effects

The wave-induced response is calculated using a linear strip theory program, where the linear analysis is based on several simplifying assumptions. The ship is divided into vertical strips and the linear response of each strip to a sinusoidal wave excitation is calculated. This simplification works well for most cases, but the non-linear effects are particularly important for finer form, higher speed, less wall-sided vessels such as container ship. Although most FPSOs are neither, the effect has been identified in several studies. ISSC (1991) presented an analysis of a FPSO where the non-linear effects on extreme wave bending moments were modelled by a bias of 0.85 in the hogging and 1.15 in the sagging condition.

Guedes Soares (1991) introduced formulas for corrections in the linear response. These formulas were dependent on the block coefficient of the vessel, and when applied to Triton they gave biases of 1.01 and 0.99 for hogging and sagging respectively. Other authors present values somewhere in between the values presented by ISSC and Guedes Soares. A factor χ_{nl} with a bias of 1.10 and a COV of 8% for the sagging condition and a bias of 0.9 and a COV of 15% was introduced to represent the non-linear effects on Triton.

4.3.1.3 Uncertainty in wave load prediction

In addition to the non-linear effects, there are other uncertainties associated with the linear strip theory programs. Different programs will use different procedures for calculating the hydrodynamic coefficients. Shellin et al (1996) identified large variations in long-term distributions of midship induced loads based on transfer functions obtained by different methods. Dogliani et al (1995) showed that the linear strip theory programs generally over-predicted the wave induced bending moments at the 10^{-8} probability level. ISSC (1991) stated that the ratio between the measured and calculated bending moments amidships was well modelled using a bias of 0.9 and a COV of 15%. These results were based on benchmark tests on a FPSO located in the North Sea, and they were adopted in the reliability analysis in this project.

4.4 Structural Reliability Analysis of Triton

For each variable the mean, standard deviation and type of distribution (e.g. Normal, Log-normal etc.) were defined. This data served as input to *CALREL*, which was used to perform

a second-order reliability analysis. The same limit state function (Eq. 4.1) was used for all models considered; only the basic variables were changed.

The characteristic values for were obtained through the analyses in chapter *2. Ultimate Strength Analysis* and *3. Loads and Load Combination*. Table 4.1 summarises the stochastic model used for Triton 2 at Area 11, the full stochastic models for the other designs, and other locations, are shown in Appendix I, together with the results.

	Condition	χ_u - LogNormal		M_u	M_{se} - Gumbel		Ψ_w	χ_w - Normal		χ_{nl} - Normal		M_{we} - Gumbel	
		Mean	STD	Const.	Mean	STD	Const.	Mean	STD	Mean	STD	Mean	STD
Sag	FL	1.00	0.15	-7887	358	42.4	0.91	0.90	0.18	1.10	0.088	-2358	-240
	PL	1.00	0.15	-7887	922	109.3	0.84	0.90	0.18	1.10	0.088	-2538	-237
	BL	1.00	0.15	-7887	1461	173.1	0.78	0.90	0.18	1.10	0.088	-2289	-229
Hog	FL	1.00	0.15	9701	768	42.4	0.91	0.90	0.18	0.90	0.135	2358	240
	PL	1.00	0.15	9701	1982	109.3	0.84	0.90	0.18	0.90	0.135	2538	237
	BL	1.00	0.15	9701	3139	173.1	0.78	0.90	0.18	0.90	0.135	2289	229

Table 4.1 Stochastic Model for Reliability Analysis of Triton 2

A negative sign on a load or strength parameter in Table 4.1, represents a sagging moment, and a positive value denotes hogging. One point of interest is that the SWBM is always positive, with the same standard deviation for both conditions. The extreme wave induced bending moment M_{we} is the same for both hog and sag, but for reasons discussed on page 69 it is corrected by χ_{nl} and χ_w in the calculations.

The main, or the most interesting, output from the structural reliability calculations is the reliability index. This value gives a measure of the reliability of the structure β. The higher value β takes, the safer the structure is believed to be. Considering Cornell's definition of β as the ratio of μ_g/σ_g, shows that higher β values may be achieved by increasing the mean value or decrease the standard deviation (reduced uncertainty) of the limit state.

DNV (1995) proposed values for P_f and β_t as shown in Table 4.2, depending on the redundancy of the structure and seriousness of failure. For a FPSO, the structure is deemed redundant and the type of failure consequence is considered to be serious because of the expensive repairs that will have be carried out. Large pollution or loss of human life is very unlikely in longitudinal hull girder failure. The target reliability for Triton was thus set to 3.71, which corresponds to an annual probability of failure, $P_f=10^{-4}$.

Class of failure	Consequence of failure	
	Less Serious	Serious
I – Redundant structure	$P_f = 10^{-3}$ ($\beta_t = 3.09$)	$P_f = 10^{-4}$ ($\beta_t = 3.71$)
II – Significant warning before the occurrence of failure in a non-redundant structure	$P_f = 10^{-4}$ ($\beta_t = 3.71$)	$P_f = 10^{-5}$ ($\beta_t = 4.26$)
III – No warning before the occurrence of failure in a non-redundant structure	$P_f = 10^{-5}$ ($\beta_t = 4.26$)	$P_f = 10^{-6}$ ($\beta_t = 4.75$)

Table 4.2 Annual P_f and β_t from DNV Classification Notes 30.6

4.4.1 Results

Three different structural designs of Triton were analysed; the initial tanker design called Triton 1, the as-built FPSO design (Triton 2), and finally the modified FPSO design (Triton 3). The Triton 3 design was developed after initial calculations showed that the Triton 2 had very high reserve strength in sagging.

The stochastic model for the structural reliability analysis of Triton 2 is shown in Table 4.1. The only difference in the models for the different designs are the M_u values used, all other variables are unchanged. It could be argued that the different scantlings would change the weight distribution, and consequently affect the VWBM and SWBM calculations. However, these calculations are not very sensitive to changes in weight distributions hence the loads obtained for Triton 2 have been used for all designs.

A reliability index was calculated for each condition, in both hog and sag, these β values were combined using;

$$\beta_a = \Phi^{-1}\left(P_{f_{FL}} + P_{f_{PL}} + P_{f_{BL}}\right) \qquad \text{Eq. 4.26}$$

to obtain the annual reliability indices β_a shown in Table 4.3. The results show that, from an ultimate-strength point of view, the increase in deck plating thickness from Triton 1 to Triton 2 was unnecessary. The sagging capacity of the midship section was satisfactory, or in fact very high ($\beta = 4.62$), in the initial design. It is also clear that the strengthening of the bottom improved the reliability in hogging to an acceptable level ($3.28 \Rightarrow 4.11$). Based on these results a third design, where only the bottom was strengthened was developed and analysed.

		Full Load	Partial Load	Ballast Load	β_a	P_f
Triton 1	Sag	4.62	5.14	6.04	4.62	$1.927 \cdot 10^{-6}$
	Hog	4.96	4.01	3.30	3.28	$5.143 \cdot 10^{-4}$
Triton 2	Sag	5.18	5.68	6.53	5.17	$1.173 \cdot 10^{-7}$
	Hog	5.55	4.74	4.12	4.11	$2.004 \cdot 10^{-5}$
Triton 3	Sag	4.71	5.24	6.13	4.69	$1.342 \cdot 10^{-6}$
	Hog	5.51	4.69	4.07	4.06	$2.498 \cdot 10^{-5}$

Table 4.3 Reliability Indices for Triton

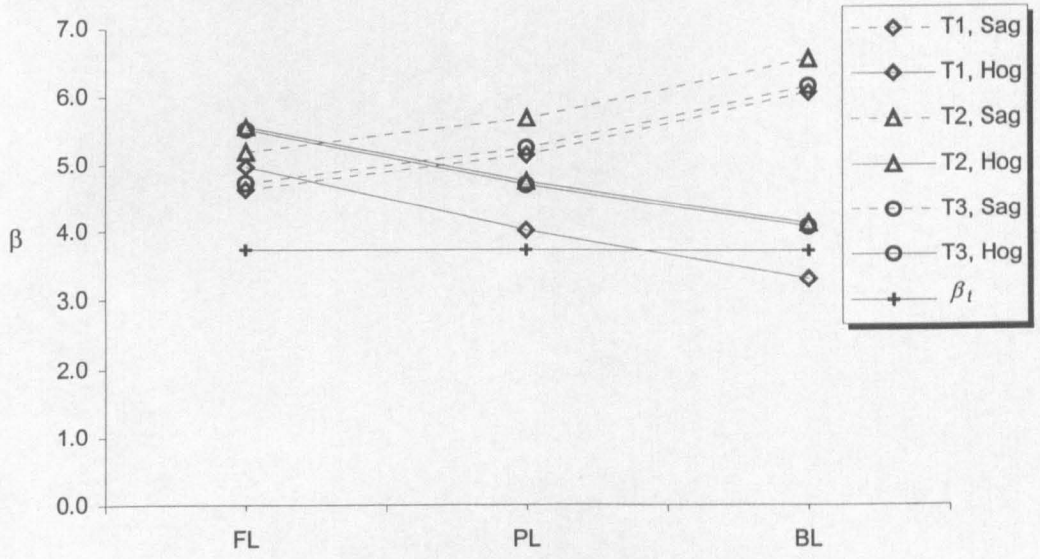

Figure 4.4 Reliability Indices for Triton

From Table 4.3 and Figure 4.4 it can be seen that the reliability index β is well above the target reliability of 3.71 in all conditions for Triton 2 and 3, indicating safe designs. The only value that drops below the target is the ballast hog condition for Triton 1, a reliability index of 3.28 corresponds to one failure in 2000 years. The low β value is mainly due to the high value of the extreme hogging stillwater bending moment in ballast condition (3139 MNm). If strict control is applied on the loading procedure, so that the calculated SWBM for ballast loading of 2300 MNm may be taken as the extreme value, a reliability index of 3.97 is achieved in hogging for the ballast condition. The annual reliability index in hogging for Triton 1 will then be 3.82, which is above the target value.

The sensitivity factors α_i show the relative importance of each variable, at the design point, within a given limit state function. A positive sign indicates that the corresponding basic variable is a "loading variable" (e.g. M_{se} and M_{we}), and a negative sign indicates a "strength

variable" (e.g. M_u). An increase in a positive sensitivity reduces the failure margin, thus reducing the reliability.

	Sagging			Hogging		
Variable	Full Load	Partial Load	Ballast Load	Full Load	Partial Load	Ballast Load
x1 - χ_u	-0.5064	-0.4815	-0.4421	-0.5598	-0.694	-0.8087
x2 - M_{se}	0.0257	0.0711	0.1264	0.0249	0.0919	0.1996
x3 - χ_w	0.4834	0.4872	0.4653	0.4404	0.4317	0.3613
x4 - χ_{nl}	0.2618	0.2698	0.263	0.3747	0.3629	0.2974
x5 - M_{we}	0.6639	0.673	0.7092	0.5929	0.4379	0.2953

Table 4.4 Sensitivity Factors, α_i

The relative importance of each basic variable on the failure function is plotted in Figure 4.5 and Figure 4.6, for the load conditions with the highest probability of failure. The variables associated with ultimate strength and wave induced bending moments are dominating in all conditions. This indicates that more effort should be put into developing better methods for predicting these variables. It is worth noting the relatively low sensitivity of the reliability to the stillwater induced bending moments.

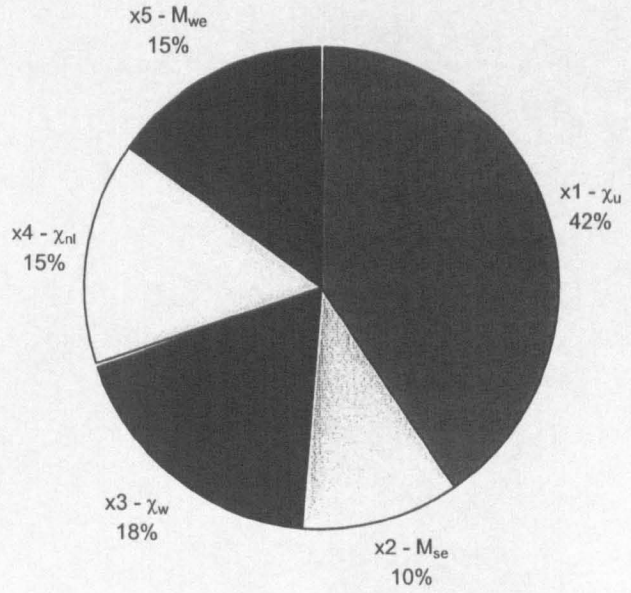

Figure 4.5 Sensitivity of Variables, Triton 2 Ballast Load Hogging

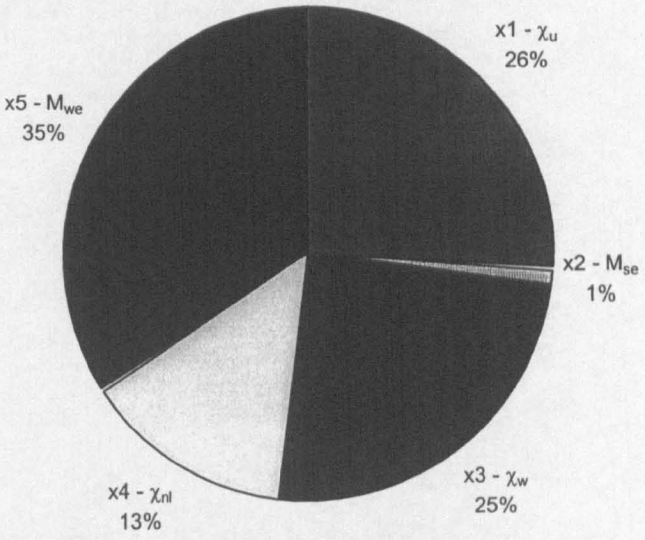

Figure 4.6 Sensitivity of Variables, Triton 2 Full Load Sagging

4.4.2 Sensitivity Analysis

A study was carried out to investigate the sensitivity of β with respect to the distribution parameters for Triton 2. Whereas the sensitivity factors relate to the relative importance of each variable, at the design point, a sensitivity analysis consider the changes in the reliability index with changes in the basic variables.

In Figure 4.7 the reliability index is plotted against different values of M_{sw}, M_w and M_u. Each graph is produced by changing the variable considered and its standard deviation (to maintain constant COV). The shapes of the curves indicate that the relationships between the variables and β are non-linear. The curves may be used to find the value of M_u giving the a required target reliability, or to establish maximum allowable stillwater loads under certain conditions.

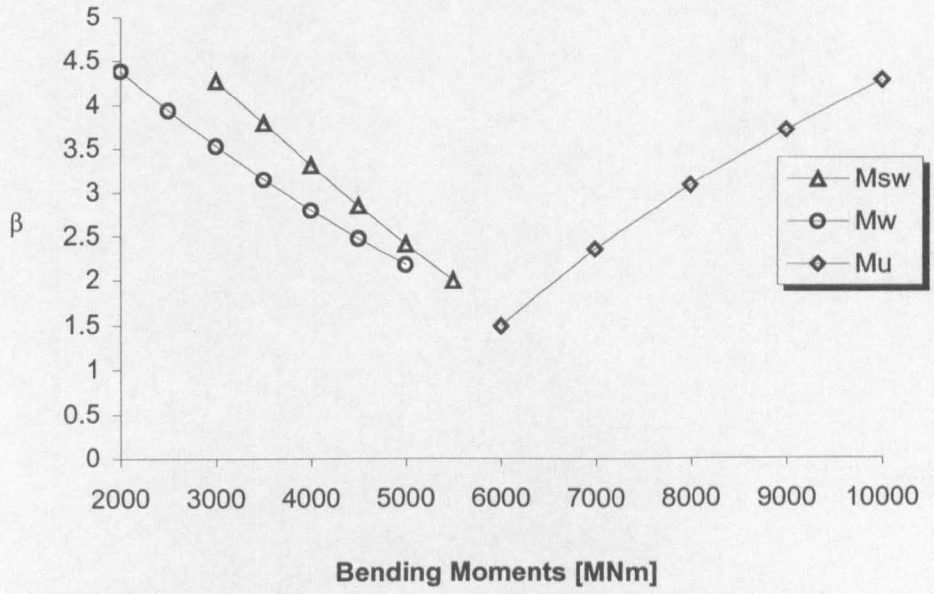

Figure 4.7 Sensitivity Study of Basic Variables for Triton 2 in Ballast Load (Hogging)

4.4.3 Reliability of FPSO at Different Locations

It was shown in chapter 3.4 that the wave statistics (H_s and T_z) influence the VWBM calculations. It is obvious that the wave statistics also will influence the structural reliability of the vessel. This effect was investigated by calculating the reliability of Triton 2 in the three loading conditions (Full, Partial and Ballast) in various locations. The extreme wave loads and the load combination factors were changed to represent the different conditions, no other variables were changed. The results from the analysis are summarised in Table 4.5 for sagging and Table 4.6 for hogging.

Location	Full Load	Partial Load	Ballast Load	β_a	P_f
Area 11	5.18	5.68	6.53	5.17	$1.17 \cdot 10^{-7}$
Central North Sea	6.31	6.87	7.71	6.31	$1.40 \cdot 10^{-10}$
Northern North Sea	4.18	4.69	5.54	4.16	$1.57 \cdot 10^{-5}$
West of Shetlands	3.74	4.37	5.30	3.72	$9.85 \cdot 10^{-5}$

Table 4.5 Reliability Indices for Triton 2 in Sagging

Location	Full Load	Partial Load	Ballast Load	β_a	P_f
Area 11	5.55	4.74	4.12	4.11	$2.004 \cdot 10^{-5}$
Central North Sea	6.55	5.31	4.66	4.62	$1.927 \cdot 10^{-6}$
Northern North Sea	4.65	3.92	3.44	3.40	$3.371 \cdot 10^{-4}$
West of Shetlands	3.91	3.47	3.19	3.09	$1.018 \cdot 10^{-3}$

Table 4.6 Reliability Indices for Triton 2 in Hogging

As expected there is a significant reduction in β_a from the central North Sea to the more severe area west of Shetlands. A reliability index of 3.09 is well below the target reliability chosen for Triton. The value obtained for the northern parts of the North Sea is also too low, due to the low reliability in the ballast condition. This may be acceptable if appropriate heavy weather countermeasures are taken to avoid ballast load during storm conditions. A separate study must be carried out to investigate the resulting reliability of the vessel, when heavy weather countermeasures are taken into account.

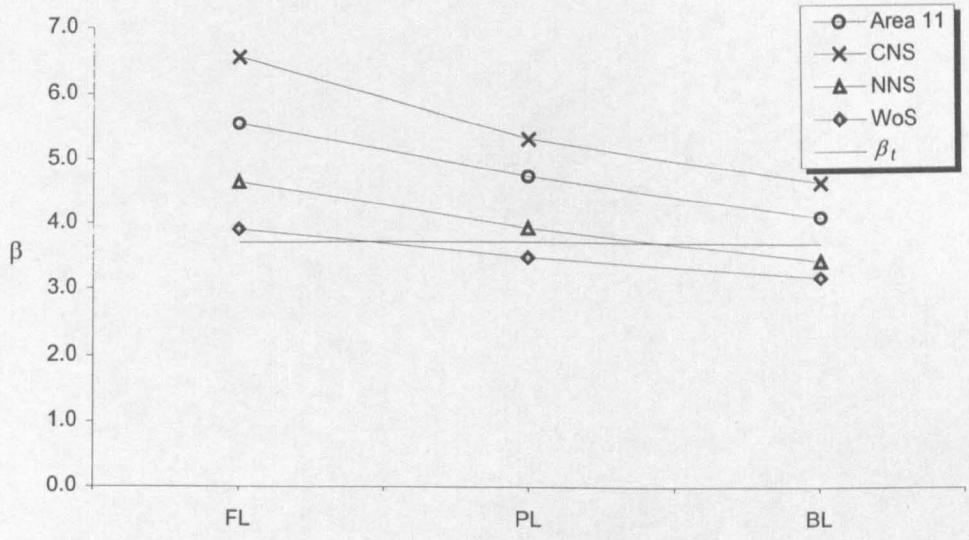

Figure 4.8 Reliability Indices for Triton 2 in Hogging.

4.5 Partial Safety Factors

A level 1 code is a conventional deterministic code in which the nominal values of the strengths of the structural members are governed by a number of partial coefficients. The safety and serviceability of the structure is achieved by use of suitable partial factors in the design. The main reason for using partial safety factors (*psf*), as opposed to single safety factors is that this is the only way to achieve a reasonable standard of reliability for different designs within a code. The most consistent standard is obtained when a safety factor is assigned to each of the main sources of uncertainties. These reliability based safety factors, γ_i, account for uncertainties in loads, load effects and limit values, and for the relative degrees of seriousness of the various limit states. Thus, for the reliability analysis of a mid-ship section ultimate strength, it will be reasonable to assign safety factors, γ_i, to the capacity of the cross-section M_u and to the two loads M_{sw} and M_w.

These partial coefficients are related to the level 2 design point, with the co-ordinates $(\beta\alpha_1, \beta\alpha_2, \ldots, \beta\alpha_n)$, where α_i is defined by Eq. 4.16. If the values of the design point $\bar{x}^*$ were to be used as the design values $\bar{x}_d$ in a deterministic level 1 design calculation, the resulting structure would have a reliability index β and a reliability $\Re = 1-\Phi(-\beta)$. Thus, if $\Re$ is an acceptable reliability for the structure, a satisfactory set of partial coefficients is given by:

$$\gamma_i = \frac{x_{sp_i}}{x_{d_i}} = \frac{x_{sp_i}}{\bar{x}_i^*} \qquad \text{Eq. 4.27}$$

where x_{sp_i} is the specified, or nominal, value of the resistance variable x_i, and by

$$\gamma_j = \frac{x_{d_j}}{x_{sp_j}} = \frac{\bar{x}_j^*}{x_{sp_j}} \qquad \text{Eq. 4.28}$$

where x_{sp_j} is the specified value of the loading variable x_j. Based on the limit state function (Eq. 4.1) the partial safety factors for the mid-ship section ultimate strength, γ_u, γ_s and γ_w could be defined by:

$$\gamma_u = \frac{x_{sp_s}}{\bar{x}_u^*} = \frac{1}{\chi_u^*} \qquad \text{Eq. 4.29}$$

$$\gamma_s = \frac{\bar{x}_s^*}{x_{sp_s}} = \frac{m_s^*}{m_{sp_s}} \qquad \text{Eq. 4.30}$$

$$\gamma_w = \frac{\bar{x}_w^*}{x_{sp_w}} = \frac{\psi \cdot \chi_{nl}^* \cdot \chi_w^* \cdot m_w^*}{m_{sp_w}} \qquad \text{Eq. 4.31}$$

where m_{sp_s} is the mean value of the still-water bending moment in different conditions, and m_{sp_w} is the characteristic value of the wave-bending moment. In this project, the most probable extreme values of SWBM and VWBM have been used as nominal values. The nominal values could also be based on the load manual, or they could be defined from rule requirements. The M_u giving the required reliability level, may be estimated using the relationship:

$$M_u > \gamma_u \cdot (\gamma_w M_w + \gamma_s M_s) \qquad \text{Eq. 4.32}$$

or

$$M_u > \gamma_w^* M_w + \gamma_s^* M_{sw} \qquad \text{Eq. 4. 33}$$

where

$$\gamma_w^* = \gamma_u \cdot \gamma_w \quad \text{and} \quad \gamma_s^* = \gamma_u \cdot \gamma_s. \qquad \text{Eq. 4. 34}$$

The *psf* γ_w account for non-linear effects, uncertainties on the 2D-linear strip theory and statistical uncertainties associated with the wave data. This means that the extreme value calculated for the hogging wave bending moment should be multiplied by this γ_w in a deterministic analysis. Similarly, the UBM obtained from the ultimate bending moment analysis and the extreme stillwater bending moments calculated, should be multiplied by their respective safety factors, which account for uncertainties in these variables.

Using Eq. 4.29-31 the partial safety factors for the mid-ship section ultimate strength was obtained at the target reliability ($\beta = 3.71$) design point for all conditions in both hogging and sagging. The full details of the design point of each condition are shown in Appendix I. The partial safety factors for hogging and sagging are plotted against load condition in Figure 4.9 and Figure 4.10 respectively.

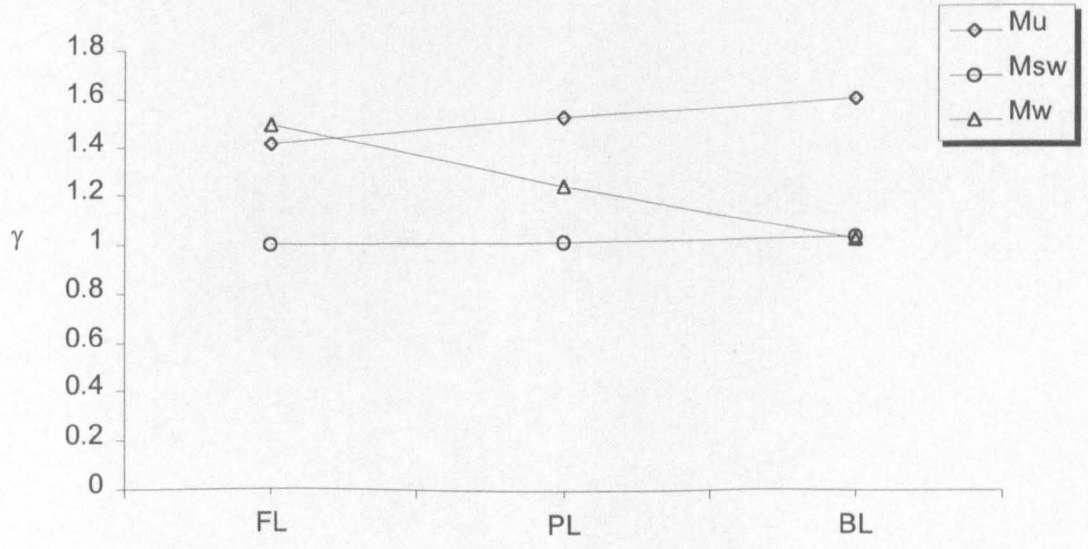

Figure 4.9 Partial Safety Factors Hogging

The uncertainty on wave load results in partial coefficients in the range from 1.5 to 1.0 depending on the loading condition. The relatively high uncertainty on ultimate strength

(COV of 15%) is reflected in a safety factor γ_u of approximately 1.5, increasing with SWBM. A safety factor of 1.0 is found for the stillwater load, indicating that there is very low uncertainty on stillwater loads.

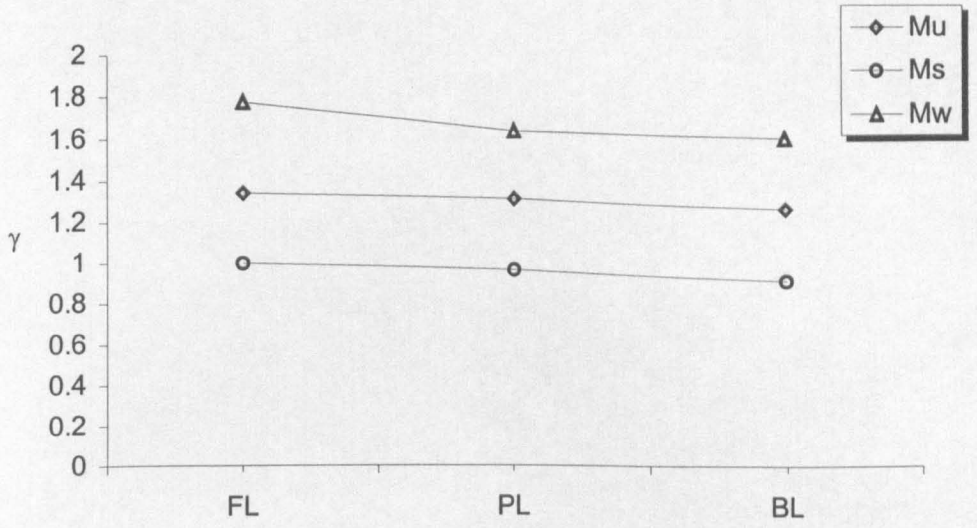

Figure 4.10 Partial Safety Factors Sagging

It is important to remember that the SWBM is always a hogging moment for Triton, and it will act in the opposite direction of a sagging VWBM. This does not affect the sign of the partial safety factors, but the sagging strength and VWBM will have opposite signs to SWBM in the sagging condition.

From Figure 4.10 it can be seen that the factor related to wave bending moment, γ_w is approximately 1.7 and, γ_s takes a value of ~1.0 in all conditions. The uncertainty on ultimate strength gives a factor of nearly 1.35 for the partial safety factor on M_u.

4.5.1 Calibration of Partial Safety Factors

When developing design codes it is desirable to obtain partial safety factors that are applicable to a wide range of designs and conditions, not just one particular load condition for one ship. The partial coefficients are optimised at a particular safety level, typically β_t = 3.71, and the factors calculated for one design might not give a good results for other designs. A more general set of partial safety factors is obtained by an optimisation procedure, where the factors for several vessels (and load conditions) are calibrated to reduce the total deviation from the target reliability. An optimisation algorithm may be defined as:

objective function ?

$$K = \sum_{i=1}^{i=m} \sum_{j=1}^{j=n} (\beta_{i,j} - \beta_t)^2 \qquad \text{Eq. 4.35}$$

where $\beta_{i,j}$ is the reliability index of the j^{th} load condition of the i^{th} ship, m and n is the number of load conditions and ship designs respectively and K is the sum of the squares of deviations in $\beta_{i,j}$ from β_t.

The optimisation process could be considered as a 3-dimensional problem, with ship type and loading condition along two axes and β along the third, where the goal is to minimise K by changing γ_w^* and γ_s^*. If it is not possible to minimise K to an acceptable value (i.e. the spread is too large), it is necessary to reduce the number of ships or load conditions, or increase the number of partial safety factors. On the other hand, if a good fit is obtained it might be useful to introduce a fourth "dimension" of optimisation. For example, the effect of different wave statistics could be included in the safety factors, by adding a summation term to Eq.4.35

Figure 4.11 shows an example, where the reliability indices for 10 ship designs with five load conditions are plotted in 3D. Ideally, all points on the surface in Figure 4.11 should be above a plane defined by the target reliability, but this is not always required.

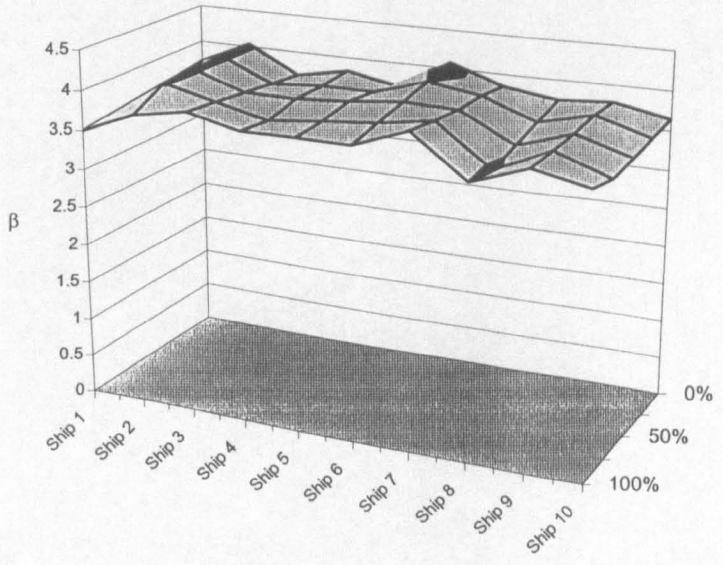

Figure 4.11 β-Values for a Range of Vessels and Load Conditions

An optimisation of partial safety factors for a full range of ship designs is beyond the scope of this project. However, the procedure is the same for one ship as for a class of ship, thus the calibration was included for completeness. Based on the assumption that the basic variables vary linearly between load conditions, a set of partial safety factors was optimised for Triton in hogging and sagging respectively. These factors could be used in the design of a similar FPSO with the same operation profile and expected wave loading.

The first step was to determine the M_{ut} required to achieve a β of 3.71 in all load conditions in both hog and sag. The partial safety factors were then optimised by minimising K in Eq. 4.33 under the constraint that $M_u > M_{ut}$. Then the new M_u based on γ_w^*, γ_s^*, and the nominal values of wave- and still water bending moments, was applied in the reliability analysis to check the resulting reliability index, β. The results of the optimisations are shown in Table 4.7.

	Hogging			Sagging		
	Full Load	Partial Load	Ballast Load	Full Load	Partial Load	Ballast Load
M_{sw}	768	1982	3139	-358	-922	-1461
M_w	2358	2538	2289	2358	2538	2289
M_{ut}	6084	7825	8977	5166	4299	2877
β_t	3.71	3.71	3.71	3.71	3.71	3.71
γ_u	1.22	1.22	1.22	1.68	1.68	1.68
γ_s	1.05	1.05	1.05	1.14	1.14	1.14
γ_w	1.77	1.77	1.77	1.47	1.47	1.47
γ_s^*	1.28	1.28	1.28	1.92	1.92	1.92
γ_w^*	2.16	2.16	2.16	2.48	2.48	2.48
M_u	6084	8031	8977	5166	4530	2877
β	3.71	3.84	3.71	3.71	3.81	3.71

Table 4.7 Calibration of Partial Safety Factors

The two sets of partial safety factors shown in Table 4.7 are supposed to represent the uncertainty on the separate basic variables for all three load conditions. They are optimised to give the lowest *total* deviation from the target reliability, they are not immediately related to the factors obtained at the design point for each load condition shown in Figure 4.9 and Figure 4.10. The optimisation of *psf* for the sagging condition give relatively high values for γ_s^* and γ_w^*. It is important to keep in mind that the stillwater bending moment has a negative sign, so that these high values cancels each other out when the required ultimate bending moment is calculated.

The β-values obtained by calculations based on partial safety factors for Triton, are quite close to the target reliability (see also Figure 4.12). There are some deviations in the values obtained for the partial loading condition for both hogging and sagging, but the results are within acceptable limits. This indicates that the *psf* give a good representation of the ultimate strength model for all load conditions. The next step in the calibration of *psf* would be to analyse a class of vessels, and then optimise a set of partial safety factors to represent this class of ships.

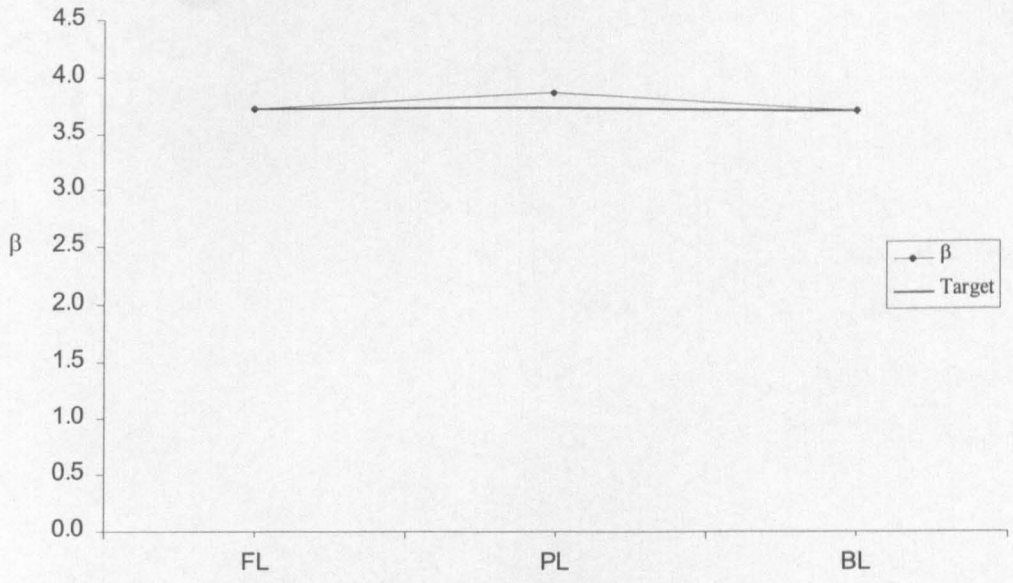

Figure 4.12 Reliability Indices for Triton in Hogging, Based on Partial Safety Factors

The partial safety factors may be used in the design of vessels that are similar to Triton. If the loads are known, a design value for M_u may be obtained using the partial safety factors. A vessel designed with this ultimate bending moment will satisfy a reliability requirement of 3.7, as long as the operational profile (Stillwater loads) and wave loading is the same as for Triton.

4.6 Conclusions

The reliabilities of three different structural designs of Triton were investigated. The structural reliability analysis was based on input from the ultimate strength and load analyses. For each design annual reliability indices β_a were obtained for both hogging and sagging condition. These values were compared with the proposed target value from DNV of one failure in 10,000 or $\beta_a = 3.71$.

The reliability analysis showed that the as-built FPSO design, Triton 2, has annual reliability indices of 5.17 and 4.11 in the sagging and hogging respectively. This indicates that the vessel is safe against longitudinal collapse of the hull girder. The hogging β value corresponds to one failure in ~50,000 years, or one failure a year in 50,000 structures.

The initial tanker design Triton 1 has a probability of failure of 5.143×10^{-4} per year in hogging. This equals a β_a value of 3.28, or roughly one failure in 2,000 years. If some control is applied on the loading procedure of the FPSO, a reliability index of 3.97 is obtained in hogging for the ballast condition. This gives an annual reliability index in hogging for Triton 1 of 3.82, which is above the target value.

Based on the relatively high reliability index obtained for Triton 2 in sagging, a design (Triton 3) where only the bottom structure was strengthened was analysed. This design has a reliability index in sagging of 4.69, which is an improvement from the value of 5.17 for Triton 2. As a part of the design process, an optimisation should be carried out in order to reduce the excess strength in both sagging and hogging.

The results show that, from an ultimate-strength point of view, the strengthening of the deck structure from Triton 1 to Triton 2 was unnecessary. The sagging capacity of the midship section was satisfactory, or in fact very high ($\beta = 4.62$), in the initial design. The hogging reliability was increased from one failure in 2,000 for Triton 1 to one in 50,000 for Triton 2, so the strengthening of the bottom structure reduced the probability of failure to an acceptable value. However, if the load control discussed above is applied, the initial design would satisfy the target reliability.

The influence of wave statistics (H_s and T_z) on the reliability of Triton 2 was investigated by calculating the reliability of the vessel in various locations. It was found that the annual reliability indices for sagging ranged from 3.72 west of Shetlands to 6.31 in the central North Sea, and in hogging the values were between 3.09 and 4.62, for the same areas. These results show the importance of carrying out a site-specific analysis, and the necessity of obtaining ample wave data for that location.

Two sets of partial safety factors were optimised to represent the uncertainty on the separate basic variables in all three load conditions. For hogging, partial safety factors of a 1.22, 1.05 and 1.77 were obtained for γ_u, γ_s and γ_w respectively, whereas in sagging the values obtained were 1.68 for γ_u, 1.14 for γ_s and 2.16 for γ_w. Using these safety factors in a deterministic analysis will give a design with a reliability index of approximately 3.71.

When assessing the reliability of structures it is important to remember the notional nature of the structural reliability analysis. Different formulations of the limit state function will give significantly different results.

5 Conclusions and Discussion

The purpose of this chapter is to summarise the conclusions made in the preceding chapters, and discuss the results of the analysis. Some recommendations for further work are made based on the experiences drawn from this project.

The aim of the project was to establish a realistic structural response of FPSOs, with a probabilistic environmental loading and to carry out a structural reliability analysis of Triton considering the ultimate limit-state. A limit state function for the longitudinal collapse of the hull girder was defined and the basic variables were obtained through ultimate strength and load analyses.

The ultimate bending moments were calculated using Lloyds Register's LRPASS Programs 20202 and 20203. Three different mid-ship sections for Triton have been analysed. Triton 1 is the initial tanker design, Triton 2 is the improved, as-built, FPSO design and Triton 3 is an intermediate design, where only the bottom panels have been strengthened. The Triton 3 design was developed after initial calculations showed that the Triton 2 had very high reserve strength in sagging. The focus of the analyses has been on Triton 2, since this is the as-built design.

The ultimate bending moment capacity was increased by 18% and 16 % in sagging and hogging respectively from Triton 1 to Triton 2. For Triton 3, an increase in the hogging capacity of 15% was achieved, whereas the sagging capacity was just marginally increased (3%). A traditional elastic analysis showed that all three designs satisfied the IACS rule requirements for section modulus and 2nd moment of area.

Only vertical bending moment has been considered, the hull girder loads are divided into still water induced and wave induced components. The still-water vertical bending moments for each loading condition were calculated using Autohydro 4.0. The SWBM obtained was taken as the mean, μ_{sw}, of the still-water bending moment distribution, and a COV of 15% was applied. This COV value only represents minor deviations from the load manual. Gross errors were not taken into account in the analysis. It was assumed that appropriate load control systems are installed on the FPSO.

The loading pattern of the vessel is such that the ship will always have a hogging stillwater bending moment, ranging from 564 MNm in full load to 2300 MNm in the ballast condition. The extreme SWBM values for the ballast load condition will tend to be conservative due to two assumptions. Firstly, the SWBM was assumed to follow a normal distribution in both hog and sag (this will also affect Full and Partial conditions), and secondly the effect of heavy weather countermeasures was not included in the analysis. Both these assumptions will produce lower values for the annual reliability than what might be actual reliability of the vessel.

A procedure for calculating the long-term distribution of the wave induced bending moments based on short-term response was used. Transfer functions for VWBM response were calculated using the 2-D strip theory program TRIBON Hydro from Kockums Computer Systems. Non-linearities were accounted for by a model uncertainty factor χ_{nl} in the reliability analysis. Based on the wave-induced response, short-term responses in irregular waves were calculated using the principle of linear superposition and wave statistics. The short-term responses were combined with long-term wave statistics for the North Sea to determine the long-term probability of exceedance of different wave-induced vertical bending moments. A Weibull distribution was fitted to the resulting distribution. Then the most probable extreme values per year for each load condition were calculated.

The vertical mooring forces on the FPSO are small, and have insignificant influence on the bending moment response. The same transfer functions, and consequently the same wave loads, was used for Triton 1, 2 and 3, neglecting the slightly different weight distributions caused by variations in the scantling variations between the designs.

The two loading components have been considered independent and Ferry Borges – Castenheta load combination method has been applied to obtain load combination factors for the Full Load, Partial Load (50 % loaded) and Ballast condition. As no information on the loading procedures for the FPSO was available, a simplified operation profile based on the production capacity was estimated, and a rectangular pulse process was fitted.

The reliability analysis was carried out using the SORM analysis in *CALREL*. Annual reliability indices (β_a) and probabilities of failures were calculated for hogging and sagging conditions. These values were compared with a target reliability of 3.71 as proposed by

DNV (1992). The reliability analysis showed that the as-built FPSO design, Triton 2, has annual reliability indices of 5.17 and 4.11 in the sagging and hogging respectively. These β values indicate that the vessel is safe against longitudinal collapse of the hull girder. The β value for hogging corresponds to one failure in ~50,000 years, or one failure a year in 50,000 structures.

The initial tanker design Triton 1 has a probability of failure of 5.143×10^{-4} per year in hogging. This equals a β_a value of 3.28, or roughly one failure in 2,000 years, which is lower than the target reliability. However, if some control is applied to the loading procedure of the FPSO, so that the extreme ballast SWBM may be taken as 2300 MNm instead of 3139 MNm, a reliability index of 3.97 is obtained in hogging for this condition. The annual reliability index in hogging for Triton 1 is then 3.82, which is above the target value.

Based on the relatively high reliability index obtained for Triton 2 in sagging, a new design (Triton 3) where only the bottom structure was strengthened was analysed. This design has a reliability index in sagging of 4.69, which is an improvement from the value of 5.17 for Triton 2. As a part of the design process, an optimisation should be carried out in order to reduce the excess strength in both sagging and hogging.

A calculation based on changes in cross-sectional areas estimated the weight of the added material from Triton 1 to Triton 2 to be roughly 4% of the hull weight, equalling 800 tonnes. The change in the design improved the hogging reliability from 3.12 to 3.92. For Triton 3 an increase in the hogging reliability index from 3.12 to 3.90 is achieved by increasing the plate thickness in the bottom plates by 3 mm. The weight of the added material from Triton 1 to Triton 3 is around 2% of the hull weight, or approximately 400 tonnes.

The Triton FPSO will be stationed in the North Sea, close to the Gannet complex and Hogben's Global Wave Statistics Area 11 was assumed to represent the wave statistics for this location. The influence of different wave statistics (H_s and T_z) on the reliability of Triton 2 was investigated by calculating the reliability of the vessel in various locations. It was found that the annual reliability indices for sagging ranged from 3.72 west of Shetlands to 6.31 in the central North Sea, and in hogging the values were between 3.09 and 4.62, for the same areas. These results show the importance of carrying out a site-specific analysis, and the necessity of obtaining ample wave data for that location.

Considering the low probability of slamming for Triton, and keeping in mind, that slamming is only associated with sagging, and that hogging is the dominating condition for Triton, it was decided to ignore slamming induced VBM in this report. However, slamming is known to occur on FPSOs operated in harsh weather, but it is believed to constitute more of a problem in the detailed design of local elements.

The structural reliability analysis indicates that the Triton FPSO is safe against longitudinal collapse of the hull girder, if it is located at this specific site and loaded according to the load manual.

References and Bibliography

'Appraisal and Development of Structured Reliability Methodologies for FPSO Units - An Engineer's Guide - Proposal for Joint Industry Project', The Centre for Marine and Petroleum Technology (CMPT), August 1997.

'Buckling Strength Analysis', Classification notes No.30.1, Det Norske Veritas, 1995' Environmental Conditions and Environmental Loads', Classification notes No.30.5, Det Norske Veritas, 1991.

'Floating Production Systems', IIR's Third Annual Floating Production Systems Conference, March 1996.

'Guide For Building and Classing; Floating Production Storage and Offloading Systems',American Bureau of Shipping, 1996.

'Hull Structural Design Ships with Length 100 Metres and Above', Rules for Classification of Ships, Part 3 Chapter 1, Det Norske Veritas, 1997.

'Proceedings of the 11th International Ship and Offshore Structures Congress', Volume 2, ISSC, China, 1991.

'Rationalisation of safety and serviceability factors in structural codes', Report 63, CIRIA, London, 1977.

'Structural Reliability Analysis of Marine Structures', Classification notes No.30.6, Det Norske Veritas, 1992.

Adamchak, J.C.: 'An Approximate Method for Estimating the Collapse of a Ship's Hull in Preliminary Design', Ship Structures Symposium '84, Arlington, VA, USA, October 1984.

Ahilan, R.V., Bush, R.B. and Trickey, J.C.: 'FPS Mooring/Riser System Design-Advantages of Integration', Noble Denton Europe Ltd., U.K.

Ahilan, R.V., Cummins, I., Dyer, R.C. and Morris, W.D.M.: 'Reliability Analysis of FPSO Mooring Systems and the Interaction with Risers', Proceedings of the 15th International Conference, OMAE, 1996.

Band, E.G.U.: 'Analysis of Ship Data to Predict Long-Term Trends of Hull Bending Moments', ABS Report, 1966.

Bennet, R. et al.: 'Results from Full-Scale Measurements and Predictions of Wave Bending Moments Acting on Ships', Swedish Shipbuilding Research Foundation, Report no. 32, 1962.

Billingsley, D. 'Hull Girder Response to Extreme Bending Moments' Proc. SNAME STAR Symposium, Coronado, California, 1980.

Breitung, K.: 'Asymptotic Approximations for Multinormal Integrals', Journal of Engineering Mechanical Division, ASCE, Vol. 110, No. 3, pp.357-366, 1984.

Caldwell, J.B.: 'Ultimate Longitudinal Strength' Trans. RINA, 1965.

Cartwright, D.E. and Longuet-Higgins, M.S.: 'The Statistical Distribution of the Maxima of a Random Function', Proc. Roy. Soc. of London, Ser. A, Vol 237, 1956.

Chalmers, D.W.: 'Design of Ships' Structures', Ministry of Defence, London, 1993.

Chan, H.S.: 'A Three Dimensional Technique for Predicting 1st and 2nd Order Wave Hydrodynamic Forces on a Marine Vehicle Advancing in Waves', PhD Thesis, University of Glasgow, 1990.

Compton, R.: 'The Prediction of Long-Term Distributions of Bending Moment from Model Testing', Maritime Technology, 1968.

Cornell, C.A.: 'A Probability Based Structural Code', Journal of American Concrete Institute, Vol. 66, No.12, pp.974-985, 1969.

Creswell, D.J. and Dow, R.S.: 'The Application of Non-linear Analysis to Ship and Submarine Structures', Symposium on Advances in Marine Structures, ARE, Dunfermline, Scotland, May 1986.

Dalzell, J.F, Maniar N.M. and Hsu, M.W.: 'Examination of Service and Stress Data of Three Ships for Development of Hull Girder Load Criteria', SSC-287,1979.

Damonte, R., Figari, M. and Porcari, R.: 'Ultimate Bending Moment of The Ship Hull Girder', University of Genova, Int. Shipbuild. Prog., 44, no. 440, pp 299-319, 1997.

Dogliani, M., Casella, G. and Guedes Soares, C.: 'SHIPREL – Reliability Methods for Ship Structural Design', BRITE/EURAM project 4554, Lisbon, 1995.

Dow, R.S. et al: 'Evaluation of Ultimate Ship Hull Strength', Symposium on Extreme Loads Response, SNAME, Arlington, VA, 1981.

Faulkner, D.: 'Compression Strength of Welded Grillages' in Ship Structural Design Concepts, Cornell Maritime Press, 1975.

Faulkner, D.: 'Introduction to Probability Methods in Design', Advanced design for Ships and Offshore Floating Systems, University of Glasgow, 1992.

Ferro, G. and Cervetto, D.: 'Hull Girder Reliability', Ship Structure Symposium '84, Arlington, VA, USA, October 1984.

Ferro, G. and Mansour, A.E.: 'Probabilistic Analysis of Combined Slamming and Wave Induced Responses', Journal of Ship Research, Vol. 29, No. 3, September 1985.

Ferry Borges, J. and Castanheta, M.: 'Structural Safety', Laboratorio Nacional de Engenharia Civil, Lisbon, 1971.

Freudenthal, A.M., Garrelts, J.M. and Shinozuka, M.: 'The Analysis of Structural Safety', Journal of Structural Division, ASCE, Vol. 92, pp. 235-246, 1966.

Gerritsma, J. and Beukelman, W.: 'Analysis of the Modified Strip Theory for the Calculations of Ship Motions and Wave Bending Moments', Int. Shipbuilding Prog., Vol 14, 1967.

Gordo, J.M. and Guedes Soares C.: 'Approximate Method to Evaluate the Hull Girder Collapse Strength', Universidade Técnica de Lisboa, 1996.

Gordo, J.M., Guedes Soares, C. and Faulkner, D.: 'Approximate Assessment of the Ultimate Longitudinal Strength of the Hull Girder', Journal of Ship Research, vol. 40, no.1, pp 60-69, 1996.

Guedes Soares, C.: 'Probabilistic Models for Load Effects in Ship Structures', Division of Marine Structures, The Norwegian Institute of Technology, Report UR-84-38, 1985.

Guedes Soares, C. and Moan, T.: 'Statistical Analysis of Stillwater Load Effects in Ship Structures', Transactions of the Society of Naval Architecture and Ocean Engineers, New York, Vol.96, 1988.

Guedes Soares, C.: 'Stochastic Models of Wave Induced Load Effects', COMETT, Instituto Superior Técnico, 1993.

Hasofer, A.M. and Lind, N.C.: 'An exact and Invariant First-Order Reliability Format', Journal of Structural Division, ASCE, Vol. 100, pp. 111-121, 1974.

Hogben, N. : 'Ocean wave statistics : a statistical survey of wave characteristics estimated visually from the voluntary observing ships sailing along the shipping routes of the world' HMSO, London, 1967.

Hogben, N., Da Cuna, L.F. and Ollivier, H.N.: 'Global Wave Statistics', British Maritime Technology, London, 1986.

Hsao H. Chen, Hsien Y. Jan, Conlon, J.F., Liu, D.: 'New Approach to The Design and Evaluation of Double Hull Tanker Structures', SNAME Centennial Meeting, 1993.

Inglis, R.B.: 'Production Facilities Selection for Deep Water Oil and Gas Field Development', Institution of Engineers and Shipbuilders in Scotland, April 1996.

Kaminski, M.L.: 'Reliability Analysis of FPSOs Hull Girder Cross Sectional Strength', Proceedings of the 16th International Conference, OMAE, 1997.

Key, J.W., Schumaker, F.E. and Theisinger, E.J.: 'Design and Analysis of Turret Mooring Systems for Tanker-Based Storage or Production Facilities', OTC 5250, 1986.

Larrabee, R.D. and Cornell, C.A,: 'Combination of Various Load Processes', Journal of Structural Division, ASCE, Vol 107, pp. 223-238, 1981.

Lewis, E.V.: 'A Study of Midships Bending Moments in Irregular Head Seas' Journal of Ship Research, Vol. 1, 1957.

Lewis, E.V.: 'Predicting Long-Term Distributions of Wave-Induced Bending Moment on Ship Hulls', SNAME, 1967.

Lewis, E.V., Hoffman, D., et al: 'Load Criteria for Ship's Structural Design', SSC Report SSC-240, 1973.

Lewis, E.V. et al: 'Load Criteria for Ship Structural Design', Ship Structure Comitte, Report No. SSC-224, Washington, DC, USA, 1975.

MacGregor, J. and Smith, S.N.: 'Some Techno-Economic Considerations in the Design of North Sea Production Monohulls'. Presented at IMarE/RINA Offshore-94, February 1994.

Manners, W.: 'Improving The Acceptability of Reliability-based Safety Factors for the Design of Structural Systems', Reliability and Optimisation of Structural Systems '88, Proc. 2nd IFIP W.G7.5 Conference, London, 1988.

Mano, H., Kawabe, H., Iwakawa, K. and Mitsumune N.: 'Statistical Character of the Demand on Longitudinal Strength (second report) – Long Term Distribution of Stillwater Bending Moment', Journal of Soc. Naval Architects of Japan, Vol. 142, pp. 255-263, 1977.

Mansour, A.E. and d'Olivera, J.: 'Hull Bending Moment Due to Ship Bottom Slamming in Regular Waves', Journal of Ship Research, Vol. 19, No. 2, June 1975.

Mansour, A.E. and Lozow, J.: 'Stochastic Theory of the Slamming Response of Marine Vehicles in Random Seas', Journal of Ship Research, Vol. 26, No. 4, December 1982.

Mansour, A.E. and Thayamballi, A.: 'Probability Based Ship Design; Loads and Load Combinations', SSC-373, Ship Structure Committee, 1994.

Mansour, A.E., Lin, Y.H. and Paik, J.K.: 'Ultimate Strength of Ships under Combined Vertical and Horizontal Moments', Proc. 6th Intl Symp., PRADS, Seoul, Korea, 1995, pp 2.844-2.851.

Mansour, A.E., Wirsching, P., Luckett, M., Plumpton, A., et al.: 'Assessment of Reliability of Ship Structures ', SSC-398, Ship Structure Committee, 1997.

Miller, N.S.: 'The Factors Affecting the Choice of FPS with Special Reference to Tanker Based Systems', 2nd International Conference - The Way Forward for Floating Production Systems, London, 1986.

Moan, T. and Jiao, G.: 'Characteristic Stillwater Load Effects for Production Ships' Report MK/R 104/88, The Norwegian Institute of Technology, 1988.

Nordenstrøm, N.: 'Methods for Predicting Long-Term Distributions of Wave Loads and Probability of Failure of Ships', DNV, Research and Development Report 71-2-s, 1971.

Ochi, M.: 'Extreme Loads Response Symposium', Sponsored by the Ship Structure Committee and the SNAME, New York, 1981.

Ochi, M. and Motter, L.E.: 'Prediction of Slamming Characteristics and Hull Response for Ship Design' Transactions of SNAME, Vol 81, 1973.

Paik, J.K. and Mansour, A.E.: 'A Simple Formulation for Predicting the Ultimate Strength of Ships', Jnl of Marine Science and Technology, vol. 1, pp 52-62, 1995.

Rackwitz, R. and Fiessler, B.: 'An Algorithm for Calculation of Structural Reliability under Combined Loading', Berichte zur Sicherheitstheorie der Bauwerke, Lab. f. Konstr. Ingb., München, 1977.

Rowe, S.J. and Welsh, M.: 'Concept Design of FPSOs for Harsh Environments', BMT Offshore Limited, BMT Ship Design Limited.

Rutherford, S.E. and Caldwell, J.B.: 'Ultimate Longitudinal Strength of Ships: A Case Study', SNAME, New Jersey, 1990.

Rutherford, S.E.: 'Hull Strength under Bending and Shear - Program Manual', Lloyd's Register of Shipping, Hull Structures Report No. 83/39, June 1983.

Rutherford, S.E.: 'Stiffened Compression Panels: the Analytical Approach', Lloyd's Register of Shipping, Internal Report No.82/26/R2, June 1982.

Salvesen, N., Tuck, E.O. and Faltinsen, O.: 'Ship Motions and Sea Loads', Trans. SNAME, Vol. 78, 1970.

Shellin, T., Östergaard, C. and Guedes Soares, C.: 'Uncertainty Assessment of Low Frequency Wave Induced Load Effects for Containerships', Marine Structures, Vol.9, no. 3-4, pp. 313-332.

Smith, C.S.: 'Influence of Local Compressive Failure on Ultimate Longitudinal Strength of a Ship's Hull', PRADS, Tokyo, October 1977.

St. Denis, M. and Pierson, W.J.: 'Prediction of Extreme Ship Responses in Rough Seas of the North Atlantic', Proc. Symposium on the Dynamics of Marine Vehicles and Structures in Waves, 1974.

Søding, H.: 'Calculation of Long-Term Extreme Loads and Fatigue Loads of Marine Structures', Symposium on the Dynamics of Marine Vehicles and Structures in Waves, London, 1974.

Teixeira, A.P.: 'Reliability of Marine Structures in the Context of Risk Based Design', MSc Thesis, University of Glasgow, 1997.

Thayamballi, A., Kutt, L. and Chen, Y.N.: 'Advanced Strength and Structural Reliability Assessment of the Ship's Hull Girder', Symposium on Advances in Marine Structures, ARE, Dunfermline, Scotland, May 1986.

Thaymaballi, A.K., Chen, Y-K and Chen, H-H.: 'Deterministic and Reliability Based Retrospective Strength Assessments of Ocean-going Vessels', Annual Meeting, SNAME, New York, November 1987.

Tvedt, L.: 'Second Order Reliability by an Exact Integral', Reliability and Optimisation of Structural Systems '88, Proc. 2nd IFIP W.G7.5 Conference, London, 1988.

Viner, A.C.: 'Development of Ship Strength Formulations', Symposium on Advances in Marine Structures, ARE, Dunfermline, Scotland, May 1986.

Wang, X. and Moan, T.: 'Stochastic and Deterministic Combinations of Still and Wave Bending Moments in Ships', Marine Structures 9, Elsevier Science Limited,1996.

Wang, X., Guoyang J. and Moan, T.: 'Analysis of Oil Production Ships Considering Load Combination, Ultimate Strength and Structural Reliability', 1995.

Wang, X.: 'Ultimate Strength and Reliability Analysis of a Midship Transverse Frame in an Offshore Production Ship', OMAE 1996.

Appendix A

Input to LR.PASS and Drawing of Midship Section of Triton

Triton 1

Length: 233 m
Breadth: 42 m
Depth: 21.3 m

Material properties (MP):
1= 245 N/mm^2
2= 326 N/mm^2

E= 210000 N/mm^2

Bottom & Side Shell:

Element no.	CID	a	b	t_p	h_w	t_w	b_f	t_f	Area	Z	Y	Pos.	MP
1	0	10	4120	410	18	410	17.5	0	0	14555	0	0	1	2
2	1	11	4120	820	18	450	11.5	150	18	22635	0	820	1	2
3	2	11	4120	820	18	450	11.5	150	18	22635	0	1640	1	2
4	3	11	4120	820	18	450	11.5	150	18	22635	0	2460	1	2
5	4	11	4120	820	18	450	11.5	150	18	22635	0	3280	1	2
6	5	12	4120	820	16.5	450	11.5	150	18	21405	0	4100	1	2
7	6	12	4120	820	16.5	450	11.5	150	18	21405	0	4920	1	2
8	7	12	4120	820	16.5	450	11.5	150	18	21405	0	5740	1	2
9	8	12	4120	820	16.5	450	11.5	150	18	21405	0	6560	1	2
10	9	12	4120	820	16.5	450	11.5	150	18	21405	0	7380	1	2
11	10	12	4120	820	16.5	450	11.5	150	18	21405	0	8200	1	2
12	11	12	4120	820	16.5	450	11.5	150	18	21405	0	9020	1	2
13	12	12	4120	820	16.5	450	11.5	150	18	21405	0	9840	1	2
14	13	12	4120	820	16.5	450	11.5	150	18	21405	0	10660	1	2
15	14	12	4120	820	16.5	450	11.5	150	18	21405	0	11480	1	2
16	15	12	4120	820	16.5	450	11.5	150	18	21405	0	12300	1	2
17	16	12	4120	820	16.5	450	11.5	150	18	21405	0	13120	1	2
18	17	12	4120	820	16.5	450	11.5	150	18	21405	0	13940	1	2
19	18	12	4120	820	16.5	450	11.5	150	18	21405	0	14760	1	2
20	19	13	4120	820	16.5	410	14.5	0	0	19475	0	15580	1	2
21	20	14	4120	820	16.5	500	11.5	150	18	21980	0	16400	1	2
22	21	14	4120	820	16.5	500	11.5	150	18	21980	0	17220	1	2
23	22	14	4120	820	16.5	500	11.5	150	18	21980	0	18040	1	2
24	23	14	4120	820	16.5	500	11.5	150	18	21980	0	18860	1	2
25	BK	15	4120	2828	16.5	400	13	50	18	52762	1050	19910	1	2
26	24	16	4120	800	16	435	11.5	150	15	20053	2100	21000	2	2
27	25	16	4120	800	16	435	11.5	150	15	20053	2920	21000	2	2
28	26	16	4120	800	16	435	11.5	150	15	20053	3740	21000	2	2
29	27	16	4120	800	16	435	11.5	150	15	20053	4560	21000	2	2
30	28	16	4120	800	16	435	11.5	150	15	20053	5380	21000	2	2
31	29	17	4120	800	16	410	13	0	0	18130	6200	21000	2	1
32	30	18	4120	800	17.5	435	11.5	150	15	21253	7020	21000	2	1
33	31	18	4120	800	17.5	435	11.5	150	15	21253	7840	21000	2	1
34	32	18	4120	800	17.5	435	11.5	150	15	21253	8660	21000	2	1
35	33	19	4120	800	17.5	385	11.5	150	15	20678	9480	21000	2	1
36	34	19	4120	800	17.5	385	11.5	150	15	20678	10300	21000	2	1
37	35	20	4120	800	17.5	410	13	0	0	19330	11120	21000	2	1
38	36	19	4120	800	17.5	385	11.5	150	15	20678	11940	21000	2	1
39	37	19	4120	800	17.5	385	11.5	150	15	20678	12760	21000	2	1
40	38	19	4120	800	17.5	385	11.5	150	15	20678	13580	21000	2	1
41	39	19	4120	800	17.5	385	11.5	150	15	20678	14400	21000	2	1
42	40	19	4120	800	17.5	385	11.5	150	15	20678	15220	21000	2	1
43	41	20	4120	800	17.5	410	13	0	0	19330	16040	21000	2	1
44	42	21	4120	800	17.5	400	11.5	100	16	20200	16860	21000	2	1
45	43	22	4120	800	17.5	350	11.5	100	12	19225	17680	21000	2	1
46	44	22	4120	800	17.5	350	11.5	100	12	19225	18500	21000	2	1
47	45	23	4120	800	16	300	11	90	16	17540	19320	21000	2	2
48	46	23	4120	800	16	300	11	90	16	17540	20140	21000	2	2
49	47	23	4120	800	16	300	11	90	16	17540	20960	21000	2	2

Upper Deck

Element	no.	CID	a	b	t_p	h_w	t_w	b_f	t_f	Area	Z	Y	Pos.	MP
50	1	24	4120	820	16.5	250	12	90	16	17970	22051	410	3	2
51	2	24	4120	820	16.5	250	12	90	16	17970	22014	1230	3	2
52	3	24	4120	820	16.5	250	12	90	16	17970	21977	2050	3	2
53	4	24	4120	820	16.5	250	12	90	16	17970	21941	2870	3	2
54	5	24	4120	820	16.5	250	12	90	16	17970	21904	3690	3	2
55	6	24	4120	820	16.5	250	12	90	16	17970	21867	4510	3	2
56	7	24	4120	820	16.5	250	12	90	16	17970	21830	5330	3	2
57	8	24	4120	820	16.5	250	12	90	16	17970	21794	6150	3	2
58	9	24	4120	820	16.5	250	12	90	16	17970	21757	6970	3	2
59	10	24	4120	820	16.5	250	12	90	16	17970	21720	7790	3	2
60	11	24	4120	820	16.5	250	12	90	16	17970	21683	8610	3	2
61	12	24	4120	820	16.5	250	12	90	16	17970	21646	9430	3	2
62	13	24	4120	820	16.5	250	12	90	16	17970	21610	10250	3	2
63	14	24	4120	820	16.5	250	12	90	16	17970	21573	11070	3	2
64	15	24	4120	820	16.5	250	12	90	16	17970	21536	11890	3	2
65	16	24	4120	820	16.5	250	12	90	16	17970	21499	12710	3	2
66	17	24	4120	820	16.5	250	12	90	16	17970	21463	13530	3	2
67	18	24	4120	820	16.5	250	12	90	16	17970	21426	14350	3	2
68	19	25	4120	740	16.5	250	12	90	16	16650	21396	15090	3	2
69	20	25	4120	740	16.5	250	12	90	16	16650	21363	15830	3	2
70	21	25	4120	740	16.5	250	12	90	16	16650	21330	16570	3	2
71	22	25	4120	740	16.5	250	12	90	16	16650	21297	17310	3	2
72	23	26	4120	820	17.5	400	16	0	0	20750	21143	18130	3	2
73	24	27	4120	820	17.5	300	11	90	16	19090	21177	18950	3	2
74	25	27	4120	820	17.5	300	11	90	16	19090	21140	19770	3	2
Inner bottom & Long. Bhd.														
75	1	28	4120	820	16	450	11.5	150	18	20995	2460	820	3	2
76	2	28	4120	820	16	450	11.5	150	18	20995	2460	1640	3	2
77	3	28	4120	820	16	450	11.5	150	18	20995	2460	2460	3	2
78	4	28	4120	820	16	450	11.5	150	18	20995	2460	3280	3	2
79	5	28	4120	820	16	450	11.5	150	18	20995	2460	4100	3	2
80	6	28	4120	820	16	450	11.5	150	18	20995	2460	4920	3	2
81	7	28	4120	820	16	450	11.5	150	18	20995	2460	5740	3	2
82	8	28	4120	820	16	450	11.5	150	18	20995	2460	6560	3	2
83	9	28	4120	820	16	450	11.5	150	18	20995	2460	7380	3	2
84	10	28	4120	820	16	450	11.5	150	18	20995	2460	8200	3	2
85	11	28	4120	820	16	450	11.5	150	18	20995	2460	9020	3	2
86	12	28	4120	820	16	450	11.5	150	18	20995	2460	9840	3	2
87	13	28	4120	820	16	450	11.5	150	18	20995	2460	10660	3	2
88	14	28	4120	820	16	450	11.5	150	18	20995	2460	11480	3	2
89	15	28	4120	820	16	450	11.5	150	18	20995	2460	12300	3	2
90	16	28	4120	820	16	450	11.5	150	18	20995	2460	13120	3	2
91	17	28	4120	820	16	450	11.5	150	18	20995	2460	13940	3	2
92	18	28	4120	820	16	450	11.5	150	18	20995	2460	14760	3	2
93	24	29	4120	785	17.5	450	11.5	125	18	21163	2876	15750	3	2
94	25	29	4120	785	17.5	450	11.5	125	18	21163	3568	16350	3	2
95	26	29	4120	785	17.5	450	11.5	125	18	21163	4260	16950	3	2
96	27	29	4120	785	17.5	450	11.5	125	18	21163	4952	17550	3	2
97	28	29	4120	785	17.5	450	11.5	125	18	21163	5644	18150	3	2
98	30	30	4120	800	15.5	450	11.5	125	18	19825	7020	18419	2	1
99	31	30	4120	800	15.5	450	11.5	125	18	19825	7840	18419	2	1

Element	no.	CID	a	b	t_p	h_w	t_w	b_f	t_f	Area	Z	Y	Pos.	MP
100	32	30	4120	800	15.5	450	11.5	125	18	19825	8660	18419	2	1
101	33	30	4120	800	15.5	450	11.5	125	18	19825	9480	18419	2	1
102	34	30	4120	800	15.5	450	11.5	125	18	19825	10300	18419	2	1
103	35	31	4120	800	14	410	13	0	0	16530	11120	18465	2	1
104	36	32	4120	800	14	400	11.5	100	16	17400	11940	18440	2	1
105	37	32	4120	800	14	400	11.5	100	16	17400	12760	18440	2	1
106	38	32	4120	800	14	400	11.5	100	16	17400	13580	18440	2	1
107	39	32	4120	800	14	400	11.5	100	16	17400	14400	18440	2	1
108	40	33	4120	800	13.5	350	12	100	17	16700	15220	18450	2	1
109	41	34	4120	800	13.5	700	12	150	12	21000	16040	18329	2	1
110	42	33	4120	800	13.5	350	12	100	17	16700	16860	18450	2	1
111	43	33	4120	800	13.5	350	12	100	17	16700	17680	18450	2	1
112	44	35	4120	800	13.5	300	13	90	17	16230	18500	18466	2	1
113	45	36	4120	800	16	800	14	150	14	26100	19320	18409	2	2
114	46	37	4120	800	16	250	12	90	16	17240	20140	18487	2	2
115	47	37	4120	800	16	250	12	90	16	17240	20960	18487	2	2
Stringers:														
116	1	38	4120	820	13	150	12	0	0	12460	6100	20155	3	1
117	2	38	4120	820	13	150	12	0	0	12460	6100	19335	3	1
118	3	38	4120	820	13	150	12	0	0	12460	10900	20155	3	1
119	4	38	4120	820	13	150	12	0	0	12460	10900	19335	3	1
120	5	38	4120	820	13	150	12	0	0	12460	15700	20155	3	1
121	6	38	4120	820	13	150	12	0	0	12460	15700	19335	3	1
Center Long Bhd.:														
122	26	39	4120	910	15.5	450	11.5	125	18	21530	2900	-100	2	2
123	27	39	4120	910	15.5	450	11.5	125	18	21530	3810	-100	2	2
124	28	39	4120	910	15.5	450	11.5	125	18	21530	4720	-100	2	2
125	29	39	4120	910	15.5	450	11.5	125	18	21530	5630	-100	2	2
126	30	40	4120	800	14	400	13	100	18	18200	6485	-100	2	2
127	31	40	4120	800	14	400	13	100	18	18200	7285	-100	2	2
128	32	40	4120	800	14	400	13	100	18	18200	8085	-100	2	2
129	33	40	4120	800	14	400	13	100	18	18200	8885	-100	2	2
130	34	41	4120	800	13	400	13	100	18	17400	9685	-100	2	2
131	35	42	4120	800	13	350	12	100	17	16300	10485	-100	2	2
132	36	42	4120	800	13	350	12	100	17	16300	11285	-100	2	2
133	37	42	4120	800	13	350	12	100	17	16300	12085	-100	2	2
134	38	42	4120	800	13	350	12	100	17	16300	12885	-100	2	2
135	39	42	4120	800	13	350	12	100	17	16300	13685	-100	2	2
136	40	43	4120	800	13	300	13	90	17	15830	14485	-100	2	2
137	41	43	4120	800	13	300	13	90	17	15830	15285	-100	2	2
138	42	44	4120	800	13	300	11	90	16	15140	16085	-100	2	2
139	43	44	4120	800	13	300	11	90	16	15140	16885	-100	2	2
140	44	44	4120	800	13	300	11	90	16	15140	17685	-100	2	2
141	45	45	4120	800	15.5	250	12	90	16	16840	18485	-100	2	2
142	46	45	4120	800	15.5	250	12	90	16	16840	19285	-100	2	2
143	47	45	4120	800	15.5	250	12	90	16	16840	20085	-100	2	2
144	48	45	4120	800	15.5	250	12	90	16	16840	20910	-100	2	2
Keelson:														
145	A	46	4120	1230	17.5	250	12	90	16	25965	820	-100	2	2
146	B	46	4120	1230	17.5	250	12	90	16	25965	1640	-100	2	2
Wing Girder:														
147	A	47	4120	1230	14.5	150	12	0	0	19635	820	15580	2	2
148	B	47	4120	1230	14.5	150	12	0	0	19635	1640	15580	2	2
Deck Corner:														
149		49	4120	500	16	300	17.5	0	0	13250	21000	21300	3	2
Deck/Center Long Bhd. Element:														
150		50	4120	250	16.5	400	15.5	0	0	10325	22200	-100	3	2

Triton 2

Length: 233 m
Breadth: 42 m
Depth: 21.3 m

Material properties (MP):
1= 245 N/mm^2
2= 326 N/mm^2

E= 210000 N/mm^2

Bottom & Side Shell:

Element no.	CID	a	b	t_p	h_w	t_w	b_f	t_f	Area	Z	Y	Pos.	MP
1	0	10	4120	410	21	410	17.5	0	0	15785	0	0	1	2
2	1	11	4120	820	21	450	11.5	150	18	25095	0	820	1	2
3	2	11	4120	820	21	450	11.5	150	18	25095	0	1640	1	2
4	3	11	4120	820	21	450	11.5	150	18	25095	0	2460	1	2
5	4	11	4120	820	21	450	11.5	150	18	25095	0	3280	1	2
6	5	12	4120	820	19.5	450	11.5	150	18	23865	0	4100	1	2
7	6	12	4120	820	19.5	450	11.5	150	18	23865	0	4920	1	2
8	7	12	4120	820	19.5	450	11.5	150	18	23865	0	5740	1	2
9	8	12	4120	820	19.5	450	11.5	150	18	23865	0	6560	1	2
10	9	12	4120	820	19.5	450	11.5	150	18	23865	0	7380	1	2
11	10	12	4120	820	19.5	450	11.5	150	18	23865	0	8200	1	2
12	11	12	4120	820	19.5	450	11.5	150	18	23865	0	9020	1	2
13	12	12	4120	820	19.5	450	11.5	150	18	23865	0	9840	1	2
14	13	12	4120	820	19.5	450	11.5	150	18	23865	0	10660	1	2
15	14	12	4120	820	19.5	450	11.5	150	18	23865	0	11480	1	2
16	15	12	4120	820	19.5	450	11.5	150	18	23865	0	12300	1	2
17	16	12	4120	820	19.5	450	11.5	150	18	23865	0	13120	1	2
18	17	12	4120	820	19.5	450	11.5	150	18	23865	0	13940	1	2
19	18	12	4120	820	19.5	450	11.5	150	18	23865	0	14760	1	2
20	19	13	4120	820	19.5	410	14.5	0	0	21935	0	15580	1	2
21	20	14	4120	820	19.5	500	11.5	150	18	24440	0	16400	1	2
22	21	14	4120	820	19.5	500	11.5	150	18	24440	0	17220	1	2
23	22	14	4120	820	19.5	500	11.5	150	18	24440	0	18040	1	2
24	23	14	4120	820	19.5	500	11.5	150	18	24440	0	18860	1	2
25	BK	15	4120	2828	19.5	400	13	50	18	61246	1050	19910	1	2
26	24	16	4120	800	16	435	11.5	150	15	20053	2100	21000	2	2
27	25	16	4120	800	16	435	11.5	150	15	20053	2920	21000	2	2
28	26	16	4120	800	16	435	11.5	150	15	20053	3740	21000	2	2
29	27	16	4120	800	16	435	11.5	150	15	20053	4560	21000	2	2
30	28	16	4120	800	16	435	11.5	150	15	20053	5380	21000	2	2
31	29	17	4120	800	16	410	13	0	0	18130	6200	21000	2	1
32	30	18	4120	800	17.5	435	11.5	150	15	21253	7020	21000	2	1
33	31	18	4120	800	17.5	435	11.5	150	15	21253	7840	21000	2	1
34	32	18	4120	800	17.5	435	11.5	150	15	21253	8660	21000	2	1
35	33	19	4120	800	17.5	385	11.5	150	15	20678	9480	21000	2	1
36	34	19	4120	800	17.5	385	11.5	150	15	20678	10300	21000	2	1
37	35	20	4120	800	17.5	410	13	0	0	19330	11120	21000	2	1
38	36	19	4120	800	17.5	385	11.5	150	15	20678	11940	21000	2	1
39	37	19	4120	800	17.5	385	11.5	150	15	20678	12760	21000	2	1
40	38	19	4120	800	17.5	385	11.5	150	15	20678	13580	21000	2	1
41	39	19	4120	800	17.5	385	11.5	150	15	20678	14400	21000	2	1
42	40	19	4120	800	17.5	385	11.5	150	15	20678	15220	21000	2	1
43	41	20	4120	800	17.5	410	13	0	0	19330	16040	21000	2	1
44	42	21	4120	800	17.5	400	11.5	100	16	20200	16860	21000	2	1
45	43	22	4120	800	17.5	350	11.5	100	12	19225	17680	21000	2	1
46	44	22	4120	800	17.5	350	11.5	100	12	19225	18500	21000	2	1
47	45	23	4120	800	19	300	11	90	16	19940	19320	21000	2	2
48	46	23	4120	800	19	300	11	90	16	19940	20140	21000	2	2
49	47	23	4120	800	19	300	11	90	16	19940	20960	21000	2	2

Upper Deck

Element	no.	CID	a	b	t_p	h_w	t_w	b_f	t_f	Area	Z	Y	Pos.	MP
50	1	24	4120	820	19.5	250	12	90	16	20430	22051	410	3	2
51	2	24	4120	820	19.5	250	12	90	16	20430	22014	1230	3	2
52	3	24	4120	820	19.5	250	12	90	16	20430	21977	2050	3	2
53	4	24	4120	820	19.5	250	12	90	16	20430	21941	2870	3	2
54	5	24	4120	820	19.5	250	12	90	16	20430	21904	3690	3	2
55	6	24	4120	820	19.5	250	12	90	16	20430	21867	4510	3	2
56	7	24	4120	820	19.5	250	12	90	16	20430	21830	5330	3	2
57	8	24	4120	820	19.5	250	12	90	16	20430	21794	6150	3	2
58	9	24	4120	820	19.5	250	12	90	16	20430	21757	6970	3	2
59	10	24	4120	820	19.5	250	12	90	16	20430	21720	7790	3	2
60	11	24	4120	820	19.5	250	12	90	16	20430	21683	8610	3	2
61	12	24	4120	820	19.5	250	12	90	16	20430	21646	9430	3	2
62	13	24	4120	820	19.5	250	12	90	16	20430	21610	10250	3	2
63	14	24	4120	820	19.5	250	12	90	16	20430	21573	11070	3	2
64	15	24	4120	820	19.5	250	12	90	16	20430	21536	11890	3	2
65	16	24	4120	820	19.5	250	12	90	16	20430	21499	12710	3	2
66	17	24	4120	820	19.5	250	12	90	16	20430	21463	13530	3	2
67	18	24	4120	820	19.5	250	12	90	16	20430	21426	14350	3	2
68	19	25	4120	740	19.5	250	12	90	16	18870	21396	15090	3	2
69	20	25	4120	740	19.5	250	12	90	16	18870	21363	15830	3	2
70	21	25	4120	740	19.5	250	12	90	16	18870	21330	16570	3	2
71	22	25	4120	740	19.5	250	12	90	16	18870	21297	17310	3	2
72	23	26	4120	820	19.5	400	16	0	0	22390	21143	18130	3	2
73	24	27	4120	820	19.5	300	11	90	16	20730	21177	18950	3	2
74	25	27	4120	820	19.5	300	11	90	16	20730	21140	19770	3	2
Inner bottom & Long. Bhd.														
75	1	28	4120	820	16	450	11.5	150	18	20995	2460	820	3	2
76	2	28	4120	820	16	450	11.5	150	18	20995	2460	1640	3	2
77	3	28	4120	820	16	450	11.5	150	18	20995	2460	2460	3	2
78	4	28	4120	820	16	450	11.5	150	18	20995	2460	3280	3	2
79	5	28	4120	820	16	450	11.5	150	18	20995	2460	4100	3	2
80	6	28	4120	820	16	450	11.5	150	18	20995	2460	4920	3	2
81	7	28	4120	820	16	450	11.5	150	18	20995	2460	5740	3	2
82	8	28	4120	820	16	450	11.5	150	18	20995	2460	6560	3	2
83	9	28	4120	820	16	450	11.5	150	18	20995	2460	7380	3	2
84	10	28	4120	820	16	450	11.5	150	18	20995	2460	8200	3	2
85	11	28	4120	820	16	450	11.5	150	18	20995	2460	9020	3	2
86	12	28	4120	820	16	450	11.5	150	18	20995	2460	9840	3	2
87	13	28	4120	820	16	450	11.5	150	18	20995	2460	10660	3	2
88	14	28	4120	820	16	450	11.5	150	18	20995	2460	11480	3	2
89	15	28	4120	820	16	450	11.5	150	18	20995	2460	12300	3	2
90	16	28	4120	820	16	450	11.5	150	18	20995	2460	13120	3	2
91	17	28	4120	820	16	450	11.5	150	18	20995	2460	13940	3	2
92	18	28	4120	820	16	450	11.5	150	18	20995	2460	14760	3	2
93	24	29	4120	785	17.5	450	11.5	125	18	21163	2876	15750	3	2
94	25	29	4120	785	17.5	450	11.5	125	18	21163	3568	16350	3	2
95	26	29	4120	785	17.5	450	11.5	125	18	21163	4260	16950	3	2
96	27	29	4120	785	17.5	450	11.5	125	18	21163	4952	17550	3	2
97	28	29	4120	785	17.5	450	11.5	125	18	21163	5644	18150	3	2
98	30	30	4120	800	15.5	450	11.5	125	18	19825	7020	18419	2	1
99	31	30	4120	800	15.5	450	11.5	125	18	19825	7840	18419	2	1

Element	no.	CID	a	b	t_p	h_w	t_w	b_f	t_f	Area	Z	Y	Pos.	MP
100	32	30	4120	800	15.5	450	11.5	125	18	19825	8660	18419	2	1
101	33	30	4120	800	15.5	450	11.5	125	18	19825	9480	18419	2	1
102	34	30	4120	800	15.5	450	11.5	125	18	19825	10300	18419	2	1
103	35	31	4120	800	14	410	13	0	0	16530	11120	18465	2	1
104	36	32	4120	800	14	400	11.5	100	16	17400	11940	18440	2	1
105	37	32	4120	800	14	400	11.5	100	16	17400	12760	18440	2	1
106	38	32	4120	800	14	400	11.5	100	16	17400	13580	18440	2	1
107	39	32	4120	800	14	400	11.5	100	16	17400	14400	18440	2	1
108	40	33	4120	800	13.5	350	12	100	17	16700	15220	18450	2	1
109	41	34	4120	800	13.5	700	12	150	12	21000	16040	18329	2	1
110	42	33	4120	800	13.5	350	12	100	17	16700	16860	18450	2	1
111	43	33	4120	800	13.5	350	12	100	17	16700	17680	18450	2	1
112	44	35	4120	800	13.5	300	13	90	17	16230	18500	18466	2	1
113	45	36	4120	800	16	800	14	150	14	26100	19320	18409	2	2
114	46	37	4120	800	16	250	12	90	16	17240	20140	18487	2	2
115	47	37	4120	800	16	250	12	90	16	17240	20960	18487	2	2
Stringers:														
116	1	38	4120	820	13	150	12	0	0	12460	6100	20155	3	1
117	2	38	4120	820	13	150	12	0	0	12460	6100	19335	3	1
118	3	38	4120	820	13	150	12	0	0	12460	10900	20155	3	1
119	4	38	4120	820	13	150	12	0	0	12460	10900	19335	3	1
120	5	38	4120	820	13	150	12	0	0	12460	15700	20155	3	1
121	6	38	4120	820	13	150	12	0	0	12460	15700	19335	3	1
Center Long Bhd.:														
122	26	39	4120	910	15.5	450	11.5	125	18	21530	2900	-100	2	2
123	27	39	4120	910	15.5	450	11.5	125	18	21530	3810	-100	2	2
124	28	39	4120	910	15.5	450	11.5	125	18	21530	4720	-100	2	2
125	29	39	4120	910	15.5	450	11.5	125	18	21530	5630	-100	2	2
126	30	40	4120	800	14	400	13	100	18	18200	6485	-100	2	2
127	31	40	4120	800	14	400	13	100	18	18200	7285	-100	2	2
128	32	40	4120	800	14	400	13	100	18	18200	8085	-100	2	2
129	33	40	4120	800	14	400	13	100	18	18200	8885	-100	2	2
130	34	41	4120	800	13	400	13	100	18	17400	9685	-100	2	2
131	35	42	4120	800	13	350	12	100	17	16300	10485	-100	2	2
132	36	42	4120	800	13	350	12	100	17	16300	11285	-100	2	2
133	37	42	4120	800	13	350	12	100	17	16300	12085	-100	2	2
134	38	42	4120	800	13	350	12	100	17	16300	12885	-100	2	2
135	39	42	4120	800	13	350	12	100	17	16300	13685	-100	2	2
136	40	43	4120	800	13	300	13	90	17	15830	14485	-100	2	2
137	41	43	4120	800	13	300	13	90	17	15830	15285	-100	2	2
138	42	44	4120	800	13	300	11	90	16	15140	16085	-100	2	2
139	43	44	4120	800	13	300	11	90	16	15140	16885	-100	2	2
140	44	44	4120	800	13	300	11	90	16	15140	17685	-100	2	2
141	45	45	4120	800	15.5	250	12	90	16	16840	18485	-100	2	2
142	46	45	4120	800	15.5	250	12	90	16	16840	19285	-100	2	2
143	47	45	4120	800	15.5	250	12	90	16	16840	20085	-100	2	2
144	48	45	4120	800	15.5	250	12	90	16	16840	20910	-100	2	2
Keelson:														
145	A	46	4120	1230	17.5	250	12	90	16	25965	820	-100	2	2
146	B	46	4120	1230	17.5	250	12	90	16	25965	1640	-100	2	2
Wing Girder:														
147	A	47	4120	1230	14.5	150	12	0	0	19635	820	15580	2	2
148	B	47	4120	1230	14.5	150	12	0	0	19635	1640	15580	2	2
Deck Corner:														
149		49	4120	500	19	300	17.5	0	0	14750	21000	21300	3	2
Deck/Center Long Bhd. Element:														
150		50	4120	250	16.5	400	15.5	0	0	10325	22200	-100	3	2

Triton 3

Length: 233 m
Breadth: 42 m
Depth: 21.3 m

Material properties (MP):
1= 245 N/mm^2
2= 326 N/mm^2

E= 2E+05 N/mm^2

Bottom & Side Shell:

Element	no.	CID	a	b	t_p	h_w	t_w	b_f	t_f	Area	Z	Y	Pos.	MP
1	0	10	4120	410	21	410	17.5	0	0	15785	0	0	1	2
2	1	11	4120	820	21	450	11.5	150	18	25095	0	820	1	2
3	2	11	4120	820	21	450	11.5	150	18	25095	0	1640	1	2
4	3	11	4120	820	21	450	11.5	150	18	25095	0	2460	1	2
5	4	11	4120	820	21	450	11.5	150	18	25095	0	3280	1	2
6	5	12	4120	820	19.5	450	11.5	150	18	23865	0	4100	1	2
7	6	12	4120	820	19.5	450	11.5	150	18	23865	0	4920	1	2
8	7	12	4120	820	19.5	450	11.5	150	18	23865	0	5740	1	2
9	8	12	4120	820	19.5	450	11.5	150	18	23865	0	6560	1	2
10	9	12	4120	820	19.5	450	11.5	150	18	23865	0	7380	1	2
11	10	12	4120	820	19.5	450	11.5	150	18	23865	0	8200	1	2
12	11	12	4120	820	19.5	450	11.5	150	18	23865	0	9020	1	2
13	12	12	4120	820	19.5	450	11.5	150	18	23865	0	9840	1	2
14	13	12	4120	820	19.5	450	11.5	150	18	23865	0	10660	1	2
15	14	12	4120	820	19.5	450	11.5	150	18	23865	0	11480	1	2
16	15	12	4120	820	19.5	450	11.5	150	18	23865	0	12300	1	2
17	16	12	4120	820	19.5	450	11.5	150	18	23865	0	13120	1	2
18	17	12	4120	820	19.5	450	11.5	150	18	23865	0	13940	1	2
19	18	12	4120	820	19.5	450	11.5	150	18	23865	0	14760	1	2
20	19	13	4120	820	19.5	410	14.5	0	0	21935	0	15580	1	2
21	20	14	4120	820	19.5	500	11.5	150	18	24440	0	16400	1	2
22	21	14	4120	820	19.5	500	11.5	150	18	24440	0	17220	1	2
23	22	14	4120	820	19.5	500	11.5	150	18	24440	0	18040	1	2
24	23	14	4120	820	19.5	500	11.5	150	18	24440	0	18860	1	2
25	BK	15	4120	2828	19.5	400	13	50	18	61246	1050	19910	1	2
26	24	16	4120	800	16	435	11.5	150	15	20053	2100	21000	2	2
27	25	16	4120	800	16	435	11.5	150	15	20053	2920	21000	2	2
28	26	16	4120	800	16	435	11.5	150	15	20053	3740	21000	2	2
29	27	16	4120	800	16	435	11.5	150	15	20053	4560	21000	2	2
30	28	16	4120	800	16	435	11.5	150	15	20053	5380	21000	2	2
31	29	17	4120	800	16	410	13	0	0	18130	6200	21000	2	1
32	30	18	4120	800	17.5	435	11.5	150	15	21253	7020	21000	2	1
33	31	18	4120	800	17.5	435	11.5	150	15	21253	7840	21000	2	1
34	32	18	4120	800	17.5	435	11.5	150	15	21253	8660	21000	2	1
35	33	19	4120	800	17.5	385	11.5	150	15	20678	9480	21000	2	1
36	34	19	4120	800	17.5	385	11.5	150	15	20678	10300	21000	2	1
37	35	20	4120	800	17.5	410	13	0	0	19330	11120	21000	2	1
38	36	19	4120	800	17.5	385	11.5	150	15	20678	11940	21000	2	1
39	37	19	4120	800	17.5	385	11.5	150	15	20678	12760	21000	2	1
40	38	19	4120	800	17.5	385	11.5	150	15	20678	13580	21000	2	1
41	39	19	4120	800	17.5	385	11.5	150	15	20678	14400	21000	2	1
42	40	19	4120	800	17.5	385	11.5	150	15	20678	15220	21000	2	1
43	41	20	4120	800	17.5	410	13	0	0	19330	16040	21000	2	1
44	42	21	4120	800	17.5	400	11.5	100	16	20200	16860	21000	2	1
45	43	22	4120	800	17.5	350	11.5	100	12	19225	17680	21000	2	1
46	44	22	4120	800	17.5	350	11.5	100	12	19225	18500	21000	2	1
47	45	23	4120	800	19	300	11	90	16	19940	19320	21000	2	2
48	46	23	4120	800	19	300	11	90	16	19940	20140	21000	2	2
49	47	23	4120	800	19	300	11	90	16	19940	20960	21000	2	2

Upper Deck

Element	no.	CID	a	b	t_p	h_w	t_w	b_f	t_f	Area	Z	Y	Pos.	MP
50	1	24	4120	820	16.5	250	12	90	16	17970	22051	410	3	2
51	2	24	4120	820	16.5	250	12	90	16	17970	22014	1230	3	2
52	3	24	4120	820	16.5	250	12	90	16	17970	21977	2050	3	2
53	4	24	4120	820	16.5	250	12	90	16	17970	21941	2870	3	2
54	5	24	4120	820	16.5	250	12	90	16	17970	21904	3690	3	2
55	6	24	4120	820	16.5	250	12	90	16	17970	21867	4510	3	2
56	7	24	4120	820	16.5	250	12	90	16	17970	21830	5330	3	2
57	8	24	4120	820	16.5	250	12	90	16	17970	21794	6150	3	2
58	9	24	4120	820	16.5	250	12	90	16	17970	21757	6970	3	2
59	10	24	4120	820	16.5	250	12	90	16	17970	21720	7790	3	2
60	11	24	4120	820	16.5	250	12	90	16	17970	21683	8610	3	2
61	12	24	4120	820	16.5	250	12	90	16	17970	21646	9430	3	2
62	13	24	4120	820	16.5	250	12	90	16	17970	21610	10250	3	2
63	14	24	4120	820	16.5	250	12	90	16	17970	21573	11070	3	2
64	15	24	4120	820	16.5	250	12	90	16	17970	21536	11890	3	2
65	16	24	4120	820	16.5	250	12	90	16	17970	21499	12710	3	2
66	17	24	4120	820	16.5	250	12	90	16	17970	21463	13530	3	2
67	18	24	4120	820	16.5	250	12	90	16	17970	21426	14350	3	2
68	19	25	4120	740	16.5	250	12	90	16	16650	21396	15090	3	2
69	20	25	4120	740	16.5	250	12	90	16	16650	21363	15830	3	2
70	21	25	4120	740	16.5	250	12	90	16	16650	21330	16570	3	2
71	22	25	4120	740	16.5	250	12	90	16	16650	21297	17310	3	2
72	23	26	4120	820	17.5	400	16	0	0	20750	21143	18130	3	2
73	24	27	4120	820	17.5	300	11	90	16	19090	21177	18950	3	2
74	25	27	4120	820	17.5	300	11	90	16	19090	21140	19770	3	2
Inner bottom & Long. Bhd.														
75	1	28	4120	820	16	450	11.5	150	18	20995	2460	820	3	2
76	2	28	4120	820	16	450	11.5	150	18	20995	2460	1640	3	2
77	3	28	4120	820	16	450	11.5	150	18	20995	2460	2460	3	2
78	4	28	4120	820	16	450	11.5	150	18	20995	2460	3280	3	2
79	5	28	4120	820	16	450	11.5	150	18	20995	2460	4100	3	2
80	6	28	4120	820	16	450	11.5	150	18	20995	2460	4920	3	2
81	7	28	4120	820	16	450	11.5	150	18	20995	2460	5740	3	2
82	8	28	4120	820	16	450	11.5	150	18	20995	2460	6560	3	2
83	9	28	4120	820	16	450	11.5	150	18	20995	2460	7380	3	2
84	10	28	4120	820	16	450	11.5	150	18	20995	2460	8200	3	2
85	11	28	4120	820	16	450	11.5	150	18	20995	2460	9020	3	2
86	12	28	4120	820	16	450	11.5	150	18	20995	2460	9840	3	2
87	13	28	4120	820	16	450	11.5	150	18	20995	2460	10660	3	2
88	14	28	4120	820	16	450	11.5	150	18	20995	2460	11480	3	2
89	15	28	4120	820	16	450	11.5	150	18	20995	2460	12300	3	2
90	16	28	4120	820	16	450	11.5	150	18	20995	2460	13120	3	2
91	17	28	4120	820	16	450	11.5	150	18	20995	2460	13940	3	2
92	18	28	4120	820	16	450	11.5	150	18	20995	2460	14760	3	2
93	24	29	4120	785	17.5	450	11.5	125	18	21163	2876	15750	3	2
94	25	29	4120	785	17.5	450	11.5	125	18	21163	3568	16350	3	2
95	26	29	4120	785	17.5	450	11.5	125	18	21163	4260	16950	3	2
96	27	29	4120	785	17.5	450	11.5	125	18	21163	4952	17550	3	2
97	28	29	4120	785	17.5	450	11.5	125	18	21163	5644	18150	3	2
98	30	30	4120	800	15.5	450	11.5	125	18	19825	7020	18419	2	1
99	31	30	4120	800	15.5	450	11.5	125	18	19825	7840	18419	2	1

Element	no.	CID	a	b	t_p	h_w	t_w	b_f	t_f	Area	Z	Y	Pos.	MP
100	32	30	4120	800	15.5	450	11.5	125	18	19825	8660	18419	2	1
101	33	30	4120	800	15.5	450	11.5	125	18	19825	9480	18419	2	1
102	34	30	4120	800	15.5	450	11.5	125	18	19825	10300	18419	2	1
103	35	31	4120	800	14	410	13	0	0	16530	11120	18465	2	1
104	36	32	4120	800	14	400	11.5	100	16	17400	11940	18440	2	1
105	37	32	4120	800	14	400	11.5	100	16	17400	12760	18440	2	1
106	38	32	4120	800	14	400	11.5	100	16	17400	13580	18440	2	1
107	39	32	4120	800	14	400	11.5	100	16	17400	14400	18440	2	1
108	40	33	4120	800	13.5	350	12	100	17	16700	15220	18450	2	1
109	41	34	4120	800	13.5	700	12	150	12	21000	16040	18329	2	1
110	42	33	4120	800	13.5	350	12	100	17	16700	16860	18450	2	1
111	43	33	4120	800	13.5	350	12	100	17	16700	17680	18450	2	1
112	44	35	4120	800	13.5	300	13	90	17	16230	18500	18466	2	1
113	45	36	4120	800	16	800	14	150	14	26100	19320	18409	2	2
114	46	37	4120	800	16	250	12	90	16	17240	20140	18487	2	2
115	47	37	4120	800	16	250	12	90	16	17240	20960	18487	2	2
Stringers:														
116	1	38	4120	820	13	150	12	0	0	12460	6100	20155	3	1
117	2	38	4120	820	13	150	12	0	0	12460	6100	19335	3	1
118	3	38	4120	820	13	150	12	0	0	12460	10900	20155	3	1
119	4	38	4120	820	13	150	12	0	0	12460	10900	19335	3	1
120	5	38	4120	820	13	150	12	0	0	12460	15700	20155	3	1
121	6	38	4120	820	13	150	12	0	0	12460	15700	19335	3	1
Center Long Bhd.:														
122	26	39	4120	910	15.5	450	11.5	125	18	21530	2900	-100	2	2
123	27	39	4120	910	15.5	450	11.5	125	18	21530	3810	-100	2	2
124	28	39	4120	910	15.5	450	11.5	125	18	21530	4720	-100	2	2
125	29	39	4120	910	15.5	450	11.5	125	18	21530	5630	-100	2	2
126	30	40	4120	800	14	400	13	100	18	18200	6485	-100	2	2
127	31	40	4120	800	14	400	13	100	18	18200	7285	-100	2	2
128	32	40	4120	800	14	400	13	100	18	18200	8085	-100	2	2
129	33	40	4120	800	14	400	13	100	18	18200	8885	-100	2	2
130	34	41	4120	800	13	400	13	100	18	17400	9685	-100	2	2
131	35	42	4120	800	13	350	12	100	17	16300	10485	-100	2	2
132	36	42	4120	800	13	350	12	100	17	16300	11285	-100	2	2
133	37	42	4120	800	13	350	12	100	17	16300	12085	-100	2	2
134	38	42	4120	800	13	350	12	100	17	16300	12885	-100	2	2
135	39	42	4120	800	13	350	12	100	17	16300	13685	-100	2	2
136	40	43	4120	800	13	300	13	90	17	15830	14485	-100	2	2
137	41	43	4120	800	13	300	13	90	17	15830	15285	-100	2	2
138	42	44	4120	800	13	300	11	90	16	15140	16085	-100	2	2
139	43	44	4120	800	13	300	11	90	16	15140	16885	-100	2	2
140	44	44	4120	800	13	300	11	90	16	15140	17685	-100	2	2
141	45	45	4120	800	15.5	250	12	90	16	16840	18485	-100	2	2
142	46	45	4120	800	15.5	250	12	90	16	16840	19285	-100	2	2
143	47	45	4120	800	15.5	250	12	90	16	16840	20085	-100	2	2
144	48	45	4120	800	15.5	250	12	90	16	16840	20910	-100	2	2
Keelson:														
145	A	46	4120	1230	17.5	250	12	90	16	25965	820	-100	2	2
146	B	46	4120	1230	17.5	250	12	90	16	25965	1640	-100	2	2
Wing Girder:														
147	A	47	4120	1230	14.5	150	12	0	0	19635	820	15580	2	2
148	B	47	4120	1230	14.5	150	12	0	0	19635	1640	15580	2	2
Deck Corner:														
149		49	4120	500	16	300	17.5	0	0	13250	21000	21300	3	2
Deck/Center Long Bhd. Element:														
150		50	4120	250	16.5	400	15.5	0	0	10325	22200	-100	3	2

ORDINARY SECTION

LOCATION	LONG. NO.	SCANTLING
UPPER DECK	1 - 22	250X 90X12 /16 I.A AH
	24 & 25	300X 90X11 /16 I.A AH
BOTTOM & SIDE SHELL	1 - 18	450X11.5 AH + 150X18 FB (T) AH
	20 - 23	500X150X11.5/18 I.A AH
	24	435X11.5 AH + 150X15 FB (T) AH
	25 - 28	435X11.5 AH + 150X15 FB (T) AH 435X11.5 DH + 150X15 FB (T) DH (FR.64-1850 - FR.84-1850 ONLY)
	30 - 32	435X11.5 + 150X15 FB (T) 435X11.5 D + 150X15 FB (T) D
	33 & 34	385X11.5 + 150X15 FB (T) 385X11.5 D + 150X15 FB (T) D
	36 - 40	385X11.5 + 120X15 FB (T) 385X11.5 D + 120X15 FB (T) D
	42	400X100X11.5/16 I.A
	43 & 44	350X100X12 /17 I.A
	45 - 47	300X 90X11 /15 I.A AH
INNER BTM. & LONG BHD.	1 - 18	450X11.5 AH + 150X18 FB (T) AH
	24 - 28	450X125X11.5/18 I.A AH
	30 - 34	450X125X11.5/18 I.A
	36 - 39	400X100X11.5/16 I.A
	40	350X100X12 /17 I.A
	41	700x12(W)+150X12 FB (T)
	42 - 43	350X100X12 /17 I.A
	44	300X 90X13 /17 I.A
	45	950x14(W) AH +150X14 FB (L3) AH
	46 & 47	250X 90X12 /15 I.A AH
CENTER LONG. BHD.	26 - 29	450X125X11.5/19 I.A AH
	30 - 34	400X100X13 /18 I.A AH
	35 - 39	350X100X12 /17 I.A AH
	40 - 41	300X 90X13 /17 I.A AH
	42 - 44	300X 90X11 /16 I.A AH
	45 - 47	300X 90X11 /15 I.A AH

DET. OF BUCK. STIFF.

MARKS : 130 X 12 FB
FR.54 ~ FR.92
UPPER DECK

MARKS PLATES TO BE LOCALLY INCREASED (SEE SHELL EXPANSION & CON-PRO & DECK PLAN)

SIZE: 420x297

Appendix B

Output from LR.PASS 20203

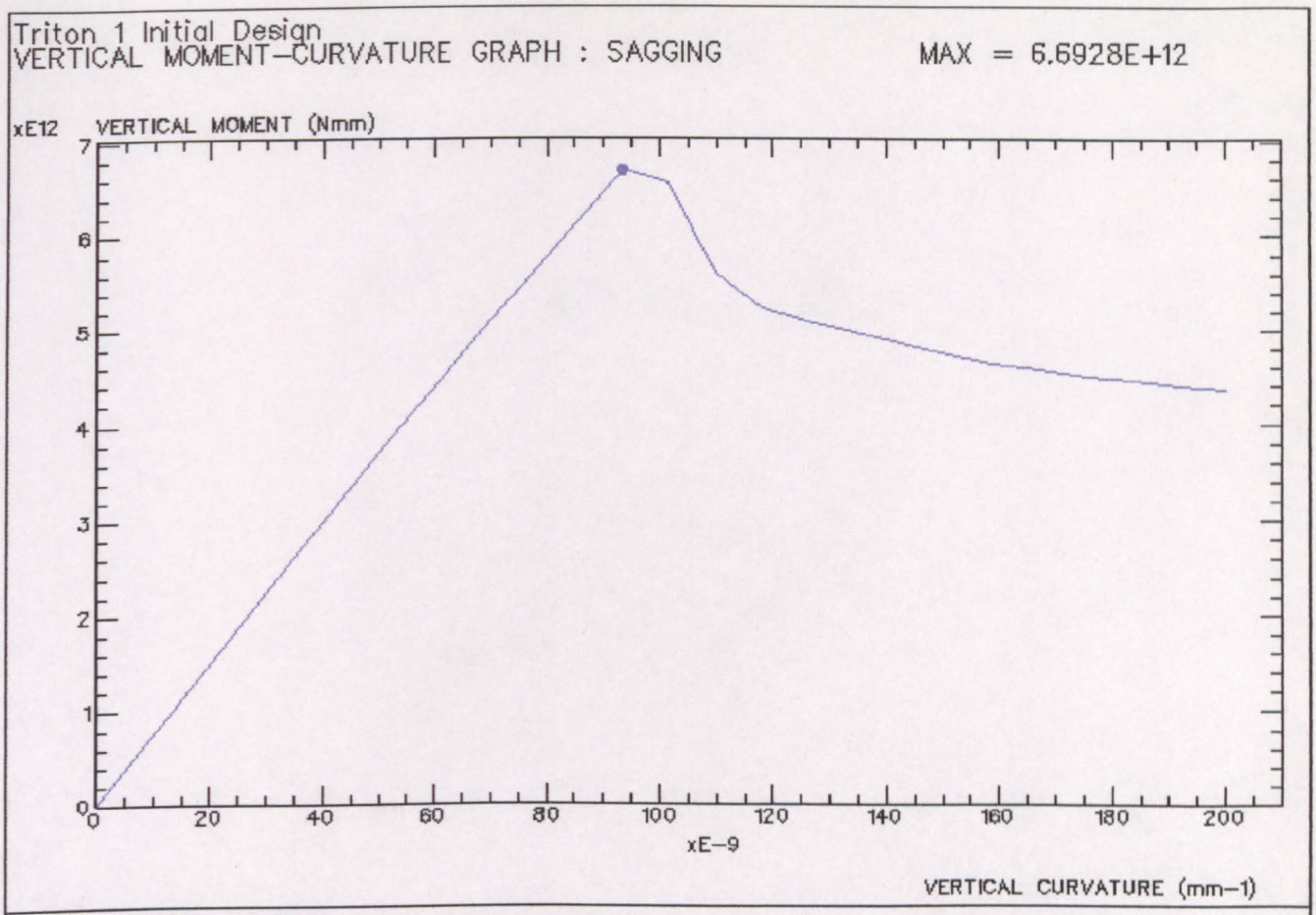
Triton 1 Initial Design
VERTICAL MOMENT-CURVATURE GRAPH : SAGGING
MAX = 6.6928E+12
xE12
VERTICAL MOMENT (Nmm)
0
1
2
3
4
5
6
7
0
20
40
60
80
100
120
140
160
180
200
xE-9
VERTICAL CURVATURE (mm-1)

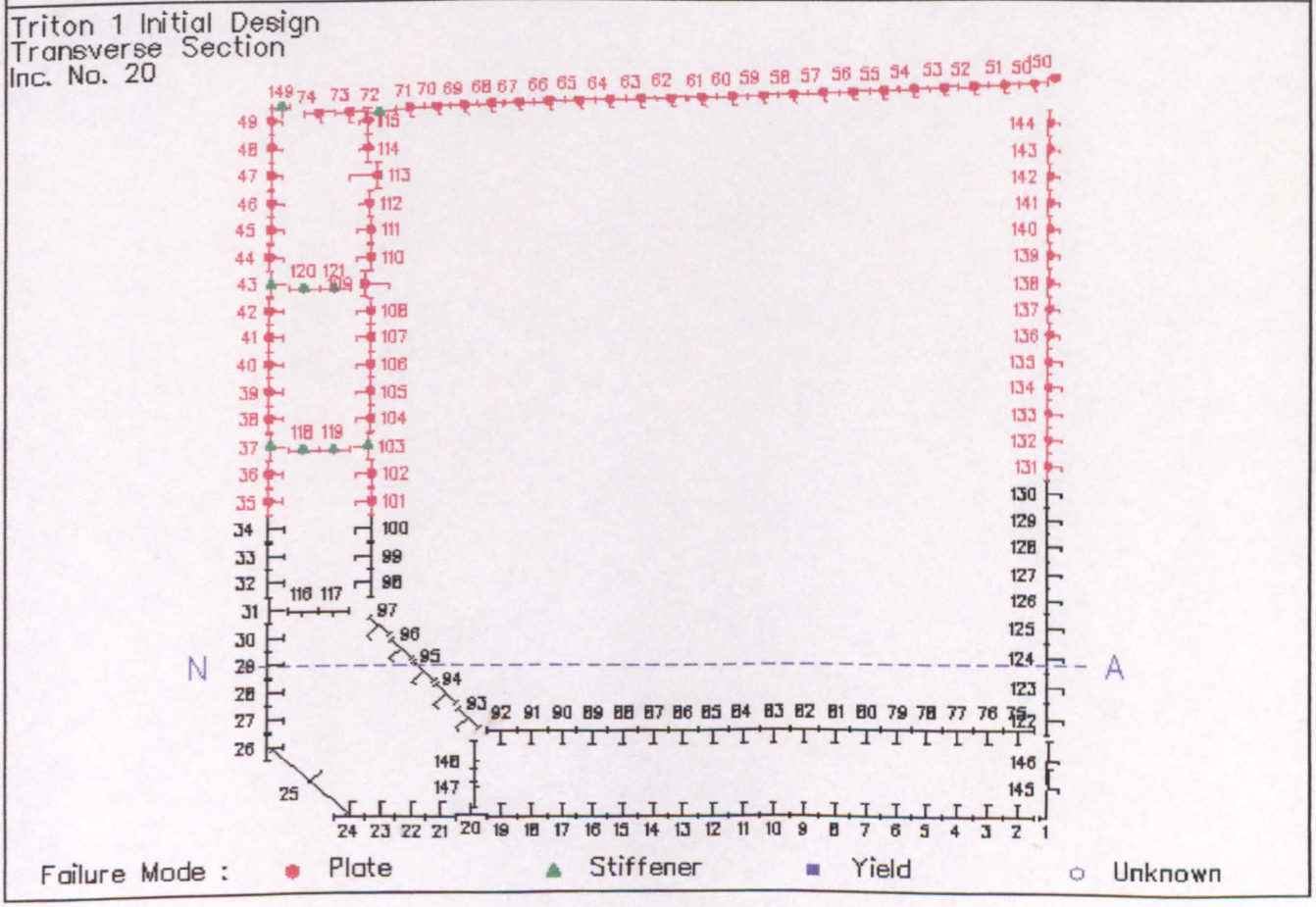
Triton 1 Initial Design
Transverse Section
Inc. No. 20
N
A
Failure Mode :
Plate
Stiffener
Yield
Unknown

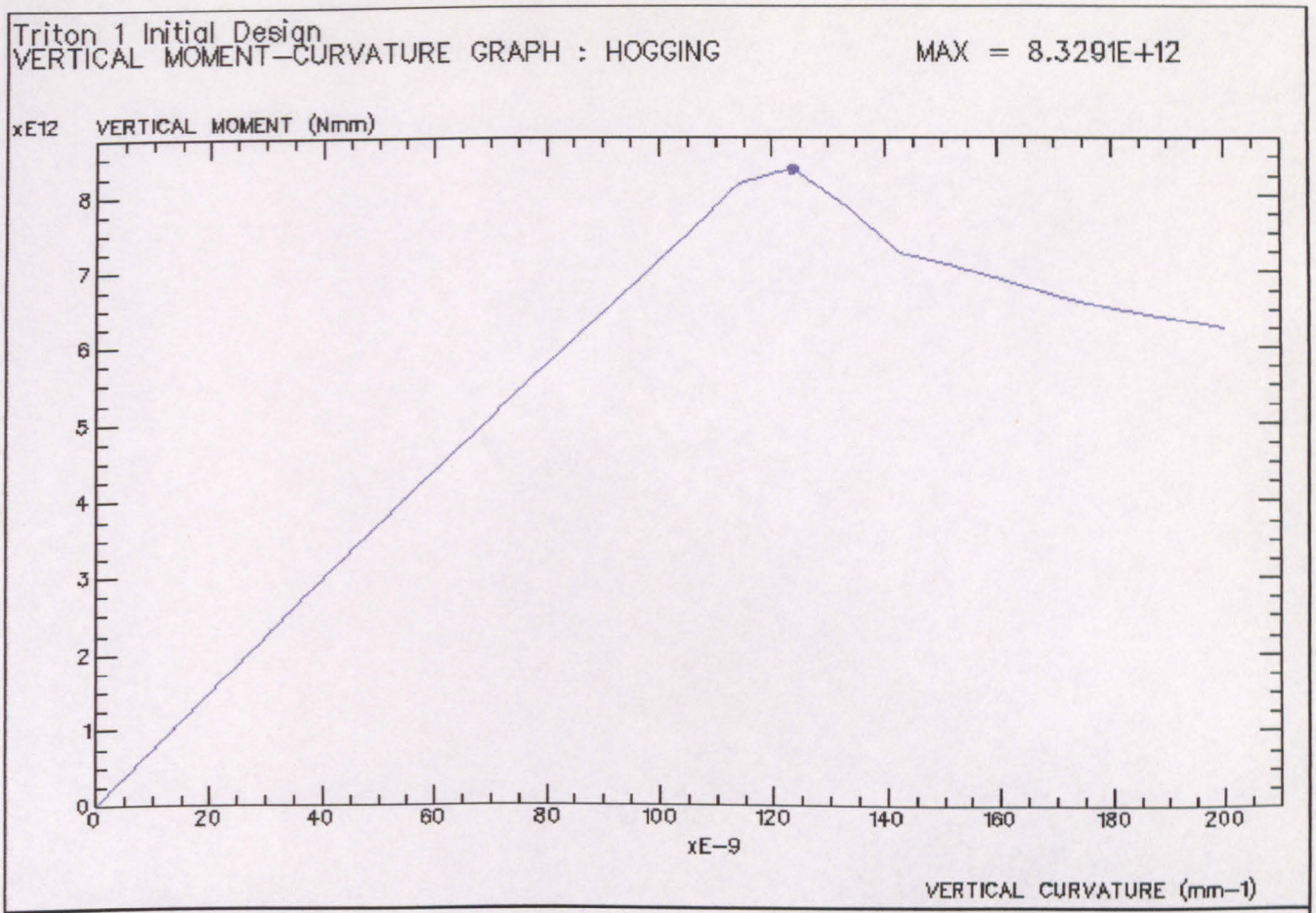
Triton 1 Initial Design
VERTICAL MOMENT–CURVATURE GRAPH : HOGGING
MAX = 8.3291E+12
xE12
VERTICAL MOMENT (Nmm)
0
1
2
3
4
5
6
7
8
0
20
40
60
80
100
120
140
160
180
200
xE-9
VERTICAL CURVATURE (mm-1)

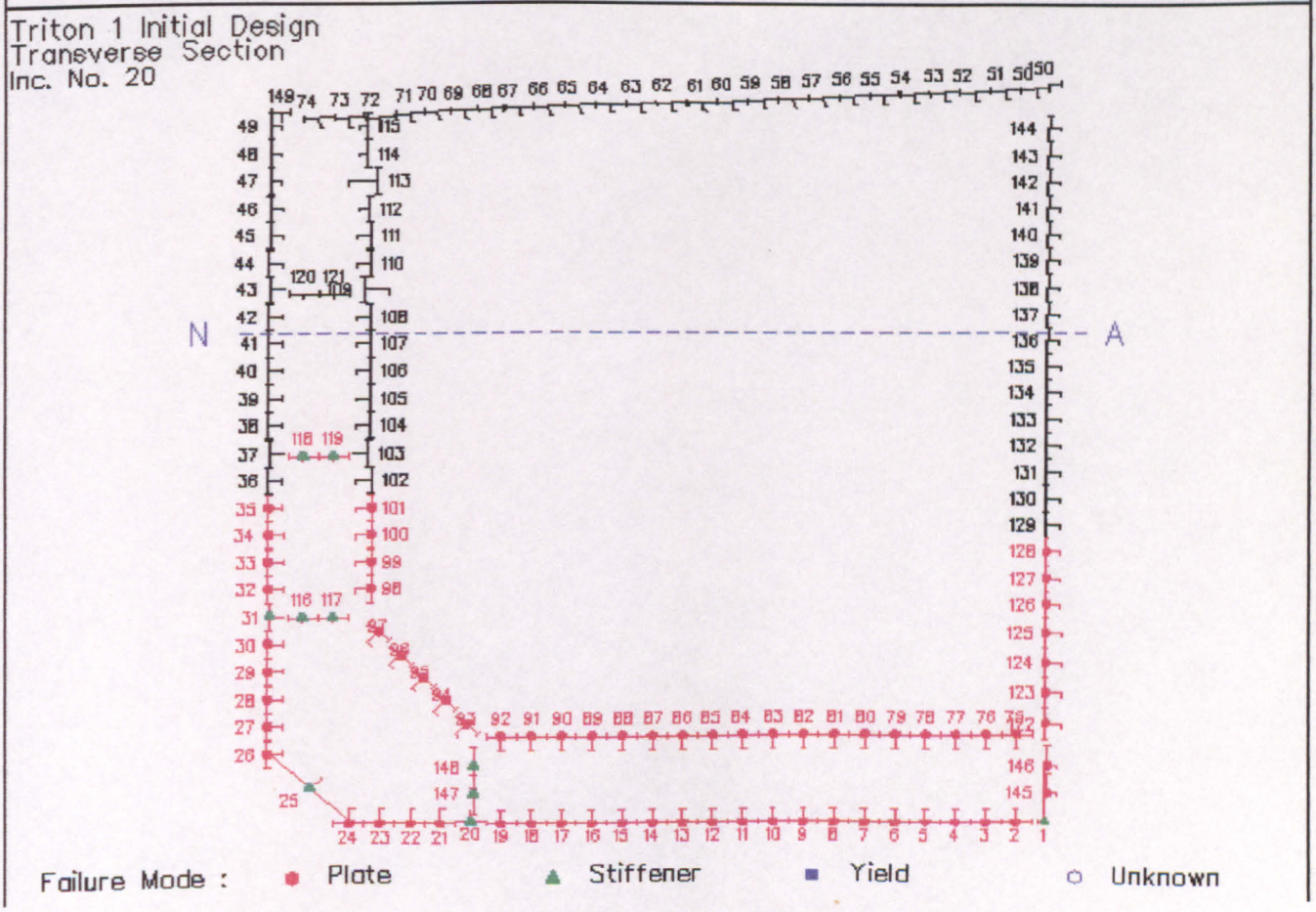
Triton 1 Initial Design
Transverse Section
Inc. No. 20
N
A
Failure Mode :
Plate
Stiffener
Yield
Unknown

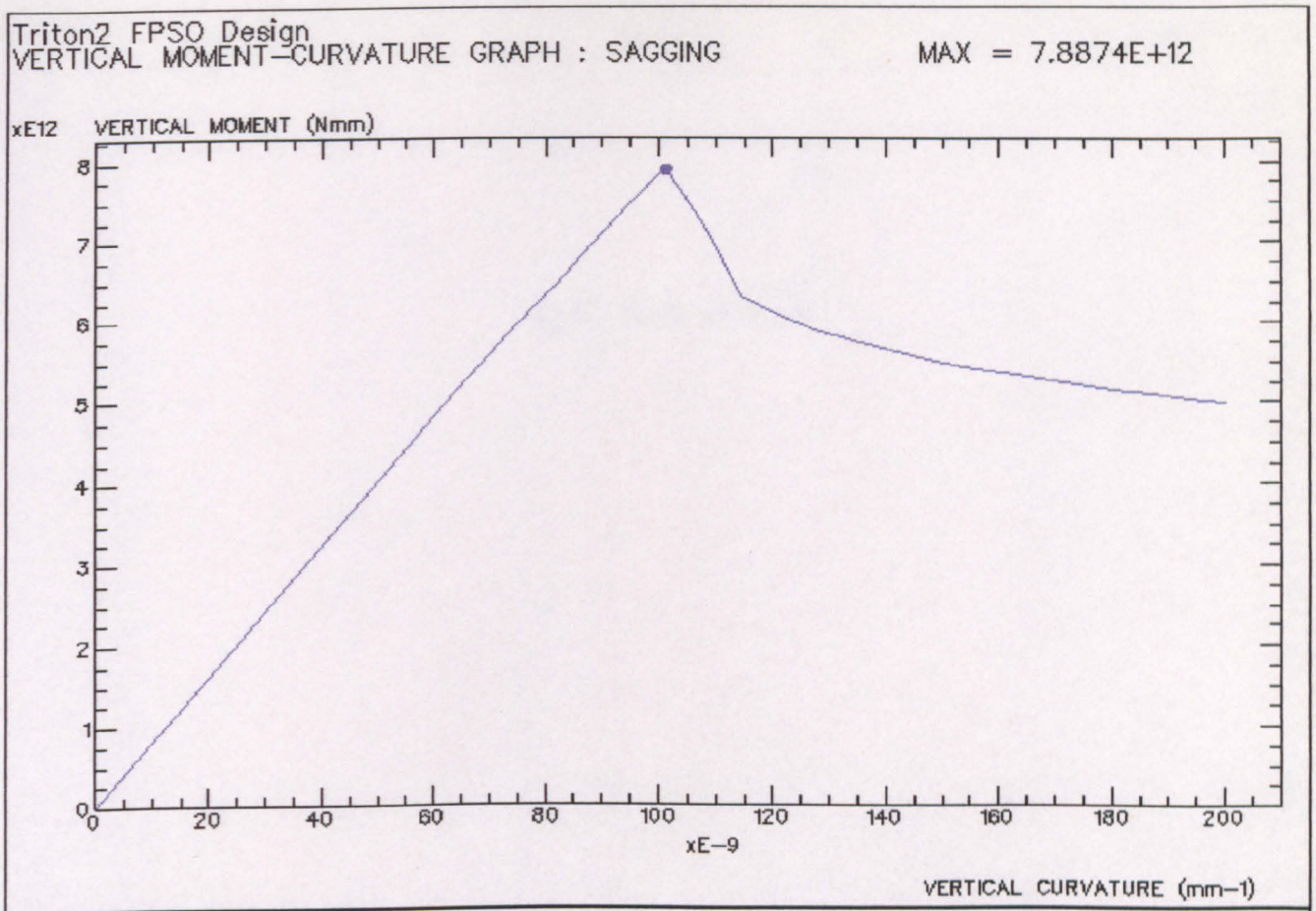
Triton2 FPSO Design
VERTICAL MOMENT-CURVATURE GRAPH : SAGGING
MAX = 7.8874E+12
xE12 VERTICAL MOMENT (Nmm)
0
1
2
3
4
5
6
7
8
0
20
40
60
80
100
120
140
160
180
200
xE-9
VERTICAL CURVATURE (mm-1)

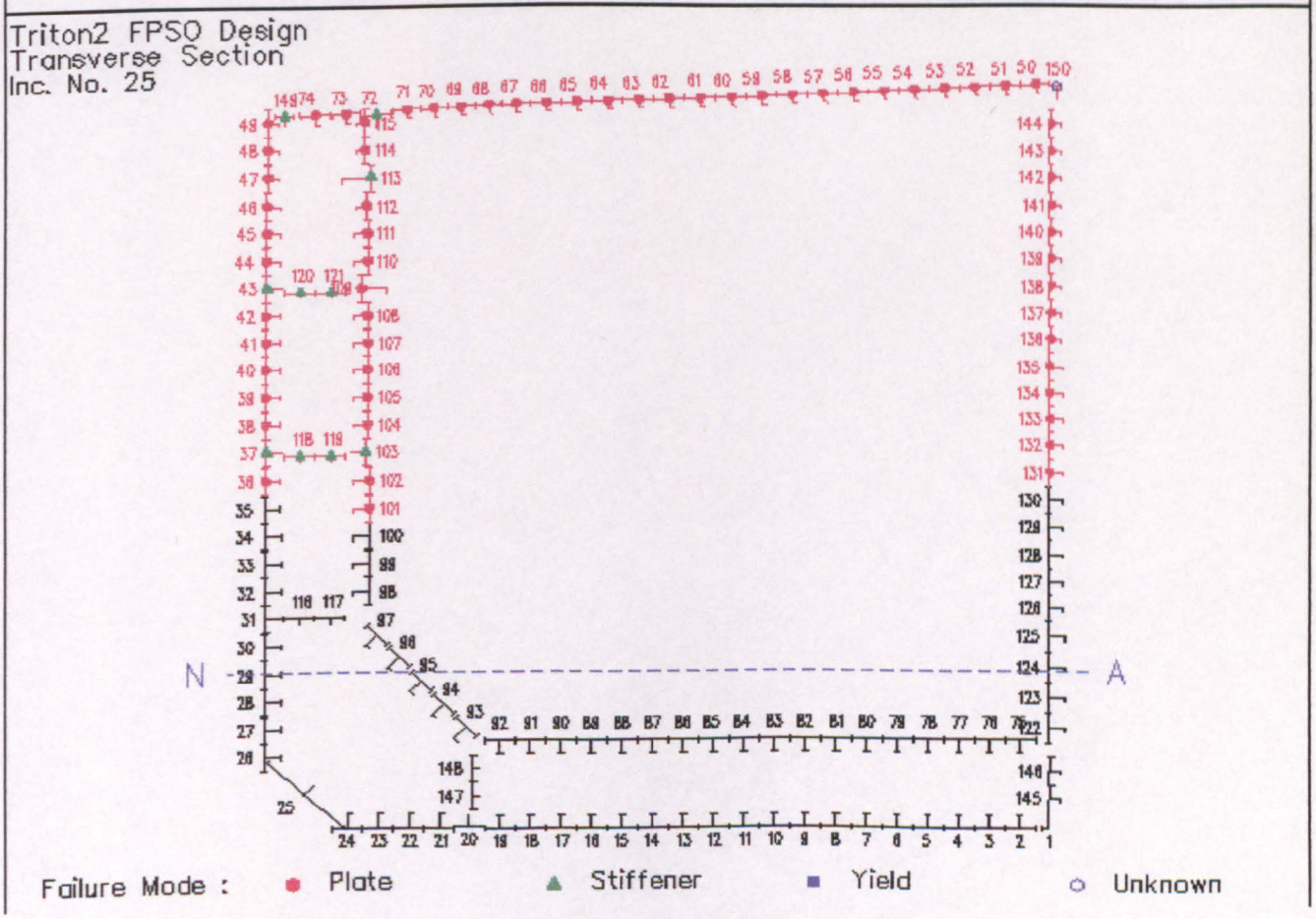
Triton2 FPSO Design
Transverse Section
Inc. No. 25
N
A
Failure Mode : Plate Stiffener Yield Unknown

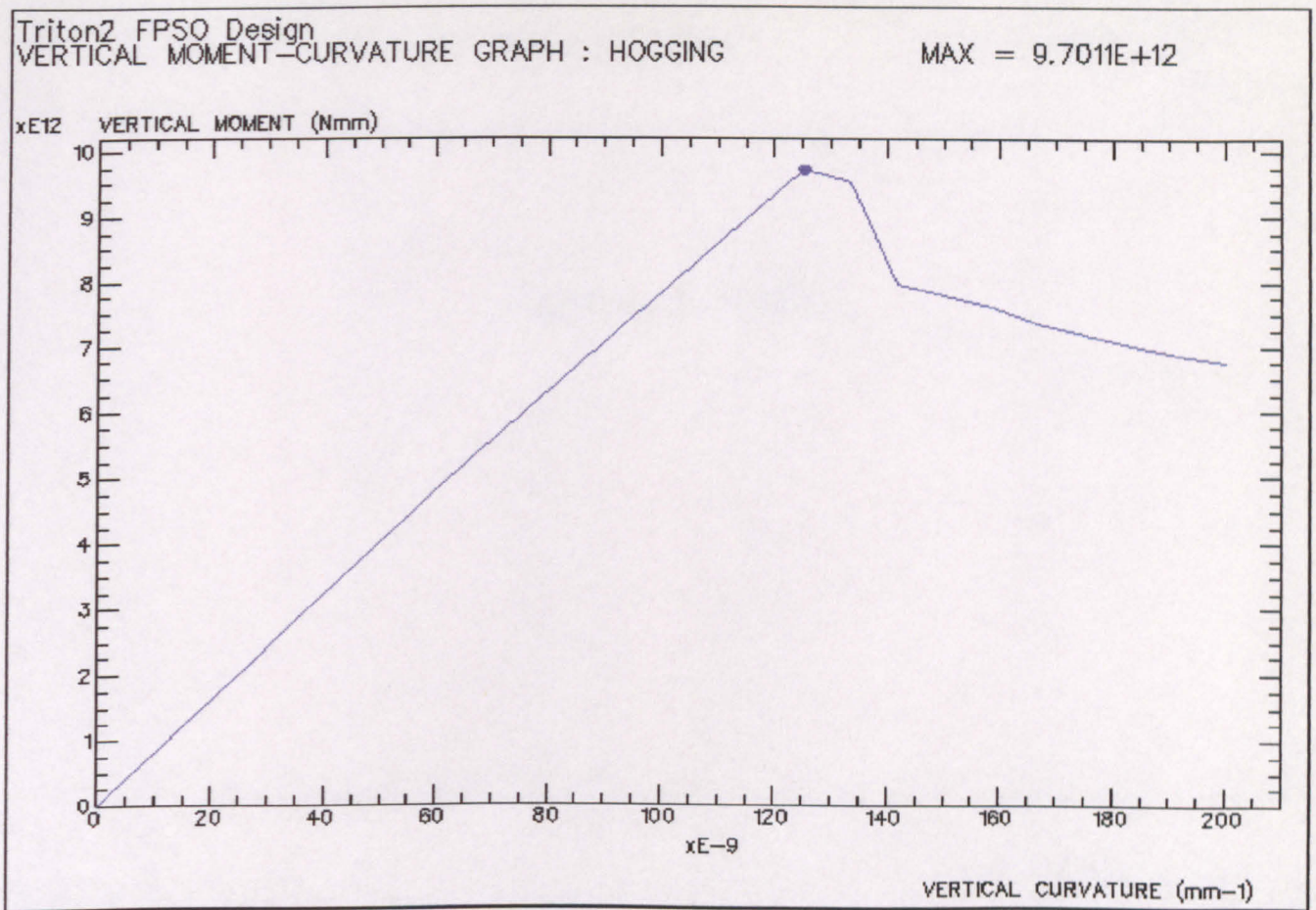
Triton2 FPSO Design
VERTICAL MOMENT-CURVATURE GRAPH : HOGGING
MAX = 9.7011E+12
xE12 VERTICAL MOMENT (Nmm)
10
9
8
7
6
5
4
3
2
1
0
0 20 40 60 80 100 120 140 160 180 200
xE-9
VERTICAL CURVATURE (mm-1)

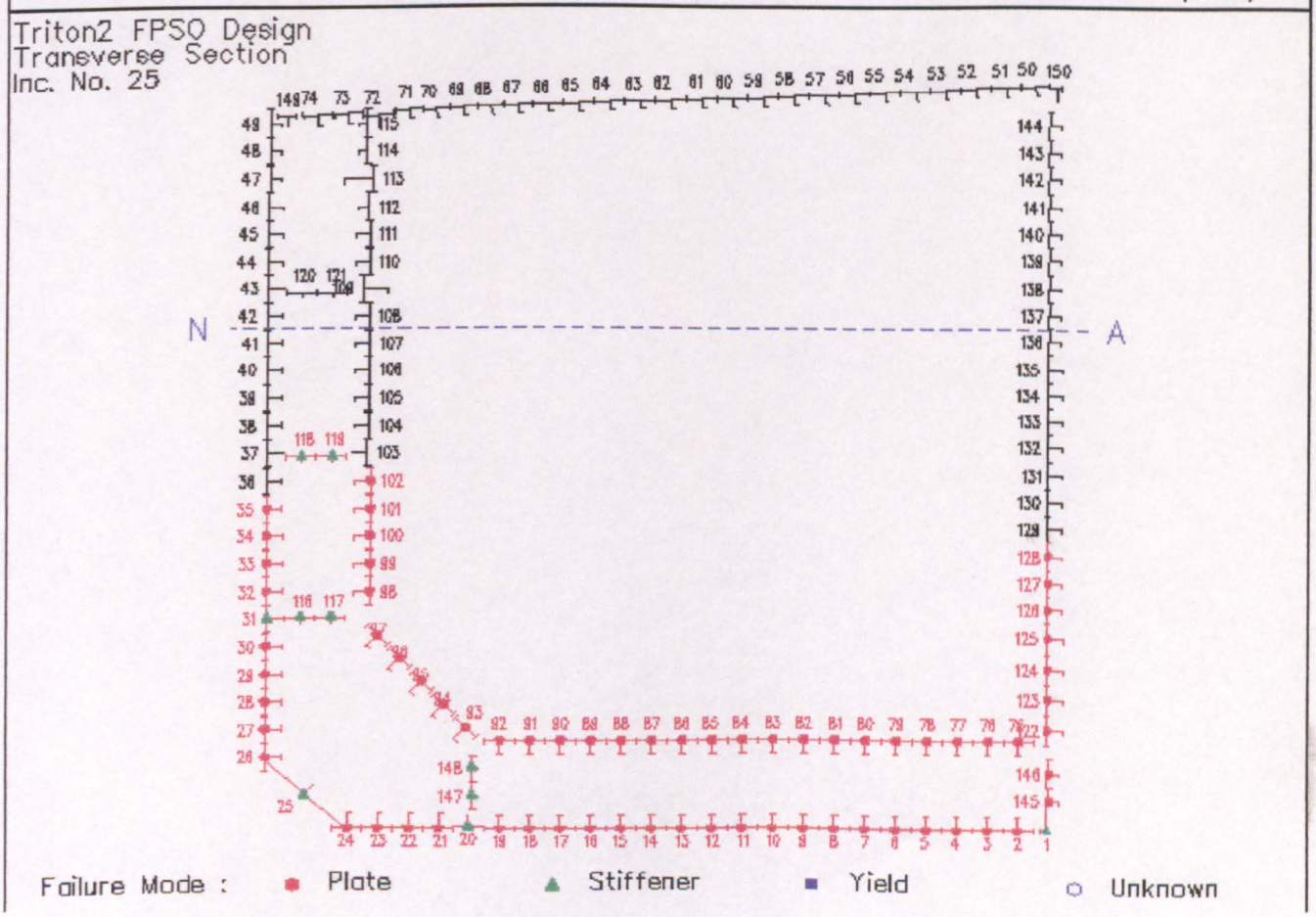
Triton2 FPSO Design
Transverse Section
Inc. No. 25
N
A
Failure Mode : Plate Stiffener Yield Unknown

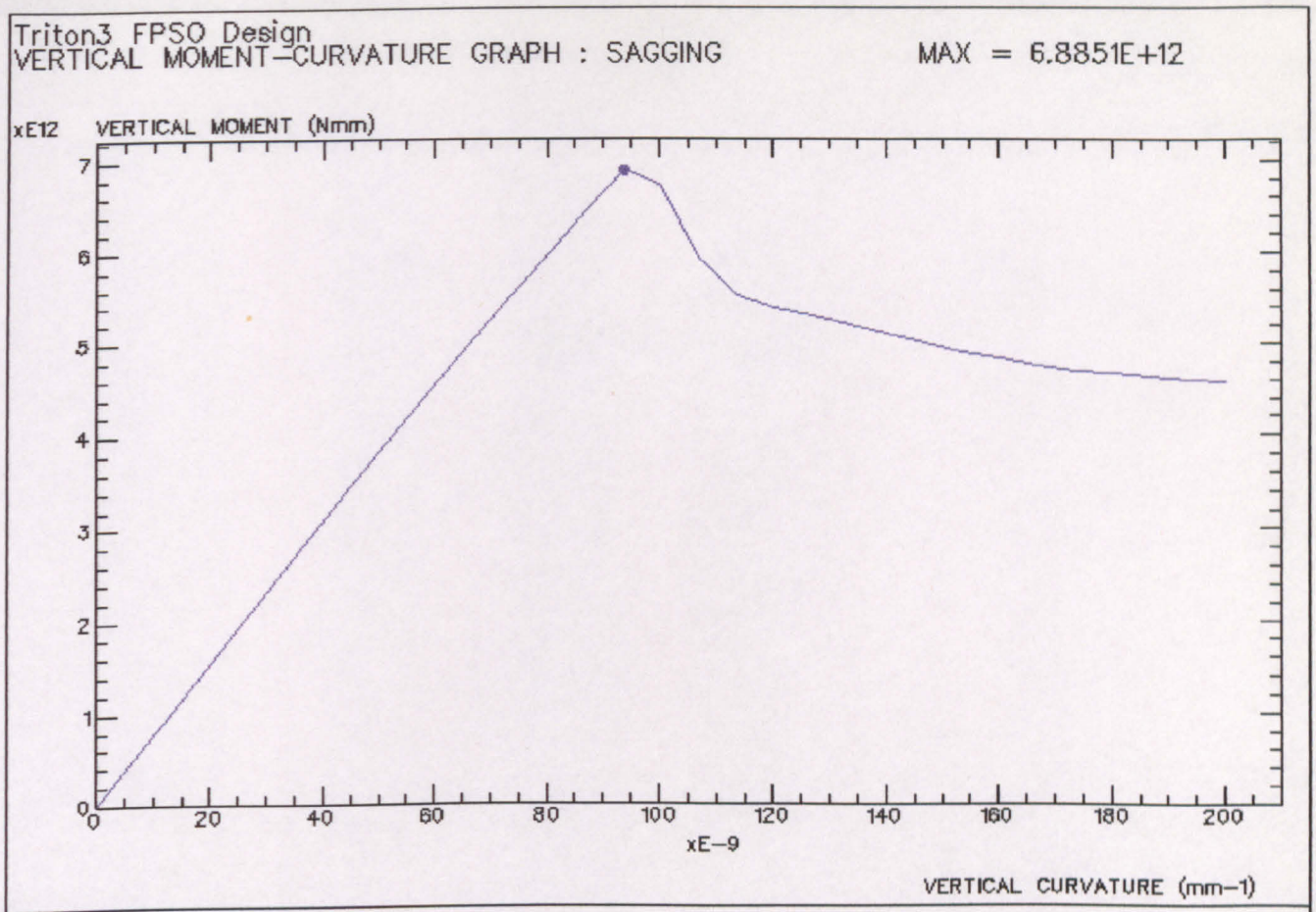
Triton3 FPSO Design
VERTICAL MOMENT-CURVATURE GRAPH : SAGGING
MAX = 6.8851E+12
xE12
VERTICAL MOMENT (Nmm)
0
1
2
3
4
5
6
7
0
20
40
60
80
100
120
140
160
180
200
xE-9
VERTICAL CURVATURE (mm-1)

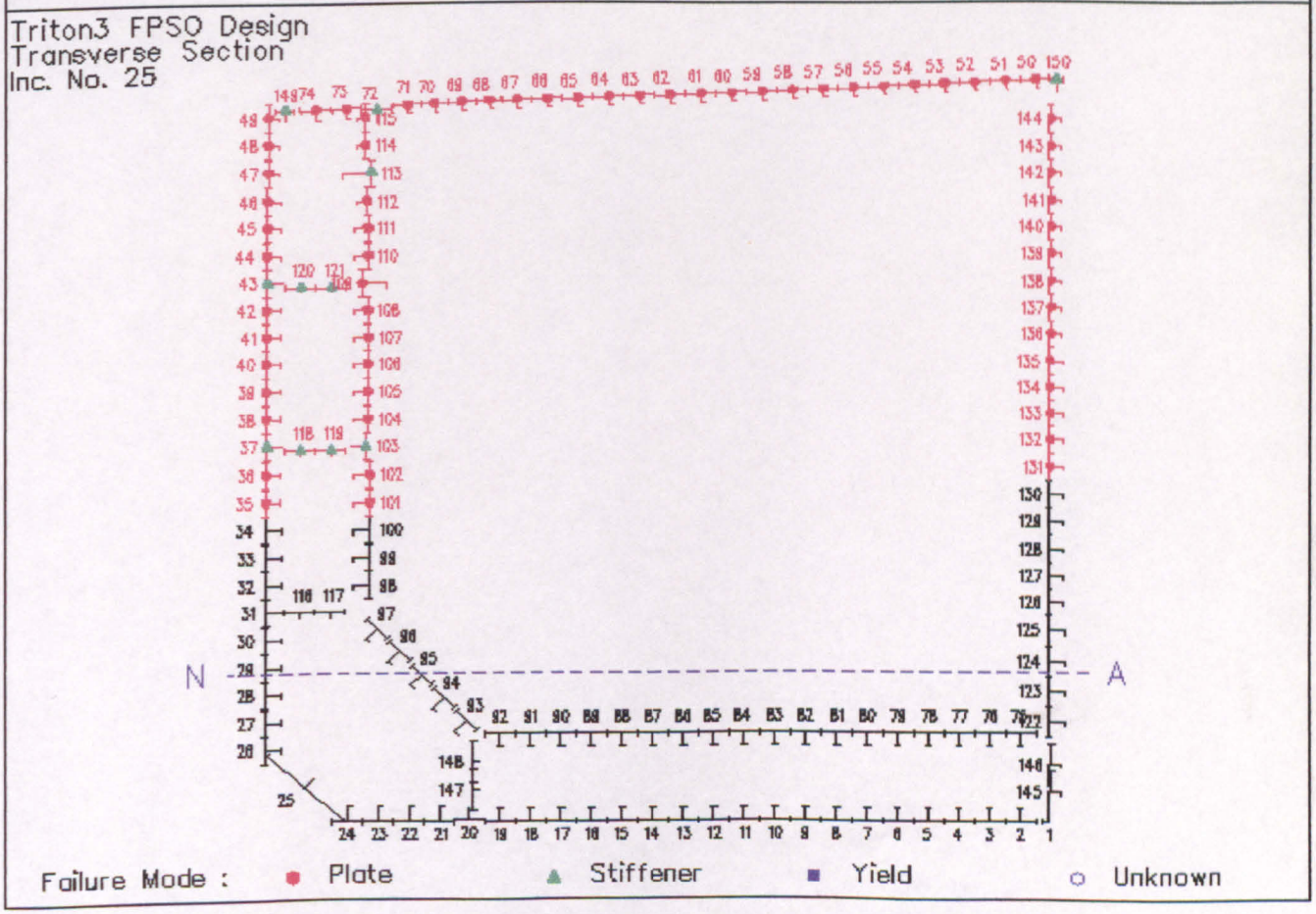
Triton3 FPSO Design
Transverse Section
Inc. No. 25
N
A
Failure Mode :
Plate
Stiffener
Yield
Unknown

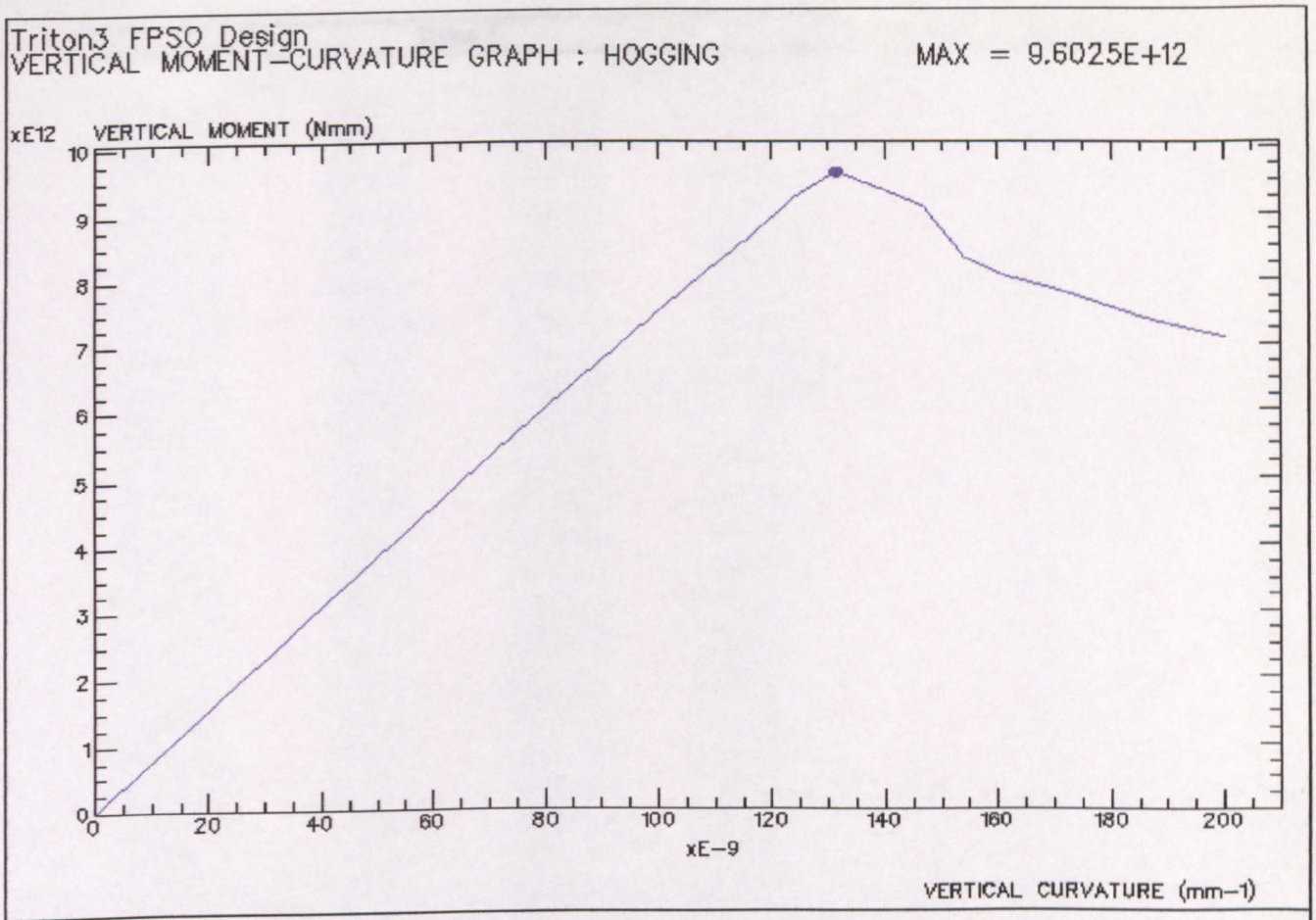
Triton3 FPSO Design
VERTICAL MOMENT-CURVATURE GRAPH : HOGGING
MAX = 9.6025E+12
xE12 VERTICAL MOMENT (Nmm)
0
1
2
3
4
5
6
7
8
9
10
0
20
40
60
80
100
120
140
160
180
200
xE-9
VERTICAL CURVATURE (mm-1)

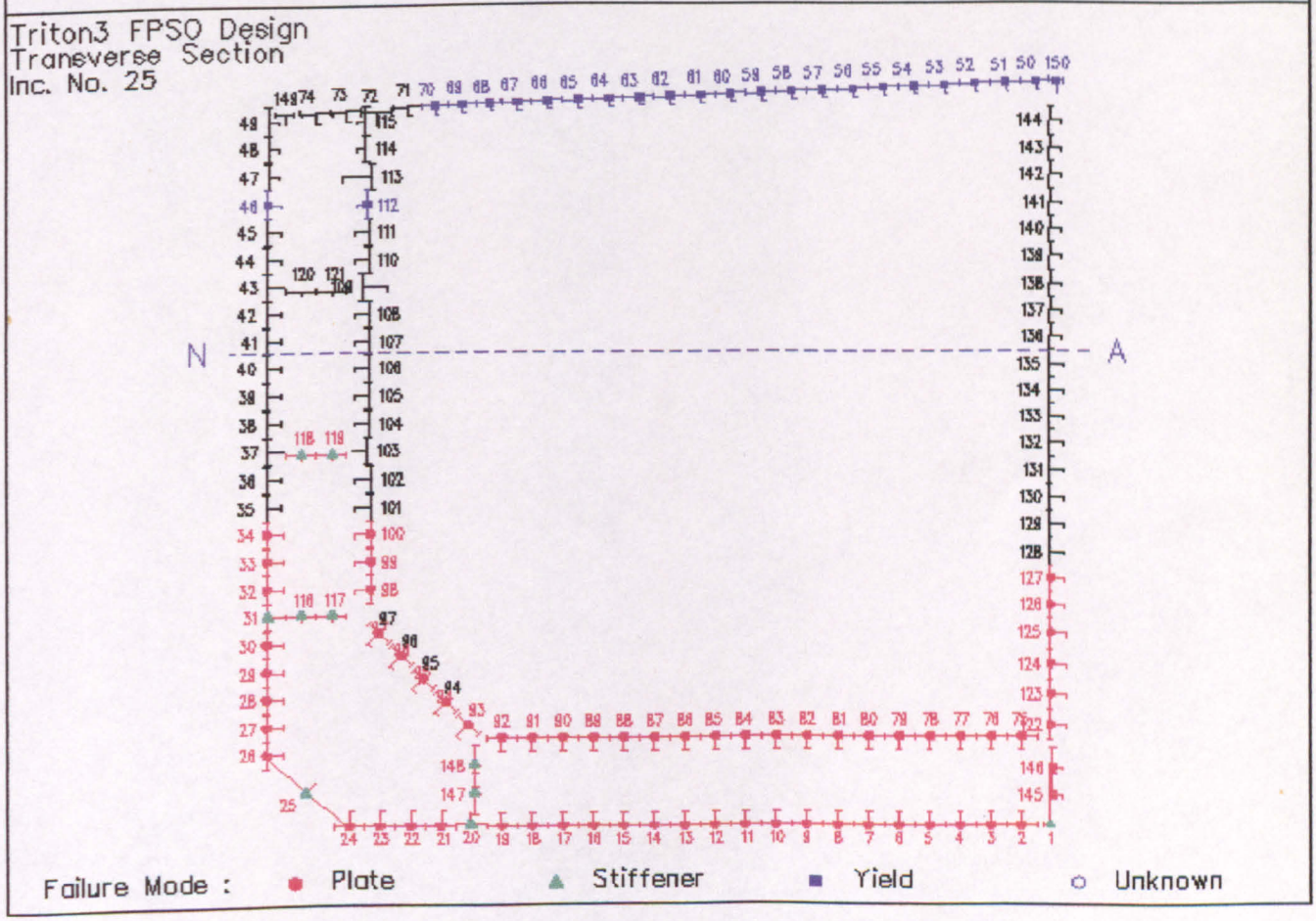
Triton3 FPSO Design
Transverse Section
Inc. No. 25
N
A
Failure Mode : Plate Stiffener Yield Unknown

Triton 1			
Sagging		Hogging	
Curvature	VBM	Curvature	VBM
0.00E+00	0	0.00E+00	0
-3.59E-08	-2686.58	8.99E-09	673.2
-4.41E-08	-3300.46	1.85E-08	1385.7
-5.23E-08	-3889.06	2.81E-08	2098.2
-6.05E-08	-4456.34	3.76E-08	2810.4
-6.87E-08	-5019.8	4.72E-08	3516.1
-7.69E-08	-5582.45	5.67E-08	4187.8
-8.51E-08	-6141.49	6.63E-08	4847.6
-9.33E-08	-6692.77	7.58E-08	5505.9
-1.02E-07	-6570.57	8.54E-08	6163.5
-1.10E-07	-5606.85	9.49E-08	6822.4
-1.18E-07	-5229.85	1.04E-07	7481.8
-1.26E-07	-5104.84	1.14E-07	8140.8
-1.34E-07	-4980.28	1.24E-07	8329.1
-1.43E-07	-4868.16	1.33E-07	7851.1
-1.51E-07	-4750.41	1.43E-07	7229.0
-1.59E-07	-4652.31	1.52E-07	7052.3
-1.67E-07	-4576.56	1.62E-07	6856.5
-1.75E-07	-4503.17	1.71E-07	6645.4
-1.84E-07	-4464.25	1.81E-07	6495.4
-1.92E-07	-4415.79	1.90E-07	6365.6
-2.00E-07	-4372.68	2.00E-07	6246.7

Triton 2			
Sagging		Hogging	
Curvature	VBM	Curvature	VBM
0.00E+00	0	0.00E+00	0
-4.30E-08	-3482.62	1.85E-08	1495.9
-4.96E-08	-4010.29	2.82E-08	2273.5
-5.61E-08	-4528.47	3.78E-08	3050.8
-6.27E-08	-5029.64	4.75E-08	3826.2
-6.92E-08	-5526.75	5.71E-08	4583.3
-7.57E-08	-6022.99	6.67E-08	5314.2
-8.23E-08	-6519.02	7.64E-08	6040.2
-8.88E-08	-7010.29	8.60E-08	6765.8
-9.54E-08	-7499.57	9.57E-08	7492.7
-1.02E-07	-7898.56	1.05E-07	8219.9
-1.08E-07	-7050.71	1.15E-07	8946.8
-1.15E-07	-6280.36	1.25E-07	9669.1
-1.22E-07	-6052.3	1.34E-07	9462.6
-1.28E-07	-5879.04	1.44E-07	7907.2
-1.35E-07	-5742.23	1.54E-07	7726.3
-1.41E-07	-5624.52	1.63E-07	7467.6
-1.48E-07	-5524.1	1.73E-07	7228.9
-1.54E-07	-5429.24	1.82E-07	7021.6
-1.61E-07	-5344.65	1.92E-07	6861.2
-1.67E-07	-5274.08	2.02E-07	6743.3
-1.74E-07	-5210.98	2.11E-07	6637.3
-1.8038E-07	-5146.66	2.21E-07	6566.81
-1.8692E-07	-5090.37	2.31E-07	6525.68
-1.9346E-07	-5027.66	2.40E-07	6482.78

Triton 3			
Sagging		Hogging	
Curvature	VBM	Curvature	VBM
0.00E+00	0	0.00E+00	0
9.36E-09	728.0	-3.35E-08	-2607.82
1.70E-08	1318.9	-4.02E-08	-3124.82
2.46E-08	1909.6	-4.69E-08	-3635.5
3.22E-08	2500.4	-5.35E-08	-4122.82
3.99E-08	3090.5	-6.02E-08	-4602.07
4.75E-08	3678.8	-6.68E-08	-5078.01
5.51E-08	4262.5	-7.35E-08	-5552.77
6.27E-08	4836.3	-8.01E-08	-6023.69
7.04E-08	5399.1	-8.68E-08	-6490.04
7.80E-08	5960.6	-9.35E-08	-6913
8.56E-08	6521.1	-1.00E-07	-6708.67
9.32E-08	7073.9	-1.07E-07	-5908.09
1.01E-07	7627.6	-1.13E-07	-5522.48
1.08E-07	8181.5	-1.20E-07	-5389.69
1.16E-07	8735.1	-1.27E-07	-5305.93
1.24E-07	9288.4	-1.33E-07	-5196.11
1.31E-07	9728.2	-1.40E-07	-5097.76
1.39E-07	9515.3	-1.47E-07	-4999.56
1.47E-07	9185.0	-1.53E-07	-4907.99
1.54E-07	8557.3	-1.60E-07	-4828.66
1.62E-07	8092.9	-1.67E-07	-4761.89
1.69E-07	7939.4	-1.73E-07	-4706.55
1.77E-07	7727.5	-1.80E-07	-4676.31
1.85E-07	7491.0	-1.87E-07	-4638.33
1.92E-07	7322.8	-1.93E-07	-4604.78
2.00E-07	7182.5	-2.00E-07	-4565.08

Appendix C

Cross Section Failure

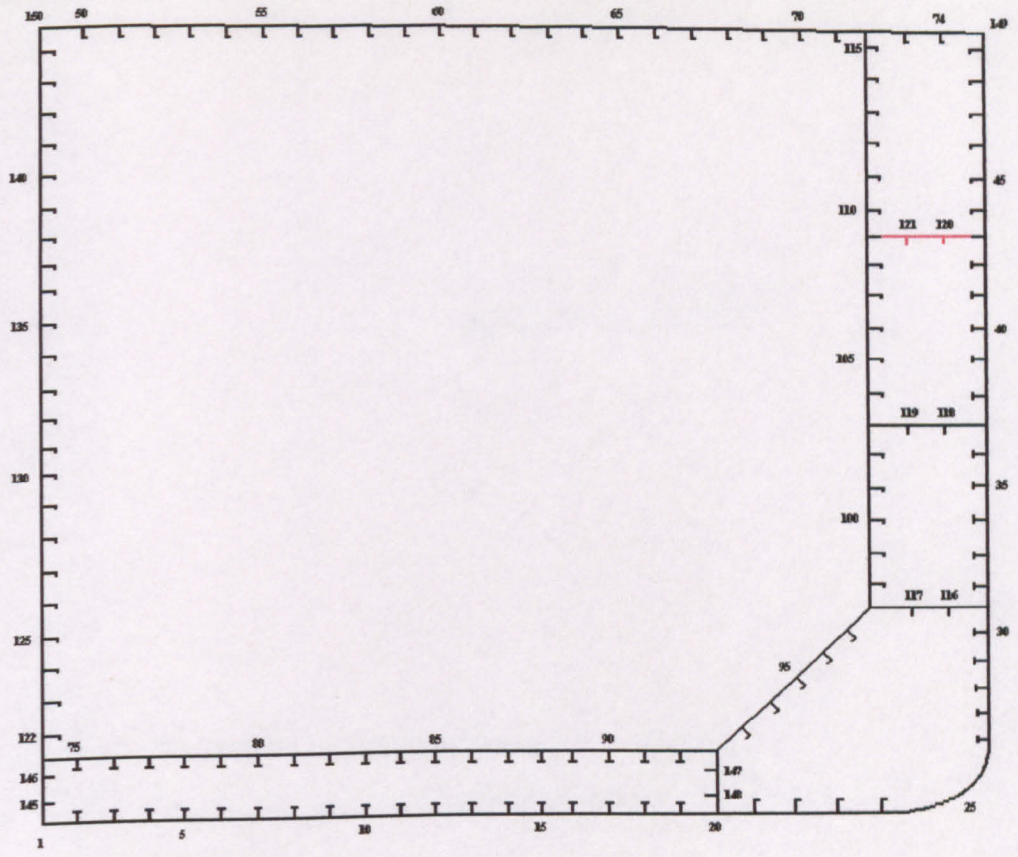

Curvature:-0.9*10-7 mm

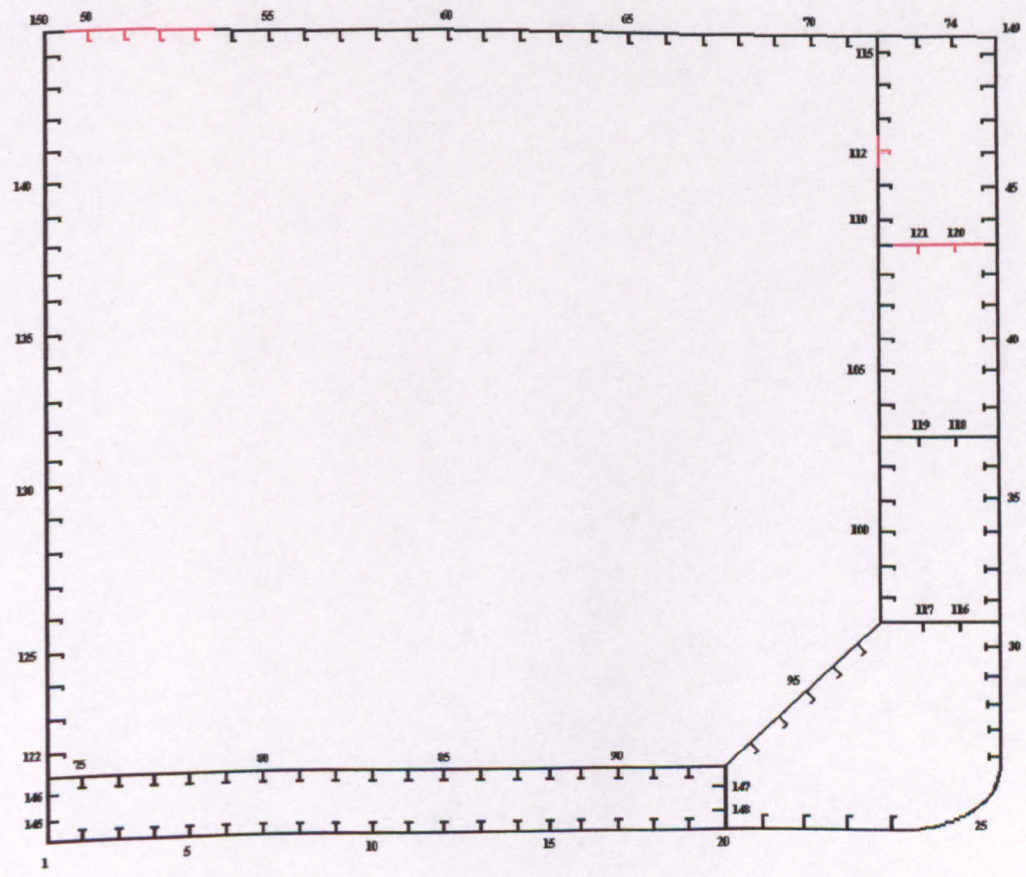

Curvature:-1.0*10-7 mm

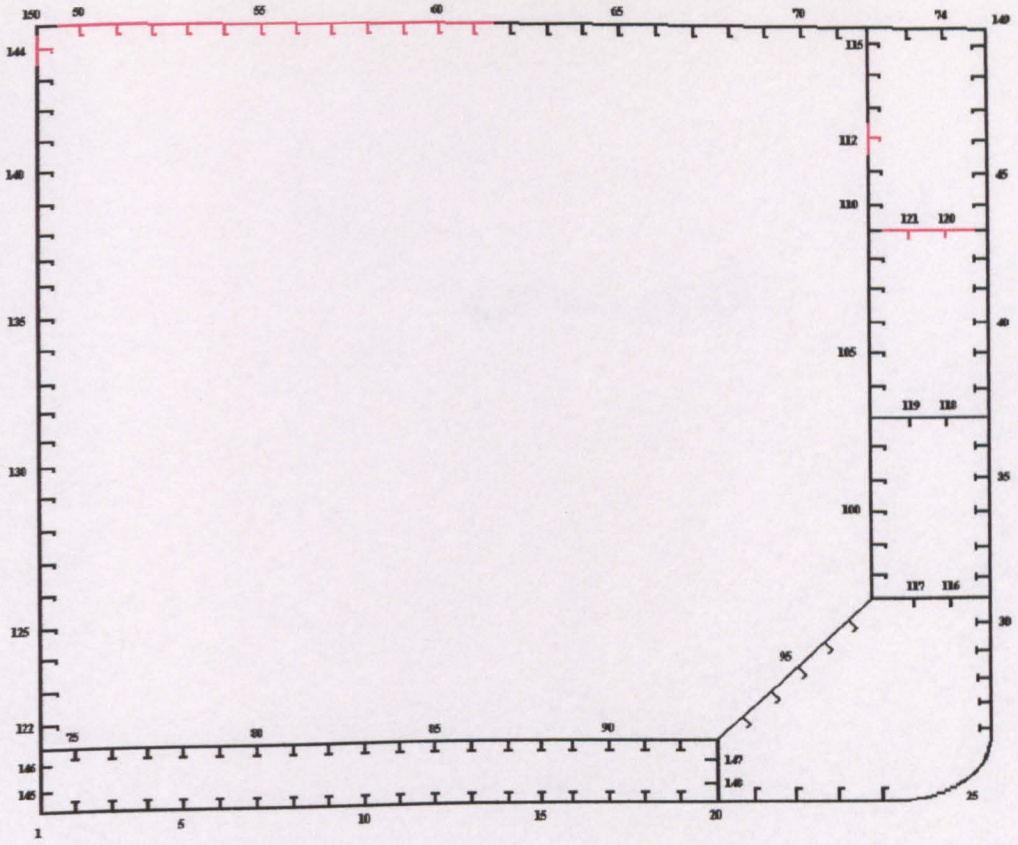

Curvature:-1.02*10-7 mm

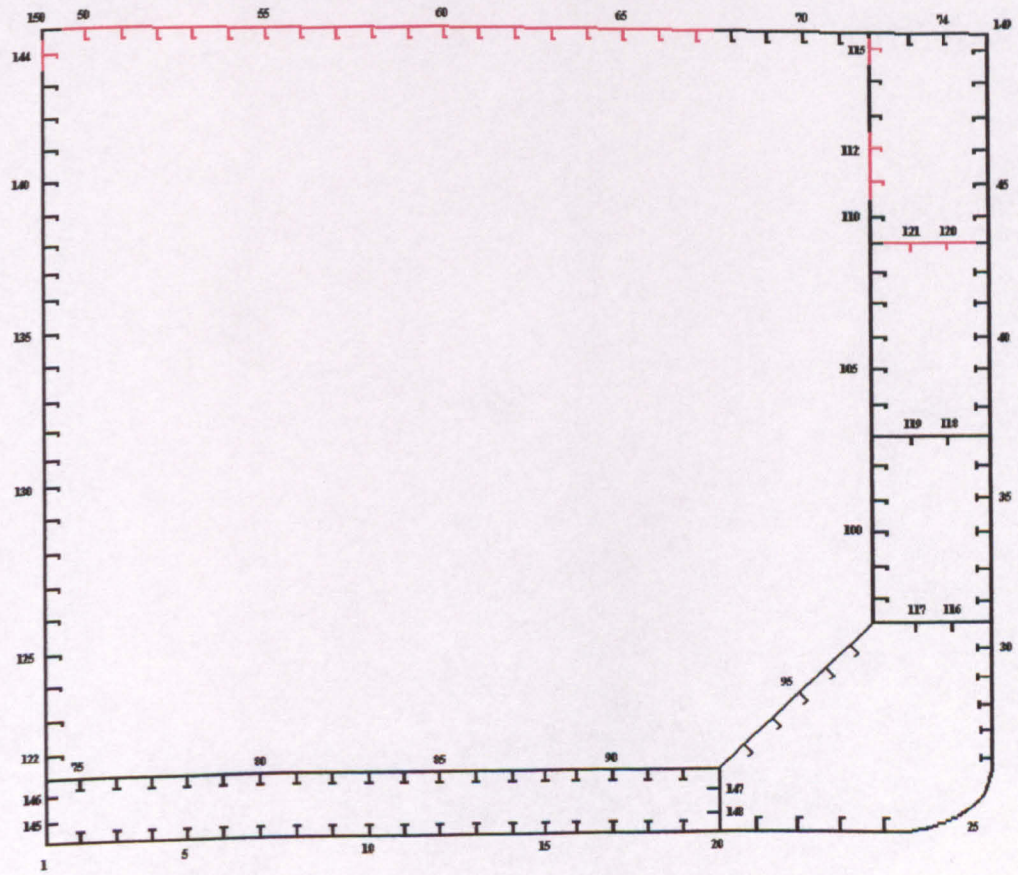

Curvature:-1.04*10-7 mm

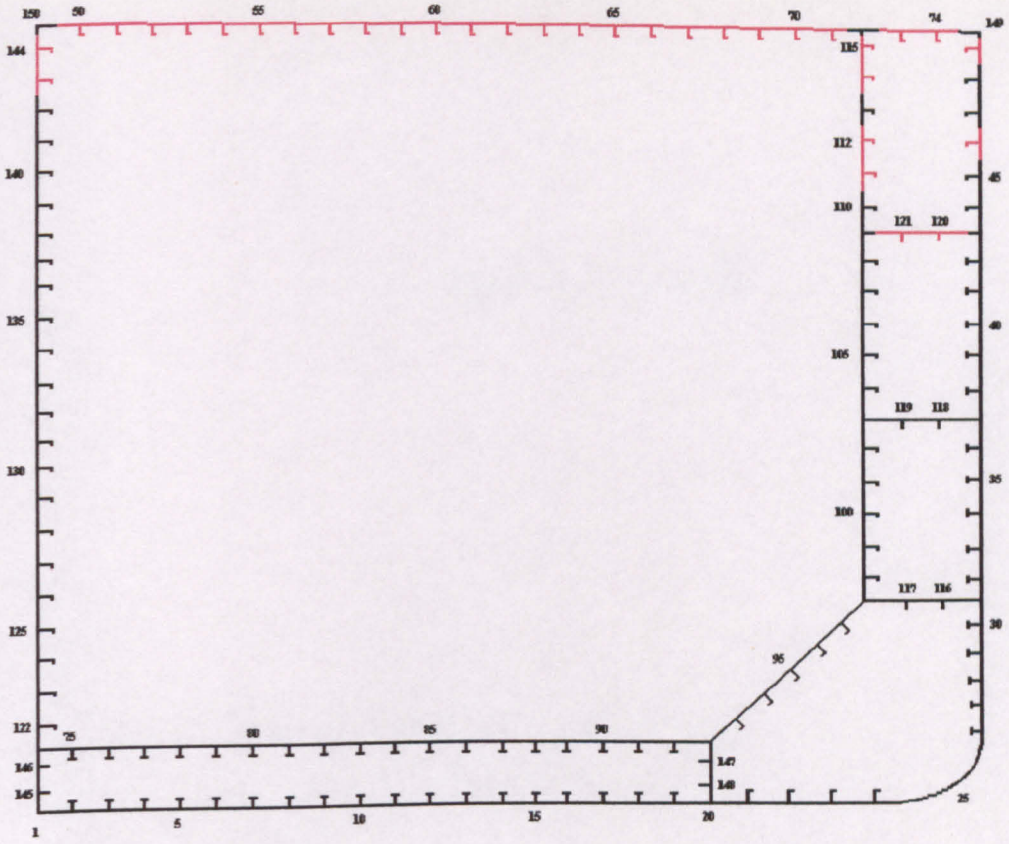

Curvature: -1.06*10-7 mm

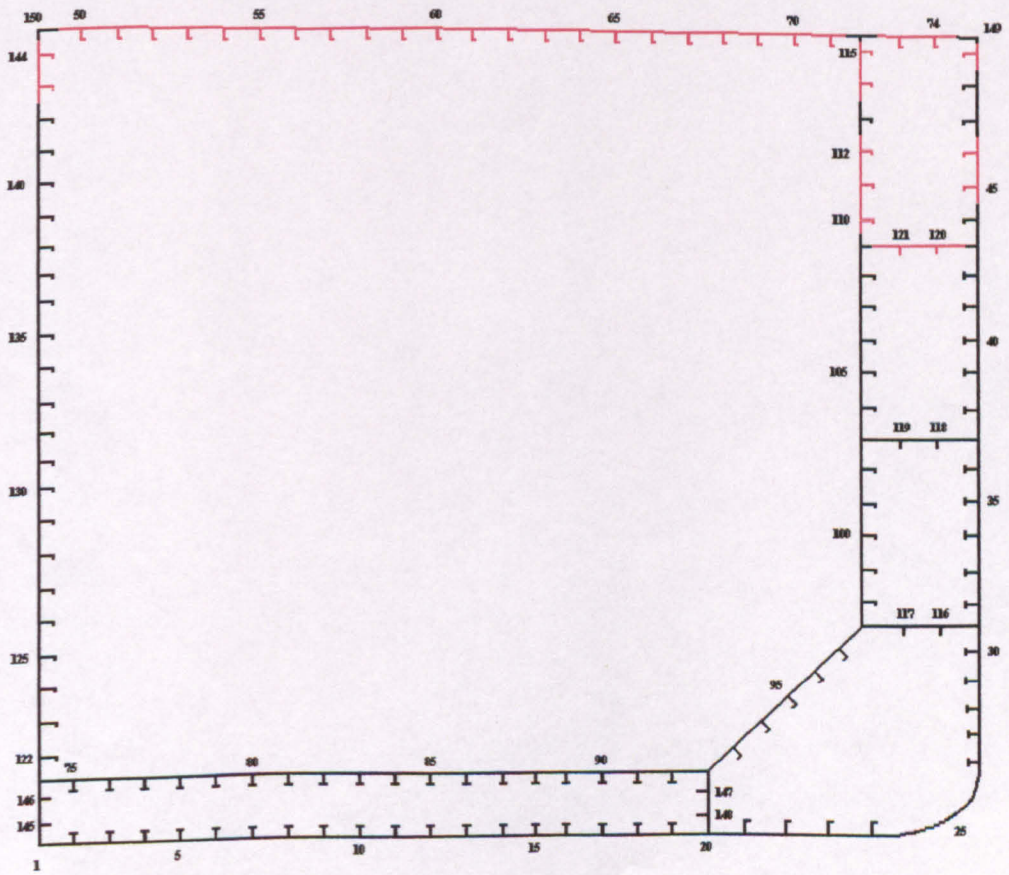

Curvature: -1.08*10-7 mm

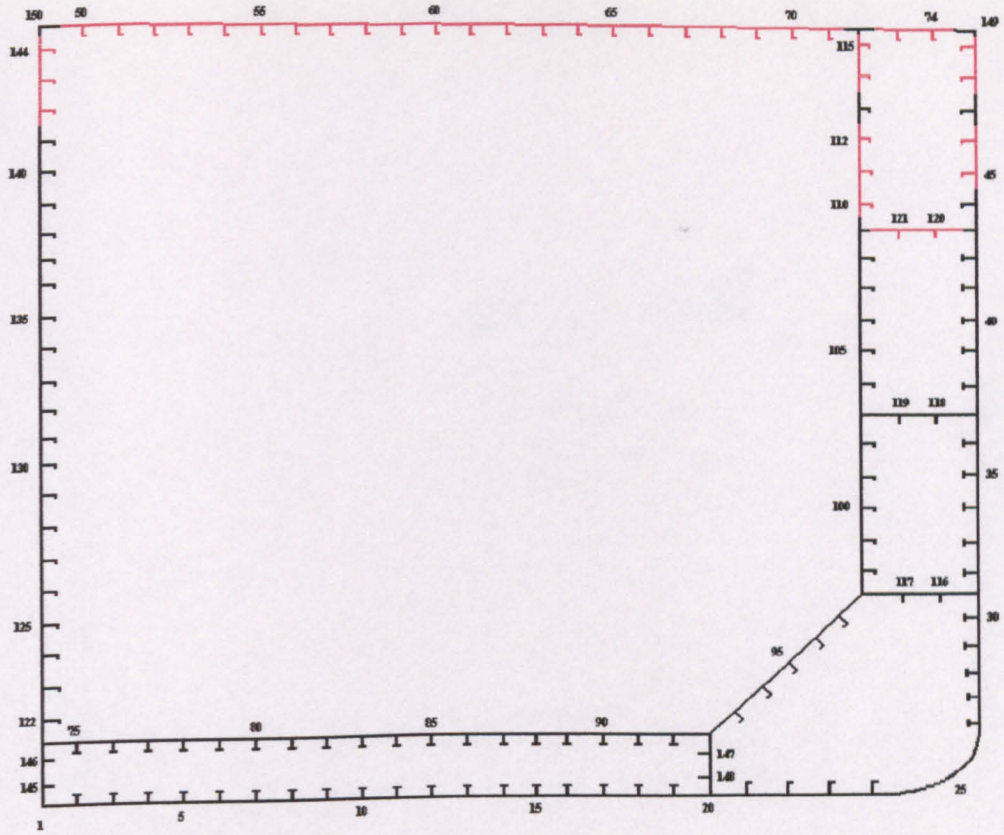

Curvature: -1.1*10-7 mm

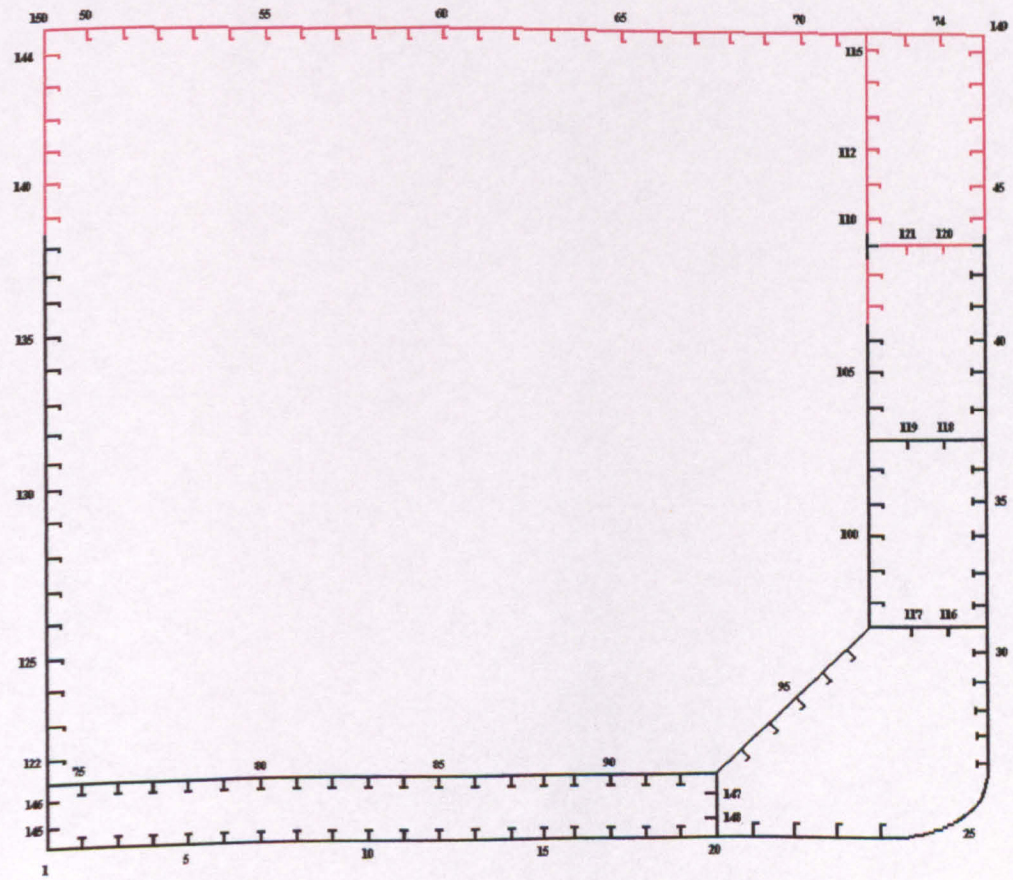

Curvature: -1.2*10-7 mm

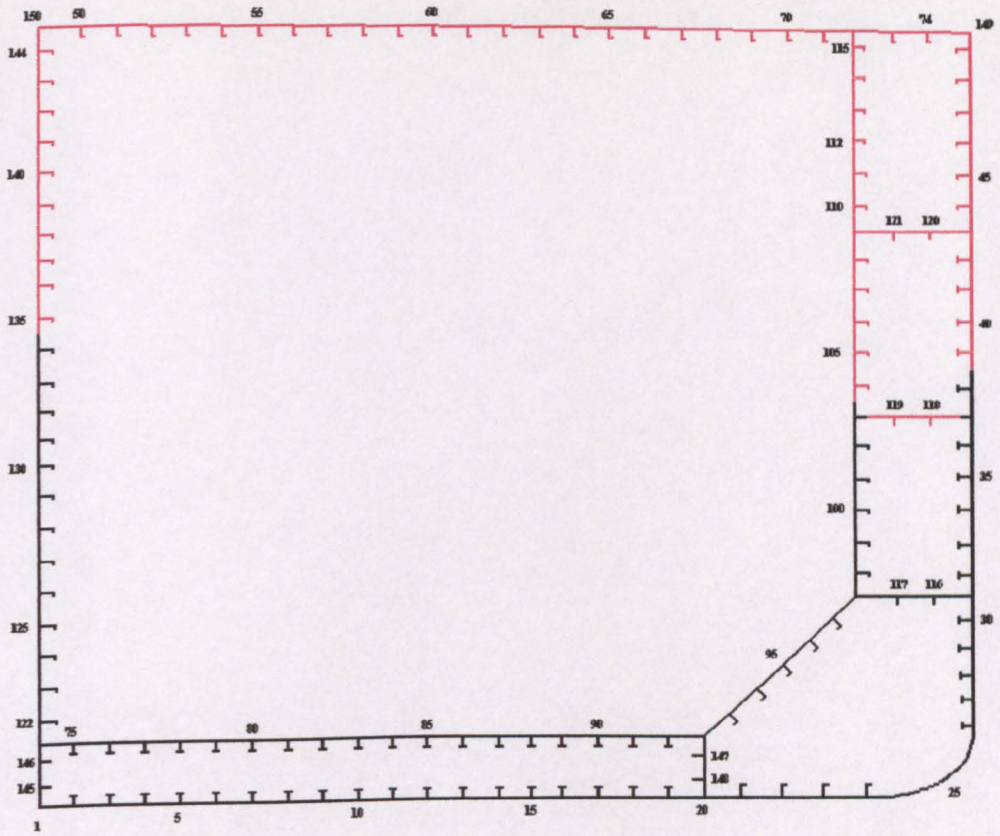

Curvature: -1.5*10-7 mm

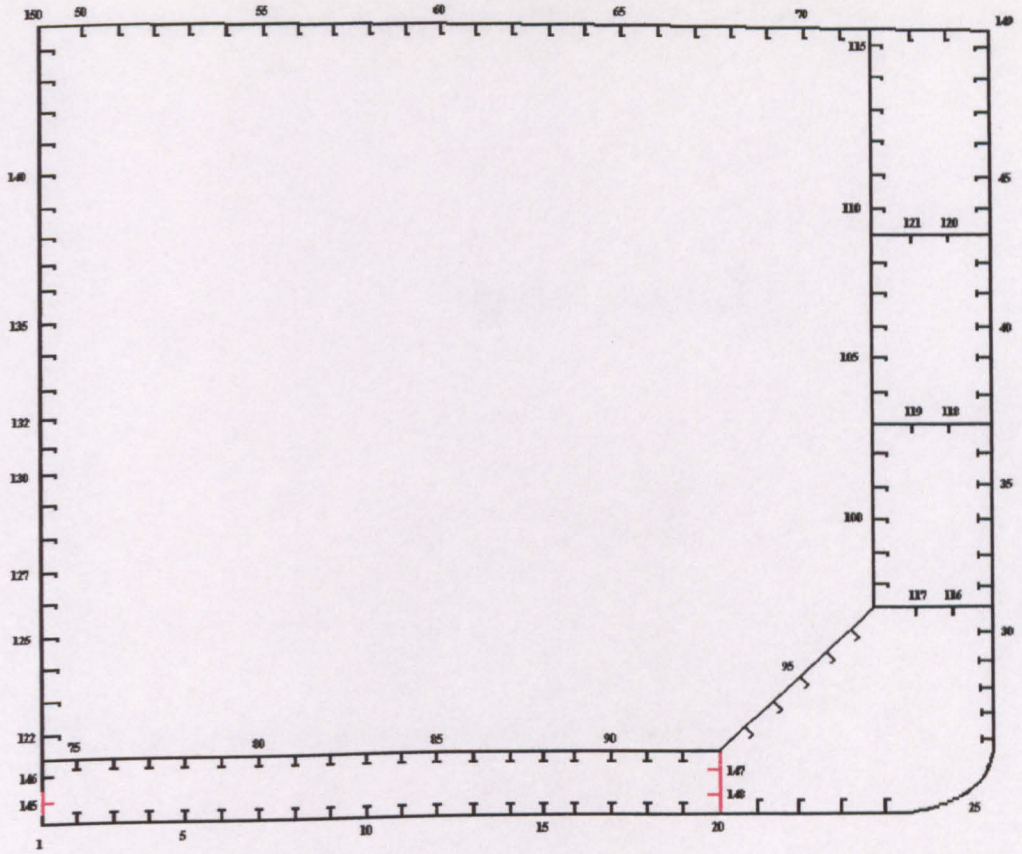

Curvature: 1.2*10-7 mm

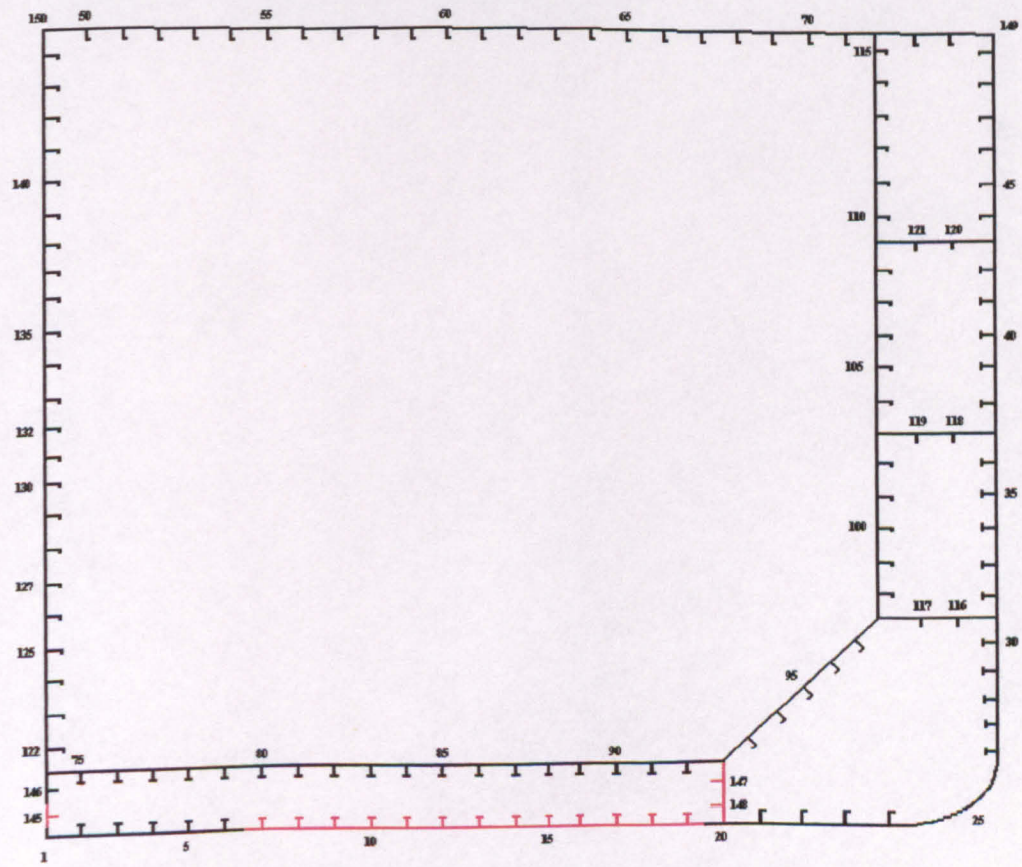

Curvature: 1.25*10-7 mm

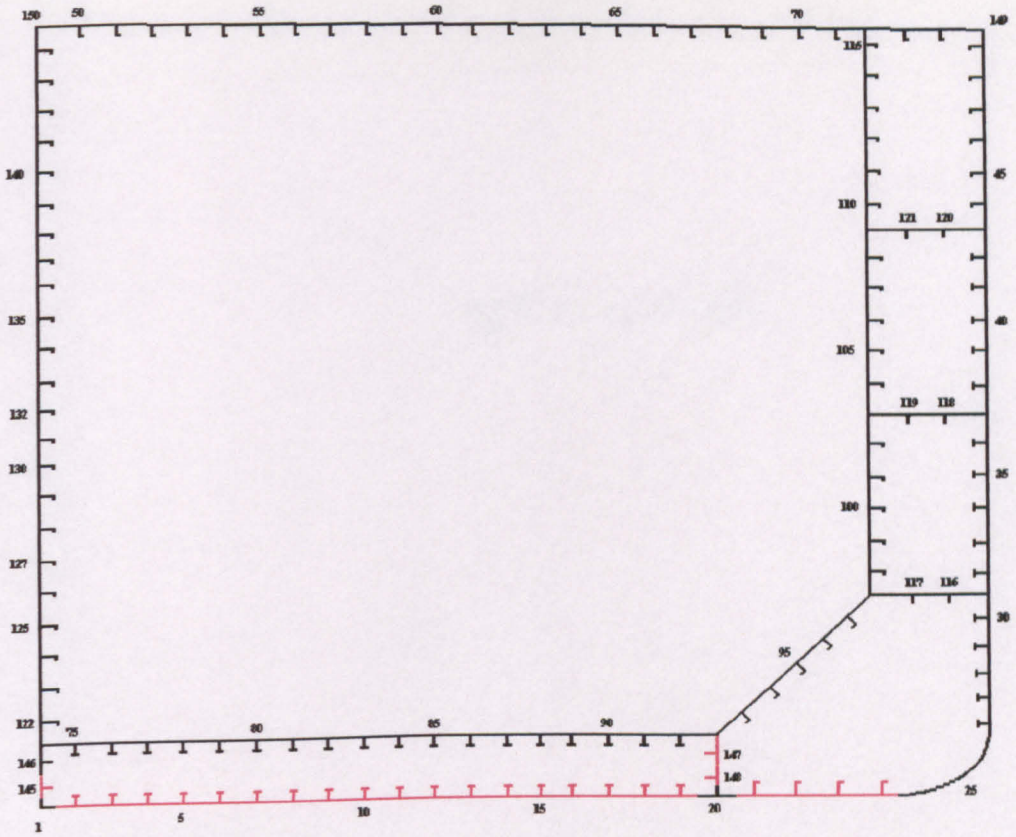

Curvature: 1.275 *10-7 mm

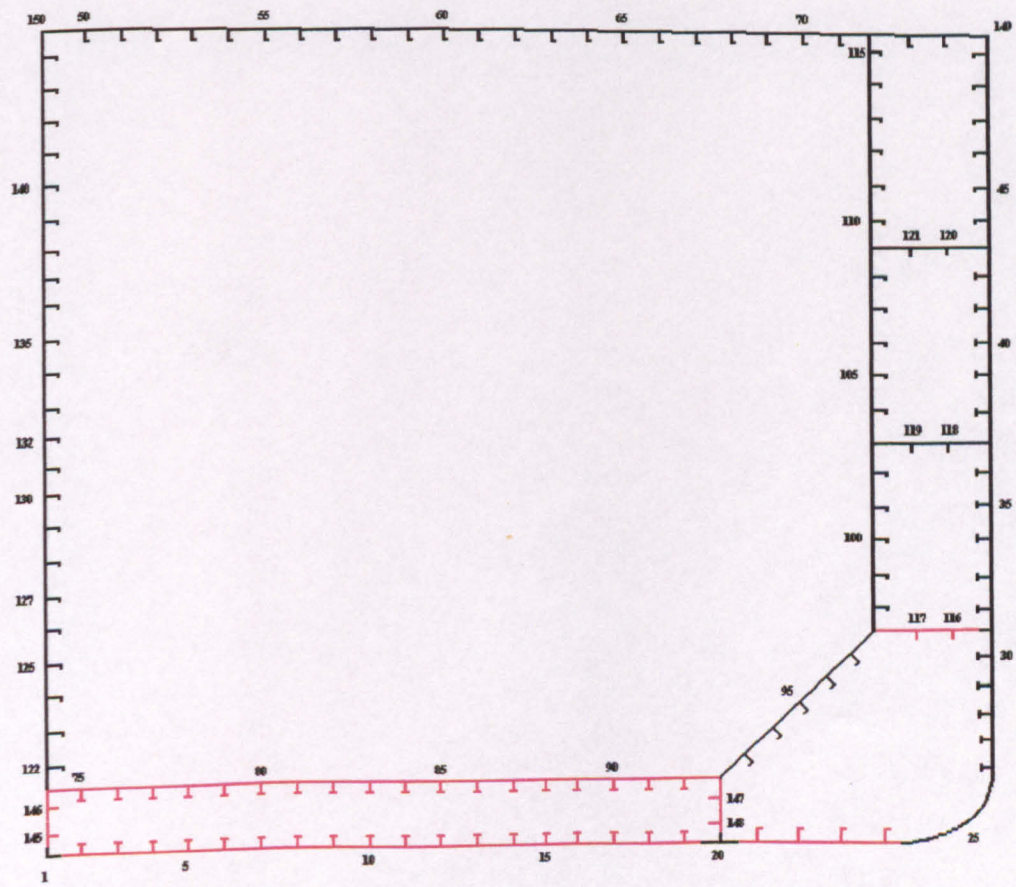

Curvature: 1.35*10-7 mm

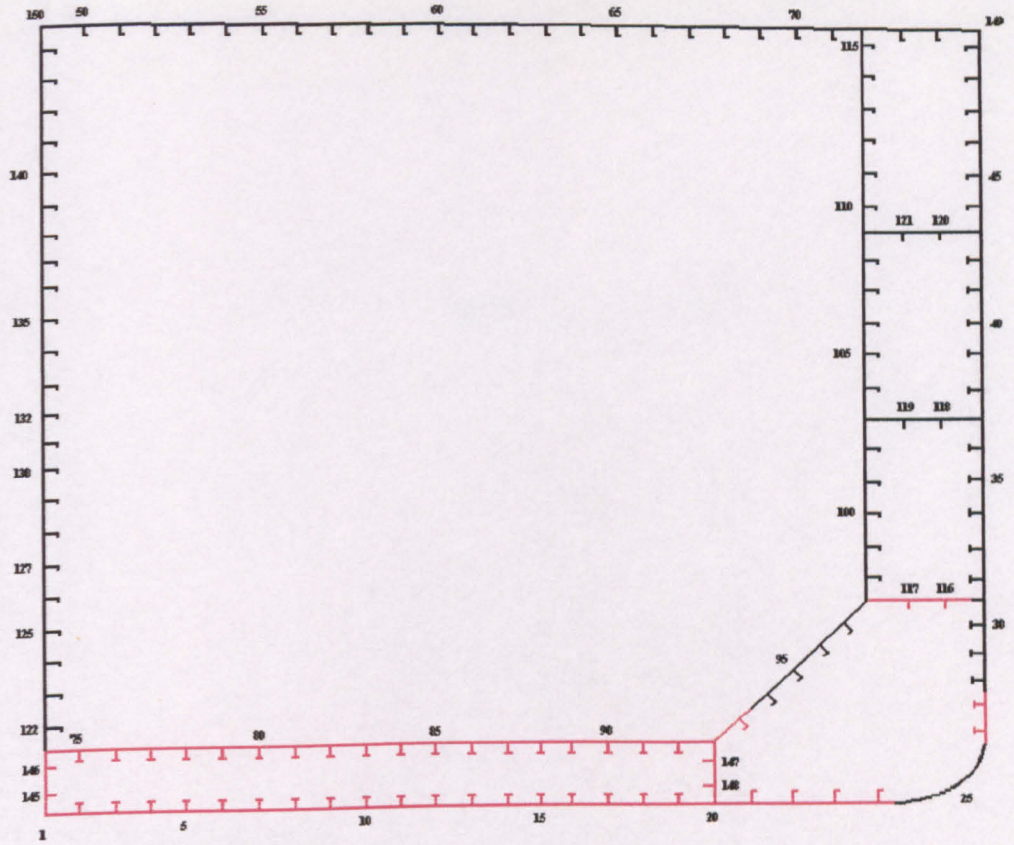

Curvature: 1.375 *10-7 mm

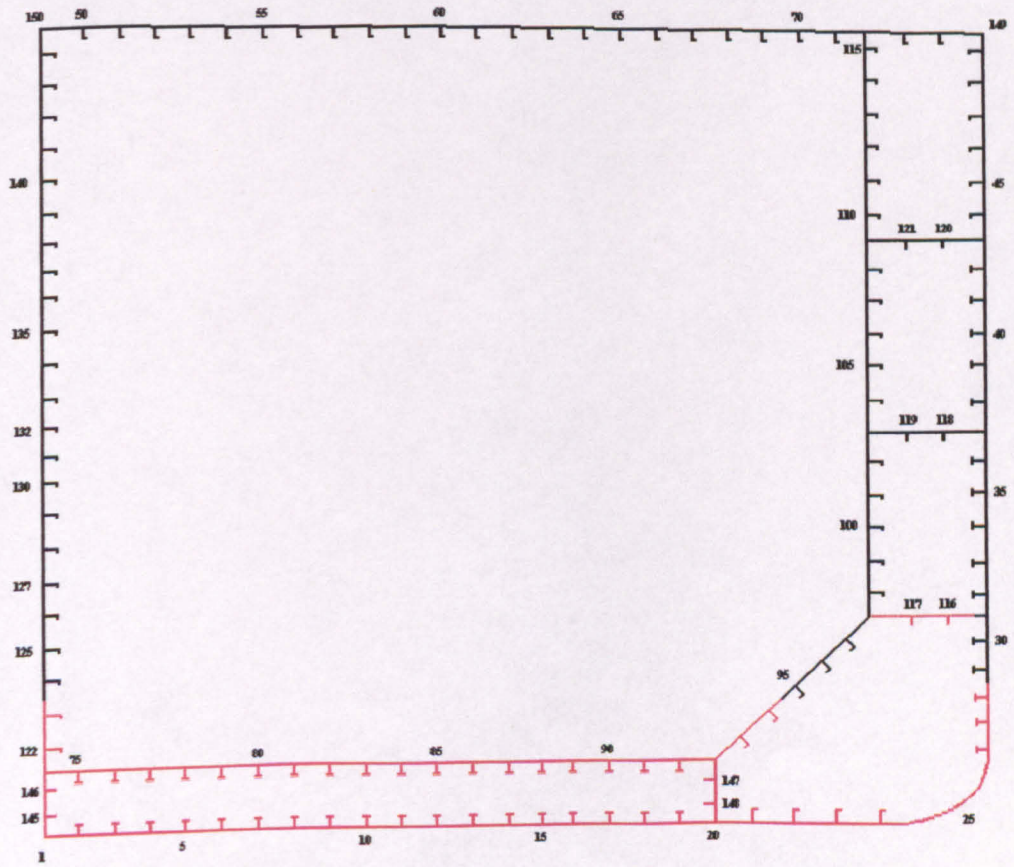

Curvature: 1.45 *10-7 mm

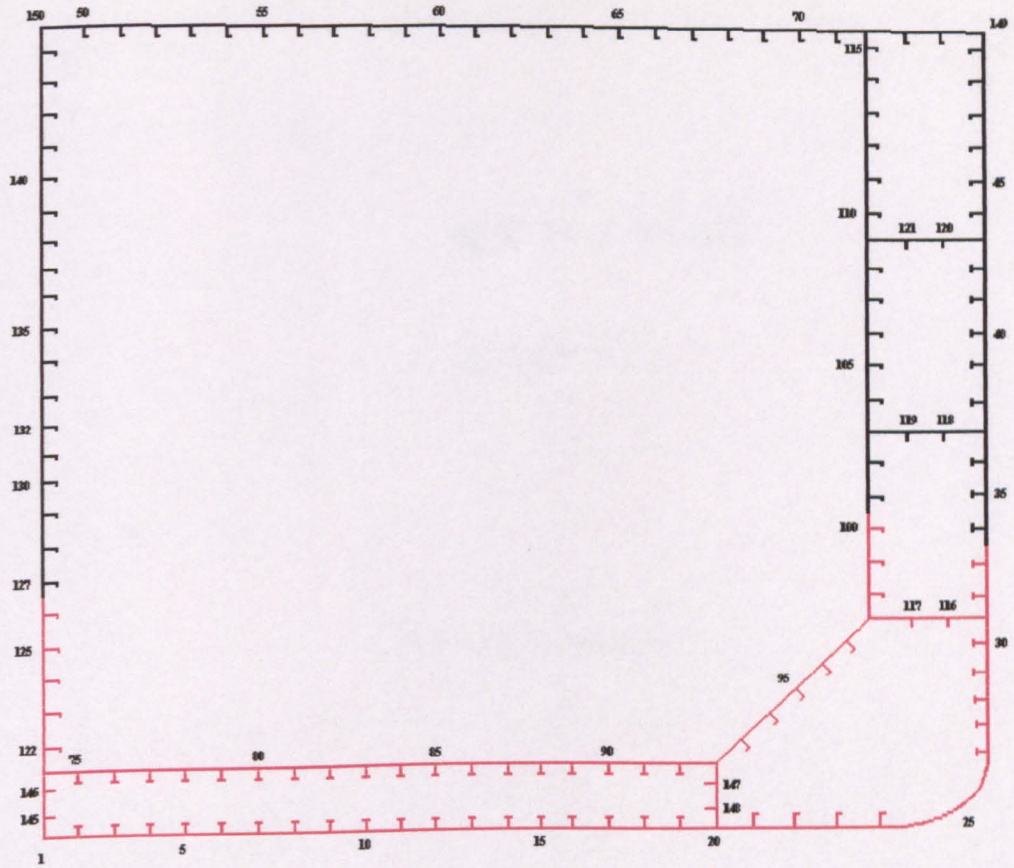

Curvature: 1.75 *10-7 mm

Appendix D

IACS Requirements

IACS Requirements.

Triton:

L := 233 T := 14.7 B := 42 D := 21.3

DWT := 105000 C_b := 0.78

Wave Coefficient:

$$C := \text{if}\left(90 \le L \le 300, 10.75 - \left(\frac{300 - L}{100}\right)^{1.5}, 10.75\right)$$

$$C := \text{if}\left(350 \le L \le 500, 10.75 - \left(\frac{L - 350}{150}\right)^{1.5}, C\right)$$

C = 10.202

Wave Bending Moments:

Hog:

$M_{w.h} := 190 \cdot C \cdot L^2 \cdot B \cdot C_b$

$M_{w.h} = 3.447 \cdot 10^9$ Nm

Sag:

$M_{w.s} := 110 \cdot C \cdot L^2 \cdot B \cdot (C_b + 0.7)$

$M_{w.s} = 3.787 \cdot 10^9$ Nm

Still Water Bending Moments:

Hog:

$M_{sw.h} := C \cdot L^2 \cdot B \cdot (122.5 - 15 \cdot C_b)$

$M_{sw.h} = 2.577 \cdot 10^9$ Nm

Sag:

$M_{sw.s} := 65 \cdot C \cdot L^2 \cdot B \cdot (C_b + 0.7)$

$M_{sw.s} = 2.238 \cdot 10^9$ Nm

Total Values:

Hog:

$M_{t.h} := M_{sw.h} + M_{w.h}$

$M_{t.h} = 6.025 \cdot 10^9$ Nm

Sag:

$M_{t.s} := M_{sw.s} + M_{w.s}$

$M_{t.s} = 6.025 \cdot 10^9$ Nm

DNV, Rules for Ships, Section 5, LONGITUDINAL STRENGTH

C300 Section Modulus

302 The midship section modulus about the transverse neutral axis is not to be less than:

$f_1 := 1.0$ (Material factor depending on material strength group)

$$Z_0 := \frac{C}{f_1} \cdot L^2 \cdot B \cdot (C_b + 0.7) \cdot 1000 \qquad Z_0 = 3.443 \cdot 10^{10} \quad mm^3$$

303 The section modulus requirements about the transverse neutral axis based on cargo and ballast conditions are given by:

$\sigma_1 := 175$

$$Z := \frac{|M_{t.s}|}{\sigma_1} \cdot 1000 \qquad Z = 3.443 \cdot 10^{10} \quad mm^3$$

C400 Moment of Inertia

401 The midship section moment of inertia about the transverse neutral axis is not to be less than:

$$I := 3 \cdot C \cdot L^3 \cdot B \cdot (C_b + 0.7) \cdot 10000 \qquad I = 2.406 \cdot 10^{14} \quad mm^4$$

Appendix E

Weight Distributions and Hull Geometry

Weight Distribution, Triton, Full Load

	Lightweight		Full Load		Fixed weights & Topside		Total	
	Weight	LCG	Weight	LCG	Weight	LCG	LCG	Weight
Step 1	124.00	-1.825	269.40	-2.171			-2.062	393.40
Step 2	365.00	3.180	746.00	3.401			3.328	1111.00
Step 3	226.00	8.057	558.80	8.038			8.043	784.80
Step 4	67.00	10.414	195.60	10.406			10.408	262.60
Step 5	769.00	15.262					15.262	769.00
Step 6	163.00	20.013	16.20	20.000			20.012	179.20
Step 7	359.00	22.008	24.50	22.000			22.007	383.50
Step 8	379.00	24.411	24.50	24.400			24.410	403.50
Step 9	399.00	26.810	24.50	26.800			26.809	423.50
Step 10	420.00	29.210	24.50	29.200			29.209	444.50
Step 11	584.00	32.433	33.70	32.400			32.431	617.70
Step 12	509.00	36.019	26.90	36.000			36.018	535.90
Step 13	350.00	39.627	1218.00	39.628			39.628	1568.00
Step 14	424.00	43.685	1896.00	43.729			43.721	2320.00
Step 15	345.00	47.776	2277.00	47.837			47.829	2622.00
Step 16	341.00	51.896	2429.00	51.912	100.00	50.000	51.843	2870.00
Step 17	345.00	56.007	2511.00	56.031			56.028	2856.00
Step 18	337.00	60.138	2594.00	60.151			60.150	2931.00
Step 19	336.00	64.258	2676.00	64.271			64.270	3012.00
Step 20	334.00	68.378	2758.00	68.390	1951.22	70.260	69.113	5043.22
Step 21	332.00	72.498	2840.00	72.510			72.509	3172.00
Step 22	330.00	76.618	2922.00	76.630			76.629	3252.00
Step 23	331.00	80.743	1850.50	80.740			80.740	2181.50
Step 24	331.00	84.859	1850.50	84.860			84.860	2181.50
Step 25	330.00	88.979	1850.50	88.980			88.980	2180.50
Step 26	328.00	93.099	1850.50	93.100			93.100	2178.50
Step 27	327.00	97.219	1850.50	97.220			97.220	2177.50
Step 28	326.00	101.339	1850.50	101.340	1047.22	99.350	100.693	3223.72
Step 29	325.00	105.459	1850.50	105.460			105.460	2175.50
Step 30	324.00	109.582	1357.00	109.580	100.00	108.140	109.500	1781.00
Step 31	351.00	113.645	1357.00	113.700			113.689	1708.00
Step 32	322.00	117.819	1357.00	117.820			116.500	1679.00
Step 33	321.00	121.939	1357.00	121.940			121.940	1678.00
Step 34	320.00	126.059	1357.00	126.060			126.060	1677.00
Step 35	319.00	130.179	1357.00	130.180	2272.42	129.960	130.053	3948.42
Step 36	318.00	134.299	1357.00	134.300			134.300	1675.00
Step 37	317.00	138.419	2344.00	138.420			138.420	2661.00
Step 38	316.00	142.539	2344.00	142.540			142.540	2660.00
Step 39	315.00	146.659	2344.00	146.660			146.660	2659.00
Step 40	314.00	150.780	2344.00	150.780			150.780	2658.00
Step 41	314.00	154.900	2344.00	154.900			154.900	2658.00
Step 42	314.00	159.020	2344.00	159.020	1315.80	161.920	159.980	3973.80
Step 43	313.00	163.140	2344.00	163.140			163.140	2657.00
Step 44	313.00	167.260	2357.00	167.259			167.259	2670.00
Step 45	313.00	171.380	2351.00	171.379			171.379	2664.00
Step 46	312.00	175.500	2346.00	175.499			175.499	2658.00
Step 47	312.00	179.620	2340.00	179.619			179.619	2652.00
Step 48	312.00	183.740	2335.00	183.739			183.739	2647.00
Step 49	312.00	187.860	2329.00	187.859			187.859	2641.00
Step 50	313.00	191.980	2324.00	191.979			191.979	2637.00
Step 51	314.00	196.100	2240.00	196.072			196.075	2554.00
Step 52	314.00	200.220	2054.00	200.189			200.193	2368.00
Step 53	546.00	204.920	1868.00	204.306			204.445	2414.00
Step 54	979.00	208.450	1682.00	208.422	571.78	208.525	208.449	3232.78
Step 55	547.00	212.019	1496.00	212.537			212.398	2043.00
Step 56	315.00	216.700	1310.00	216.651			216.660	1625.00
Step 57	315.00	220.820	1124.00	220.763			220.775	1439.00
Step 58	757.00	228.747					228.747	757.00
Total	20888.00	113.890	93082.10	125.474			123.142	121328.54

Weight Distribution, Triton, Partial Load

	Lightweight		Full Load		Fixed weights & Topside		Total	
	Weight	LCG	Weight	LCG	Weight	LCG	LCG	Weight
Step 1	124.00	-1.825	103.60	-2.1			-1.931	227.60
Step 2	365.00	3.180	504.40	3.5			3.362	869.40
Step 3	226.00	8.057	435.50	8.0			8.051	661.50
Step 4	67.00	10.414	133.40	10.4			10.411	200.40
Step 5	769.00	15.262					15.262	769.00
Step 6	163.00	20.013	16.20	20.0			20.012	179.20
Step 7	359.00	22.008	24.50	22.0			22.007	383.50
Step 8	379.00	24.411	24.50	24.4			24.410	403.50
Step 9	399.00	26.810	24.50	26.8			26.809	423.50
Step 10	420.00	29.210	24.50	29.2			29.209	444.50
Step 11	584.00	32.433	33.70	32.4			32.431	617.70
Step 12	509.00	36.019	26.90	36.0			36.018	535.90
Step 13	350.00	39.627	1218.00	39.6			39.628	1568.00
Step 14	424.00	43.685	1896.00	43.7			43.721	2320.00
Step 15	345.00	47.776	2277.00	47.8			47.829	2622.00
Step 16	341.00	51.896	1359.00	51.9	100.00	50.000	51.810	1800.00
Step 17	345.00	56.007	1441.00	56.0			56.034	1786.00
Step 18	337.00	60.138	1523.00	60.2			60.155	1860.00
Step 19	336.00	64.258	1605.00	64.3			64.275	1941.00
Step 20	334.00	68.378	1687.00	68.4	1951.22	70.260	69.311	3972.22
Step 21	332.00	72.498	1770.00	72.5			72.513	2102.00
Step 22	330.00	76.618	1851.00	76.6			76.632	2181.00
Step 23	331.00	80.743	1234.00	80.7			80.741	1565.00
Step 24	331.00	84.859	1234.00	84.9			84.860	1565.00
Step 25	330.00	88.979	1234.00	89.0			88.980	1564.00
Step 26	328.00	93.099	1234.00	93.1			93.100	1562.00
Step 27	327.00	97.219	1234.00	97.2			97.220	1561.00
Step 28	326.00	101.339	1234.00	101.3	1047.22	99.350	100.541	2607.22
Step 29	325.00	105.459	1234.00	105.5			105.460	1559.00
Step 30	324.00	109.582	1234.00	109.6	100.00	108.140	109.494	1658.00
Step 31	351.00	113.645	1234.00	113.7			113.688	1585.00
Step 32	322.00	117.819	1234.00	117.8			116.500	1556.00
Step 33	321.00	121.939	1234.00	121.9			121.940	1555.00
Step 34	320.00	126.059	1234.00	126.1			126.060	1554.00
Step 35	319.00	130.179	1234.00	130.2	2272.42	129.960	130.049	3825.42
Step 36	318.00	134.299	1234.00	134.3			134.300	1552.00
Step 37	317.00	138.419	1663.00	138.4			138.420	1980.00
Step 38	316.00	142.539	1661.00	142.5			142.540	1977.00
Step 39	315.00	146.659	1659.00	146.7			146.660	1974.00
Step 40	314.00	150.780	1656.00	150.8			150.780	1970.00
Step 41	314.00	154.900	1654.00	154.9			154.900	1968.00
Step 42	314.00	159.020	1649.00	159.0	1315.80	161.920	160.184	3278.80
Step 43	313.00	163.140	1650.00	163.1			163.140	1963.00
Step 44	313.00	167.260	1654.00	167.3			167.259	1967.00
Step 45	313.00	171.380	1649.00	171.4			171.379	1962.00
Step 46	312.00	175.500	1644.00	175.5			175.499	1956.00
Step 47	312.00	179.620	1639.00	179.6			179.619	1951.00
Step 48	312.00	183.740	1634.00	183.7			183.739	1946.00
Step 49	312.00	187.860	1628.00	187.9			187.859	1940.00
Step 50	313.00	191.980	1623.00	192.0			191.979	1936.00
Step 51	314.00	196.100	1729.00	196.1			196.078	2043.00
Step 52	314.00	200.220	1599.00	200.2			200.197	1913.00
Step 53	546.00	204.920	1470.00	204.3			204.475	2016.00
Step 54	979.00	208.450	1341.00	208.4	571.78	208.525	208.454	2891.78
Step 55	547.00	212.019	1212.00	212.5			212.381	1759.00
Step 56	315.00	216.700	1082.00	216.7			216.668	1397.00
Step 57	315.00	220.820	953.60	220.8			220.785	1268.60
Step 58	757.00	228.747	1414.30	227.9			228.195	2171.30
Total	20888.00	113.890	69118.60	128.9			125.027	97365.04

Weight Distribution, Triton, Ballast Load

	Lightweight		Ballast Load		Fixed weights & Topside		Total	
	Weight	LCG	Weight	LCG	Weight	LCG	LCG	Weight
Step 1	124.00	-1.825					-1.825	124.00
Step 2	365.00	3.180	265.40	3.540			3.332	630.40
Step 3	226.00	8.057	275.50	8.050			8.053	501.50
Step 4	67.00	10.414	43.30	10.407			10.411	110.30
Step 5	769.00	15.262					15.262	769.00
Step 6	163.00	20.013	16.20	20.000			20.012	179.20
Step 7	359.00	22.008	24.50	22.000			22.007	383.50
Step 8	379.00	24.411	24.50	24.400			24.410	403.50
Step 9	399.00	26.810	24.50	26.800			26.809	423.50
Step 10	420.00	29.210	24.50	29.200			29.209	444.50
Step 11	584.00	32.433	33.70	32.400			32.431	617.70
Step 12	509.00	36.019	26.90	36.000			36.018	535.90
Step 13	350.00	39.627	1218.00	39.628			39.628	1568.00
Step 14	424.00	43.685	1896.00	43.729			43.721	2320.00
Step 15	345.00	47.776	2277.00	47.837			47.829	2622.00
Step 16	341.00	51.896	289.40	51.950	100.00	50.000	51.658	730.40
Step 17	345.00	56.007	332.00	56.063			56.034	677.00
Step 18	337.00	60.138	374.00	60.179			60.160	711.00
Step 19	336.00	64.258	416.00	64.295			64.278	752.00
Step 20	334.00	68.378	457.00	68.411	1951.22	70.260	69.723	2742.22
Step 21	332.00	72.498	499.00	72.529			72.517	831.00
Step 22	330.00	76.618	541.00	76.647			76.636	871.00
Step 23	331.00	80.743	819.00	80.741			80.742	1150.00
Step 24	331.00	84.859	822.00	84.861			84.860	1153.00
Step 25	330.00	88.979	824.00	88.981			88.980	1154.00
Step 26	328.00	93.099	826.00	93.100			93.100	1154.00
Step 27	327.00	97.219	829.00	97.221			97.220	1156.00
Step 28	326.00	101.339	831.00	101.341	1047.22	99.350	100.395	2204.22
Step 29	325.00	105.459	834.00	105.461			105.460	1159.00
Step 30	324.00	109.582	836.00	109.581	100.00	108.140	109.467	1260.00
Step 31	351.00	113.645	839.00	113.701			113.684	1190.00
Step 32	322.00	117.819	841.00	117.820			116.500	1163.00
Step 33	321.00	121.939	844.00	121.940			121.940	1165.00
Step 34	320.00	126.059	846.00	126.061			126.060	1166.00
Step 35	319.00	130.179	849.00	130.180	2272.42	129.960	130.035	3440.42
Step 36	318.00	134.299	851.00	134.301			134.300	1169.00
Step 37	317.00	138.419	854.90	138.418			138.418	1171.90
Step 38	316.00	142.539	851.20	142.538			142.538	1167.20
Step 39	315.00	146.659	847.50	146.658			146.658	1162.50
Step 40	314.00	150.780	843.80	150.778			150.779	1157.80
Step 41	314.00	154.900	840.10	154.898			154.899	1154.10
Step 42	314.00	159.020	836.40	159.018	1315.80	161.920	160.567	2466.20
Step 43	313.00	163.140	832.70	163.138			163.139	1145.70
Step 44	313.00	167.260	829.00	167.258			167.259	1142.00
Step 45	313.00	171.380	825.30	171.378			171.379	1138.30
Step 46	312.00	175.500	821.60	175.498			175.499	1133.60
Step 47	312.00	179.620	817.90	179.618			179.619	1129.90
Step 48	312.00	183.740	814.20	183.738			183.739	1126.20
Step 49	312.00	187.860	810.50	187.858			187.859	1122.50
Step 50	313.00	191.980	806.80	191.978			191.979	1119.80
Step 51	314.00	196.100	874.60	196.104			196.103	1188.60
Step 52	314.00	200.220	886.10	200.224			200.223	1200.10
Step 53	546.00	204.920	897.70	204.344			204.562	1443.70
Step 54	979.00	208.450	909.30	208.464	571.78	208.525	208.473	2460.08
Step 55	547.00	212.019	920.80	212.584			212.373	1467.80
Step 56	315.00	216.700	932.40	216.704			216.703	1247.40
Step 57	315.00	220.820	944.00	220.823			220.822	1259.00
Step 58	757.00	228.747	2828.70	227.090			227.440	3585.70
Total	20888.00	113.890	41574.90	134.418			126.757	69821.34

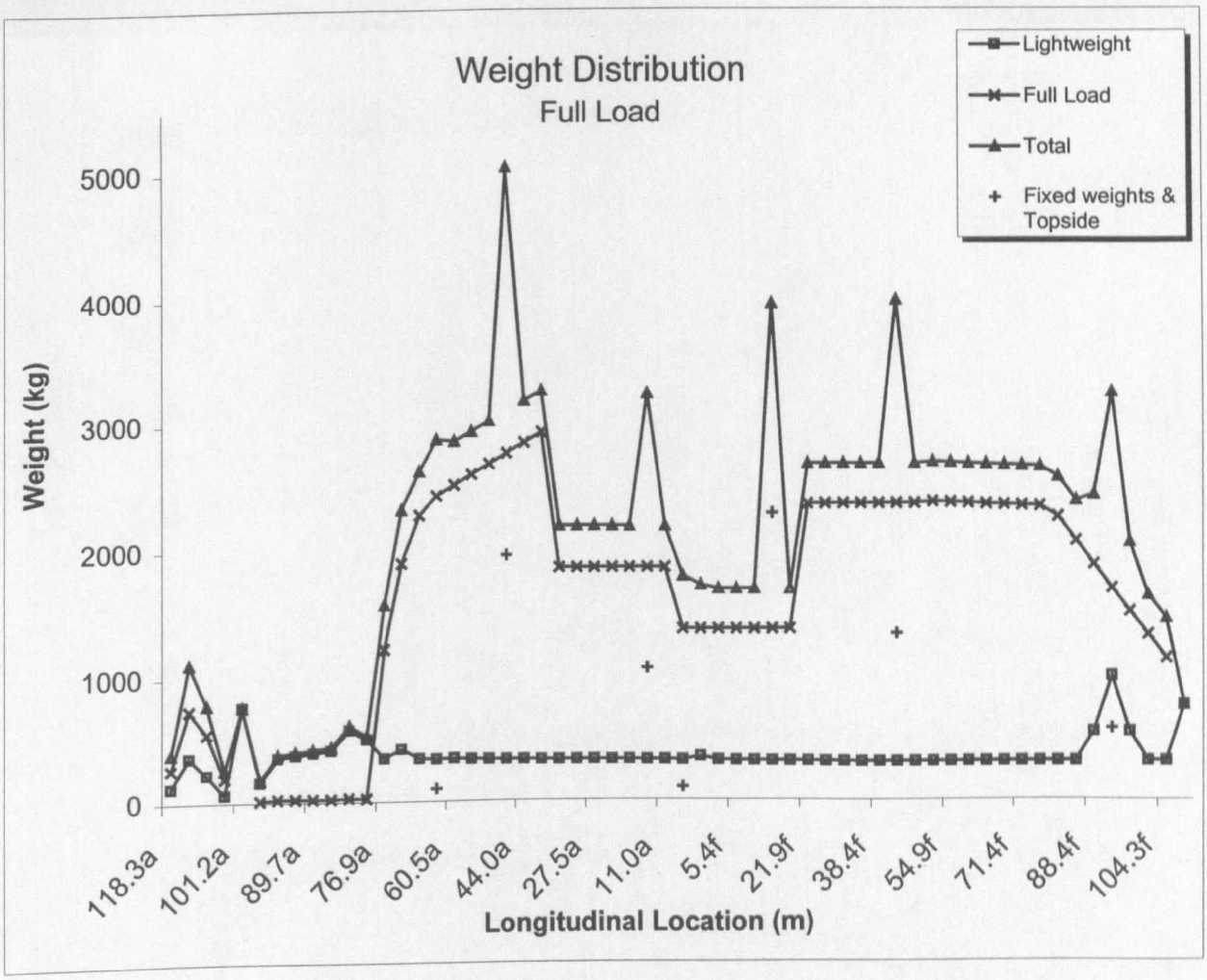
Weight Distribution
Full Load
Lightweight
Full Load
Total
Fixed weights & Topside
Weight (kg)
5000
4000
3000
2000
1000
0
118.3a
101.2a
89.7a
76.9a
60.5a
44.0a
27.5a
11.0a
5.4f
21.9f
38.4f
54.9f
71.4f
88.4f
104.3f
Longitudinal Location (m)

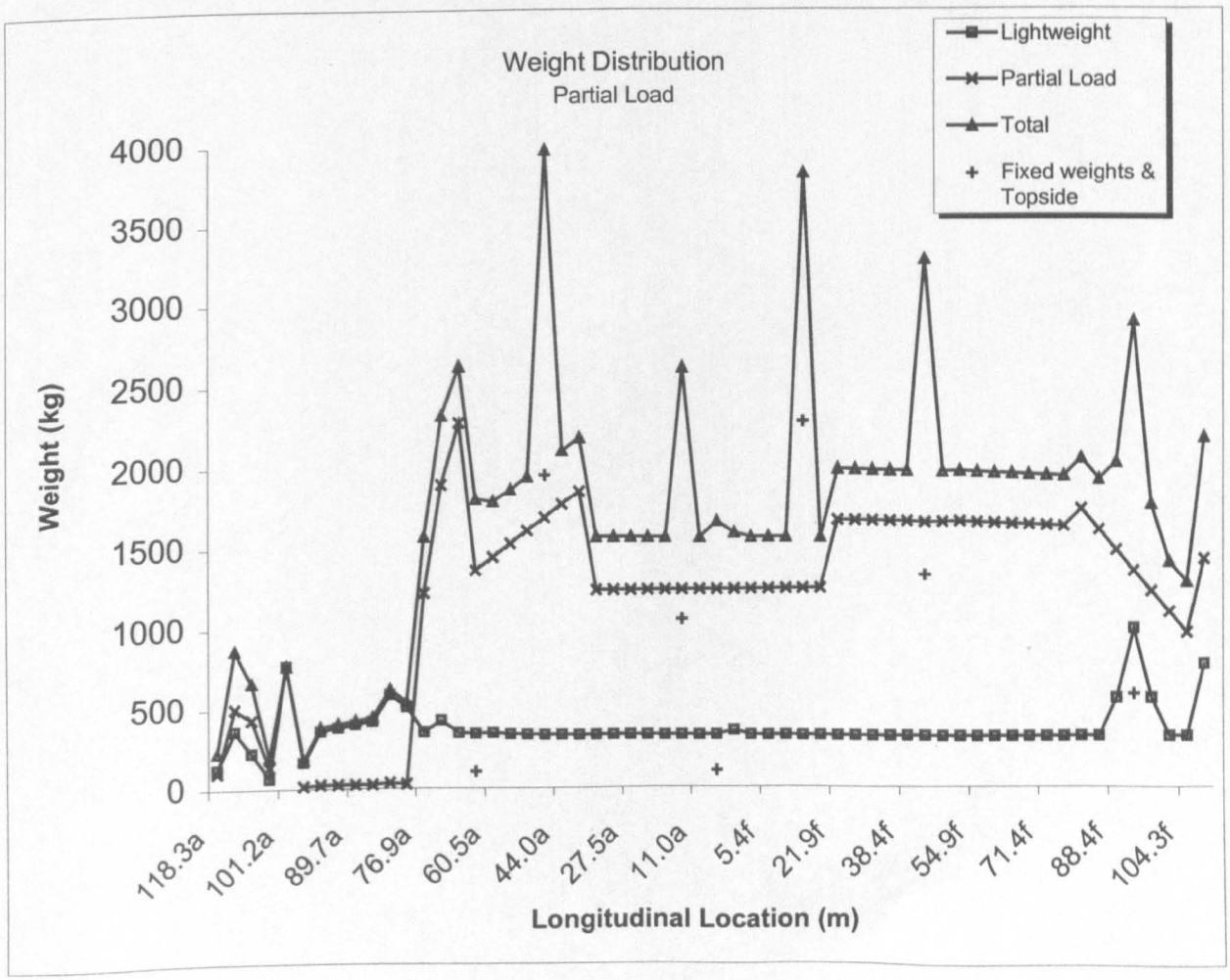
Weight Distribution
Partial Load
Lightweight
Partial Load
Total
Fixed weights & Topside
Weight (kg)
4000
3500
3000
2500
2000
1500
1000
500
0
118.3a
101.2a
89.7a
76.9a
60.5a
44.0a
27.5a
11.0a
5.4f
21.9f
38.4f
54.9f
71.4f
88.4f
104.3f
Longitudinal Location (m)

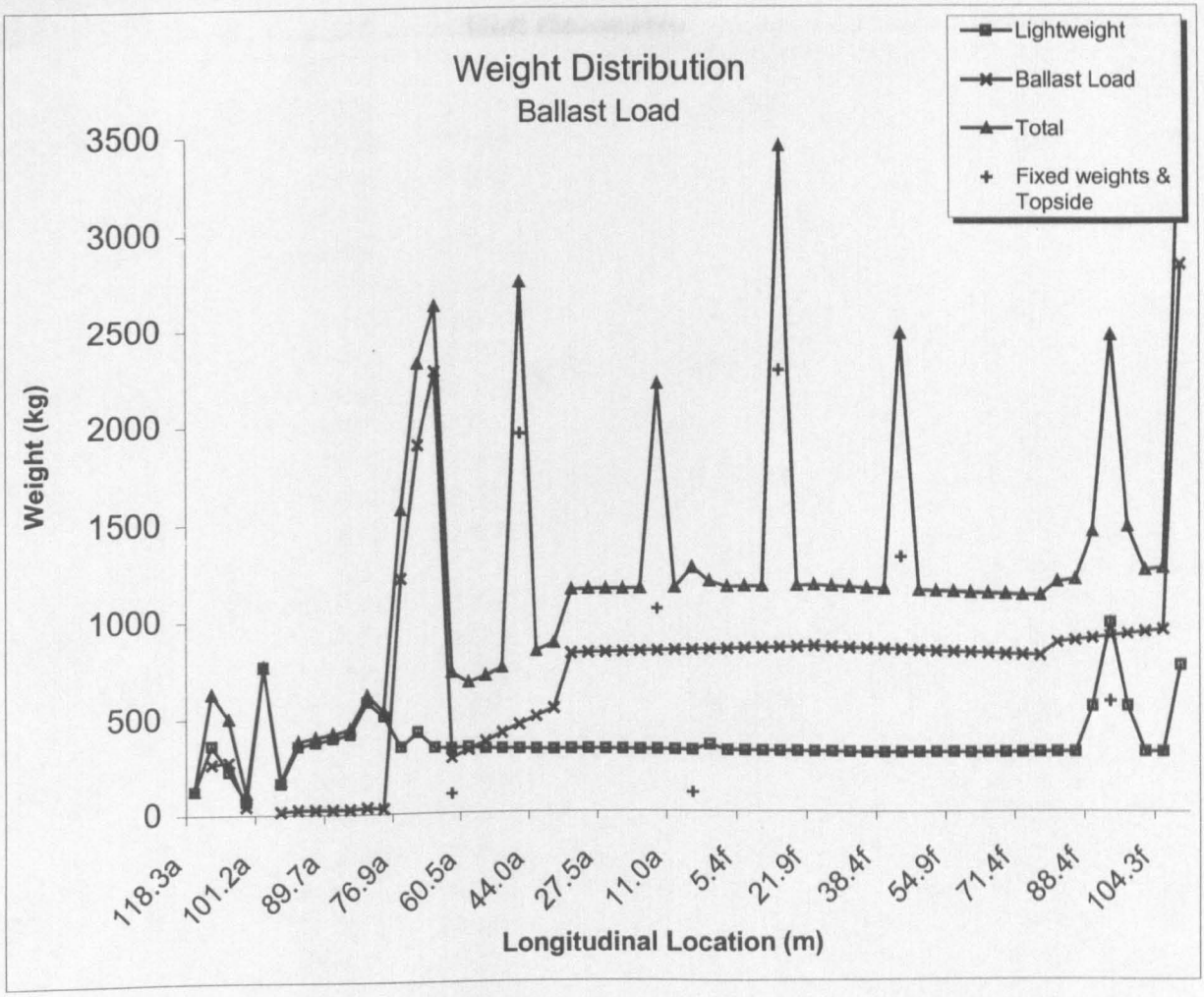
Weight Distribution
Ballast Load
Lightweight
Ballast Load
Total
Fixed weights & Topside
Weight (kg)
3500
3000
2500
2000
1500
1000
500
0
118.3a
101.2a
89.7a
76.9a
60.5a
44.0a
27.5a
11.0a
5.4f
21.9f
38.4f
54.9f
71.4f
88.4f
104.3f
Longitudinal Location (m)

Hull Geometry

	1		
AP, 1	12	0.000	0.000
116.500		0.000	11.300
		1.000	11.550
		2.000	11.800
		3.000	12.100
		4.000	12.500
		5.000	12.950
		6.000	13.500
		8.000	15.100
		8.900	16.000
		9.450	17.000
		9.850	18.500
		9.850	21.300
	0		
2	12	0.250	5.825
110.675		0.000	9.800
		1.000	9.950
		2.000	10.200
		4.000	10.850
		5.000	11.200
		6.000	11.600
		8.000	12.600
		10.000	14.100
		11.000	15.000
		12.000	16.550
		12.300	17.500
		12.500	18.500
		12.500	21.300
	0		
3	17	0.500	11.650
104.850		0.000	0.050
		1.000	0.500
		1.500	1.150
		1.800	2.000
		1.900	3.000
		1.750	4.000
		1.500	5.000
		1.350	6.000
		1.450	7.000
		2.000	8.000
		3.000	8.850
		6.000	10.000
		10.000	11.800
		12.000	13.300
		13.000	14.100
		14.000	15.450
		14.500	16.500
		14.950	18.500
		14.950	21.300
	0		
4	15	0.750	17.475
99.025		0.000	0.000
		1.000	0.100
		2.000	0.500
		3.000	1.650
		3.550	4.000
		4.000	6.150
		5.000	7.600
		6.000	8.400
		8.000	9.350
		10.000	10.200
		12.000	11.250
		14.000	12.800
		16.000	15.200
		17.050	18.500
		17.050	21.300
	0		
5	15	1.000	23.300
93.200		0.000	0.000
		1.000	0.000
		2.000	0.100
		3.000	0.450
		4.000	1.100
		5.000	2.400
		6.000	4.700
		7.000	6.200
		8.000	7.300
		10.000	8.650
		14.000	10.900
		16.000	12.600
		18.000	15.450
		18.800	18.500
		18.800	21.300
	0		
6	16	1.250	29.125
87.375		0.000	0.000
		2.000	0.000
		3.000	0.100
		4.000	0.350
		5.000	0.800
		6.000	1.500
		8.000	4.000
		10.000	6.300
		12.000	7.900
		14.000	9.250
		16.000	10.750
		18.000	12.900
		19.150	14.700
		20.000	17.550
		20.100	18.500
		20.100	21.300
	0		

7	13	1.500	34.950
81.550		0.000	0.000
		4.000	0.050
		5.000	0.200
		6.000	0.600
		8.000	1.750
		10.000	3.650
		12.000	5.650
		14.000	7.400
		16.000	9.000
		18.000	10.950
		20.000	14.200
		20.900	18.500
		20.900	21.300
	0		
8	12	1.750	40.775
75.725		0.000	0.000
		5.000	0.000
		7.000	0.350
		8.000	0.700
		10.000	1.850
		16.000	7.100
		18.000	9.150
		19.000	10.300
		20.000	12.050
		20.500	13.300
		21.000	16.000
		21.000	21.300
	0		
9	12	2.000	46.600
69.900		0.000	0.000
		6.000	0.000
		8.000	0.200
		10.000	0.850
		12.000	1.900
		14.000	3.350
		16.000	5.100
		18.000	7.300
		20.000	10.150
		20.500	11.200
		21.000	13.600
		21.000	21.300
	0		
10	12	2.250	52.425
64.075		0.000	0.000
		8.700	0.000
		10.000	0.250
		12.000	0.950
		14.000	2.050
		16.000	3.450
		18.000	5.400
		19.000	6.700
		20.000	8.400
		20.700	10.000
		21.000	11.800
		21.000	21.300
	0		
11	11	2.500	58.250
58.250		0.000	0.000
		10.100	0.000
		12.000	0.350
		14.000	1.100
		16.000	2.250
		18.000	3.900
		19.000	5.000
		20.000	6.650
		20.600	8.000
		21.000	9.900
		21.000	21.300
	0		
12	10	3.000	69.900
46.600		0.000	0.000
		13.300	0.000
		15.000	0.300
		16.000	0.650
		18.000	1.750
		19.000	2.500
		20.000	3.750
		20.650	5.000
		21.000	6.700
		21.000	21.300
	0		
13	8	3.500	81.550
34.950		0.000	0.000
		16.200	0.000
		18.000	0.450
		19.000	1.000
		20.000	1.900
		20.500	2.500
		21.000	3.800
		21.000	21.300
	0		

14	7	4.000	93.200
23.300		0.000	0.000
		18.300	0.000
		19.000	0.100
		20.000	0.700
		20.500	1.150
		21.000	2.500
		21.000	21.300
	0		
15	7	4.500	104.850
11.650		0.000	0.000
		19.200	0.000
		20.000	0.300
		20.500	0.650
		20.750	1.000
		21.000	1.850
		21.000	21.300
	0		
Midship, 16	7	5.000	116.500
0.000		0.000	0.000
		19.200	0.000
		20.000	0.300
		20.500	0.650
		20.750	1.000
		21.000	1.850
		21.000	21.300
	0		
17	7	7.000	163.100
46.600		0.000	0.000
		19.200	0.000
		20.000	0.300
		20.500	0.650
		20.750	1.000
		21.000	1.850
		21.000	21.300
	0		
18	7	7.500	174.750
58.250		0.000	0.000
		18.800	0.000
		20.000	0.450
		20.500	0.900
		20.750	1.400
		21.000	2.500
		21.000	21.300
	0		
19	9	8.000	186.400
69.900		0.000	0.000
		17.100	0.000
		18.000	0.150
		19.000	0.600
		20.000	1.500
		20.500	2.400
		20.800	4.000
		20.900	4.900
		20.900	21.300
	0		
20	10	8.250	192.225
75.725		0.000	0.000
		15.600	0.000
		16.000	0.050
		17.000	0.250
		18.000	0.600
		19.000	1.300
		20.000	2.700
		20.450	4.000
		20.600	6.000
		20.600	21.300
	0		
21	11	8.500	198.050
81.550		0.000	0.000
		13.500	0.000
		15.000	0.150
		16.000	0.400
		17.000	0.800
		18.000	1.450
		19.000	2.500
		19.500	3.450
		20.000	5.100
		20.150	6.900
		20.150	21.300
	0		
22	11	8.750	203.875
87.375		0.000	0.000
		11.900	0.000
		13.000	0.150
		14.000	0.350
		16.000	1.150
		17.000	1.850
		18.000	3.000
		19.000	5.100
		19.300	8.000
		19.300	16.000
		19.500	21.300
	0		

23	15	9.000	209.700
93.200		0.000	0.000
		9.000	0.000
		10.000	0.100
		12.000	0.400
		13.000	0.700
		14.000	1.200
		15.000	1.800
		16.000	2.700
		17.000	4.000
		17.500	5.350
		17.700	6.000
		18.000	8.200
		18.000	14.000
		18.150	18.000
		18.350	21.300
	0		
24	14	9.250	215.525
99.025		0.000	0.000
		6.300	0.000
		8.000	0.200
		10.000	0.600
		12.000	1.450
		13.000	2.150
		14.000	3.150
		15.000	4.600
		15.550	6.000
		16.000	8.200
		16.100	10.300
		16.100	14.000
		16.400	18.000
		16.700	21.300
	0		
25	14	9.500	221.350
104.850		0.000	0.000
		3.600	0.000
		6.000	0.350
		8.000	1.000
		10.000	2.200
		11.000	3.100
		12.000	4.500
		12.700	6.000
		13.100	8.000
		13.400	14.000
		13.500	16.000
		13.800	18.000
		14.200	20.000
		14.500	21.300
	0		
26	15	9.625	224.263
107.763		0.000	0.000
		2.400	0.000
		4.000	0.250
		6.000	0.900
		8.000	2.000
		9.000	2.850
		10.000	4.100
		10.900	6.000
		11.350	8.000
		11.500	10.000
		11.650	14.000
		11.850	16.000
		12.250	18.000
		12.700	20.000
		13.100	21.300
	0		
27	15	9.750	227.175
110.675		0.000	0.000
		0.800	0.000
		2.000	0.150
		4.000	0.750
		6.000	1.900
		7.000	2.700
		8.000	4.000
		9.000	6.000
		9.400	8.000
		9.400	12.000
		9.500	14.000
		9.800	16.000
		10.300	18.000
		11.000	20.000
		11.600	21.300
	0		
28	16	9.875	230.088
113.588		0.000	0.100
		1.000	0.300
		2.000	0.650
		4.000	1.750
		5.000	2.600
		6.000	4.000
		6.900	6.000
		7.200	8.000
		7.000	10.000
		6.700	12.000
		6.600	13.600
		6.800	15.000
		7.100	16.000
		7.950	18.000
		9.000	20.000
		9.750	21.300
	0		

FP, 29	17	10.000	233.000
116.500		0.000	0.600
		1.000	1.000
		2.000	1.700
		3.000	2.700
		4.000	4.050
		4.750	6.000
		4.950	8.000
		4.800	9.000
		4.400	10.000
		4.000	10.800
		3.000	11.850
		0.000	13.600
		0.000	15.200
		2.000	16.000
		4.000	17.300
		6.000	19.500
		7.400	21.300
	0		

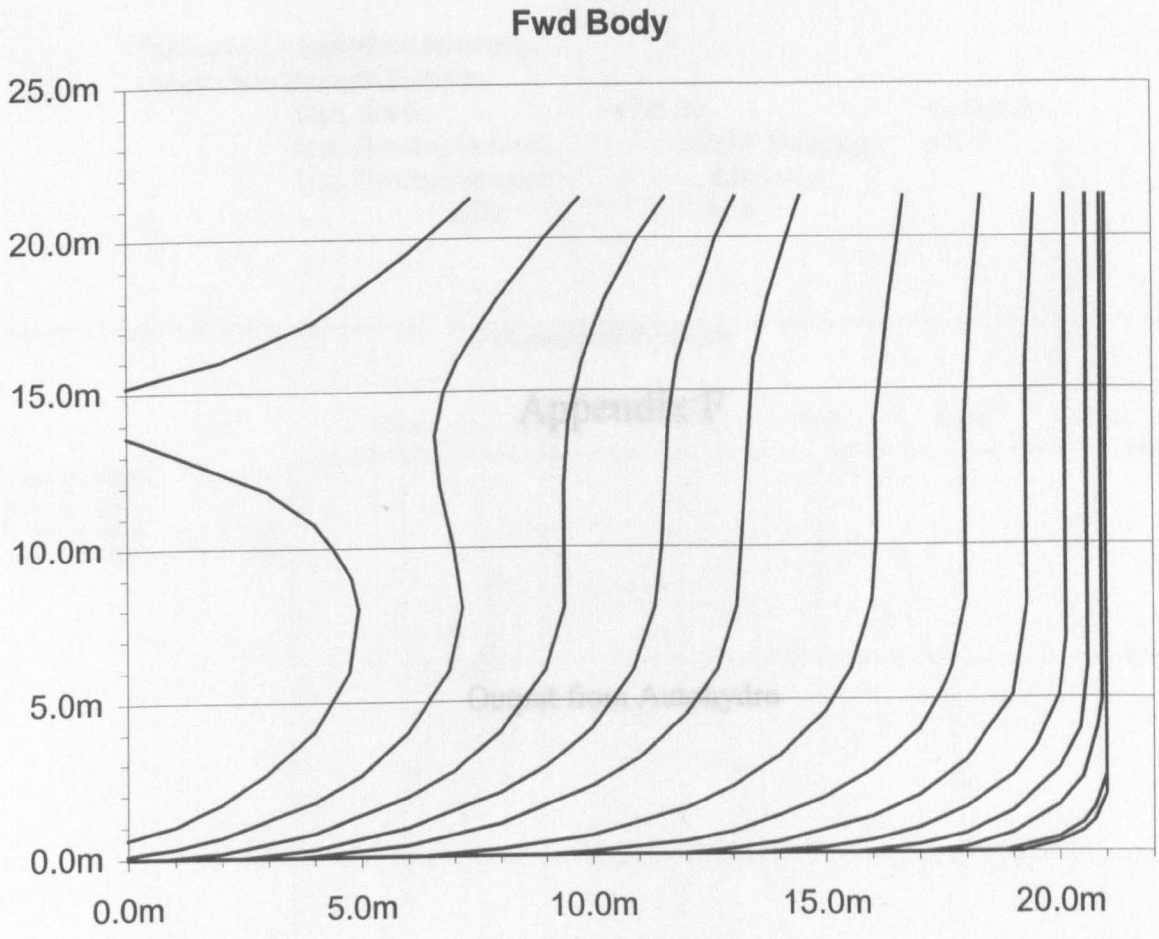
Fwd Body
25.0m
20.0m
15.0m
10.0m
5.0m
0.0m
0.0m
5.0m
10.0m
15.0m
20.0m

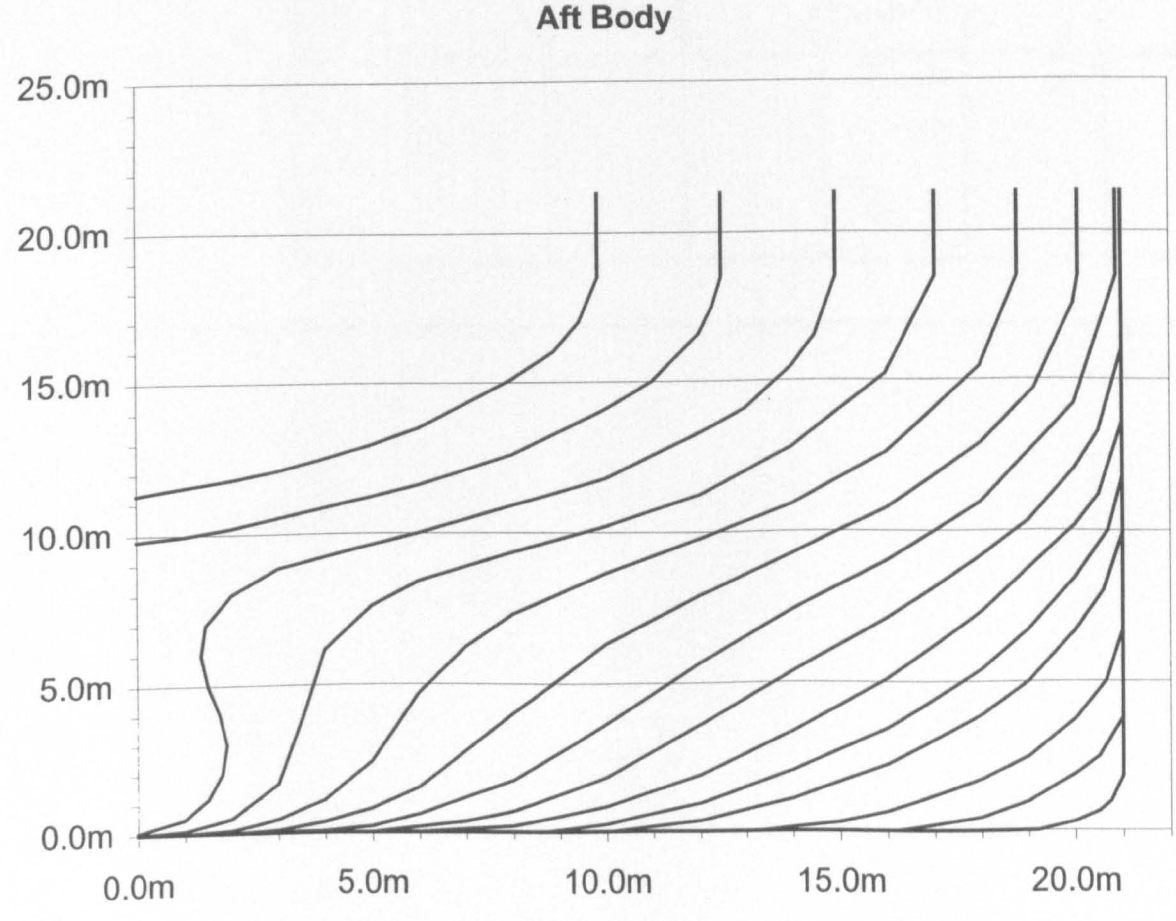
Aft Body
25.0m
20.0m
15.0m
10.0m
5.0m
0.0m
0.0m
5.0m
10.0m
15.0m
20.0m

Appendix F

Output from Autohydro

Full Load, Longitudinal Strength

Longitudinal Strength Summary

Max. Shear:	4795.89	at 39.882a
Max. Bending Moment:	57517 (Hogging)	at 0.000
Max. Bending Moment:	564 MNm	
STD	84.6	

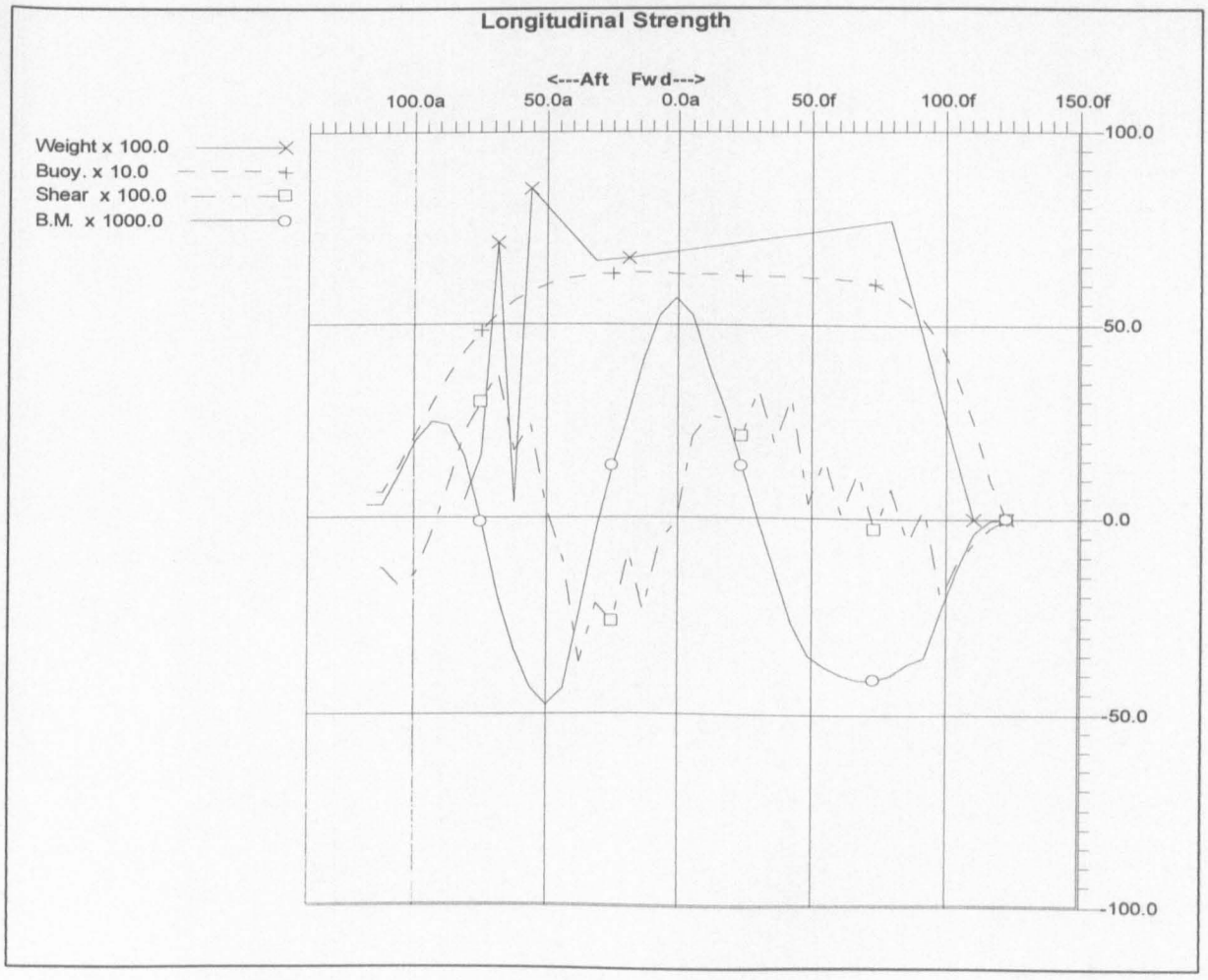

Partial Load, Longitudinal Strength

Longitudinal Strength Summary

Max. Shear:	4294.35	at 39.882a
Max. Bending Moment:	147971 (Hogging)	at 6.918a
Max. Bending Moment:	1452 MNm	
STD	217.7	

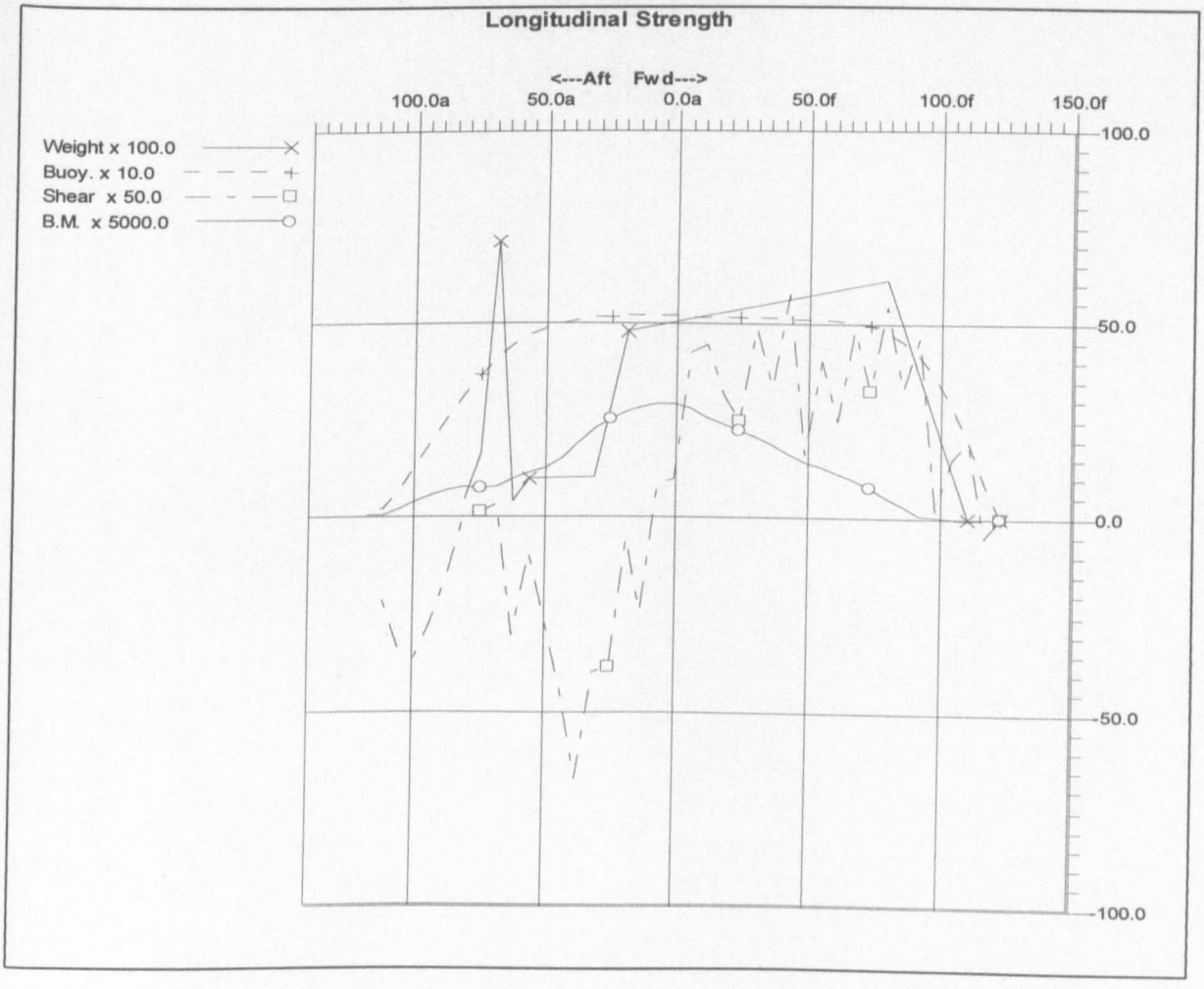

Ballast Load, Longitudinal Strength

Longitudinal Strength Summary

Max. Shear:	5680.73		at 68.724a
Max. Bending Moment:	234425	(Hogging)	at 0.000
Max. Bending Moment:	2300	MNm	
STD	345.0		

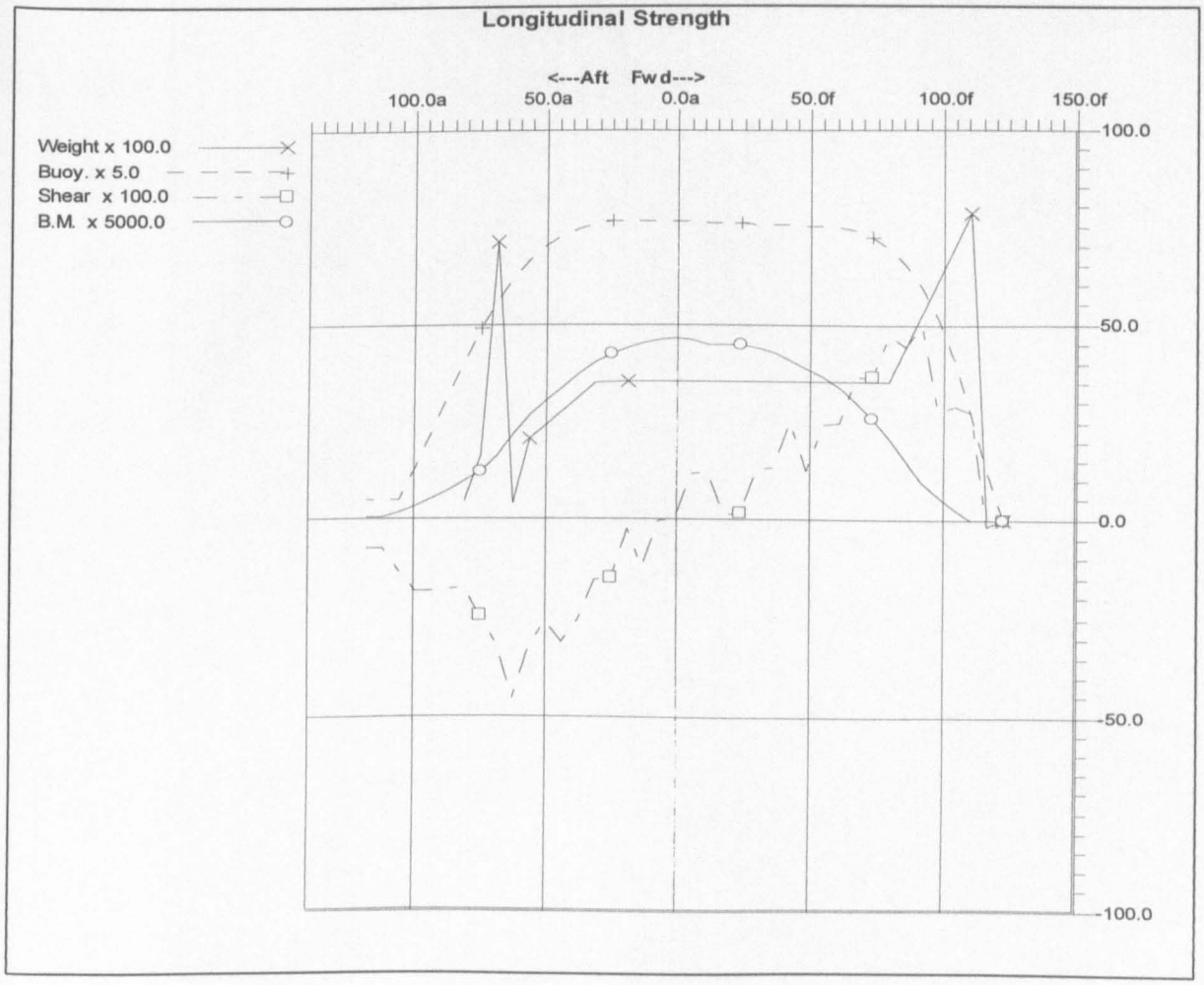

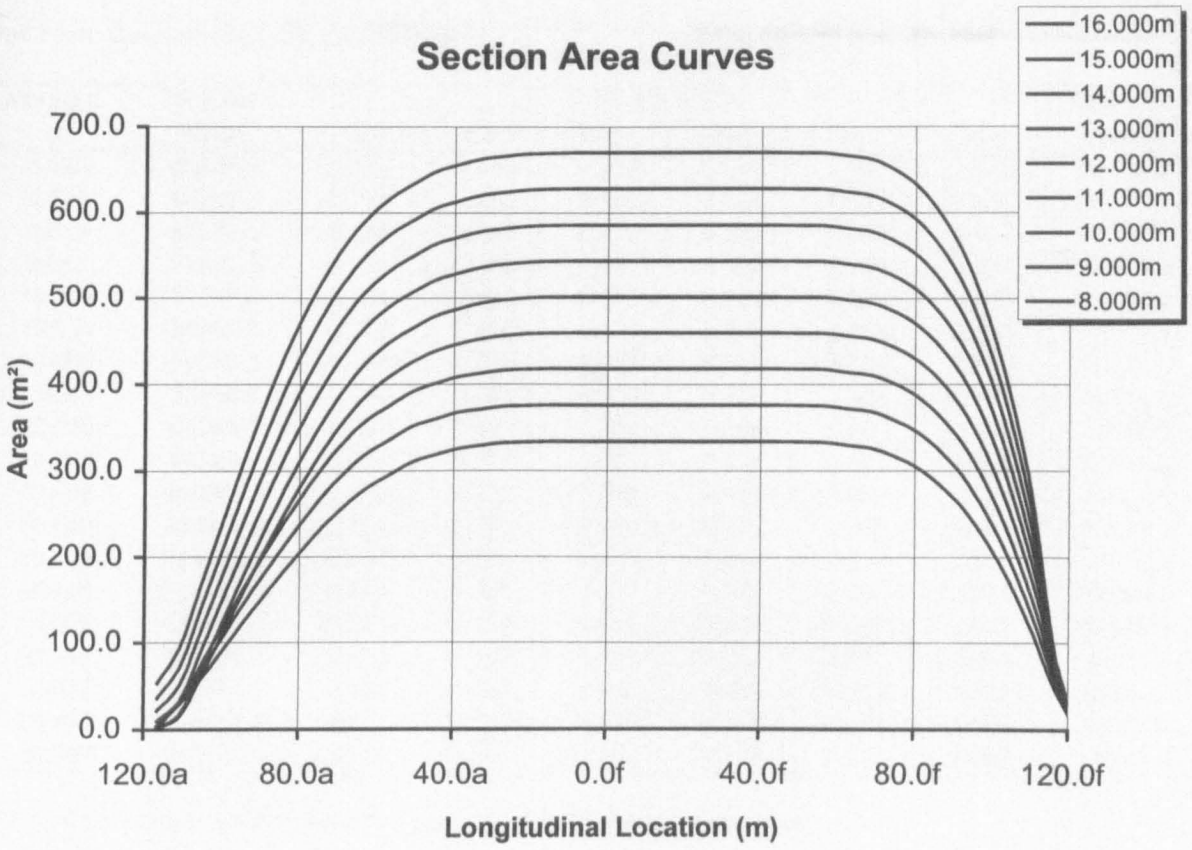
Section Area Curves
16.000m
15.000m
14.000m
13.000m
12.000m
11.000m
10.000m
9.000m
8.000m
700.0
600.0
500.0
400.0
300.0
200.0
100.0
0.0
Area (m²)
120.0a
80.0a
40.0a
0.0f
40.0f
80.0f
120.0f
Longitudinal Location (m)

Hull Form Coefficients (with appendages) Trim: Aft 0.15 deg., No heel

draught	Volume	Coefficients						WS Area
m	Cu.m	Cp	Cb	Cms	Cwp	Cv	Cws	Sq.m
8.023	60509.9	0.775	0.749	0.967	0.841	0.890	2.859	10718.1
8.521	64617.6	0.778	0.753	0.969	0.846	0.890	2.830	10972.3
9.019	68752.3	0.781	0.758	0.970	0.852	0.889	2.807	11233.8
9.517	72921.9	0.784	0.762	0.972	0.857	0.888	2.788	11496.4
10.014	77117.8	0.781	0.760	0.973	0.858	0.886	2.767	11783.8
10.511	81352.8	0.778	0.758	0.974	0.858	0.884	2.746	12058.3
11.009	85629.1	0.776	0.757	0.976	0.858	0.882	2.725	12327.5
11.507	89932.2	0.780	0.761	0.977	0.864	0.881	2.718	12602.4
12.005	94265.6	0.783	0.766	0.978	0.869	0.881	2.711	12868.9
12.503	98625.9	0.787	0.770	0.978	0.874	0.881	2.705	13132.7
13.002	103009.3	0.790	0.774	0.979	0.878	0.882	2.699	13391.9
13.500	107412.3	0.794	0.778	0.980	0.881	0.882	2.694	13648.9
13.999	111833.4	0.797	0.781	0.981	0.884	0.884	2.681	13859.5
14.499	116271.6	0.800	0.785	0.981	0.887	0.885	2.675	14099.0
14.998	120725.3	0.803	0.788	0.982	0.890	0.886	2.669	14336.4
15.497	125192.3	0.806	0.792	0.982	0.892	0.887	2.664	14571.5
15.997	129673.7	0.808	0.795	0.983	0.895	0.888	2.662	14821.1
16.497	134168.1	0.811	0.798	0.984	0.897	0.890	2.661	15067.7
16.997	138672.8	0.814	0.801	0.984	0.898	0.891	2.659	15310.0

NOTE: Coefficients calculated based on true waterline length at given draft

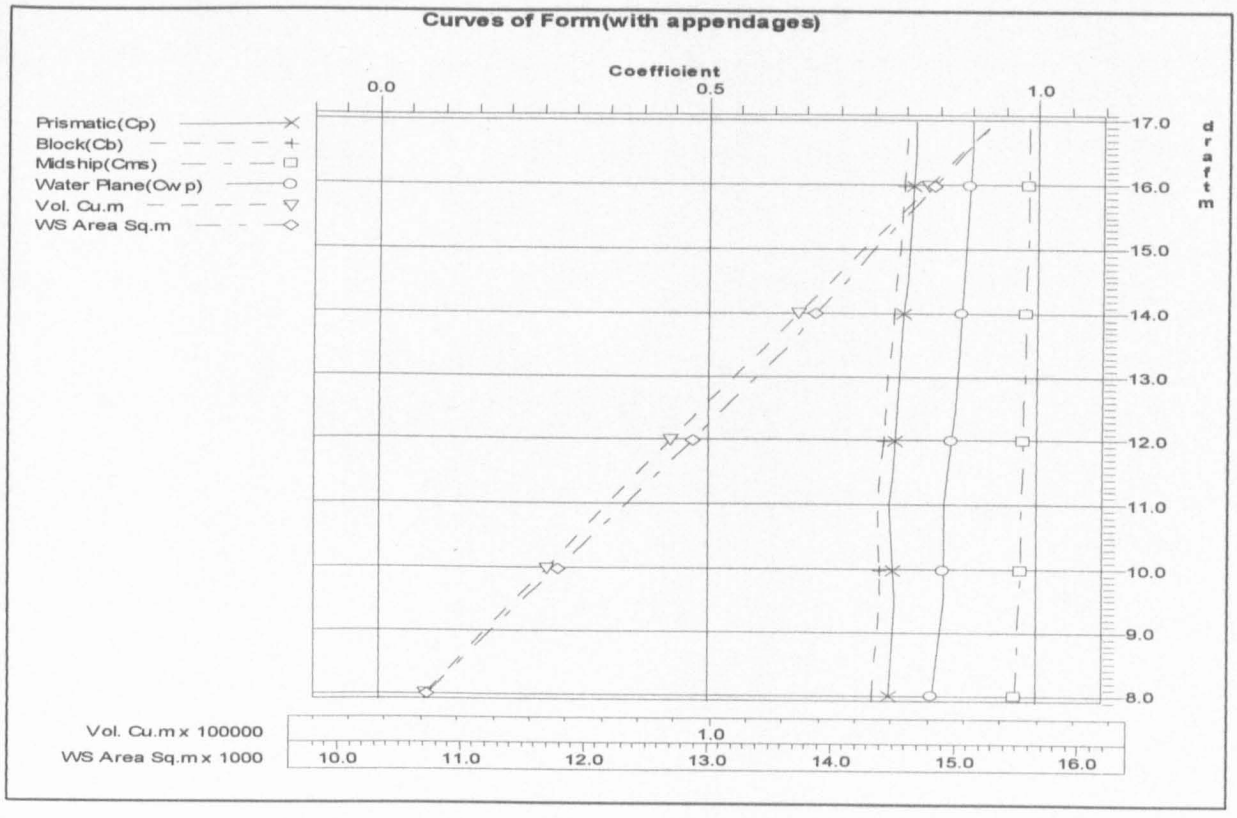

Appendix G

Scatter Diagrams and Transfer Functions

Scatter Diagram, Area 11

	1.75	3.5	6.5	8.5	10.5	12.5	14.5	16.5	18.5	20.5	21
0.25	6.33E-02	4.13E-02	2.35E-03	9.16E-04	5.23E-04	0.00E+00	0.00E+00	0.00E+00	0.00E+00	1.31E-04	6.54E-04
0.5	4.45E-03	1.13E-01	1.43E-02	3.40E-03	9.16E-04	1.31E-04	1.31E-04	1.31E-04	0.00E+00	0.00E+00	3.40E-03
1	4.97E-03	1.68E-01	6.17E-02	1.07E-02	2.62E-03	9.16E-04	3.92E-04	5.23E-04	3.92E-04	0.00E+00	1.57E-03
1.5	3.79E-03	7.42E-02	8.28E-02	2.14E-02	6.80E-03	1.57E-03	5.23E-04	5.23E-04	1.31E-04	1.31E-04	1.31E-04
2	2.88E-03	2.04E-02	5.18E-02	2.46E-02	6.41E-03	1.05E-03	3.92E-04	1.31E-04	0.00E+00	0.00E+00	3.92E-04
2.5	1.57E-03	9.68E-03	2.81E-02	2.18E-02	7.98E-03	1.83E-03	2.62E-04	0.00E+00	1.31E-04	0.00E+00	1.31E-04
3	5.23E-04	5.23E-03	1.74E-02	1.16E-02	7.45E-03	1.83E-03	2.62E-04	3.92E-04	1.31E-04	0.00E+00	0.00E+00
3.5	1.44E-03	1.70E-03	9.16E-03	1.36E-02	5.89E-03	2.62E-03	1.31E-04	1.31E-04	0.00E+00	0.00E+00	0.00E+00
4	5.23E-04	1.70E-03	4.71E-03	5.89E-03	3.92E-03	1.44E-03	3.92E-04	0.00E+00	1.31E-04	0.00E+00	0.00E+00
4.5	5.23E-04	7.85E-04	4.05E-03	4.71E-03	2.62E-03	1.57E-03	5.23E-04	3.92E-04	0.00E+00	1.31E-04	0.00E+00
5	1.31E-04	2.62E-04	3.92E-04	5.23E-04	7.85E-04	2.62E-04	0.00E+00	0.00E+00	0.00E+00	0.00E+00	0.00E+00
5.5	3.92E-04	1.31E-04	5.23E-04	1.05E-03	9.16E-04	0.00E+00	0.00E+00	0.00E+00	0.00E+00	0.00E+00	0.00E+00
6	2.62E-04	1.31E-04	5.23E-04	1.05E-03	5.23E-04	3.92E-04	1.31E-04	1.31E-04	0.00E+00	0.00E+00	0.00E+00
6.5	0.00E+00	0.00E+00	6.54E-04	6.54E-04	1.05E-03	3.92E-04	1.31E-04	0.00E+00	0.00E+00	0.00E+00	0.00E+00
7	1.31E-04	1.31E-04	0.00E+00	2.62E-04	1.31E-04	2.62E-04	0.00E+00	0.00E+00	0.00E+00	0.00E+00	0.00E+00
7.5	0.00E+00	0.00E+00	0.00E+00	2.62E-04	2.62E-04	1.31E-04	1.31E-04	0.00E+00	0.00E+00	0.00E+00	0.00E+00
8	1.31E-04	1.31E-04	2.62E-04	3.92E-04	0.00E+00	0.00E+00	0.00E+00	0.00E+00	0.00E+00	0.00E+00	0.00E+00
8.5	0.00E+00	0.00E+00	0.00E+00	0.00E+00	1.31E-04	0.00E+00	0.00E+00	1.31E-04	0.00E+00	0.00E+00	0.00E+00
9	0.00E+00	0.00E+00	0.00E+00	1.31E-04	1.31E-04	0.00E+00	0.00E+00	0.00E+00	0.00E+00	0.00E+00	0.00E+00
9.5	0.00E+00	0.00E+00	0.00E+00	2.62E-04	1.31E-04	0.00E+00	0.00E+00	0.00E+00	0.00E+00	0.00E+00	0.00E+00

Scatter Diagram, Central North Sea

	2.5	3.5	4.5	5.5	6.5	7.5	8.5
0.25	4.04E-03	7.06E-03	2.02E-03	1.01E-03	0.00E+00	0.00E+00	0.00E+00
0.75	1.41E-02	9.18E-02	4.34E-02	7.06E-03	1.01E-03	0.00E+00	0.00E+00
1.25	0.00E+00	5.15E-02	1.19E-01	2.93E-02	5.05E-03	1.01E-03	0.00E+00
1.75	0.00E+00	2.02E-03	1.12E-01	5.85E-02	1.11E-02	2.02E-03	0.00E+00
2.25	0.00E+00	0.00E+00	3.13E-02	8.78E-02	1.61E-02	3.03E-03	0.00E+00
2.75	0.00E+00	0.00E+00	2.02E-03	6.66E-02	2.62E-02	3.03E-03	0.00E+00
3.25	0.00E+00	0.00E+00	0.00E+00	2.62E-02	3.83E-02	4.04E-03	0.00E+00
3.75	0.00E+00	0.00E+00	0.00E+00	4.04E-03	3.73E-02	6.05E-03	0.00E+00
4.25	0.00E+00	0.00E+00	0.00E+00	0.00E+00	2.32E-02	1.01E-02	0.00E+00
4.75	0.00E+00	0.00E+00	0.00E+00	0.00E+00	7.06E-03	1.31E-02	1.01E-03
5.25	0.00E+00	0.00E+00	0.00E+00	0.00E+00	1.01E-03	1.11E-02	2.02E-03
5.75	0.00E+00	0.00E+00	0.00E+00	0.00E+00	0.00E+00	6.05E-03	2.02E-03
6.25	0.00E+00	0.00E+00	0.00E+00	0.00E+00	0.00E+00	2.02E-03	3.03E-03
6.75	0.00E+00	0.00E+00	0.00E+00	0.00E+00	0.00E+00	0.00E+00	2.02E-03
7.25	0.00E+00	0.00E+00	0.00E+00	0.00E+00	0.00E+00	0.00E+00	1.01E-03

Scatter Diagram, Northern North Sea

	0.5	1.5	2.5	3.5	4.5	5.5	6.5	7.5	8.5	9.5	10.5	11.5	12.5	13.5
0.5	0.00E+00	2.00E-03	1.02E-01	1.96E+00	3.56E+00	1.70E+00	5.22E-01	3.82E-01	2.33E-01	1.10E-01	2.50E-02	2.00E-02	1.00E-02	0.00E+00
1.5	0.00E+00	0.00E+00	4.00E-02	3.22E+00	1.01E+01	9.64E+00	4.85E+00	2.25E+00	1.07E+00	6.40E-01	2.44E-01	1.01E-01	4.10E-02	0.00E+00
2.5	0.00E+00	0.00E+00	4.00E-03	1.65E-01	2.79E+00	9.88E+00	7.44E+00	3.64E+00	1.35E+00	3.38E-01	1.61E-01	2.30E-02	1.10E-02	0.00E+00
3.5	0.00E+00	0.00E+00	0.00E+00	3.00E-03	1.51E-01	2.06E+00	7.43E+00	3.87E+00	1.39E+00	3.64E-01	1.15E-01	5.00E-02	1.60E-02	2.00E-03
4.5	0.00E+00	0.00E+00	0.00E+00	0.00E+00	2.00E-03	1.47E-01	2.37E+00	4.36E+00	1.57E+00	5.07E-01	7.60E-02	5.70E-02	2.30E-02	4.00E-03
5.5	0.00E+00	0.00E+00	0.00E+00	0.00E+00	0.00E+00	1.20E-02	1.65E-01	2.43E+00	1.55E+00	5.00E-01	1.12E-01	4.40E-02	1.60E-02	8.00E-03
6.5	0.00E+00	0.00E+00	0.00E+00	0.00E+00	0.00E+00	0.00E+00	8.00E-03	3.10E-01	1.41E+00	3.94E-01	1.49E-01	4.20E-02	1.30E-02	7.00E-03
7.5	0.00E+00	0.00E+00	0.00E+00	0.00E+00	0.00E+00	0.00E+00	0.00E+00	2.50E-02	4.86E-01	3.65E-01	9.30E-02	4.20E-02	1.30E-02	4.00E-03
8.5	0.00E+00	0.00E+00	0.00E+00	0.00E+00	0.00E+00	0.00E+00	0.00E+00	2.00E-03	4.70E-02	2.79E-01	5.40E-02	2.30E-02	1.20E-02	4.00E-03
9.5	0.00E+00	0.00E+00	0.00E+00	0.00E+00	0.00E+00	0.00E+00	0.00E+00	0.00E+00	6.00E-03	8.80E-02	5.00E-02	1.10E-02	3.00E-03	1.00E-03
10.5	0.00E+00	0.00E+00	0.00E+00	0.00E+00	0.00E+00	0.00E+00	0.00E+00	0.00E+00	1.00E-03	6.00E-03	3.60E-02	1.20E-02	2.00E-03	1.00E-03
11.5	0.00E+00	0.00E+00	0.00E+00	0.00E+00	0.00E+00	0.00E+00	0.00E+00	0.00E+00	0.00E+00	2.00E-03	9.00E-03	7.00E-03	1.00E-03	0.00E+00
12.5	0.00E+00	0.00E+00	0.00E+00	0.00E+00	0.00E+00	0.00E+00	0.00E+00	0.00E+00	0.00E+00	0.00E+00	1.00E-03	4.00E-03	1.00E-03	0.00E+00
13.5	0.00E+00	0.00E+00	0.00E+00	0.00E+00	0.00E+00	0.00E+00	0.00E+00	0.00E+00	0.00E+00	0.00E+00	0.00E+00	1.00E-03	0.00E+00	0.00E+00

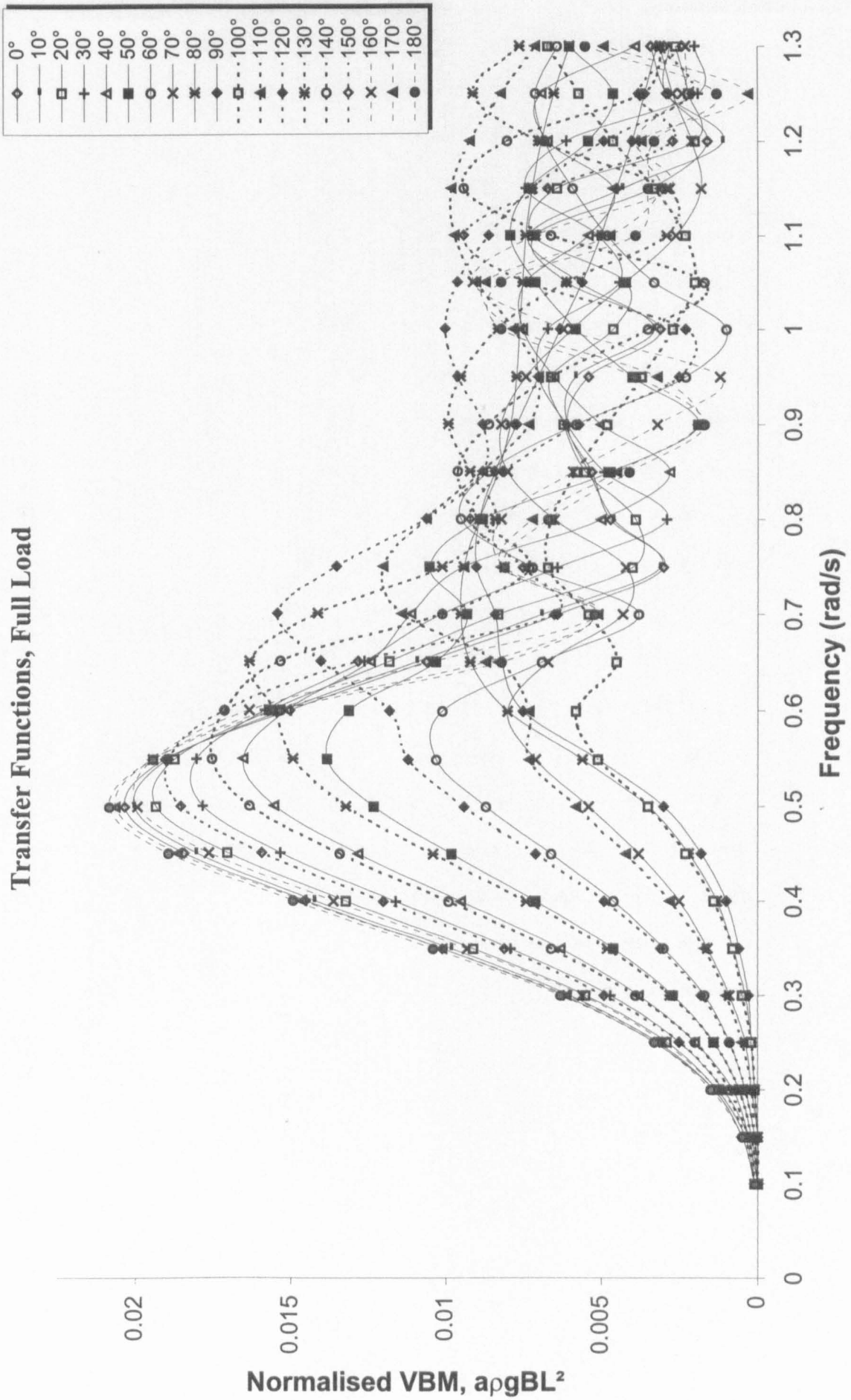
Transfer Functions, Full Load
0°
10°
20°
30°
40°
50°
60°
70°
80°
90°
100°
110°
120°
130°
140°
150°
160°
170°
180°
0
0.1
0.2
0.3
0.4
0.5
0.6
0.7
0.8
0.9
1
1.1
1.2
1.3
Frequency (rad/s)
0.02
0.015
0.01
0.005
0
Normalised VBM, aρgBL²

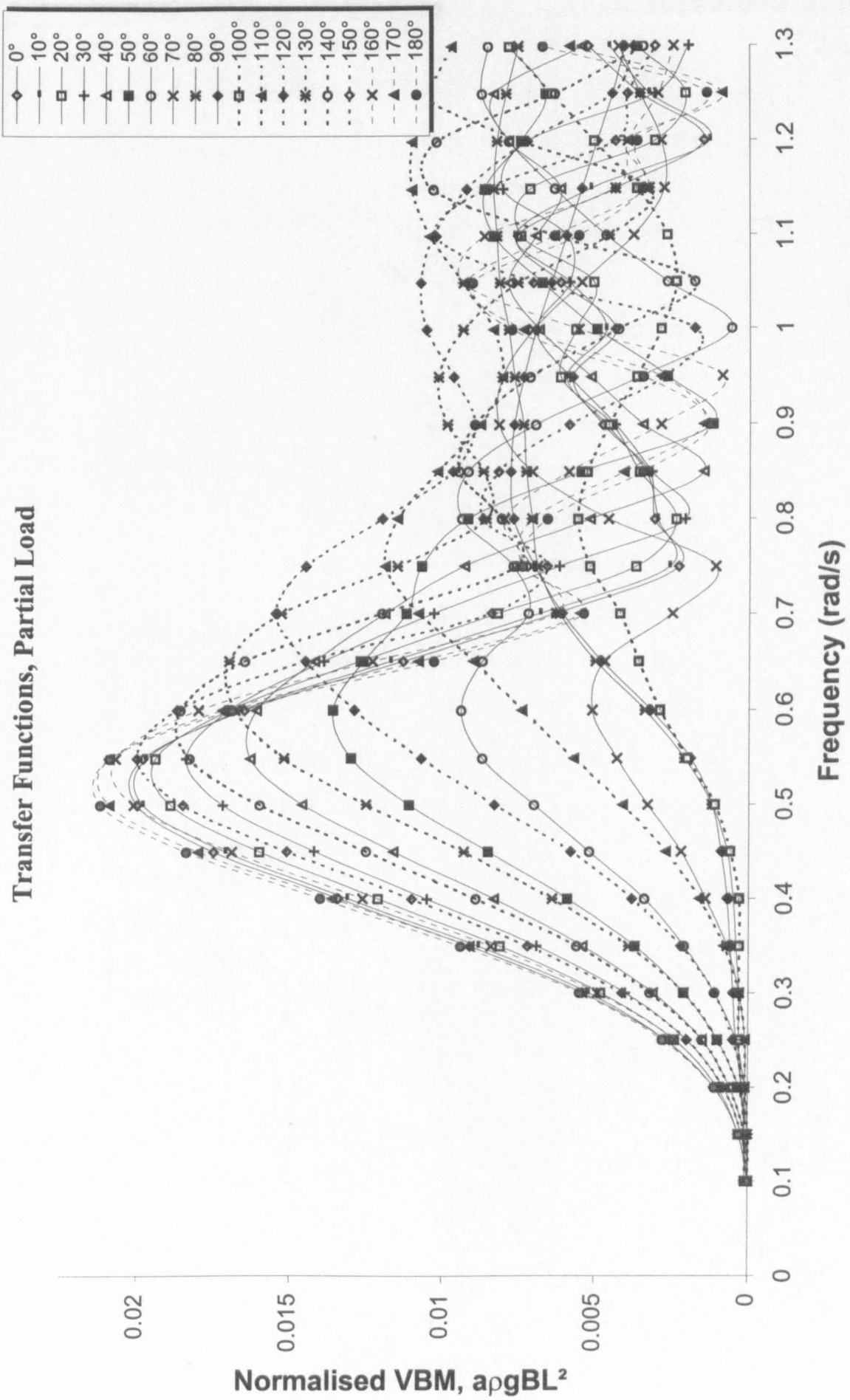
Transfer Functions, Partial Load
0°
10°
20°
30°
40°
50°
60°
70°
80°
90°
100°
110°
120°
130°
140°
150°
160°
170°
180°
0.02
0.015
0.01
0.005
0
Normalised VBM, aρgBL²
0
0.1
0.2
0.3
0.4
0.5
0.6
0.7
0.8
0.9
1
1.1
1.2
1.3
Frequency (rad/s)

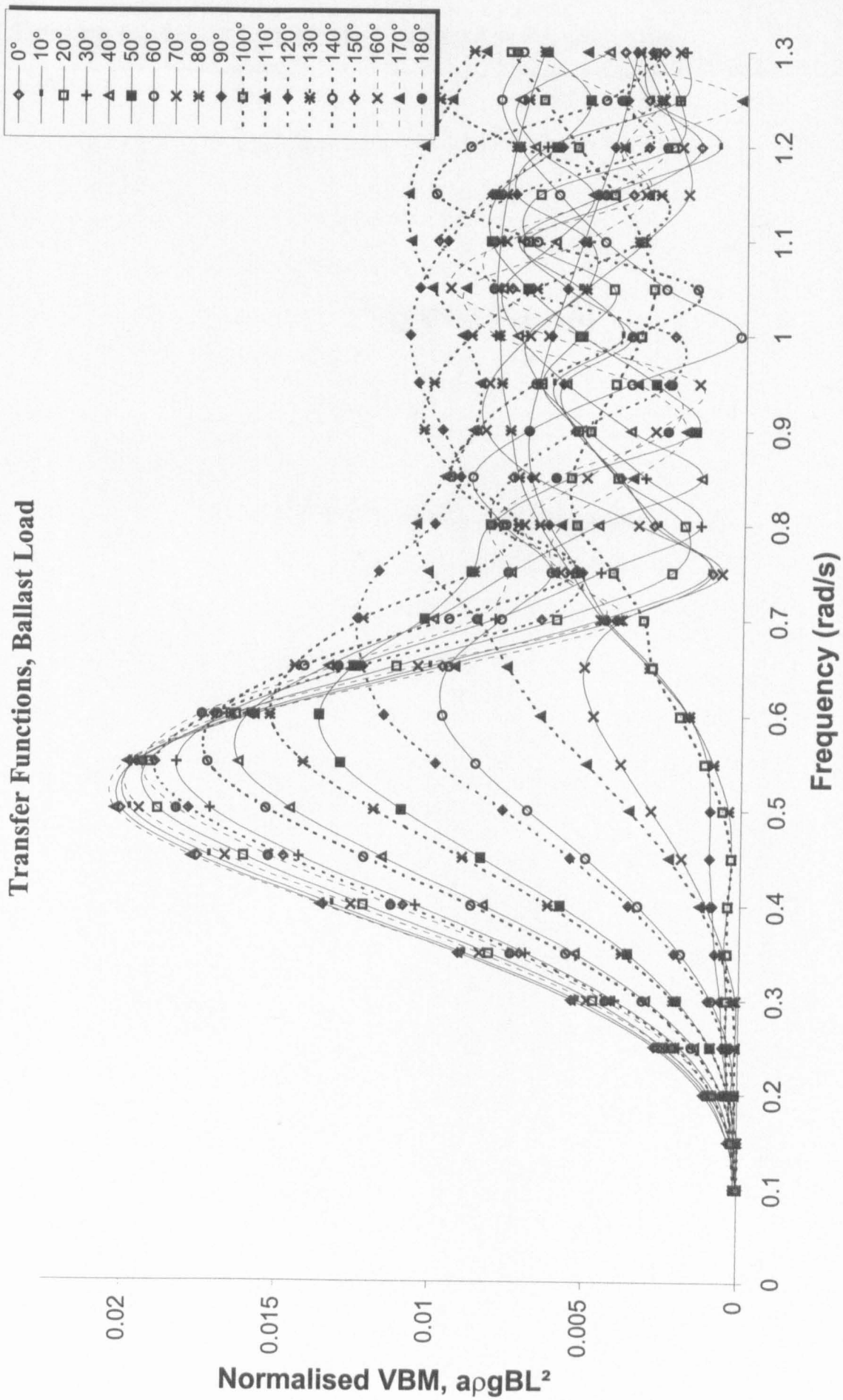
Transfer Functions, Ballast Load
0°
10°
20°
30°
40°
50°
60°
70°
80°
90°
100°
110°
120°
130°
140°
150°
160°
170°
180°
0
0.005
0.01
0.015
0.02
Normalised VBM, aρgBL²
0
0.1
0.2
0.3
0.4
0.5
0.6
0.7
0.8
0.9
1
1.1
1.2
1.3
Frequency (rad/s)

Appendix H

Extreme Load Model & Load Combination

Extreme model for Combination of Environmental Loads

Load Condition: Full Load, Hogging.

Input file for Long Term Wave Results: LT := READPRN(trifull4_res)

$T_d := 73$	Number of days spent in loading condition pr. year.
$T_h := 24$	Duration of condition (hours).
$T_z := 9.5$	Average mean zero crossing period of waves.
$\gamma := 0.5772$	Euler Constant

Extreme Stillwater Load (one year):

$\mu_s := 564$	Mean value of Still-Water Bending Moment	
$cov_s := 0.15$	Coefficient of variation of Still-Water Bending Moment	
$\sigma_s := \mu_s \cdot cov_s$	Standard deviation of Still-Water Bending Moment	$\sigma_s = 84.6$
$T_d = 73$	Number of days spent in condition over one year.	
$T_h = 24$	Duration of condition (hours).	
$n_s := \frac{T_d}{T_h} \cdot 24$	Number of occurrences in one year.	$n_s = 73$

Gumbel parameters:

$u_{ns} := qnorm\left[\left(1 - \frac{1}{n_s}\right), \mu_s, \sigma_s\right]$ $u_{ns} = 750.6$

$f_s := dnorm(u_{ns}, \mu_s, \sigma_s)$ $f_s = 4.14 \cdot 10^{-4}$

$F_s := pnorm(u_{ns}, \mu_s, \sigma_s)$ $F_s = 0.986$

$\alpha_{ns} := \left(\frac{1 - F_s}{f_s}\right)$ $\alpha_{ns} = 33.1$

Extreme Distribution:

$\mu_{es} := (u_{ns} + \gamma \cdot \alpha_{ns})$ $\mu_{es} = 769.7$

$\sigma_{es} := \frac{\pi}{\sqrt{6}} \cdot \alpha_{ns}$ $\sigma_{es} = 42.4$

Still Water Bending Moment, one year normal distribution:

$VBM_s := 0, 10 .. 1000$

$f_s(VBM_s) := dnorm(VBM_s, u_{ns}, \alpha_{ns})$

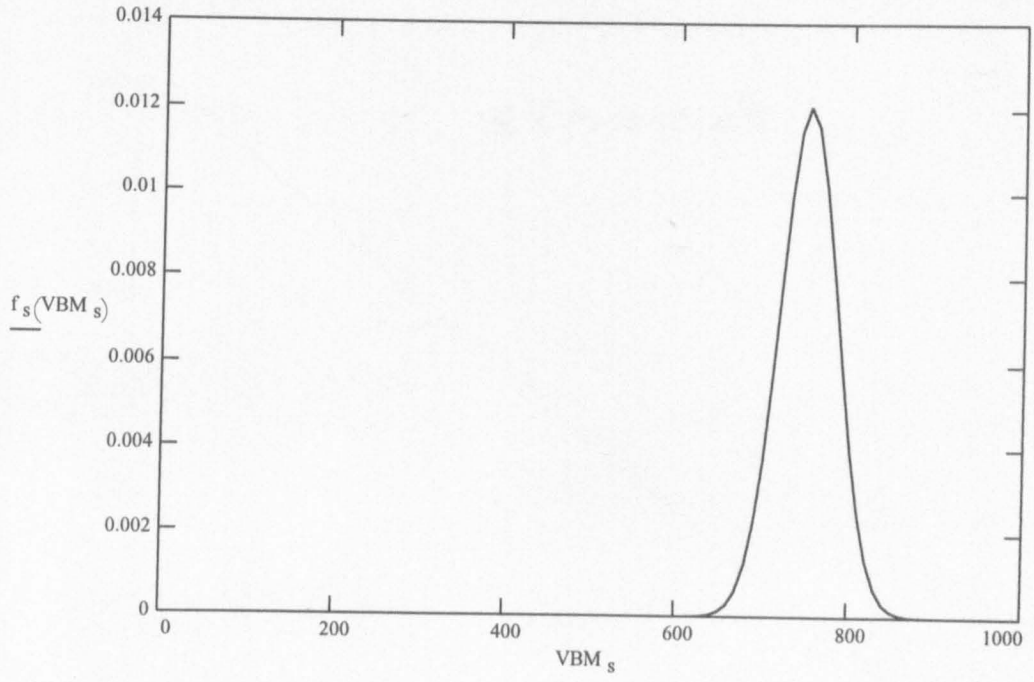

Extreme Wave Induced Bending Moment:

Data from Long Term Calculations

$VBM := LT^{<0>}$ $Qx := LT^{<1>}$ $n := 0 .. 14$

Weibull fit:

$$Fit(VBM, w, k) := \exp\left[-\left(\frac{VBM}{w}\right)^{k}\right]$$

$$SSE(w, k) := \sum_{n} \left(\log(|Qx_n|) - \log(|Fit(VBM_n, w, k)|)\right)^2$$

Initial guess for Weibull Parameters:

$w := 140$ $k := 0.98$

Given

$SSE(w, k) = 0$ $1 = 1$ $\begin{pmatrix} w \\ k \end{pmatrix} := Minerr(w, k)$

Gumbel parameters:

$w = 124.9$ $k = 0.898$ $SSE(w, k) = 0.5612$ (error)

$LT =$

	0	1
0	0	1
1	250	0.07734
2	500	0.01557
3	750	0.00373
4	$1 \cdot 10^3$	0.00107
5	$1.25 \cdot 10^3$	$3.30422 \cdot 10^{-4}$
6	$1.5 \cdot 10^3$	$1.02169 \cdot 10^{-4}$
7	$1.75 \cdot 10^3$	$3.08543 \cdot 10^{-5}$
8	$2 \cdot 10^3$	$8.98725 \cdot 10^{-6}$
9	$2.25 \cdot 10^3$	$2.47679 \cdot 10^{-6}$
10	$2.5 \cdot 10^3$	$6.33212 \cdot 10^{-7}$
11	$2.75 \cdot 10^3$	$1.48085 \cdot 10^{-7}$
12	$3 \cdot 10^3$	$3.14269 \cdot 10^{-8}$
13	$3.25 \cdot 10^3$	$6.02693 \cdot 10^{-9}$
14	$3.5 \cdot 10^3$	$1.04181 \cdot 10^{-9}$

$$Weibull_n := \exp\left[-\left(\frac{VBM_n}{w}\right)^k\right]$$

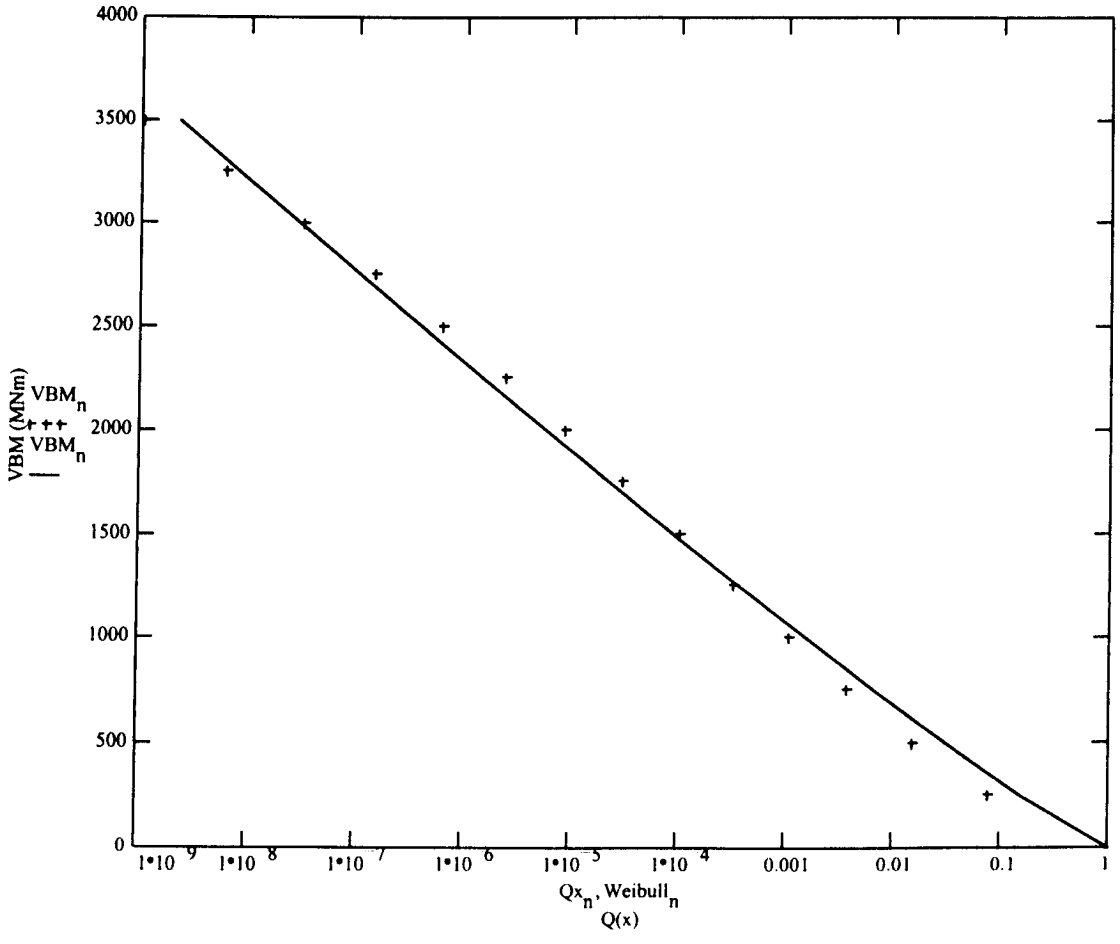

Extreme model (one year):

$T_z = 9.5$ Average mean zero crossing period of waves.

$T_d = 73$ Time spent in loading condition pr. year (days).

$T_c := T_d \cdot 3600 \cdot 24$ Time spent in loading condition pr. year (seconds).

$n := \frac{T_c}{T_z}$ Number of peaks counted in the time period T_c. $n = 6.639 \cdot 10^5$

Gumbel parameters:

$u_{nw.y} := w \cdot \left(\ln(n)^{\frac{1}{k}}\right)$ $u_{nw.y} = 2250.6$

$\alpha_{nw.y} := \frac{w}{k} \cdot \left(\ln(n)^{\frac{1}{k}-1}\right)$ $\alpha_{nw.y} = 187$

The mean and standard deviation of the extreme distribution:

$\mu_{ew.y} := u_{nw.y} + \gamma \cdot \alpha_{nw.y}$ $\mu_{ew.y} = 2358.5$

$\sigma_{ew.y} := \frac{\pi}{\sqrt{6}} \cdot \alpha_{nw.y}$ $\sigma_{ew.y} = 239.8$

$COV_{ew.y} := \frac{\pi}{\sqrt{6} \cdot \left(\gamma + \ln(n)^{\frac{1}{k}}\right)}$ $COV_{ew.y} = 0.07$

Wave Induced Bending Moment, one year normal distribution:

$VBM_w := 0, 10 .. 3500$

$f_s(VBM_w) := dnorm(VBM_w, u_{nw.y}, \alpha_{nw.y})$

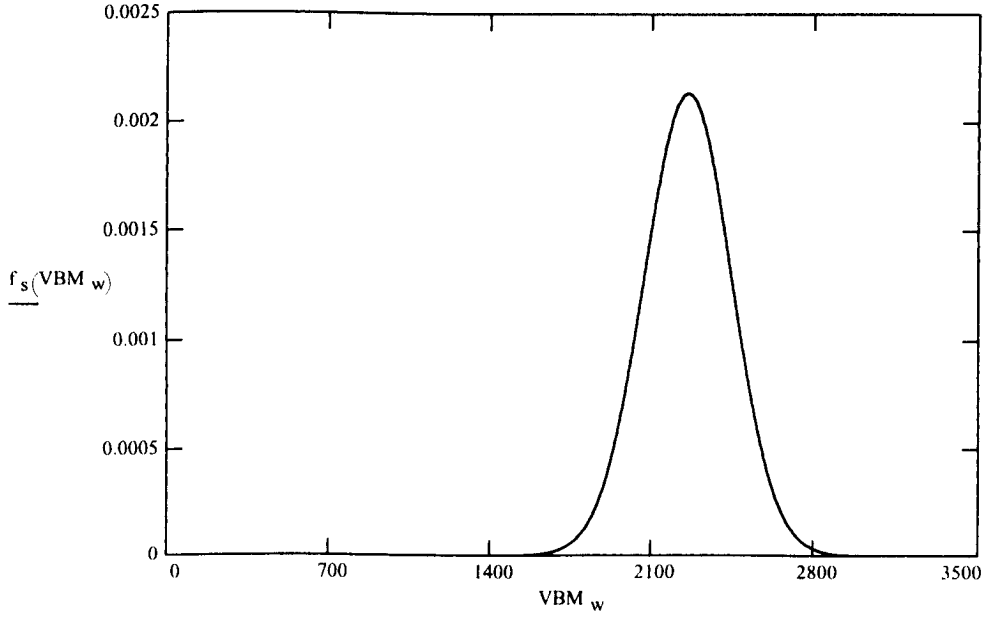

Extreme model (one Load Condition):

$T_z = 9.5$ Average mean zero crossing period of waves (seconds).

$T_h = 24$ Duration of load condition (hours)

$T_c = T_h \cdot 3600$ Duration of load condition (seconds)

$n = \frac{T_c}{T_z}$ Number of peaks counted in the time period T_c. $n = 9.095 \cdot 10^3$

Gumbel parameters:

$u_{nw} = w \cdot \left(\ln(n)^{\frac{1}{k}}\right)$ $u_{nw} = 1464.6$

$\alpha_{nw} = \frac{w}{k} \cdot \left(\ln(n)^{\frac{1-k}{k}}\right)$ $\alpha_{nw} = 179$

The mean and standard deviation of the extreme distribution:

$\mu_{ew} = u_{nw} + \gamma \cdot \alpha_{nw}$ $\mu_{ew} = 1567.9$

$\sigma_{ew} = \frac{\pi}{\sqrt{6}} \cdot \alpha_{nw}$ $\sigma_{ew} = 229.5$

$COV_{ew} = \frac{\pi}{\sqrt{6} \cdot \left(\gamma + \ln(n)^{\frac{1}{k}}\right)}$ $COV_{ew} = 0.1$

Wave Induced Bending Moment, one voyage normal distribution:

$VBM_{w.v} := 0, 10 .. 2500$

$f_s(VBM_{w.v}) := dnorm(VBM_{w.v}, u_{nw}, \alpha_{nw})$

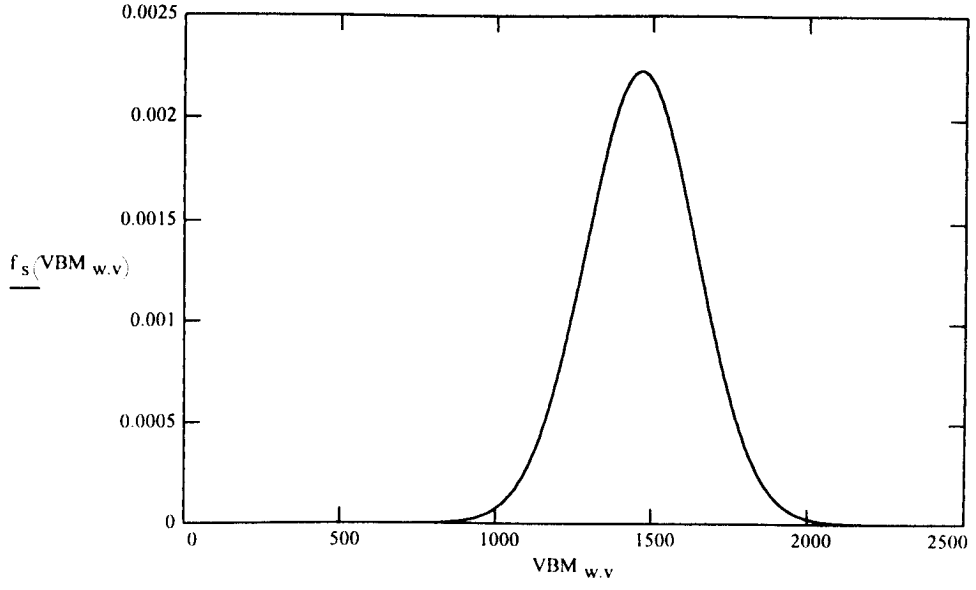

Load Combination, Ferry-Borges Castenheta's Method

Probability distribution of the maximum of the combined process:

$VBM_t := 2000, 2050 .. 4000$ $a(VBM_t) := 0.5$ $i := 1 .. 20$

$$F_t(VBM_t) := \left[\int_{-1 \cdot 10^4}^{VBM_t} \exp\left[-\exp\left[-\frac{(VBM_t - z) - u_{nw}}{\alpha_{nw}} \right] \right] \cdot dnorm(z, \mu_s, \sigma_s)\, dz \right]^{n_s}$$

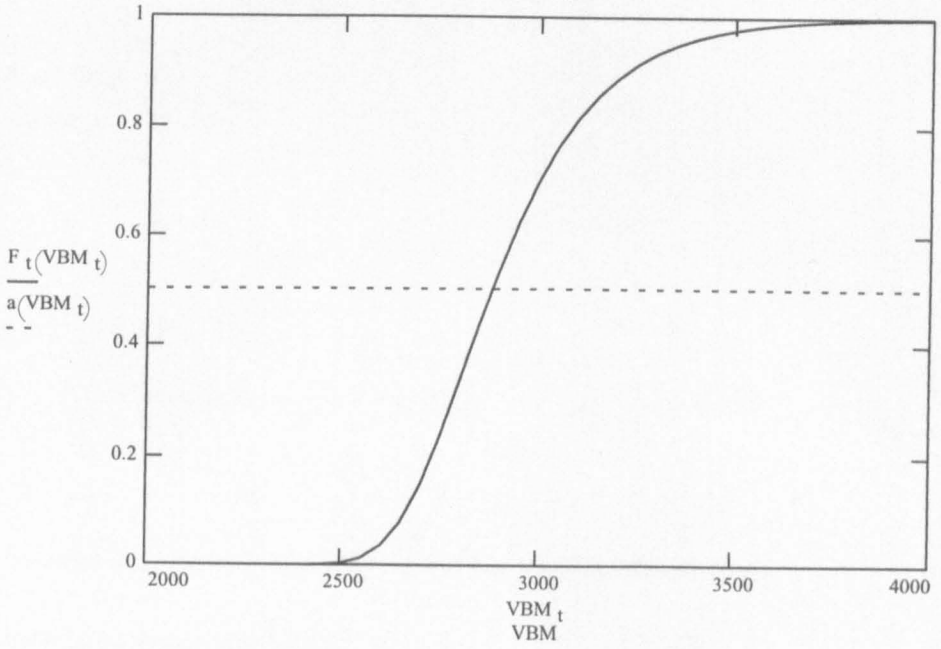

VBM	$F_t(VBM_t)$
2000	0
2050	0
2100	0
2150	0
2200	0
2250	0
2300	0
2350	0
2400	0
2450	0
2500	0.003
2550	0.012
2600	0.036
2650	0.08
2700	0.148
2750	0.236
2800	0.335
2850	0.437
2900	0.535
2950	0.623
3000	0.699
3050	0.763
3100	0.815
3150	0.856
3200	0.889
3250	0.915
3300	0.935
3350	0.951
3400	0.962
3450	0.971
3500	0.978
3550	0.984
3600	0.988
3650	0.991
3700	0.993
3750	0.995
3800	0.996
3850	0.997
3900	0.998
3950	0.998
4000	0.999

Extreme Combined Bending Moment at the 0.5 exceedance level:

Initial guess (User defined):

$VBM_t := 2800$

At the 0.5 exceedance level:

$VBM_{t0.5} := root(F_t(VBM_t) - 0.5, VBM_t)$

$VBM_{t0.5} = 2881.7$ MNm

Gumbel Distribution Function of the Still Water Bending Moment:

$VBM_s := 500, 520 .. 1000$ $a(VBM_s) := 0.5$

$$F_{es}(VBM_s) := \exp\left(-\exp\left(-\frac{VBM_s - u_{ns}}{\alpha_{ns}}\right)\right)$$

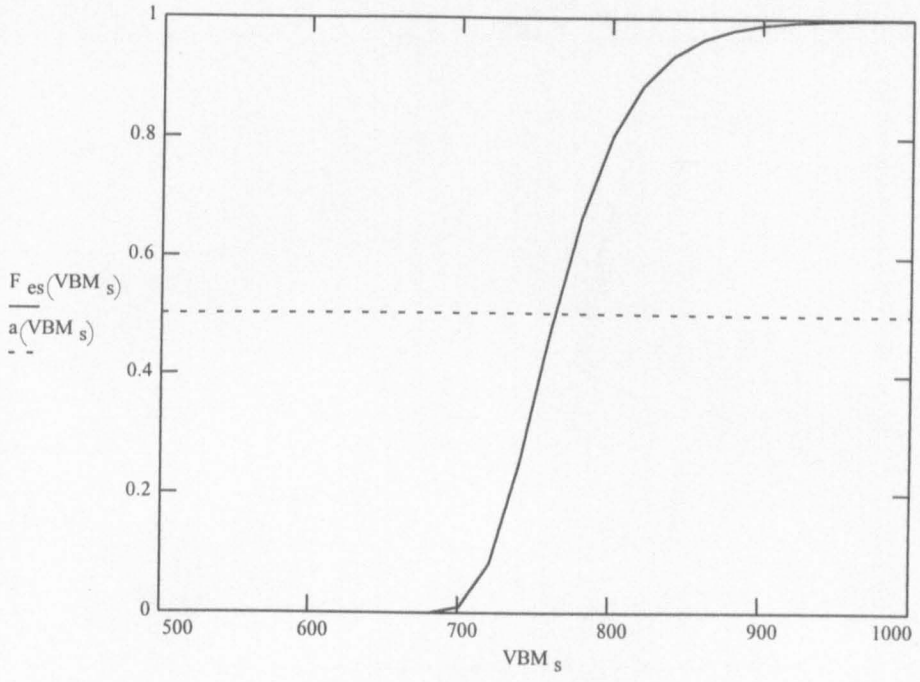

VBM	$F_{es}(VBM_s)$
500	0
520	0
540	0
560	0
580	0
600	0
620	0
640	0
660	0
680	0
700	0.01
720	0.08
740	0.252
760	0.471
780	0.663
800	0.799
820	0.884
840	0.935
860	0.964
880	0.98
900	0.989
920	0.994
940	0.997
960	0.998
980	0.999
1000	0.999

Extreme Still Water Bending Moment at the 0.5 exceedance level:

Initial guess (User defined):

$VBM_s := 750$

$VBM_{s0.5} := root(F_{es}(VBM_s) - 0.5, VBM_s)$

$VBM_{s0.5} = 762.7$ MNm

Gumbel Distribution Function of the Wave Induced Bending Moment, One year:

$VBM_w := 0, 100 .. 4000$ $a(VBM_w) := 0.5$

$$F_{ew}(VBM_w) := \exp\left(-\exp\left(-\frac{VBM_w - u_{nw.y}}{\alpha_{nw.y}}\right)\right)$$

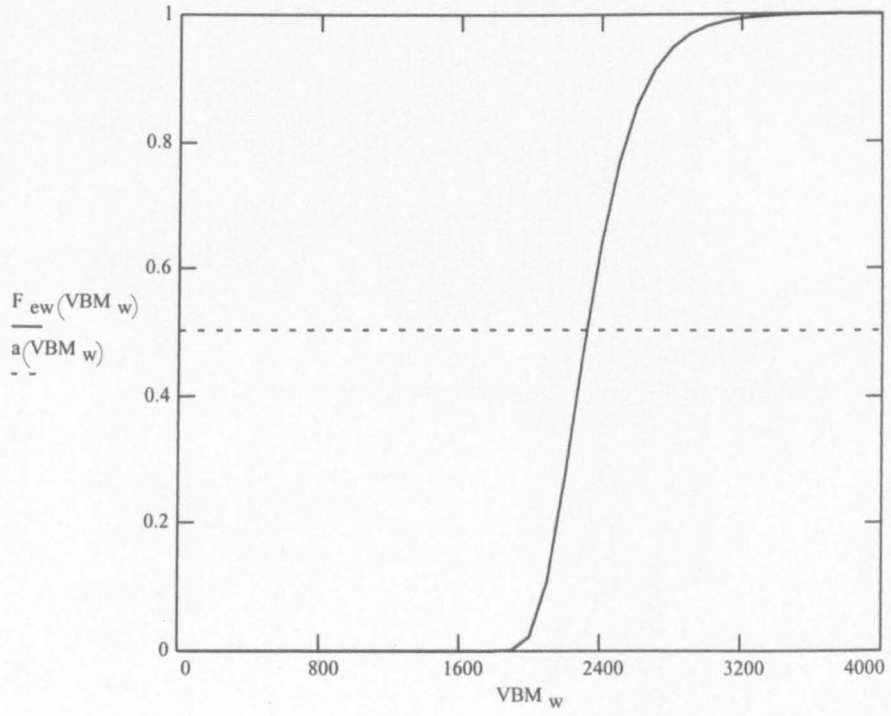

VBM	$F_{ew}(VBM_w)$
0	0
100	0
200	0
300	0
400	0
500	0
600	0
700	0
800	0
900	0
1000	0
1100	0
1200	0
1300	0
1400	0
1500	0
1600	0
1700	0
1800	0
1900	0.001
2000	0.022
2100	0.107
2200	0.27
2300	0.464
2400	0.638
2500	0.768
2600	0.857
2700	0.914
2800	0.948
2900	0.969
3000	0.982
3100	0.989
3200	0.994
3300	0.996
3400	0.998
3500	0.999
3600	0.999
3700	1
3800	1
3900	1
4000	1

Extreme Wave Bending Moment at the 0.5 exceedance level:

Initial guess (User defined):

$VBM_w := 2500$

$VBM_{w0.5} := root(F_{ew}(VBM_w) - 0.5, VBM_w)$

$VBM_{w0.5} = 2319.1$ MNm

Load Combination factor:

$VBM := 0, 100 .. 5000$ $\quad a(VBM_t) := 0.5$

$$F_t(VBM) := \left[\int_{-1 \cdot 10^4}^{VBM} \exp\left[-\exp\left[-\frac{(VBM - z) - u_{nw}}{\alpha_{nw}} \right] \right] \cdot dnorm(z, \mu_s, \sigma_s)\, dz \right]^{n_s}$$

$$F_{es}(VBM) := \exp\left(-\exp\left(-\frac{VBM - u_{ns}}{\alpha_{ns}} \right) \right)$$

$$F_{ew}(VBM) := \exp\left(-\exp\left(-\frac{VBM - u_{nw.y}}{\alpha_{nw.y}} \right) \right)$$

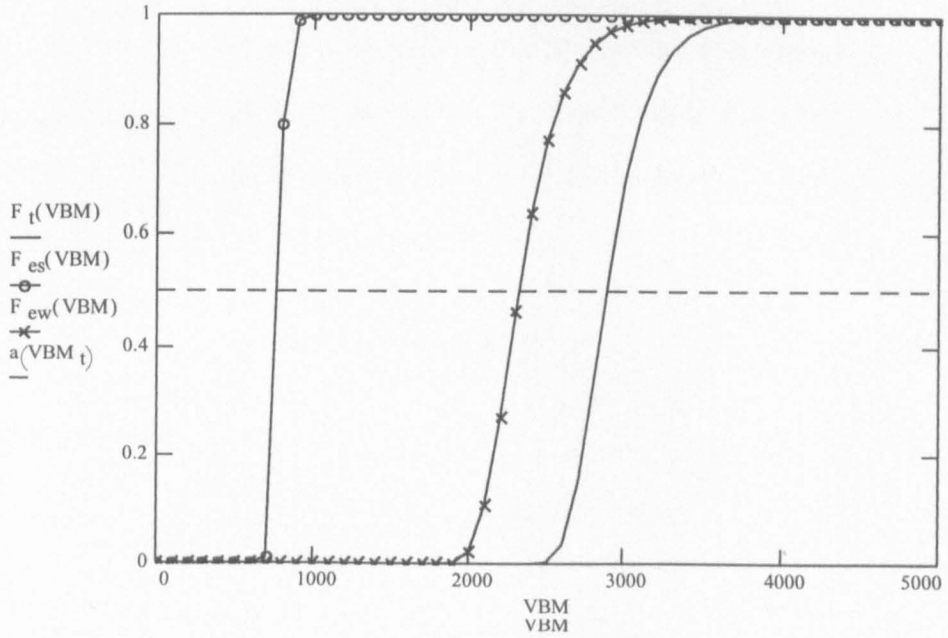

$$\psi_w := \frac{VBM_{t0.5} - VBM_{s0.5}}{VBM_{w0.5}} \qquad \psi_w = 0.91$$

Extreme model for Combination of Environmental Loads

Load Condition: Ballast Load, Hog.

Input filename for Long Term Wave Results: $LT := READPRN(triball4_{res})$

$T_d := 73$	Number of days spent in loading condition pr. year.
$T_h := 24$	Duration of condition (hours).
$T_z := 9.5$	Average mean zero crossing period of waves.
$\gamma := 0.5772$	Euler Constant

Extreme Stillwater Bending Moment (one year):

$\mu_s := 2300$ MNm	Mean value of Still-Water Bending Moment	
$cov_s := 0.15$	Coefficient of variation of Still-Water Bending Moment	
$\sigma_s := \mu_s \cdot cov_s$	Standard deviation of Still-Water Bending Moment	$\sigma_s = 345$ MNm
$T_d = 73$	Number of days spent in condition pr. year.	
$T_h = 24$	Duration of condition (hours).	
$n_s := \frac{T_d}{T_h} \cdot 24$	Number of occurrences pr. year.	$n_s = 73$

Gumbel parameters:

$u_{ns} := qnorm\left[\left(1 - \frac{1}{n_s}\right), \mu_s, \sigma_s\right]$ $u_{ns} = 3061$ MNm

$f_s := dnorm(u_{ns}, \mu_s, \sigma_s)$ $f_s = 1.015 \cdot 10^{-4}$

$F_s := pnorm(u_{ns}, \mu_s, \sigma_s)$ $F_s = 0.986$

$\alpha_{ns} := \left(\frac{1 - F_s}{f_s}\right)$ $\alpha_{ns} = 134.9$ MNm

The mean and standard deviation of the extreme distribution:

$\mu_{es} := u_{ns} + \gamma \cdot \alpha_{ns}$ $\mu_{es} = 3138.9$ MNm

$\sigma_{es} := \frac{\pi}{\sqrt{6}} \cdot \alpha_{ns}$ $\sigma_{es} = 173.1$ MNm

Still Water Bending Moment, one year normal distribution:

$VBM_s := 2000, 2010 .. 3500$

$f_s(VBM_s) := dnorm(VBM_s, u_{ns}, \alpha_{ns})$

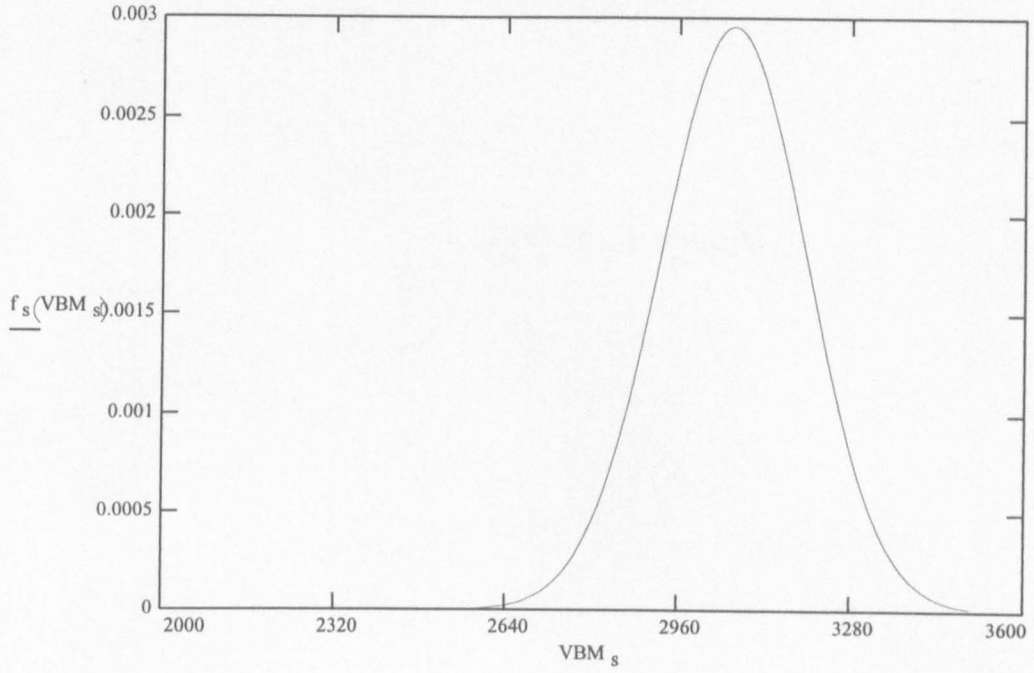

Extreme Wave Induced Bending Moment:

Data from Long Term Calculations

$VBM := LT^{<0>}$ $Qx := LT^{<1>}$ $n := 0 .. 14$

Weibull fit:

$Fit(VBM, k, b) := \exp\left[-\left(\frac{VBM}{k}\right)^b\right]$

$SSE(k, b) := \sum_n \left(\log(|Qx_n|) - \log(|Fit(VBM_n, k, b)|)\right)^2$

Initial guess for Weibull Parameters:

$k := 140$ MNm $b := 0.98$

Given

$SSE(k, b) = 0$ $1 = 1$ $\begin{pmatrix} k \\ b \end{pmatrix} := Minerr(k, b)$

Weibull parameters:

$k = 127.6$ MNm $b = 0.914$ $SSE(k, b) = 0.6714$ (error)

$LT =$

	0	1
0	0	1
1	250	0.0737
2	500	0.01435
3	750	0.00334
4	$1 \cdot 10^3$	$9.33254 \cdot 10^{-4}$
5	$1.25 \cdot 10^3$	$2.80907 \cdot 10^{-4}$
6	$1.5 \cdot 10^3$	$8.43023 \cdot 10^{-5}$
7	$1.75 \cdot 10^3$	$2.46636 \cdot 10^{-5}$
8	$2 \cdot 10^3$	$6.90615 \cdot 10^{-6}$
9	$2.25 \cdot 10^3$	$1.80727 \cdot 10^{-6}$
10	$2.5 \cdot 10^3$	$4.33072 \cdot 10^{-7}$
11	$2.75 \cdot 10^3$	$9.38282 \cdot 10^{-8}$
12	$3 \cdot 10^3$	$1.82628 \cdot 10^{-8}$
13	$3.25 \cdot 10^3$	$3.18426 \cdot 10^{-9}$
14	$3.5 \cdot 10^3$	$4.96541 \cdot 10^{-10}$

$$Weibull_n := \exp\left[-\left(\frac{VBM_n}{k}\right)^b\right]$$

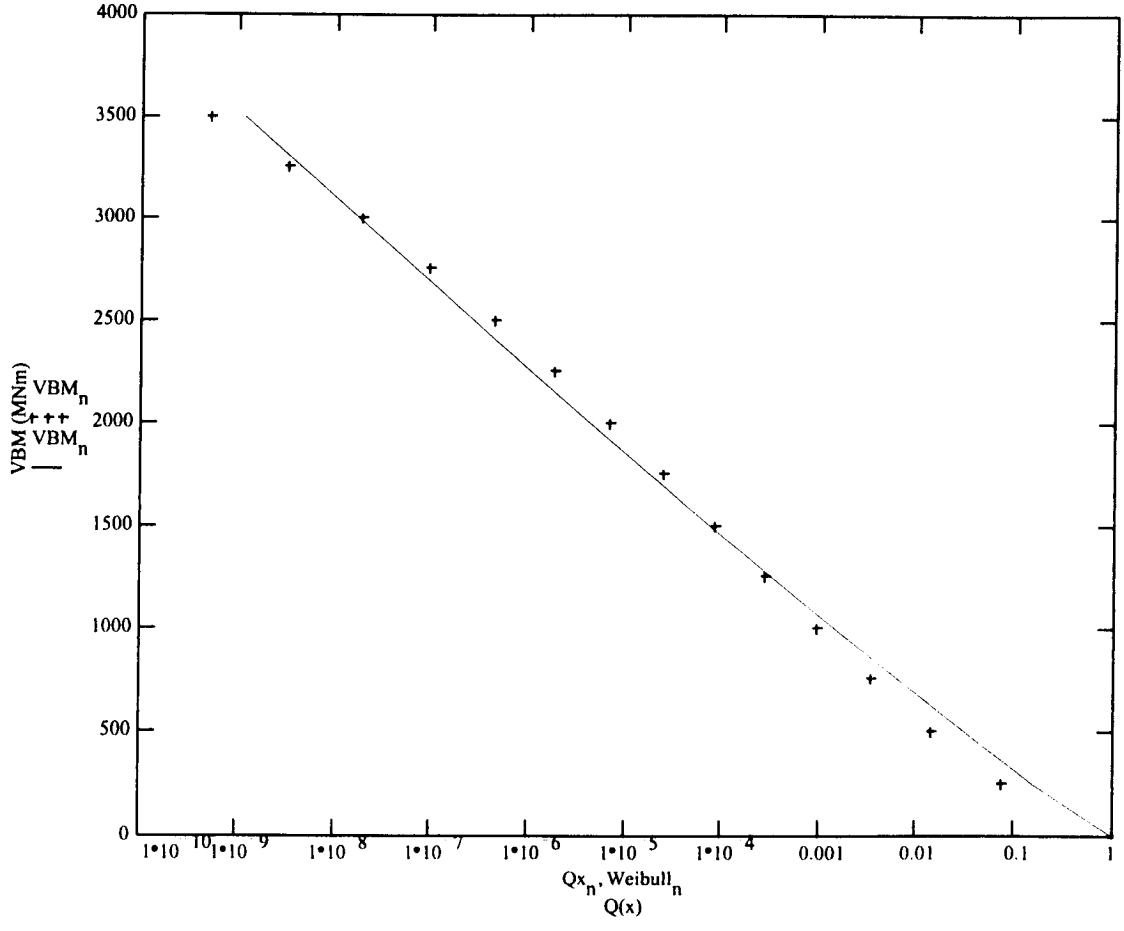

Extreme VWBM (one year):

$T_z = 9.5$ Average mean zero crossing period of waves.

$T_d = 73$ Time spent in loading condition pr. year (days).

$T_c := T_d \cdot 3600 \cdot 24$ Time spent in loading condition pr. year (seconds).

$n := \frac{T_c}{T_z}$ Number of peaks counted in the time period T_c. $n = 6.639 \cdot 10^5$

Gumbel parameters:

$u_{nw.y} := k \cdot \left(\ln(n)^{\frac{1}{b}}\right)$ $u_{nw.y} = 2186$ MNm

$\alpha_{nw.y} := \frac{k}{b} \cdot \left(\ln(n)^{\frac{1-b}{b}}\right)$ $\alpha_{nw.y} = 178.5$ MNm

The mean and standard deviation of the extreme distribution:

$\mu_{ew.y} := u_{nw.y} + \gamma \cdot \alpha_{nw.y}$ $\mu_{ew.y} = 2289$ MNm

$\sigma_{ew.y} := \frac{\pi}{\sqrt{6}} \cdot \alpha_{nw.y}$ $\sigma_{ew.y} = 228.9$ MNm

$COV_{ew.y} := \frac{\pi}{\sqrt{6} \cdot \left(\gamma + \ln(n)^{\frac{1}{b}}\right)}$ $COV_{ew.y} = 0.07$

Wave Induced Bending Moment, one year normal distribution:

$VBM_w := 0, 10 .. 3500$

$f_S(VBM_w) := dnorm(VBM_w, u_{nw.y}, \alpha_{nw.y})$

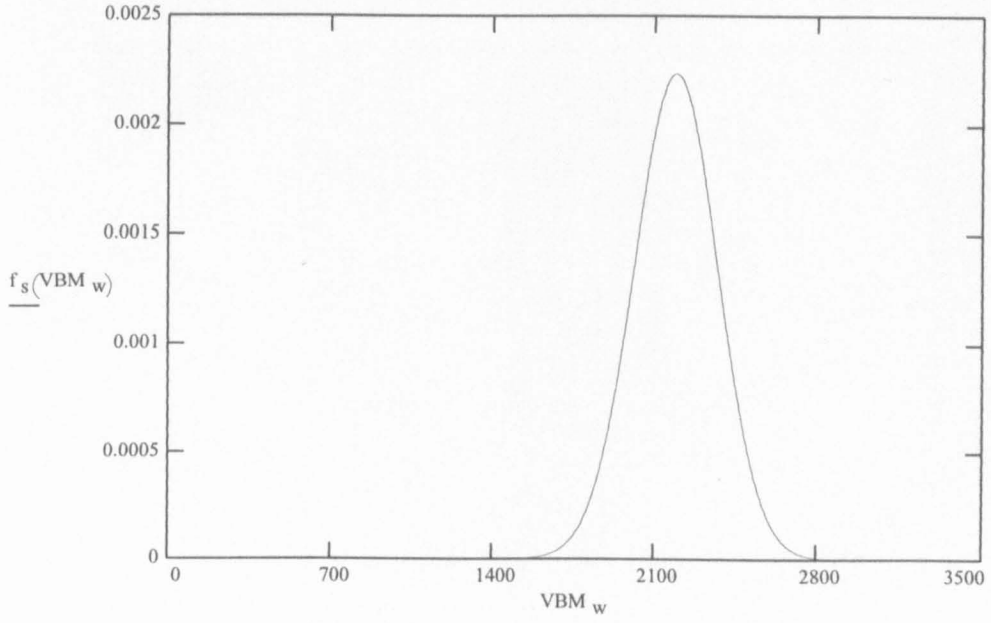

Extreme VWBM (one Load Condition):

$T_z = 9.5$ Average mean zero crossing period of waves (seconds).

$T_h = 24$ Duration of load condition (hours)

$T_c := T_h \cdot 3600$ Duration of load condition (seconds)

$n := \frac{T_c}{T_z}$ Number of peaks counted in the time period T_c. $n = 9.095 \cdot 10^3$

Gumbel parameters:

$u_{nw} := k \cdot \left(\ln(n)^{\frac{1}{b}}\right)$ $u_{nw} = 1433.2$ MNm

$\alpha_{nw} := \frac{k}{b} \cdot \left(\ln(n)^{\frac{1-b}{b}}\right)$ $\alpha_{nw} = 172.1$ MNm

The mean and standard deviation of the extreme distribution:

$\mu_{ew} := u_{nw} + \gamma \cdot \alpha_{nw}$ $\mu_{ew} = 1532.5$ MNm

$\sigma_{ew} := \frac{\pi}{\sqrt{6}} \cdot \alpha_{nw}$ $\sigma_{ew} = 220.7$ MNm

$COV_{ew} := \frac{\pi}{\sqrt{6} \cdot \left(\gamma + \ln(n)^{\frac{1}{b}}\right)}$ $COV_{ew} = 0.11$

Wave Induced Bending Moment, one voyage normal distribution:

$VBM_{w.v} := 0, 10 .. 2500$

$f_s(VBM_{w.v}) := dnorm(VBM_{w.v}, u_{nw}, \alpha_{nw})$

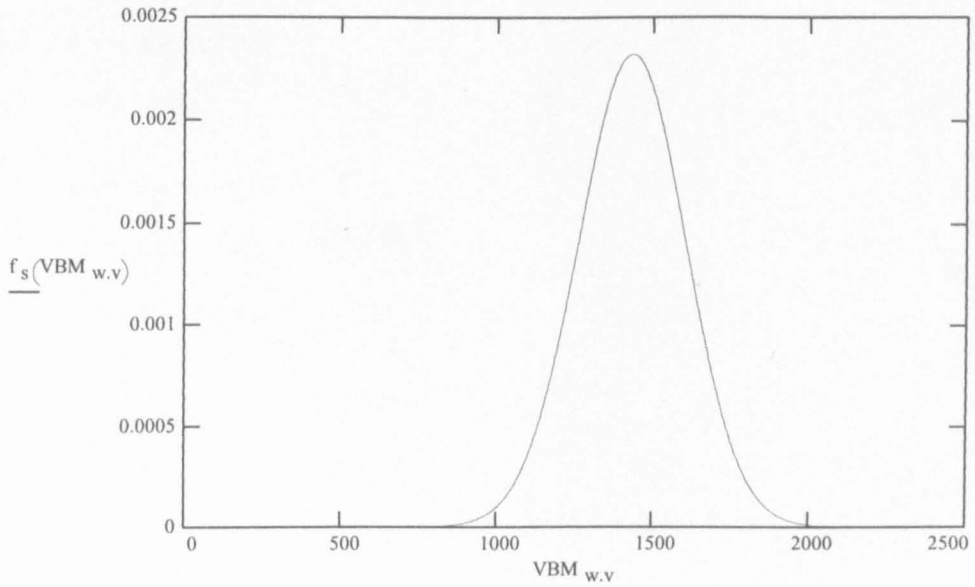

Load Combination, Ferry Borges-Castenheta's Method

Probability distribution of the maximum of the combined process:

$VBM_t := 4000, 4050 .. 6000$ $\quad a(VBM_t) := 0.5$

$$F_t(VBM_t) := \left[\int_{-1 \cdot 10^4}^{VBM_t} \exp\left[-\exp\left[-\frac{(VBM_t - z) - u_{nw}}{\alpha_{nw}} \right] \right] \cdot dnorm(z, \mu_s, \sigma_s)\, dz \right]^{n_s}$$

$WRITEPRN(FtBall_{out}) := F_t(VBM_t)$

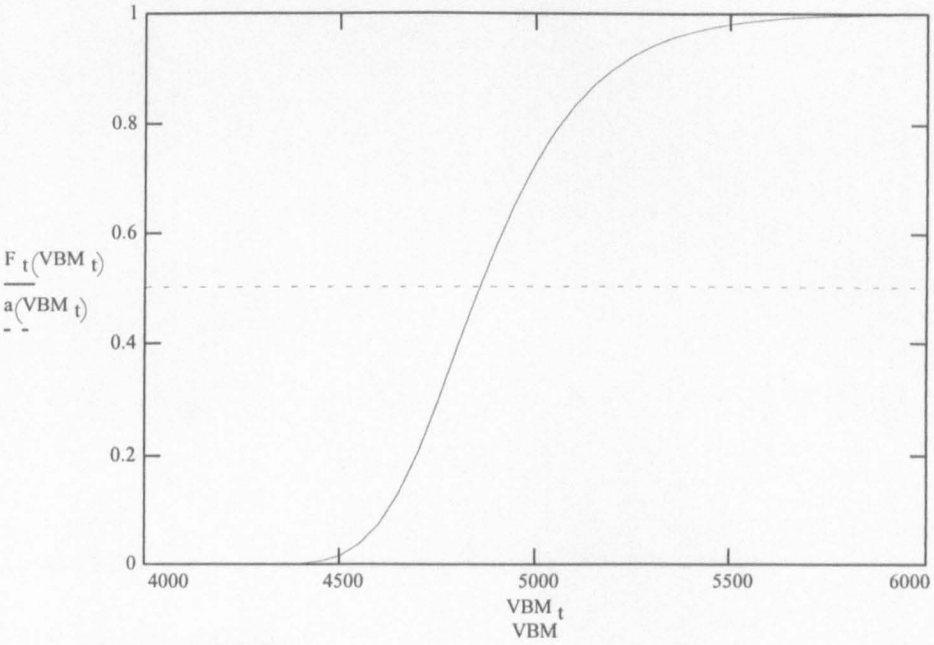

VBM	$F_t(VBM_t)$
4000	0
4050	0
4100	0
4150	0
4200	0
4250	0
4300	0
4350	0
4400	0.002
4450	0.006
4500	0.016
4550	0.038
4600	0.076
4650	0.132
4700	0.207
4750	0.294
4800	0.389
4850	0.484
4900	0.574
4950	0.655
5000	0.725
5050	0.783
5100	0.831
5150	0.87
5200	0.9
5250	0.924
5300	0.942
5350	0.956
5400	0.967
5450	0.975
5500	0.981
5550	0.986
5600	0.99
5650	0.992
5700	0.994
5750	0.996
5800	0.997
5850	0.998
5900	0.998
5950	0.999
6000	0.999

Extreme Combined Bending Moment at the 0.5 exceedance level:

Initial guess (User defined):

$VBM_t := 5000$ MNm

At the 0.5 exceedance level:

$VBM_{t0.5} := root(F_t(VBM_t) - 0.5, VBM_t)$

$VBM_{t0.5} = 4858.6$ MNm

Gumbel Distribution Function of the Still Water Bending Moment:

$VBM_s := 2500, 2550 .. 3750$ $a(VBM_s) := 0.5$

$$F_{es}(VBM_s) := \exp\left(-\exp\left(-\frac{VBM_s - u_{ns}}{\alpha_{ns}}\right)\right)$$

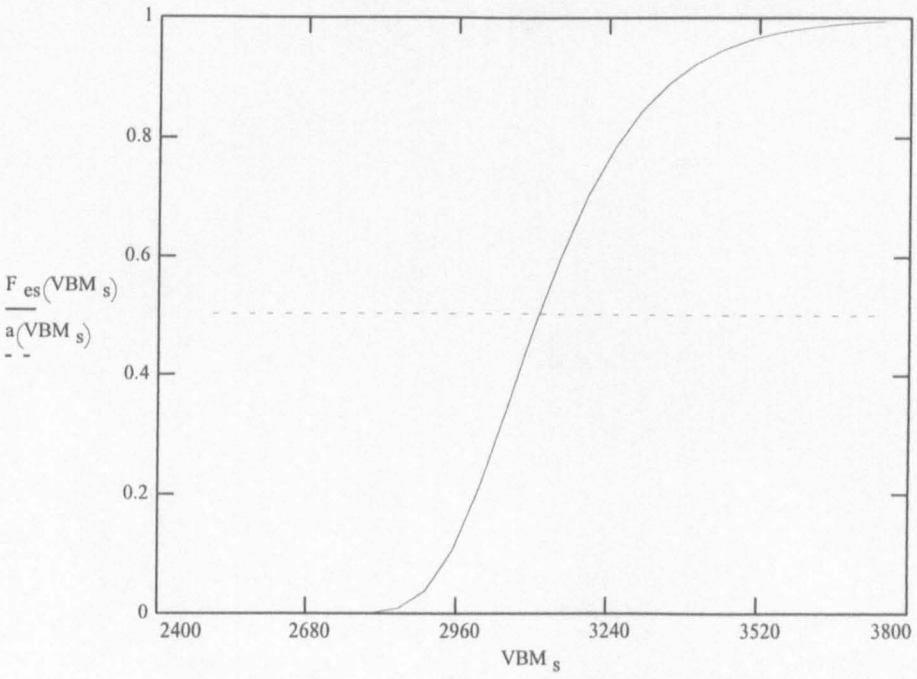

VBM	$F_{es}(VBM_s)$
2500	0
2550	0
2600	0
2650	0
2700	0
2750	0
2800	0.001
2850	0.008
2900	0.037
2950	0.103
3000	0.208
3050	0.338
3100	0.473
3150	0.596
3200	0.7
3250	0.782
3300	0.844
3350	0.889
3400	0.922
3450	0.946
3500	0.962
3550	0.974
3600	0.982
3650	0.987
3700	0.991
3750	0.994

Extreme Still Water Bending Moment at the 0.5 exceedance level:

Initial guess (User defined):

$VBM_s := 3000$ MNm

$VBM_{s0.5} := root(F_{es}(VBM_s) - 0.5, VBM_s)$

$VBM_{s0.5} = 3110.8$ MNm

Gumbel Distribution Function of the Wave Induced Bending Moment, One year:

$VBM_w := 0, 100 .. 3500$ $a(VBM_w) := 0.5$

$$F_{ew}(VBM_w) := \exp\left(-\exp\left(-\frac{VBM_w - u_{nw.y}}{\alpha_{nw.y}}\right)\right)$$

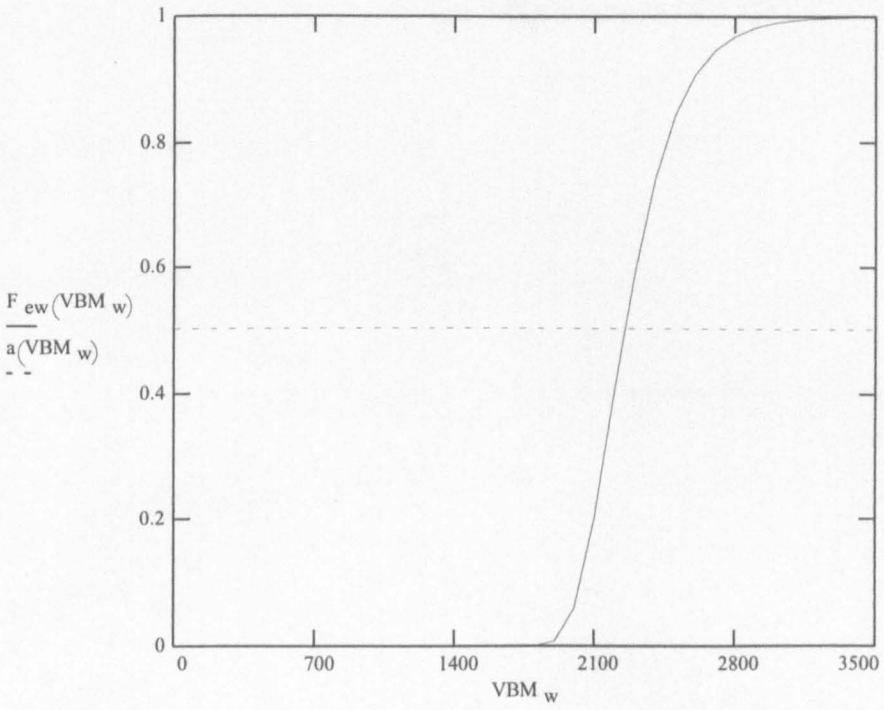

VBM_w	$F_{ew}(VBM_w)$
0	0
100	0
200	0
300	0
400	0
500	0
600	0
700	0
800	0
900	0
1000	0
1100	0
1200	0
1300	0
1400	0
1500	0
1600	0
1700	0
1800	0
1900	0.007
2000	0.059
2100	0.198
2200	0.397
2300	0.59
2400	0.74
2500	0.842
2600	0.906
2700	0.945
2800	0.968
2900	0.982
3000	0.99
3100	0.994
3200	0.997
3300	0.998
3400	0.999
3500	0.999

Extreme Wave Bending Moment at the 0.5 exceedance level:

Initial guess (User defined):

$VBM_w := 2500$ MNm

$VBM_{w0.5} := root(F_{ew}(VBM_w) - 0.5, VBM_w)$

$VBM_{w0.5} = 2251.4$ MNm

Load Combination factor:

$VBM := 0, 100 .. 6000$ $\quad a(VBM_t) := 0.5$

$$F_t(VBM) := \left[\int_{-1 \cdot 10^4}^{VBM} \exp\left[-\exp\left[-\frac{(VBM - z) - u_{nw}}{\alpha_{nw}} \right] \right] \cdot dnorm(z, \mu_s, \sigma_s)\, dz \right]^{n_s}$$

$$F_{es}(VBM) := \exp\left(-\exp\left(-\frac{VBM - u_{ns}}{\alpha_{ns}} \right) \right)$$

$$F_{ew}(VBM) := \exp\left(-\exp\left(-\frac{VBM - u_{nw.y}}{\alpha_{nw.y}} \right) \right)$$

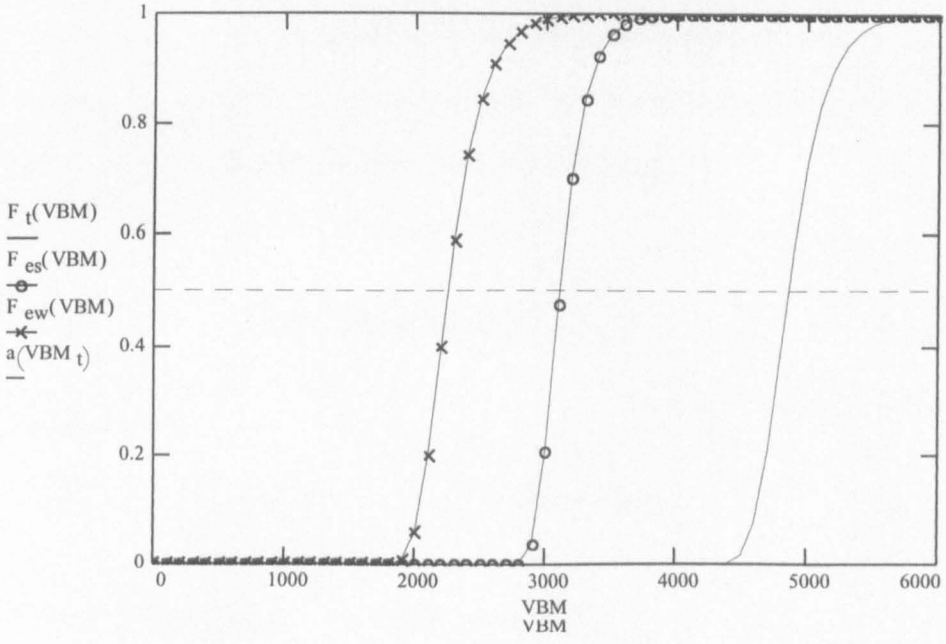

$$\psi_w := \frac{VBM_{t0.5} - VBM_{s0.5}}{VBM_{w0.5}} \qquad \psi_w = 0.78$$

Extreme model for Combination of Environmental Loads

Load Condition: Partial Load, Hog.

Input filename for Long Term Wave Results: $LT := READPRN(tripart4_{res})$

$T_d := 219$	Number of days spent in loading condition pr. year.
$T_h := 72$	Duration of condition (hours).
$T_z := 9.5$	Average mean zero crossing period of waves.
$\gamma := 0.5772$	Euler Constant

Extreme Stillwater Bending Moment (one year):

$\mu_s := 1452$ MNm	Mean value of Still-Water Bending Moment	
$cov_s := 0.15$	Coefficient of variation of Still-Water Bending Moment	
$\sigma_s := \mu_s \cdot cov_s$	Standard deviation of Still-Water Bending Moment	$\sigma_s = 217.8$ MNm
$T_d = 219$	Number of days spent in condition pr. year.	
$T_h = 72$	Duration of condition (hours).	
$n_s := \frac{T_d}{T_h} \cdot 24$	Number of occurrences pr. year.	$n_s = 73$

Gumbel parameters:

$u_{ns} := qnorm\left|\left(1 - \frac{1}{n_s}\right), \mu_s, \sigma_s\right|$ $u_{ns} = 1932.4$ MNm

$f_s := dnorm(u_{ns}, \mu_s, \sigma_s)$ $f_s = 1.608 \cdot 10^{-4}$

$F_s := pnorm(u_{ns}, \mu_s, \sigma_s)$ $F_s = 0.986$

$\alpha_{ns} := \left(\frac{1 - F_s}{f_s}\right)$ $\alpha_{ns} = 85.2$ MNm

The mean and standard deviation of the extreme distribution:

$\mu_{es} := u_{ns} + \gamma \cdot \alpha_{ns}$ $\mu_{es} = 1981.6$ MNm

$\sigma_{es} := \frac{\pi}{\sqrt{6}} \cdot \alpha_{ns}$ $\sigma_{es} = 109.3$ MNm

Still Water Bending Moment, one year normal distribution:

$VBM_s := 500, 510 .. 2500$

$f_s(VBM_s) := dnorm(VBM_s, u_{ns}, \alpha_{ns})$

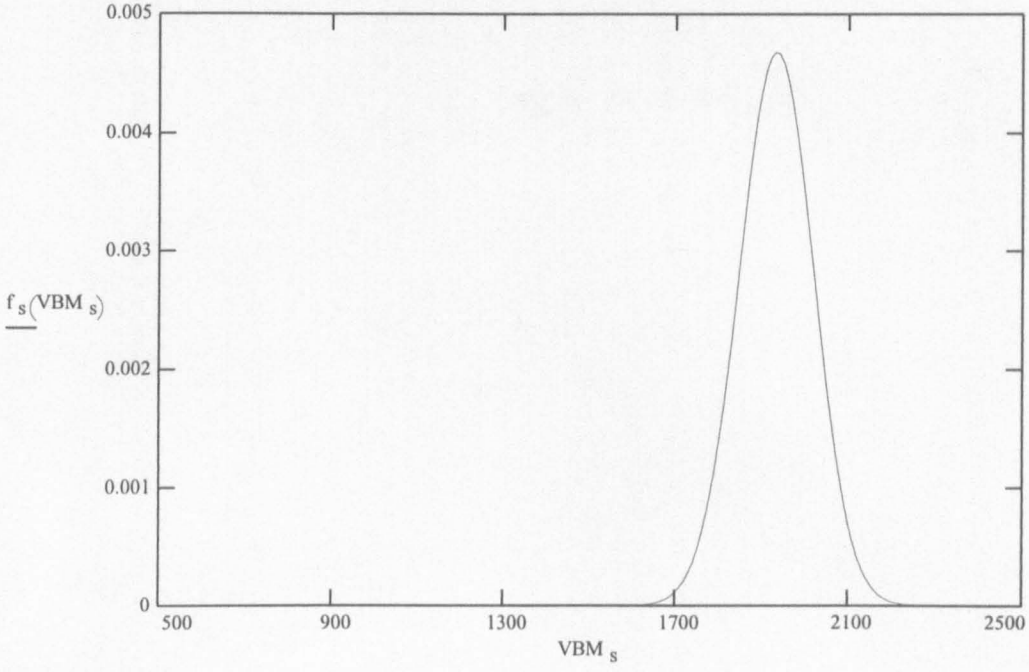

Extreme Wave Induced Bending Moment:

Data from Long Term Calculations

$VBM := LT^{<0>}$ $Qx := LT^{<1>}$ $n := 0 .. 14$

Weibull fit:

$$Fit(VBM, k, b) = \exp\left[-\left(\frac{VBM}{k}\right)^b\right]$$

$$SSE(k, b) := \sum_n \left(\log(|Qx_n|) - \log(|Fit(VBM_n, k, b)|)\right)^2$$

Initial guess for Weibull Parameters:

$k := 140$ MNm $b := 0.98$

Given

$SSE(k, b) = 0$ $1 = 1$ $\begin{pmatrix} k \\ b \end{pmatrix} := Minerr(k, b)$

Weibull parameters:

$k = 127.8$ MNm $b = 0.908$ $SSE(k, b) = 0.6304$ (error)

$LT =$

	0	1
0	0	1
1	250	0.0782
2	500	0.01542
3	750	0.00363
4	$1 \cdot 10^3$	0.00103
5	$1.25 \cdot 10^3$	$3.15015 \cdot 10^{-4}$
6	$1.5 \cdot 10^3$	$9.71326 \cdot 10^{-5}$
7	$1.75 \cdot 10^3$	$2.92894 \cdot 10^{-5}$
8	$2 \cdot 10^3$	$8.47169 \cdot 10^{-6}$
9	$2.25 \cdot 10^3$	$2.29451 \cdot 10^{-6}$
10	$2.5 \cdot 10^3$	$5.69997 \cdot 10^{-7}$
11	$2.75 \cdot 10^3$	$1.28176 \cdot 10^{-7}$
12	$3 \cdot 10^3$	$2.59175 \cdot 10^{-8}$
13	$3.25 \cdot 10^3$	$4.69947 \cdot 10^{-9}$
14	$3.5 \cdot 10^3$	$7.63408 \cdot 10^{-10}$

$$Weibull_n := \exp\left[-\left(\frac{VBM_n}{k}\right)^b\right]$$

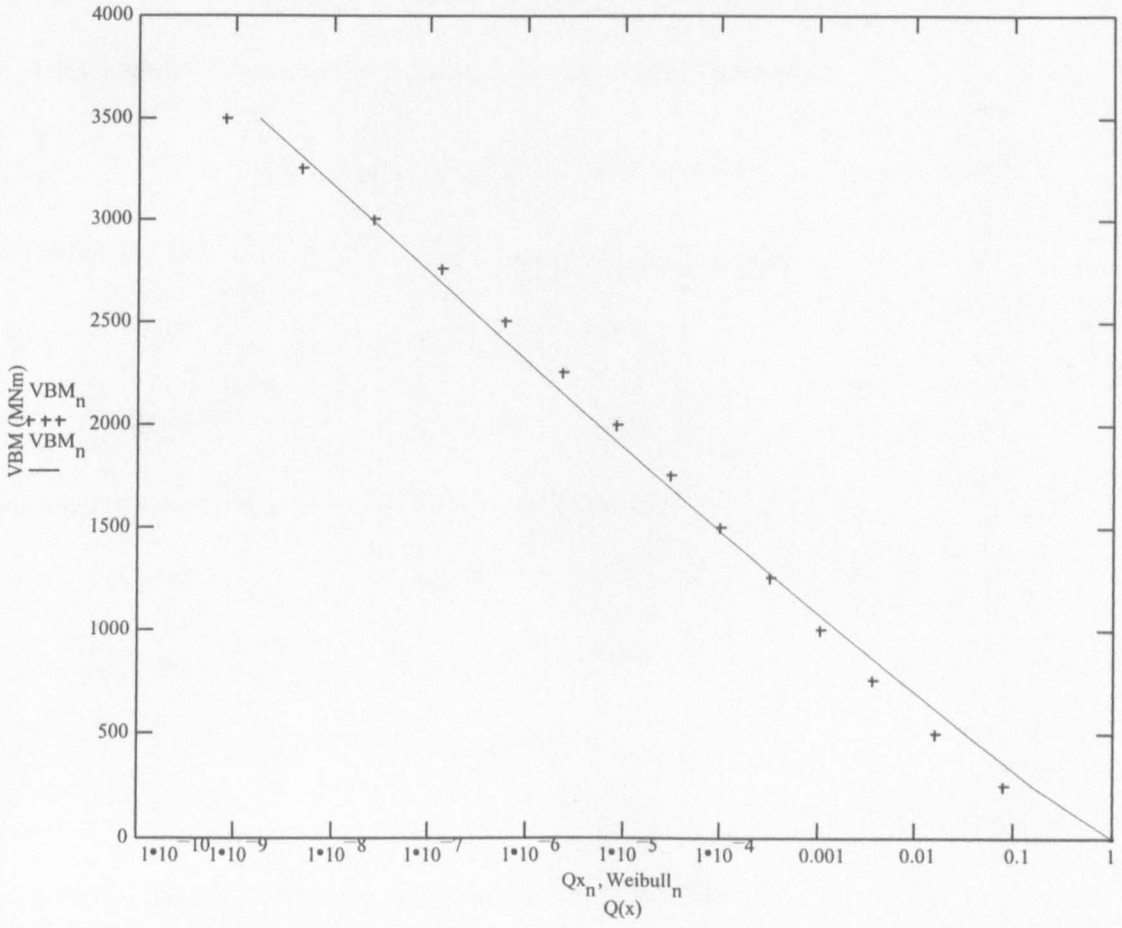

Extreme VWBM (one year):

$T_z = 9.5$ Average mean zero crossing period of waves.

$T_d = 219$ Time spent in loading condition pr. year (days).

$T_c := T_d \cdot 3600 \cdot 24$ Time spent in loading condition pr. year (seconds).

$n := \frac{T_c}{T_z}$ Number of peaks counted in the time period T_c. $n = 1.992 \cdot 10^6$

Gumbel parameters:

$u_{nw.y} := k \cdot \left(\ln(n)^{\frac{1}{b}}\right)$ $u_{nw.y} = 2431.5$ MNm

$\alpha_{nw.y} := \frac{k}{b} \cdot \left(\ln(n)^{\frac{1-b}{b}}\right)$ $\alpha_{nw.y} = 184.7$ MNm

The mean and standard deviation of the extreme distribution:

$\mu_{ew.y} := u_{nw.y} + \gamma \cdot \alpha_{nw.y}$ $\mu_{ew.y} = 2538.1$ MNm

$\sigma_{ew.y} := \frac{\pi}{\sqrt{6}} \cdot \alpha_{nw.y}$ $\sigma_{ew.y} = 236.8$ MNm

$COV_{ew.y} := \frac{\pi}{\sqrt{6} \cdot \left(\gamma + \ln(n)^{\frac{1}{b}}\right)}$ $COV_{ew.y} = 0.07$

Wave Induced Bending Moment, one year normal distribution:

$VBM_w := 0, 10 .. 3500$

$f_s(VBM_w) := dnorm(VBM_w, u_{nw.y}, \alpha_{nw.y})$

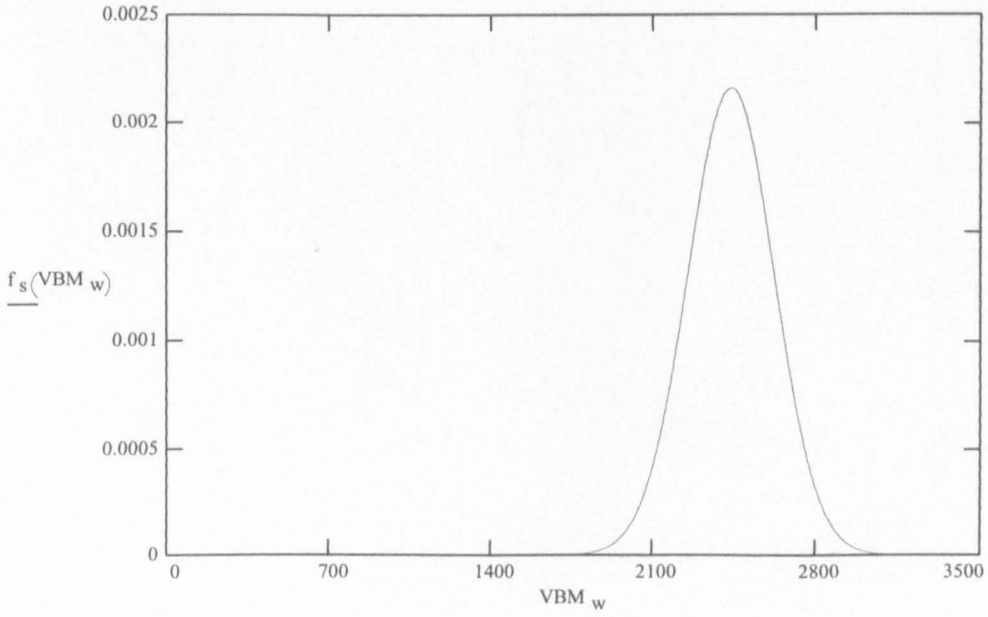

Extreme VWBM (one Load Condition):

$T_z = 9.5$ Average mean zero crossing period of waves (seconds).

$T_h = 72$ Duration of load condition (hours)

$T_c := T_h \cdot 3600$ Duration of load condition (seconds)

$n := \frac{T_c}{T_z}$ Number of peaks counted in the time period T_c. $n = 2.728 \cdot 10^4$

Gumbel parameters:

$u_{nw} := k \cdot \left(\ln(n)^{\frac{1}{b}}\right)$ $u_{nw} = 1652.4$ MNm

$\alpha_{nw} := \frac{k}{b} \cdot \left(\ln(n)^{\frac{1-b}{b}}\right)$ $\alpha_{nw} = 178.2$ MNm

The mean and standard deviation of the extreme distribution:

$\mu_{ew} := u_{nw} + \gamma \cdot \alpha_{nw}$ $\mu_{ew} = 1755.2$ MNm

$\sigma_{ew} := \frac{\pi}{\sqrt{6}} \cdot \alpha_{nw}$ $\sigma_{ew} = 228.6$ MNm

$COV_{ew} := \frac{\pi}{\sqrt{6} \cdot \left(\gamma + \ln(n)^{\frac{1}{b}}\right)}$ $COV_{ew} = 0.09$

Wave Induced Bending Moment, one voyage normal distribution:

$VBM_{w.v} := 0, 10 .. 2500$

$f_s(VBM_{w.v}) := dnorm(VBM_{w.v}, u_{nw}, \alpha_{nw})$

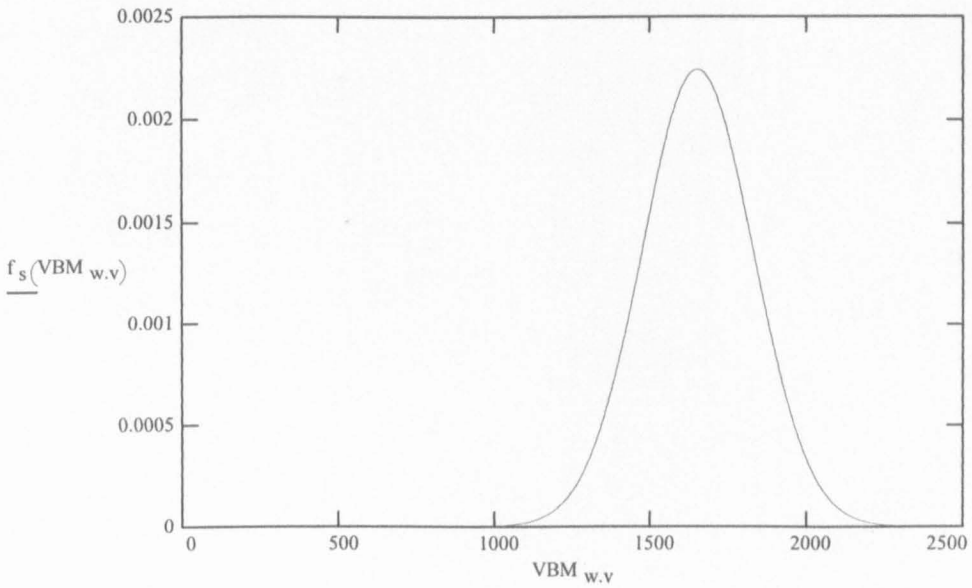

Load Combination, Ferry Borges-Castenheta's Method

Probability distribution of the maximum of the combined process:

$VBM_t := 3500, 3550 .. 5000$ $\quad a(VBM_t) := 0.5$

$$F_t(VBM_t) := \left[\int_{-1 \cdot 10^4}^{VBM_t} \exp\left[-\exp\left[-\frac{(VBM_t - z) - u_{nw}}{\alpha_{nw}} \right] \right] \cdot dnorm(z, \mu_s, \sigma_s)\, dz \right]^{n_s}$$

VBM	$F_t(VBM_t)$
3500	0
3550	0
3600	0
3650	0.002
3700	0.007
3750	0.022
3800	0.054
3850	0.107
3900	0.181
3950	0.272
4000	0.372
4050	0.472
4100	0.566
4150	0.65
4200	0.721
4250	0.781
4300	0.829
4350	0.868
4400	0.899
4450	0.922
4500	0.941
4550	0.955
4600	0.966
4650	0.974
4700	0.98
4750	0.985
4800	0.989
4850	0.991
4900	0.994
4950	0.995
5000	0.996

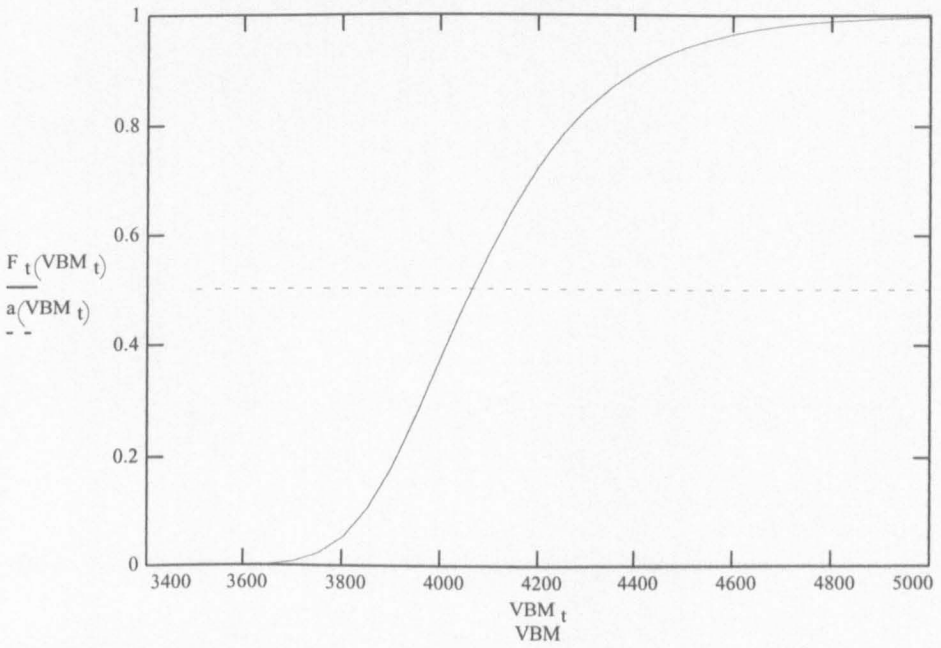

Extreme Combined Bending Moment at the 0.5 exceedance level:

Initial guess (User defined):

$VBM_t := 4000$ MNm

At the 0.5 exceedance level:

$VBM_{t0.5} := root(F_t(VBM_t) - 0.5, VBM_t)$

$VBM_{t0.5} = 4064.5$ MNm

Gumbel Distribution Function of the Still Water Bending Moment:

$VBM_s := 1500, 1525 .. 2500$ $\quad a(VBM_s) := 0.5$

$$F_{es}(VBM_s) := \exp\left(-\exp\left(-\frac{VBM_s - u_{ns}}{\alpha_{ns}}\right)\right)$$

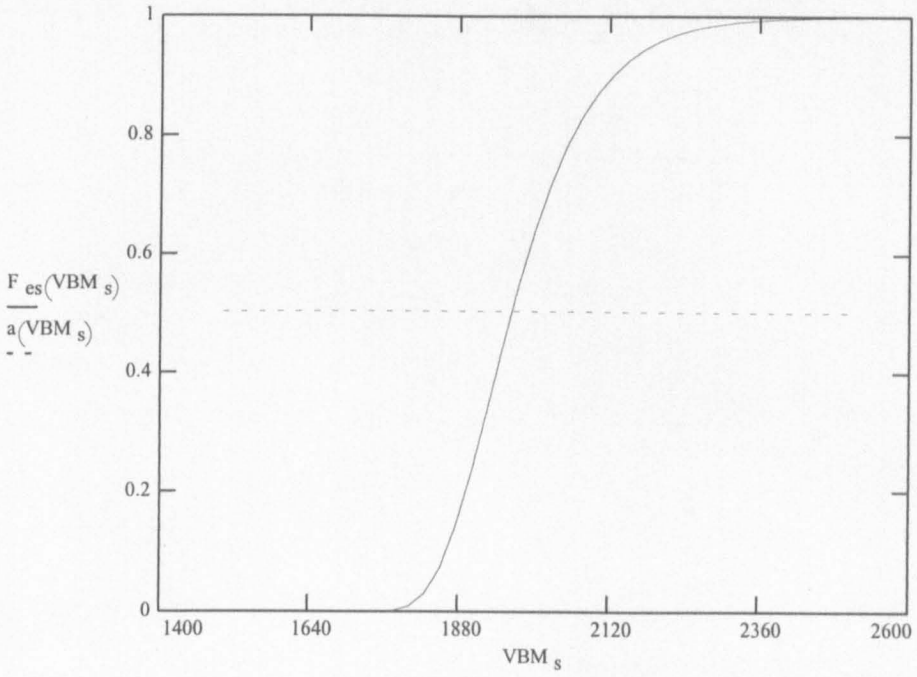

VBM	$F_{es}(VBM_s)$
1500	0
1525	0
1550	0
1575	0
1600	0
1625	0
1650	0
1675	0
1700	0
1725	0
1750	0
1775	0.002
1800	0.009
1825	0.029
1850	0.072
1875	0.141
1900	0.231
1925	0.336
1950	0.443
1975	0.545
2000	0.636
2025	0.714
2050	0.778
2075	0.829
2100	0.869
2125	0.901
2150	0.925
2175	0.944
2200	0.958
2225	0.968
2250	0.976
2275	0.982
2300	0.987
2325	0.99
2350	0.993
2375	0.994
2400	0.996
2425	0.997
2450	0.998
2475	0.998
2500	0.999

Extreme Still Water Bending Moment at the 0.5 exceedance level:

Initial guess (User defined):

$VBM_s := 2000$ MNm

$VBM_{s0.5} := \text{root}(F_{es}(VBM_s) - 0.5, VBM_s)$

$VBM_{s0.5} = 1963.7$ MNm

Gumbel Distribution Function of the Wave Induced Bending Moment, One year:

$VBM_w := 0, 100 .. 3500$ $a(VBM_w) := 0.5$

$$F_{ew}(VBM_w) := \exp\left(-\exp\left(-\frac{VBM_w - u_{nw.y}}{\alpha_{nw.y}}\right)\right)$$

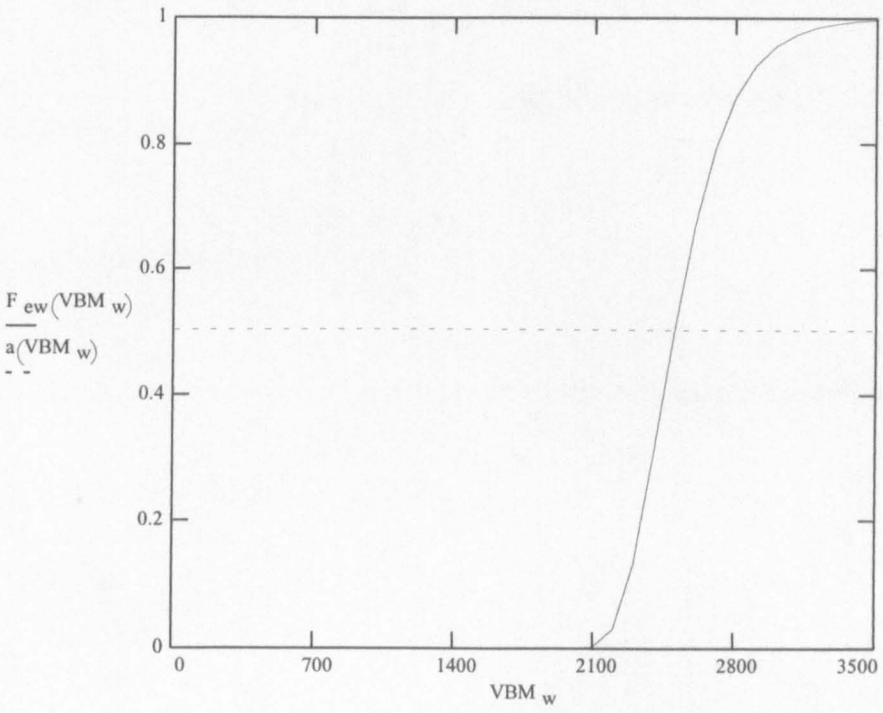

VBM	$F_{ew}(VBM_w)$
0	0
100	0
200	0
300	0
400	0
500	0
600	0
700	0
800	0
900	0
1000	0
1100	0
1200	0
1300	0
1400	0
1500	0
1600	0
1700	0
1800	0
1900	0
2000	0
2100	0.002
2200	0.03
2300	0.13
2400	0.305
2500	0.502
2600	0.669
2700	0.792
2800	0.873
2900	0.924
3000	0.955
3100	0.974
3200	0.985
3300	0.991
3400	0.995
3500	0.997

Extreme Wave Bending Moment at the 0.5 exceedance level:

Initial guess (User defined):

$VBM_w := 2500$ MNm

$VBM_{w0.5} := root(F_{ew}(VBM_w) - 0.5, VBM_w)$

$VBM_{w0.5} = 2499.2$ MNm

Load Combination factor:

$VBM := 0, 100 .. 5000$ $\quad a(VBM_t) := 0.5$

$$F_t(VBM) := \left[\int_{-1 \cdot 10^4}^{VBM} \exp\left[-\exp\left[-\frac{(VBM - z) - u_{nw}}{\alpha_{nw}} \right] \right] \cdot dnorm(z, \mu_s, \sigma_s)\, dz \right]^{n_s}$$

$$F_{es}(VBM) := \exp\left(-\exp\left(-\frac{VBM - u_{ns}}{\alpha_{ns}} \right) \right)$$

$$F_{ew}(VBM) := \exp\left(-\exp\left(-\frac{VBM - u_{nw.y}}{\alpha_{nw.y}} \right) \right)$$

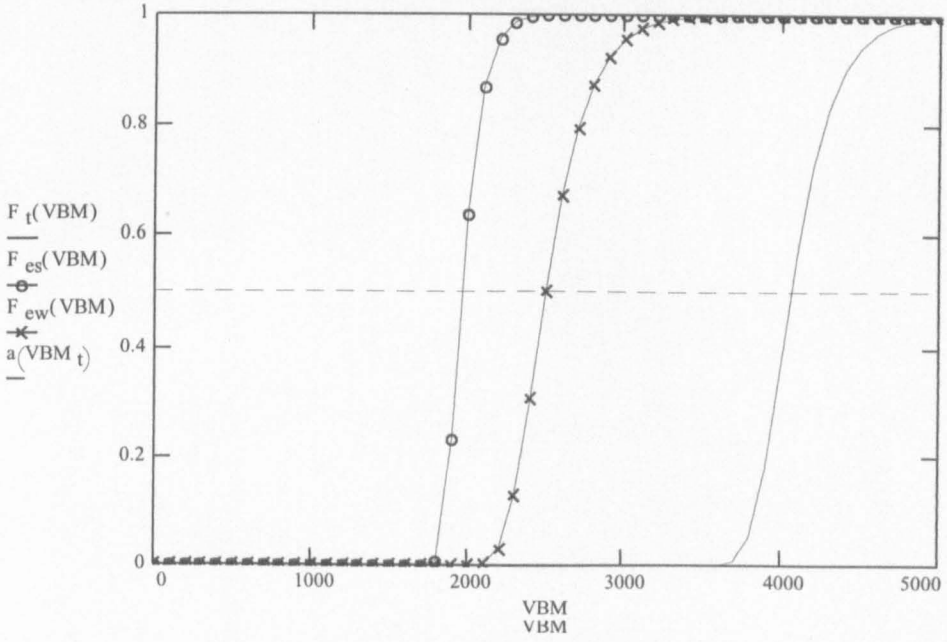

$$\psi_w := \frac{VBM_{t0.5} - VBM_{s0.5}}{VBM_{w0.5}} \qquad \psi_w = 0.84$$

Appendix I

Reliability Analysis

Stochastic models used for Triton

Area 4 Wave Statistics

Sagging

Ship	Condition	χ_u - LogNormal		M_u	M_{se} - Gumbel		Ψ_w	χ_w - Normal		χ_{nl} - Normal		M_{we} - Gumbel		β	P_f	β_t	P_f
		Mean	STD	Constant	Mean	STD	Constant	Mean	STD	Mean	STD	Mean	STD				
Triton 1	Full Load	1.00	0.15	-6693	358	42.4	0.91	0.90	0.18	1.10	0.088	-2358	-240	4.62	1.921E-06	4.62	1.927E-06
	Partial Load	1.00	0.15	-6693	922	109.3	0.84	0.90	0.18	1.10	0.088	-2538	-236.8	5.14	1.376E-07		
	Ballast	1.00	0.15	-6693	1461	173.1	0.78	0.90	0.18	1.10	0.088	-2289	-228.9	6.04	7.734E-10		
Triton 2	Full Load	1.00	0.15	-7887	358	42.4	0.91	0.90	0.18	1.10	0.088	-2358	-240	5.18	1.112E-07	5.17	1.173E-07
	Partial Load	1.00	0.15	-7887	922	109.3	0.84	0.90	0.18	1.10	0.088	-2538	-236.8	5.68	6.754E-09		
	Ballast	1.00	0.15	-7887	1461	173.1	0.78	0.90	0.18	1.10	0.088	-2289	-228.9	6.53	3.305E-11		
Triton 3	Full Load	1.00	0.15	-6885	358	42.4	0.91	0.90	0.18	1.10	0.088	-2358	-240	4.71	1.240E-06	4.69	1.342E-06
	Partial Load	1.00	0.15	-6885	922	109.3	0.84	0.90	0.18	1.10	0.088	-2538	-236.8	5.24	8.045E-08		
	Ballast	1.00	0.15	-6885	1461	173.1	0.78	0.90	0.18	1.10	0.088	-2289	-228.9	6.13	4.411E-10		

Hogging

Ship	Condition	χ_u - LogNormal		M_u	M_{se} - Gumbel		Ψ_w	χ_w - Normal		χ_{nl} - Normal		M_{we} - Gumbel		β	P_f	β_t	P_f
		Mean	STD	Constant	Mean	STD	Constant	Mean	STD	Mean	STD	Mean	STD				
Triton 1	Full Load	1.00	0.15	8329	768	42.4	0.91	0.90	0.18	0.90	0.135	2358	240	4.96	3.530E-07	3.28	5.143E-04
	Partial Load	1.00	0.15	8329	1982	109.3	0.84	0.90	0.18	0.90	0.135	2538	236.8	4.01	3.037E-05		
	Ballast	1.00	0.15	8329	3139	173.1	0.78	0.90	0.18	0.90	0.135	2289	228.9	3.30	4.835E-04		
Triton 2	Full Load	1.00	0.15	9701	768	42.4	0.91	0.90	0.18	0.90	0.135	2358	240	5.55	1.432E-08	4.11	2.004E-05
	Partial Load	1.00	0.15	9701	1982	109.3	0.84	0.90	0.18	0.90	0.135	2538	236.8	4.74	1.070E-06		
	Ballast	1.00	0.15	9701	3139	173.1	0.78	0.90	0.18	0.90	0.135	2289	228.9	4.12	1.895E-05		
Triton 3	Full Load	1.00	0.15	9603	768	42.4	0.91	0.90	0.18	0.90	0.135	2358	240	5.51	1.799E-08	4.06	2.498E-05
	Partial Load	1.00	0.15	9603	1982	109.3	0.84	0.90	0.18	0.90	0.135	2538	236.8	4.69	1.368E-06		
	Ballast	1.00	0.15	9603	3139	173.1	0.78	0.90	0.18	0.90	0.135	2289	228.9	4.07	2.352E-05		

IACS / DNV rules 0.15 0.05 0.10

Ship	Condition	χ_u - LogNormal		M_u	M_{se} - Gumbel		Ψ_w	χ_w - Normal		χ_{nl} - Normal		M_{we} - Gumbel		β	P_f	β_t	P_f
		Mean	STD	Constant	Mean	STD	Constant	Mean	STD	Mean	STD	Mean	STD				
Triton 1	Sag	1.00	0.15	-6693	2238	111.9	0.88	0.90	0.18	1.100	0.088	3787	378.7	0.92	1.788E-01	0.89	1.855E-01
	Hog	1.00	0.15	8329	2577	128.85	0.88	0.90	0.18	0.900	0.135	3447	344.7	2.47	6.756E-03		
Triton 2	Sag	1.00	0.15	-7887	2238	111.9	0.88	0.90	0.18	1.100	0.088	3787	378.7	1.74	4.093E-02	1.73	4.162E-02
	Hog	1.00	0.15	9701	2577	128.85	0.88	0.90	0.18	0.900	0.135	3447	344.7	3.20	6.872E-04		
Triton 3	Sag	1.00	0.15	-6885	2238	111.9	0.88	0.90	0.18	1.100	0.088	3787	378.7	1.07	1.423E-01	1.07	1.431E-01
	Hog	1.00	0.15	9603	2577	128.85	0.88	0.90	0.18	0.900	0.135	3447	344.7	3.16	7.889E-04		

Triton 2, Central North Sea

Condition	χ_u - LogNormal		M_u	M_{se} - Gumbel		Ψ_w	χ_w - Normal		χ_{nl} - Normal		M_{we} - Gumbel		β	P_f	β_t	P_f
	Mean	STD	Constant	Mean	STD	Constant	Mean	STD	Mean	STD	Mean	STD				
Full Load	1.00	0.15	-7887	358	42.4	0.91	0.90	0.18	1.10	0.088	-1845	161.0	6.31	1.401E-10	6.31	1.401E-10
Sagging Partial Load	1.00	0.15	-7887	922	109.3	0.84	0.90	0.18	1.10	0.088	-2008	156.3	6.87	3.230E-12		
Ballast	1.00	0.15	-7887	1461	173.1	0.78	0.90	0.18	1.10	0.088	-1810	155.2	7.71	6.328E-15		
Full Load	1.00	0.15	9701	768	42.4	0.91	0.90	0.18	0.90	0.135	1845	161.0	6.55	2.891E-11	4.62	1.927E-06
Hogging Partial Load	1.00	0.15	9701	1982	109.3	0.84	0.90	0.18	0.90	0.135	2008	156.3	5.31	5.493E-08		
Ballast	1.00	0.15	9701	3139	173.1	0.78	0.90	0.18	0.90	0.135	1810	155.2	4.66	1.583E-06		

Triton 2, Northern North Sea

Condition	χ_u - LogNormal		M_u	M_{se} - Gumbel		Ψ_w	χ_w - Normal		χ_{nl} - Normal		M_{we} - Gumbel		β	P_f	β_t	P_f
	Mean	STD	Constant	Mean	STD	Constant	Mean	STD	Mean	STD	Mean	STD				
Full Load	1.00	0.15	-7887	358	42.4	0.91	0.90	0.18	1.10	0.088	-3047	288.2	4.18	1.458E-05	4.16	1.571E-05
Sagging Partial Load	1.00	0.15	-7887	922	109.3	0.84	0.90	0.18	1.10	0.088	-3230	281.0	4.69	1.368E-06		
Ballast	1.00	0.15	-7887	1461	173.1	0.78	0.90	0.18	1.10	0.088	-2948	275.3	5.54	1.516E-08		
Full Load	1.00	0.15	9701	768	42.4	0.91	0.90	0.18	0.90	0.135	3047	288.2	4.65	1.661E-06	3.40	3.371E-04
Hogging Partial Load	1.00	0.15	9701	1982	109.3	0.84	0.90	0.18	0.90	0.135	3230	281.0	3.92	4.429E-05		
Ballast	1.00	0.15	9701	3139	173.1	0.78	0.90	0.18	0.90	0.135	2948	275.3	3.44	2.909E-04		

Triton 2, West of Shetland

Condition	χ_u - LogNormal		M_u	M_{se} - Gumbel		Ψ_w	χ_w - Normal		χ_{nl} - Normal		M_{we} - Gumbel		β	P_f	β_t	P_f
	Mean	STD	Constant	Mean	STD	Constant	Mean	STD	Mean	STD	Mean	STD				
Full Load	1.00	0.15	-7887	358	42.4	0.91	0.90	0.18	1.10	0.088	-3978	410.8	3.74	9.204E-05	3.72	9.848E-05
Sagging Partial Load	1.00	0.15	-7887	922	109.3	0.84	0.90	0.18	1.10	0.088	-4045	355.0	4.37	6.217E-06		
Ballast	1.00	0.15	-7887	1461	173.1	0.78	0.90	0.18	1.10	0.088	-3276	356.3	5.30	5.802E-08		
Full Load	1.00	0.15	9701	768	42.4	0.91	0.90	0.18	0.90	0.135	3978	410.8	3.91	4.617E-05	3.09	1.018E-03
Hogging Partial Load	1.00	0.15	9701	1982	109.3	0.84	0.90	0.18	0.90	0.135	4045	355.0	3.47	2.603E-04		
Ballast	1.00	0.15	9701	3139	173.1	0.78	0.90	0.18	0.90	0.135	3276	356.3	3.19	7.114E-04		

Results of reliability analysis for Triton 2. Partial safety factors are based on the design point in each condition, they are not optimised.

Triton 2, Full Load, Sagging

var	design point		sensitivity vectors			
	x^*	u^*	α	γ	δ	η
x1 - X_u	0.6694	-2.6160	-0.5064	-0.5064	0.7169	-1.3847
x2 - M_{se}	-359.8	0.1332	0.0257	0.0257	-0.0273	0.0011
x3 - X_w	1.3500	2.5010	0.4834	0.4834	-0.4834	-1.2091
x4 - X_{nl}	1.2190	1.3530	0.2618	0.2618	-0.2618	-0.3542
x5 - M_{we}	3765.0	3.4270	0.6639	0.6639	-0.2311	-1.3551

m_{ns} = -358 MNm
m_{nw} = 2358 MNm

γ_u = 1.49
γ_s = 1.01
γ_w = 2.39

"As Built"
M_u = 7887 MNm
β = 5.18
P_f = 1.1E-07

α - Triton 2, Full Load, Sagging

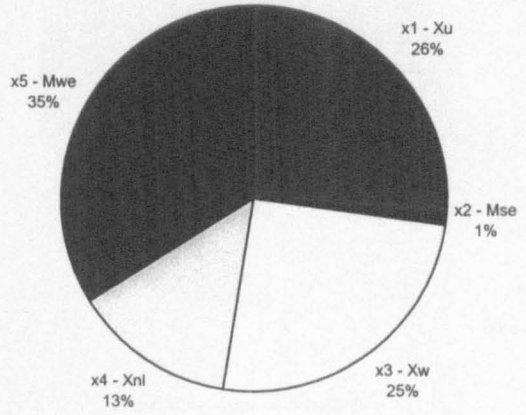

Triton 2, Partial Load, Sagging

var	design point		sensitivity vectors			
	x^*	u^*	α	γ	δ	η
x1 - X_u	0.6579	-2.7320	-0.4815	-0.4815	0.6901	-1.3722
x2 - M_{se}	-895.4	0.4211	0.0711	0.0711	-0.068	-0.0166
x3 - X_w	1.3980	2.7690	0.4872	0.4872	-0.4872	-1.3491
x4 - X_{nl}	1.2350	1.5290	0.2698	0.2698	-0.2698	-0.4126
x5 - M_{we}	4195.0	3.8050	0.673	0.673	-0.2137	-1.4952

m_{ns} = -922 MNm
m_{nw} = 2538 MNm

γ_u = 1.52
γ_s = 0.97
γ_w = 2.40

"As Built"
M_u = 7887 MNm
β = 5.68
P_f = 6.8E-09

α - Triton 2, Partial Load, Sagging

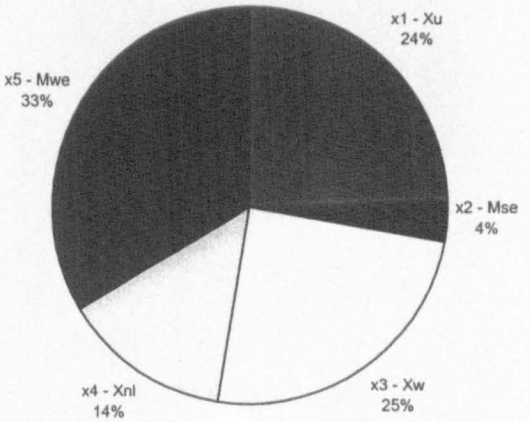

Triton 2, Ballast Load, Sagging

var	design point		sensitivity vectors			
	x^*	u^*	α	γ	δ	η
x1 - X_u	0.6429	-2.8870	-0.4421	-0.4421	0.6437	-1.3275
x2 - M_{se}	-1324.0	0.8977	0.1264	0.1264	-0.1012	-0.0798
x3 - X_w	1.4470	3.0370	0.4653	0.4653	-0.4653	-1.4131
x4 - X_{nl}	1.2510	1.7200	0.263	0.263	-0.263	-0.4524
x5 - M_{we}	4530.0	4.6140	0.7092	0.7092	-0.1889	-1.8499

m_{ns} = -1461 MNm
m_{nw} = 2289 MNm

γ_u = 1.56
γ_s = 0.91
γ_w = 2.79

"As Built"
M_u = 7887 MNm
β = 6.53
P_f = 3.3E-11

α - Triton 2, Ballast Load, Sagging

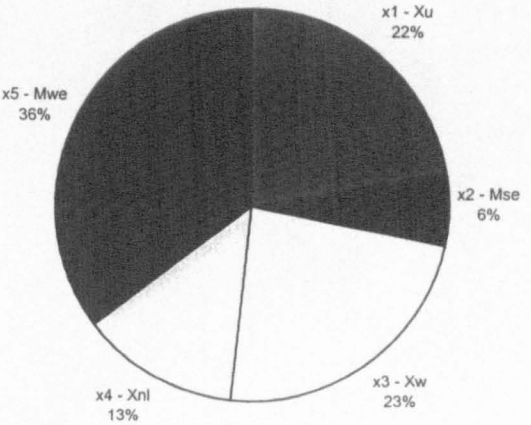

Triton 2, Full Load, Hogging

var	design point		sensitivity vectors			
	x^*	u^*	α	γ	δ	η
x1 - X_u	0.6222	-3.1060	-0.5598	-0.5598	0.8333	-1.8024
x2 - M_{se}	766.5	0.1388	0.0249	0.0249	-0.0264	0.001
x3 - X_w	1.3390	2.4390	0.4404	0.4404	-0.4404	-1.0743
x4 - X_{nl}	1.1800	2.0770	0.3747	0.3747	-0.3747	-0.7782
x5 - M_{we}	3664.0	3.2780	0.5929	0.5929	-0.2146	-1.1677

m_{ns} = 768 MNm
m_{nw} = 2358 MNm

γ_u = 1.61
γ_s = 1.00
γ_w = 2.23

"As Built"
M_u = 9701 MNm
β = 5.55
P_f = 1.4E-08

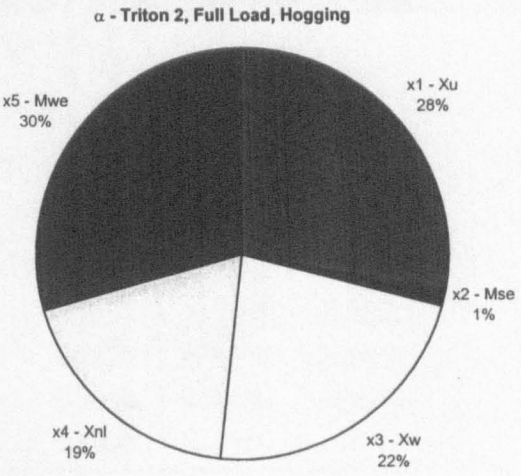

Triton 2, Partial Load, Hogging

var	design point		sensitivity vectors			
	x^*	u^*	α	γ	δ	η
x1 - X_u	0.6017	-3.3310	-0.694	-0.694	1.0562	-2.3887
x2 - M_{se}	2012.0	0.4466	0.0919	0.0919	-0.0871	-0.0236
x3 - X_w	1.2720	2.0640	0.4317	0.4317	-0.4317	-0.8911
x4 - X_{nl}	1.1340	1.7350	0.3629	0.3629	-0.3629	-0.6297
x5 - M_{we}	3158.0	2.0670	0.4379	0.4379	-0.2287	-0.5984

m_{ns} = 1982 MNm
m_{nw} = 2538 MNm

γ_u = 1.66
γ_s = 1.02
γ_w = 1.51

"As Built"
M_u = 9701 MNm
β = 4.74
P_f = 1.1E-06

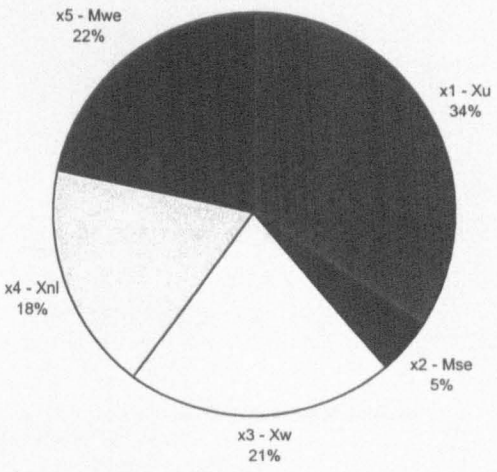

Triton 2, Ballast Load, Hogging

var	design point		sensitivity vectors			
	x^*	u^*	α	γ	δ	η
x1 - X_u	0.5949	-3.4070	-0.8087	-0.8087	1.2398	-2.8442
x2 - M_{se}	3266.0	0.8523	0.1996	0.1996	-0.1626	-0.1191
x3 - X_w	1.1720	1.5130	0.3613	0.3613	-0.3613	-0.5466
x4 - X_{nl}	1.0680	1.2460	0.2974	0.2974	-0.2974	-0.3705
x5 - M_{we}	2565.0	1.2120	0.2953	0.2953	-0.21	-0.2532

m_{ns} = 3139 MNm
m_{nw} = 2289 MNm

γ_u = 1.68
γ_s = 1.04
γ_w = 1.09

"As Built"
M_u = 9701 MNm
β = 4.12
P_f = 1.9E-05

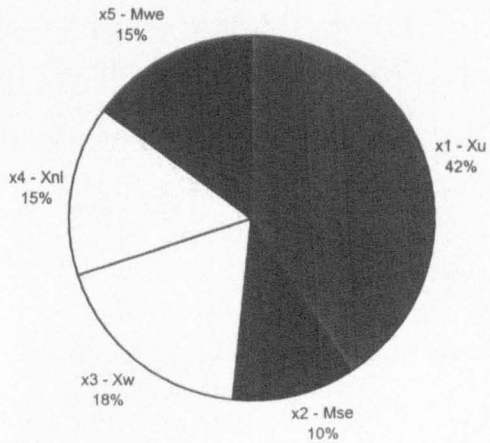

Optimisation of M_u to target reliability, $\beta = 3.71$, for Triton 2.
Partial safety factors are based on the design point
in each condition, they are not calibrated.

Triton 2, Full Load, Sagging						
var	*design point*		*sensitivity vectors*			
	x^*	u^*	α	γ	δ	η
x1 - X_u	0.7423	-1.9230	-0.5168	-0.5168	0.6785	-1.059
x2 - M_{se}	-359.7	0.1345	0.0361	0.0361	-0.0383	0.0016
x3 - X_w	1.2620	2.0100	0.5406	0.5406	-0.5406	-1.0868
x4 - X_{nl}	1.1920	1.0410	0.2799	0.2799	-0.2799	-0.2914
x5 - M_{we}	3064.0	2.2310	0.6009	0.6009	-0.2969	-0.873

m_{ns} = -358 MNm
m_{nw} = 2358 MNm

γ_u = 1.35
γ_s = 1.00
γ_w = 1.78

"As Built"
M_u = 7887
β = 5.18
P_f = 1.11E-07

Target Values:
M_{ut} = 5165.918
β_t = 3.71
P_f = 1.04E-04

Triton 2, Partial Load, Sagging						
var	*design point*		*sensitivity vectors*			
	x^*	u^*	α	γ	δ	η
x1 - X_u	0.7590	-1.7740	-0.4727	-0.4727	0.6101	-0.8988
x2 - M_{se}	-894.9	0.4251	0.1111	0.1111	-0.1061	-0.0263
x3 - X_w	1.2820	2.1240	0.5668	0.5668	-0.5668	-1.2036
x4 - X_{nl}	1.1980	1.1120	0.2966	0.2966	-0.2966	-0.3298
x5 - M_{we}	3223.0	2.2080	0.5958	0.5958	-0.2966	-0.8585

m_{ns} = -922 MNm
m_{nw} = 2538 MNm

γ_u = 1.317523
γ_s = 0.970607
γ_w = 1.638298

"As Built"
M_u = 7887
β = 5.68
P_f = 6.75E-09

Target Values:
M_{ut} = 4299.209
β_t = 3.71
P_f = 1.04E-04

Triton 2, Ballast Load, Sagging						
var	*design point*		*sensitivity vectors*			
	x^*	u^*	α	γ	δ	η
x1 - X_u	0.8005	-1.4170	-0.3757	-0.3757	0.4651	-0.5821
x2 - M_{se}	-1321.0	0.9144	0.2381	0.2381	-0.1895	-0.1534
x3 - X_w	1.2780	2.1010	0.5584	0.5584	-0.5584	-1.1729
x4 - X_{nl}	1.1970	1.0970	0.2916	0.2916	-0.2916	-0.32
x5 - M_{we}	3037.0	2.3880	0.6367	0.6367	-0.2989	-0.9761

m_{ns} = -1461 MNm

m_{nw} = 2289 MNm

γ_u = 1.249219

γ_s = 0.904175

γ_w = 1.583137

"As Built"

M_u = 7887 MNm

β = 6.53

P_f = 3.30E-11

Target Values:

M_{ut} = 2876.704 MNm

β_t = 3.71

P_f = 1.04E-04

Triton 2, Full Load, Hogging						
var	*design point*		*sensitivity vectors*			
	x^*	u^*	α	γ	δ	η
x1 - X_u	0.7059	-2.2610	-0.6034	-0.6034	0.8224	-1.4379
x2 - M_{se}	766.6	0.1428	0.0377	0.0377	-0.04	0.0013
x3 - X_w	1.2280	1.8200	0.4872	0.4872	-0.4872	-0.8865
x4 - X_{nl}	1.1050	1.5160	0.406	0.406	-0.406	-0.6156
x5 - M_{we}	2857.0	1.7700	0.482	0.482	-0.2791	-0.5799

m_{ns} = 768 MNm (From load maual)

m_{nw} = 2358 MNm (From IACS requirements)

γ_u = 1.416631

γ_s = 0.998177

γ_w = 1.496127

"As Built"

M_u = 9701 MNm

β = 5.55

P_f = 1.43E-08

Target Values:

M_{ut} = 6083.677 MNm

β_t = 3.71

P_f = 1.04E-04

Triton 2, Partial Load, Hogging						
var	*design point*		*sensitivity vectors*			
	x^*	u^*	α	γ	δ	η
x1 - X_u	0.6577	-2.7340	-0.7251	-0.7251	1.0393	-2.0678
x2 - M_{se}	2007.0	0.4100	0.1075	0.1075	-0.1033	-0.024
x3 - X_w	1.2010	1.6700	0.4444	0.4444	-0.4444	-0.7422
x4 - X_{nl}	1.0870	1.3830	0.3683	0.3683	-0.3683	-0.5093
x5 - M_{we}	2863.0	1.3270	0.3599	0.3599	-0.2452	-0.3361

m_{ns} = 1982 MNm
m_{nw} = 2538 MNm

γ_u = 1.52045
γ_s = 1.012614
γ_w = 1.237034

"As Built"
M_u = 9701 MNm
β = 4.74
P_f = 1.07E-06

Target Values:
M_{ut} = 7825.136 MNm
β_t = 3.71
P_f = 1.04E-04

Triton 2, Ballast Load, Hogging						
var	*design point*		*sensitivity vectors*			
	x^*	u^*	α	γ	δ	η
x1 - X_u	0.6236	-3.0910	-0.8163	-0.8163	1.2132	-2.6158
x2 - M_{se}	3248.0	0.7663	0.2011	0.2011	-0.1691	-0.1063
x3 - X_w	1.1450	1.3630	0.3612	0.3612	-0.3612	-0.4924
x4 - X_{nl}	1.0500	1.1140	0.2954	0.2954	-0.2954	-0.3291
x5 - M_{we}	2506.0	1.0240	0.2749	0.2749	-0.2099	-0.1994

m_{ns} = 3139 MNm
m_{nw} = 2289 MNm

γ_u = 1.603592
γ_s = 1.034724
γ_w = 1.026655

"As Built"
M_u = 9701 MNm
β = 4.12
P_f = 1.90E-05

Target Values:
M_{ut} = 8976.931 MNm
β_t = 3.71
P_f = 1.04E-04